

**UCSF**

**UC San Francisco Electronic Theses and Dissertations**

**Title**

Carbon-14 synthesis, in vitro reductive metabolism, and covalent binding to DNA of the 5-nitrofuran 2,4 diacetylamino-6-(5-nitro-2-furyl)-1,3,5-triazine

**Permalink**

<https://escholarship.org/uc/item/4v5528cb>

**Author**

Doose, Dennis R.

**Publication Date**

1983

Peer reviewed|Thesis/dissertation

CARBON-14 SYNTHESIS, IN VITRO REDUCTIVE METABOLISM, AND COVALENT BINDING  
TO DNA OF THE 5-NITROFURAN 2,4-DIACETYLAMINO-6-(5-NITRO-2-FURYL)-1,3,5-TRIAZINE  
by

Dennis R. Doose

B.S., California State Polytechnic University, Pomona, 1973

DISSERTATION

Submitted in partial satisfaction of the requirements for the degree of

DOCTOR OF PHILOSOPHY

in

PHARMACEUTICAL CHEMISTRY

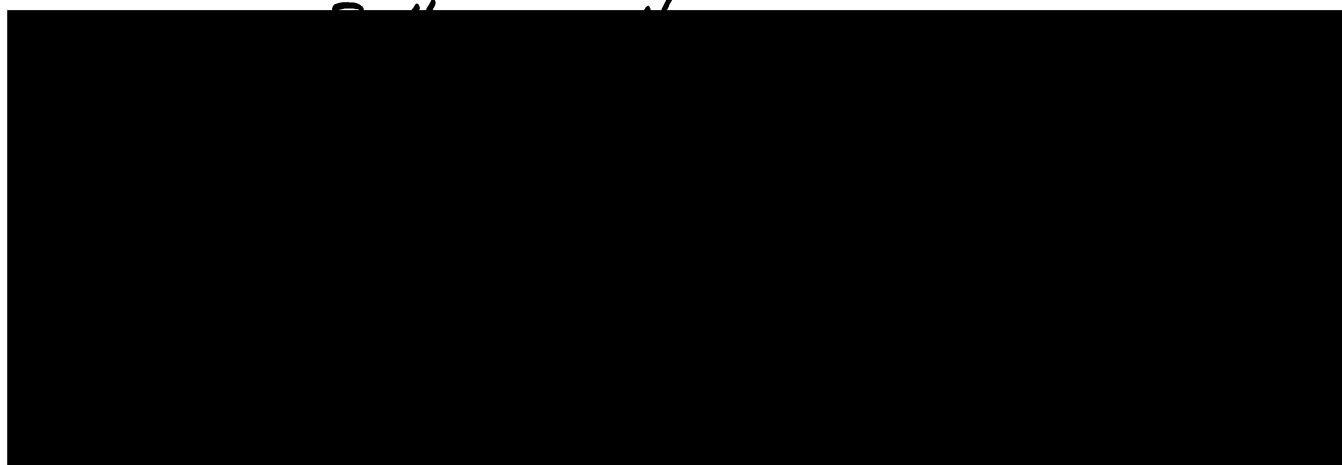
in the

GRADUATE DIVISION

of the

UNIVERSITY OF CALIFORNIA

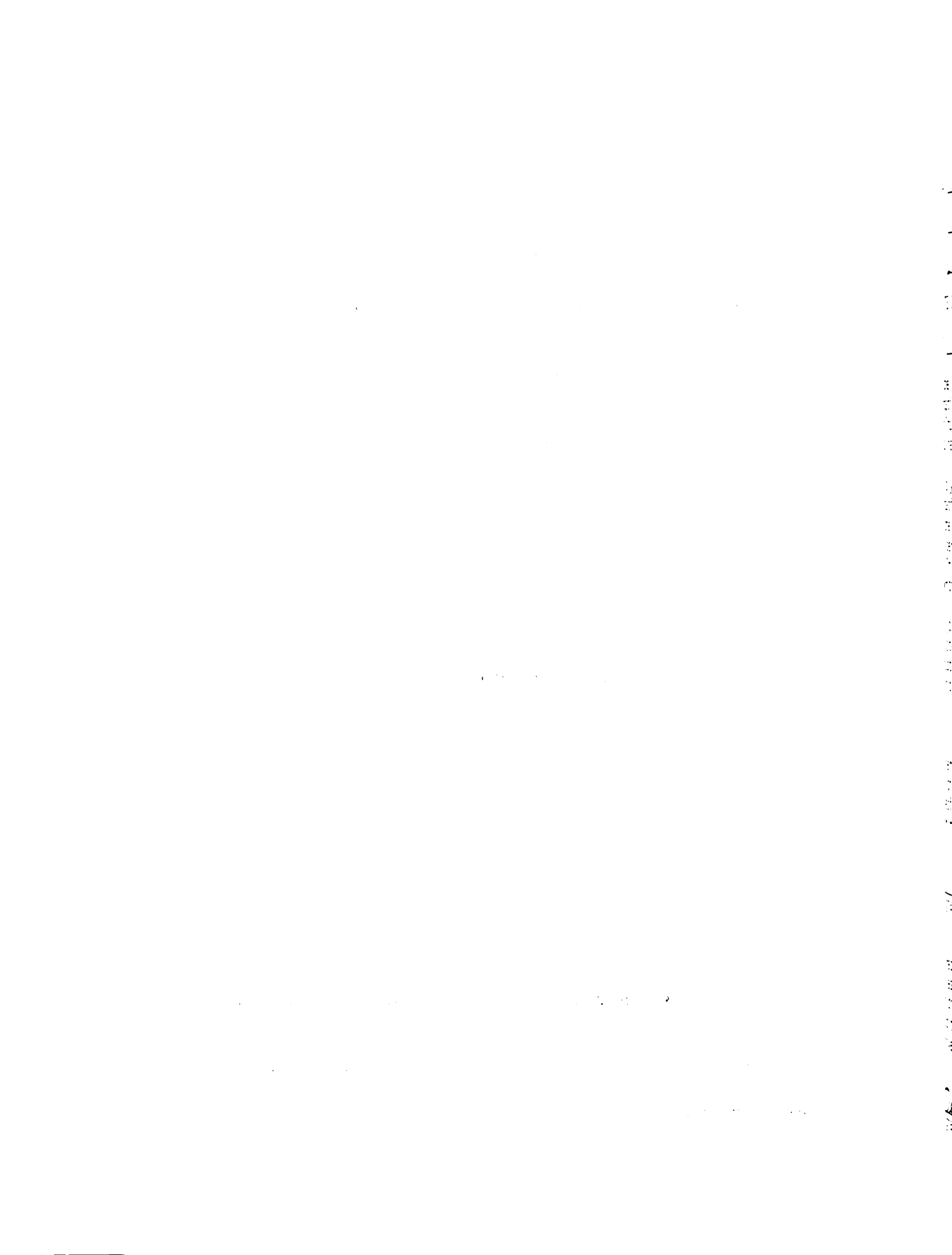
San Francisco



Date

University Librarian

Degree Conferred: . . . SEPTEMBER 7, 1983 . . . . .



To  
Carole and David,  
my family,  
for without their sacrifices, support,  
understanding and love, this achievement  
would not have been possible

## ACKNOWLEDGEMENTS

I am indebted to the following persons for their contributions to my graduate education:

Dr. Betty-ann Hoener, for her guidance and encouragement during the course of my research work.

Dr. Chin-Tzu Peng, for reading my dissertation and his suggestions and loan of glass-ware for radiochemical synthesis.

Dr. John C. Craig, for his suggestions and comments concerning matters of organic synthesis.

Dr. Paul R. Ortiz de Montellano, for reading my dissertation.

In addition, I am grateful for the support received from the National Institution of Health and Patent Funds from the Graduate Division of the University of California, San Francisco.

### ABSTRACT

The 5-nitrofurans are used in clinical and veterinary medicine as antibiotics, in animal feeds as growth promoters, and as pesticides. Like most other 5-nitrofurans, 2,4-diacetylamino-6-(5-nitro-2-furyl)-1,3,5-triazine (I), has been found to be a potent mutagen in the Ames test and carcinogenic in chronic feeding studies with rats. Activated reduced metabolites are thought to be responsible for not only these toxic effects but also the antibiotic activity of this and other 5-nitrofurans.

In order to elucidate the mechanism of the pharmacological and toxicological effects of 5-nitrofurans in general, and the metabolism and interaction of reduced metabolites of (I) with DNA in particular, in vitro anaerobic metabolism studies with (I) were conducted. Since it was necessary to use radiolabeled (I) for metabolism and DNA binding studies, a carbon-14 synthesis of (I) was developed.

Incubations of (I) using the 9000xg rat liver homogenate supernatant, rat liver microsomes, and xanthine oxidase as the source of nitroreductase were conducted. As determined by HPLC separation, two metabolites were formed. The structure of metabolite (M-2) was elucidated using spectroscopic methods and confirmed synthetically to be the corresponding 5-aminofuran. Although not definitive the same spectroscopic methods suggested that the other metabolite (M-1) was the open-chain nitrile. Of the two metabolites isolated, xanthine oxidase produced almost exclusively the 5-aminofuran (M-2) and the 9000xg rat liver homogenate supernatant produced approximately one-third (M-1) and two-thirds

(M-2). With xanthine oxidase (I) disappeared more quickly than (M-2) appeared. Both enzymes produced about equivalent total amounts of identified metabolites corresponding to approximately 50% of all metabolized (I).

Incubations of radiolabeled (I) with added DNA showed that no DNA binding occurred using the 9000xg rat liver homogenate supernatant, possibly because of extensive protein binding. Similar studies using rat liver microsomes and xanthine oxidase indicated a small amount of activated (I) was bound to DNA. A correlation between amount of metabolism and the amount of DNA binding was demonstrated in incubations using different amounts of enzyme and in incubations of different time.

These results support the following conclusions: (1) Anaerobic in vitro metabolism of the highly carcinogenic/mutagenic (I) results in reduction of the 5-nitro group to the corresponding 5-aminofuran similar to what is observed for other 5-nitrofurans, (2) nitroreductase enzymes differ significantly in the metabolites produced, (3) although metabolically activated (I) covalently binds to DNA to only a very small extent, the potency of its carcinogenic/mutagenic activity indicates the qualitative importance of this binding.

TABLE OF CONTENTS

	<u>Page</u>
Acknowledgements.....	i
Abstract.....	ii
Table of Contents.....	iv
List of Tables.....	xiii
List of Figures.....	xv
List of Abbreviations.....	xxiii
CHAPTER ONE. INTRODUCTION AND STATEMENT OF THE PROBLEM.....	1
I. 5-Nitrofurans, History and Uses.....	1
II. Pharmacology and Toxicology.....	3
III. Metabolism.....	7
IV. Mutagenicity and Carcinogenicity of 2,4-Diacetylamino-6-(5-Nitro-2-Furyl)-1,3,5-Triazine.....	11
V. Statement of the Problem.....	12
CHAPTER TWO. PHYSICAL PROPERTIES, STABILITY, AND SYNTHESIS OF 2,4-DIACETYLAMINO-6-(5-NITRO-2-FURYL)-1,3,5-TRI- AZINE.....	15
I. Physical Properties.....	15
A. Melting Range.....	16
B. Ultraviolet Absorption Spectrum.....	16
C. Proton Nuclear Magnetic Resonance Spectrum.....	16
D. Electron Ionization Mass Spectrum.....	16
E. Solubility.....	19
II. Stability Study.....	22
A. Materials and Methods.....	22



	<u>Page</u>
B. Results.....	23
C. Discussion.....	23
III. Synthesis.....	26
A. Synthesis of Biguanide.....	26
1. Materials and Methods.....	26
2. Results.....	28
B. Synthesis of 2,4-Diacetylamino-6-(5-Nitro-2-Furyl)-1,3, 5-Triazine.....	28
1. Materials and Methods.....	28
2. Results.....	30
CHAPTER THREE. RADIOCHEMICAL SYNTHESIS OF 2,4-DIACETYLAMINO-6-(5- NITRO-2-FURYL)-1,3,5-TRIAZINE.....	31
I. Background.....	31
II. Synthesis of 2,4-Diacetylamino-6-(5-Nitro-2-Furyl)-1,3,5- Triazine-(Acetyl-H-3).....	34
A. Materials and Methods.....	34
B. Results.....	36
C. Discussion.....	38
III. Synthesis of 2,4-Diacetylamino-6-(5-Nitro-2-Furyl)-1,3,5- Triazine-(Acetyl-1-C-14).....	38
A. Materials and Methods.....	38
B. Results.....	42
C. Discussion.....	42
IV. Attempted Development of Microsynthesis of 2,4-Diacetyl- amino-6-(5-Nitro-2-Furyl)-1,3,5-Triazine From 5-Nitro- 2-Bromofuran.....	44
A. Background.....	44

	<u>Page</u>
B. Synthesis of 5-Nitro-2-Bromofuran.....	44
1. Materials and Methods.....	44
2. Results.....	46
3. Discussion.....	47
C. Attempt at Lithium Halogen Exchange With 5-Nitro-2-Bromofuran.....	47
1. Background.....	47
2. Materials and Methods.....	47
3. Results.....	48
4. Discussion.....	49
D. Attempt at Grignard Reagent Formation With 5-Nitro-2-Bromofuran.....	49
1. Background.....	49
2. Materials and Methods.....	49
3. Results.....	51
4. Discussion.....	51
E. Attempt At Cyanide Substitution of Bromide on 5-Nitro-2-Bromofuran.....	52
1. Background.....	52
2. Materials and Methods.....	52
3. Results.....	53
4. Discussion.....	53
F. Summary.....	53
V. Development of Microsynthesis of 2,4-Diacetylamino-6-(5-Nitro-2-Furyl)-1,3,5-Triazine From 2-Furyllithium.....	54
A. Background.....	54
B. Development of Maximum Yield in Sufficient Purity of Ethyl 2-Furoate from Barium Carbonate.....	55

	<u>Page</u>
1. Establishment of Complete Ethylation by Diazoethane	55
a. Materials and Methods.....	55
i. Diazoethane Generation.....	55
ii. Ethyl Esterification of 2-Furoic Acid.....	56
iii. HPLC Analysis of Ethyl 2-Furoate.....	56
b. Results.....	57
2. Carboxylation of 2-Furyllithium.....	57
a. Background.....	57
b. Materials and Methods.....	57
i. Preparation of n-Butyllithium in Ether.....	57
ii. Preparation of 2-Furyllithium in Ether.....	58
iii. High Vacuum Microcarboxylation of 2-Furyl- lithium.....	59
iv. Lithium 2-Furoate Extraction, Ethylation, and HPLC Analysis.....	61
c. Results.....	62
3. Purification of Ethyl 2-Furoate for Nitration.....	62
a. Background.....	62
b. Materials and Methods.....	62
i. Silicic Acid Column Chromatography of Ethyl 2-Furoate.....	62
ii. Solvent Removal Techniques on Solutions of Ethyl 2-Furoate in Ethyl Ether and Hexanes/ Ethyl Acetate, 98/2 (V/V).....	64
c. Results.....	66
C. Development of Maximum Yield in Sufficient Purity of Ethyl 5-Nitro-2-Furoate from Ethyl 2-Furoate.....	68
1. Background.....	68

	<u>Page</u>
2. Materials and Methods.....	68
a. Nitration of Ethyl 2-Furoate.....	68
b. HPLC Analysis of Ethyl 5-Nitro-2-Furoate.....	70
c. Purification of Ethyl 5-Nitro-2-Furoate from the Nitration Reaction Mixture for Condensation with Biguanide.....	71
i. Background.....	71
ii. Silicic Acid Column Chromatography.....	71
iii. Liquid/Liquid Ether Extraction.....	73
iv. Fractional Crystallization.....	73
3. Results.....	73
D. Development of Maximum Yield in Sufficient Purity of 2,4-Diacetylamino-6-(5-Nitro-2-Furyl)-1,3,5-Triazine from Ethyl 5-Nitro-2-Furoate.....	76
1. Background.....	76
2. Biguanide Condensation, Acetylation, and Stability Studies.....	77
a. Materials and Methods.....	77
i. Biguanide Condensation with Ethyl 5-Nitro-2- Furoate.....	77
ii. HPLC Analysis of 2,4-Diamino-6-(5-Nitro-2- Furyl)-1,3,5-Triazine and 2,4-Diacetylamino- 6-(5-Nitro-2-Furyl)-1,3,5-Triazine.....	78
iii. Acetylation of 2,4-Diamino-6-(5-Nitro-2-Furyl)- 1,3,5-Triazine.....	78
iv. Stability of 2,4-Diacetylamino-6-(5-Nitro-2- Furyl)-1,3,5-Triazine.....	78
b. Results.....	79
3. Final Purification Studies.....	79

	<u>Page</u>
a. Materials and Methods.....	79
i. Silicic Acid Column Chromatography.....	79
ii. Activated Charcoal Adsorption.....	81
iii. Fractional Crystallization.....	81
b. Results.....	82
E. Microsynthesis of 2,4-Diacetylamino-6-(5-Nitro-2-Furyl)- 1,3,5-Triazine from 0.50 mmole Barium Carbonate.....	85
1. Background.....	85
2. Materials and Methods.....	85
a. Carboxylation of 2-Furyllithium.....	85
b. Acidification and Extraction of 2-Furoic Acid into Ethyl Ether.....	85
c. Ethyl Esterification and Purification of Ethyl 2-Furoate by Silicic Acid Column Chromatography.	86
d. Nitration of Ethyl 2-Furoate and Purification of Ethyl 5-Nitro-2-Furoate.....	88
e. Biguanide Condensation of Ethyl 5-Nitro-2- Furoate.....	88
f. Purification and Acetylation of 2,4-Diamino-6-(5- Nitro-2-Furyl)-1,3,5-Triazine.....	88
3. Results.....	88
F. Summary.....	89
VI. Synthesis of 2,4-Diacetylamino-6-(5-Nitro-2-Furyl)-1,3,5- Triazine-(6-C-14).....	89
A. Materials and Methods.....	89
B. Results.....	91
C. Discussion.....	91

CHAPTER FOUR. ANAEROBIC <u>IN VITRO</u> REDUCTIVE METABOLISM OF 2,4-DIACETYLAMINO-6-(5-NITRO-2-FURYL)-1,3,5-TRIAZINE.....	<u>Page</u>
	93
I. Background.....	93
II. Enzymatic Systems.....	94
A. Preparation of 9000xg Rat Liver Homogenate Supernatant	94
B. Preparation of Rat Liver Microsomes.....	94
C. Xanthine Oxidase.....	95
III. Relative Rates of Metabolism.....	96
A. Materials and Methods.....	96
1. In 9000xg Rat Liver Homogenate Supernatant.....	96
2. In Rat Liver Microsomes.....	97
3. In Xanthine Oxidase.....	98
B. Results.....	99
C. Discussion.....	105
IV. Metabolite Structural Elucidation.....	107
A. Materials and Methods.....	107
1. Preparative Scale Incubations.....	107
2. Metabolite Isolation.....	108
3. Physical Characterization of Metabolites.....	108
a. Ultraviolet Spectra.....	108
b. Electron Ionization Mass Spectra.....	110
c. Fourier Transform Proton Nuclear Magnetic Resonance Spectra.....	110
B. Results.....	110
C. Discussion.....	116
V. Preparation of 2,4-Diacetylamino-6-(5-Amino-2-Furyl)-1,3,5,-Triazine.....	117

	<u>Page</u>
A. Materials and Methods.....	117
B. Results.....	118
VI. Anaerobic <u>In Vitro</u> Metabolism of 2,4-Diacetylamino-6-(5-Nitro-2-Furyl)-1,3,5-Triazine-(Acetyl-H-3) and 2,4-Diacetylamino-6-(5-Nitro-2-Furyl)-1,3,5-Triazine-(Acetyl-1-C-14) in the 9000xg Rat Liver Homogenate Supernatant...	118
A. Background.....	118
B. Materials and Methods.....	119
1. For 2,4-Diacetylamino-6-(5-Nitro-2-Furyl)-1,3,5-Triazine-(Acetyl-H-3).....	119
2. For 2,4-Diacetylamino-6-(5-Nitro-2-Furyl)-1,3,5-Triazine-(Acetyl-1-C-14).....	120
C. Results.....	120
D. Discussion.....	125
VII. Determination of Total Mass Balance of Metabolites in the 9000xg Rat Liver Homogenate Supernatant and Xanthine Oxidase Incubation Systems with Radiolabeled 2,4-Diacetylamino-6-(5-Nitro-2-Furyl)-1,3,5-Triazine-(6-C-14) (I-C-14)	125
A. Materials and Methods.....	126
1. In the 9000xg Rat Liver Homogenate Supernatant.....	126
2. In Xanthine Oxidase.....	128
B. Results.....	129
VIII. Summary.....	142
CHAPTER FIVE. <u>IN VITRO</u> NITROREDUCTASE CATALYZED BINDING OF 2,4-DIACETYLAMINO-6-(5-NITRO-2-FURYL)-1,3,5-TRIAZINE-(6-C-14) TO DNA.....	145
I. Background.....	145
II. Using the 9000xg Rat Liver Homogenate Supernatant.....	146

	<u>Page</u>
A. Materials and Methods.....	146
B. Results.....	147
C. Discussion.....	149
III. Using Rat Liver Microsomes.....	149
A. Materials and Methods.....	149
B. Results.....	152
C. Discussion.....	154
IV. Using Xanthine Oxidase.....	158
A. Materials and Methods.....	158
B. Results.....	159
C. Discussion.....	159
V. Summary.....	163
SUMMARY AND CONCLUSIONS.....	166
REFERENCES.....	172



LIST OF TABLES

		<u>Page</u>
	CHAPTER THREE	
	RADIOCHEMICAL SYNTHESIS OF 2,4-DIACETYLAMINO- 6-(5-NITRO-2-FURYL)-1,3,5-TRIAZINE	
TABLE 3.1	ETHYL 2-FUROATE YIELDS FROM CARBOXYLATION OF 2-FURYL LITHIUM.....	63
TABLE 3.2	SOLVENT REMOVAL FROM SOLUTIONS OF ETHYL 2- FUROATE.....	67
TABLE 3.3	YIELD OF ETHYL 5-NITRO-2-FUROATE FROM 2-FURYL- LITHIUM AND BaCO <sub>3</sub> WITH SILICIC ACID COLUMN CHROMATOGRAPHIC PURIFICATION USING DIFFERENT LENGTHS OF SILICIC ACID COLUMN.....	69
TABLE 3.4	YIELDS OF ETHYL 5-NITRO-2-FUROATE AND 2,4-DI- AMINO-6-(5-NITRO-2-FURYL)-1,3,5-TRIAZINE (II) FROM NITRATION OF ETHYL 2-FUROATE FOLLOWED BY BIGUANIDE CONDENSATION.....	75
TABLE 3.5	DEPENDENCE OF YIELD OF 2,4-DIAMINO-6-(5-NITRO- 2-FURYL)-1,3,5-TRIAZINE (II) ON BIGUANIDE SOURCE, SOLVENT, AND SOLVENT VOLUME.....	80
TABLE 3.6	STABILITY OF 2,4-DIACETYLAMINO-6-(5-NITRO-2- FURYL)-1,3,5-TRIAZINE (I) AS A SUSPENSION IN ACETIC ANHYDRIDE.....	80
TABLE 3.7	PURITY AND YIELD OF (I) FOLLOWING DIFFERENT PURIFICATION TECHNIQUES.....	84

## CHAPTER FOUR

Page

ANAEROBIC IN VITRO REDUCTIVE METABOLISM OF  
2,4-DIACETYLAMINO-6-(5-NITRO-2-FURYL)-1,3,5-TRIAZINE

TABLE 4.1	RESULTS OF MASS BALANCE OF METABOLITES IN THE 9000xg RAT LIVER HOMOGENATE SUPERNATANT AND XANTHINE OXIDASE INCUBATION WITH (I-C-14) STUDIES.....	137
TABLE 4.2	RESULTS OF QUANTITATION OF RADIOACTIVITY ASSOCIATED WITH PROTEIN IN INCUBATION MIXTURES RESULTING FROM METABOLISM.....	141

## CHAPTER FIVE

IN VITRO NITROREDUCTASE CATALYZED BINDING OF  
2,4-DIACETYLAMINO-6-(5-NITRO-2-FURYL)-1,3,5-TRIAZINE-  
(6-C-14) TO DNA

TABLE 5.1	RESULTS OF QUANTITATION OF DNA BOUND RADIOACTIVITY FOLLOWING INCUBATION OF (I-C-14) WITH RAT LIVER MICROSOMES (ENZYME AMOUNT AND INCUBATION TIME DEPENDENCE AND CONTROLS).....	153
TABLE 5.2	RESULTS OF QUANTITATION OF DNA BOUND RADIOACTIVITY FOLLOWING INCUBATION OF (I-C-14) WITH RAT LIVER MICROSOMES.....	155
TABLE 5.3	RESULTS OF QUANTITATION OF DNA BOUND RADIOACTIVITY FOLLOWING INCUBATION OF (I-C-14) WITH XANTHINE OXIDASE.....	160

LIST OF FIGURES

		<u>Page</u>
CHAPTER ONE		
INTRODUCTION AND STATEMENT OF THE PROBLEM		
FIGURE 1.1	POSTULATED METABOLIC PATHWAYS OF THE 5-NITRO GROUP ON 5-NITROFURANS.....	9
FIGURE 1.2	METABOLIC PATHWAYS NOT INVOLVING THE 5-NITRO GROUP ON 5-NITROFURANS.....	10
FIGURE 1.3	DOSE RESPONSE CURVE OF THE MUTAGENICITY OF 2,4-DIACETYLAMINO-6-(5-NITRO-2-FURYL)-1,3,5-TRIAZINE (I). His <sup>+</sup> REVERTANTS OF <u>S. TYPHIMURIUM</u> TA 100 & TA 98 AS A FUNCTION OF mcgms/... plate (FROM REF. 32)	13
CHAPTER TWO		
PHYSICAL PROPERTIES, STABILITY, AND SYNTHESIS OF 2,4-DIACETYLAMINO-6-(5-NITRO-2-FURYL)-1,3,5-TRIAZINE		
FIGURE 2.1	ULTRAVIOLET ABSORPTION SPECTRUM OF 2,4-DIACETYLAMINO-6-(5-NITRO-2-FURYL)-1,3,5-TRIAZINE (I) IN 40% MeOH/H <sub>2</sub> O (V/V) AND THE REFERENCE OF 40% MeOH/H <sub>2</sub> O (V/V).....	17
FIGURE 2.2	PROTON NUCLEAR MAGNETIC RESONANCE SPECTRUM OF 2,4-DIACETYLAMINO-6-(5-NITRO-2-FURYL)-1,3,5-TRIAZINE (I) IN <u>d</u> <sub>6</sub> -DMSO.....	18
FIGURE 2.3	ELECTRON IONIZATION MASS SPECTRUM OF 2,4-DIACETYLAMINO-6-(5-NITRO-2-FURYL)-1,3,5-TRIAZINE (I).....	20

		<u>Page</u>
FIGURE 2.4	POSTULATED STRUCTURES OF IMPORTANT IONS IN THE ELECTRON IONIZATION MASS SPECTRUM OF 2,4-DIACETYLAMINO-6-(5-NITRO-2-FURYL)-1,3,5-TRIAZINE (I).....	21
FIGURE 2.5	PHOTOCHEMICAL STABILITY OF (I), PER CENT OF PEAK HEIGHT OF (I) AT TIME ZERO AS A FUNCTION OF TIME.....	24
FIGURE 2.6	ACETATE STABILITY OF (I), PEAK HEIGHT OF MONO-DESACETYL DEGRADATION PRODUCT OF (I) AS A FUNCTION OF TIME.....	25

### CHAPTER THREE

#### RADIOCHEMICAL SYNTHESIS OF 2,4-DIACETYLAMINO-6-(5-NITRO-2-FURYL)-1,3,5-TRIAZINE

FIGURE 3.1	COMMERCIAL PROCEDURES FOR RADIOLABELING 5-NITROFURANS.....	32
FIGURE 3.2	IMPORTANT CHEMICAL STRUCTURES AND POTENTIAL METABOLITES.....	33
FIGURE 3.3	MICROSCALE REFLUXING APPARATUS.....	35
FIGURE 3.4	HPLC ABSORBANCE/RADIOACTIVITY PROFILE OF PURIFIED 2,4-DIACETYLAMINO-6-(5-NITRO-2-FURYL)-1,3,5-TRIAZINE-(ACETYL-H-3).....	37
FIGURE 3.5	MICROSCALE REFLUXING TUBE (PYREX GLASS).....	39
FIGURE 3.6	HIGH VACUUM MANIFOLD (KONTES, K-925100).....	40

		<u>Page</u>
FIGURE 3.7	BREAKSEAL TUBE CONTAINING ACETIC ANHYDRIDE- 1- <sup>14</sup> C.....	41
FIGURE 3.8	HPLC ABSORBANCE/RADIOACTIVITY PROFILE OF PUR- IFIED 2,4-DIACETYLAMINO-6-(5-NITRO-2-FURYL)- 1,3,5-TRIAZINE-(ACETYL-1- <sup>14</sup> C).....	43
FIGURE 3.9	PATHWAYS FOR C-14 RADIOLABELING OF THE FURAN RING AND THE SUBSEQUENT SCHEME FOR THE TOTAL SYNTHESIS.....	45
FIGURE 3.10	HIGH VACUUM MANIFOLD (KONTES, K-925100) CAR- BOXYLATION OF 2-FURYLLITHIUM.....	60
FIGURE 3.11	SILICIC ACID COLUMN CHROMATOGRAMS OF ETHYL 2- FUROATE.....	65
FIGURE 3.12	SILICIC ACID COLUMN CHROMATOGRAM OF THE SEP- ARATION OF ETHYL 5-NITRO-2-FUROATE FROM THE NEUTRALIZED NITRATION REACTION MIXTURE.....	72
FIGURE 3.13	25 ml MICROFILTRATION FLASK.....	74
FIGURE 3.14	SILICIC ACID COLUMN CHROMATOGRAPHY OF IMPURE 2,4-DIACETYLAMINO-6-(5-NITRO-2-FURYL)-1,3,5- TRIAZINE (I) WITH ACETIC ANHYDRIDE ELUTION...	83
FIGURE 3.15	ETHER LIQUID/LIQUID EXTRACTOR.....	87
FIGURE 3.16	SYNTHETIC SCHEME FOR MICROSYNTHESIS OF 2,4-DI- ACETYLAMINO-6-(5-NITRO-2-FURYL)-1,3,5-TRI- AZINE (I).....	90
FIGURE 3.17	HPLC ABSORBANCE/RADIOACTIVITY PROFILE OF SYN- THESIZED 2,4-DIACETYLAMINO-6-(5-NITRO-2-FURYL)- 1,3,5-TRIAZINE-(6- <sup>14</sup> C).....	92

## CHAPTER FOUR

Page

ANAEROBIC IN VITRO REDUCTIVE METABOLISM OF  
2,4-DIACETYLAMINO-6-(5-NITRO-2-FURYL)-1,3,5-TRIAZINE

FIGURE 4.1	GRADIENT ELUTION 0→40% MeOH/H <sub>2</sub> O (V/V) #10 PROGRAM (WATERS GRADIENT PROGRAMER MODEL 660) HPLC ABSORBANCE PROFILE OF METABOLITES OF (I) AFTER 14 MIN INCUBATION WITH 9000xg RAT LIVER HOMOGENATE SUPERNATANT WITHOUT DNA.....	100
FIGURE 4.2	RELATIVE CHANGE IN CONCENTRATION OF (I) AND (M-2) IN INCUBATIONS WITH 9000xg RAT LIVER HOMOGENATE SUPERNATANT.....	101
FIGURE 4.3	RELATIVE CHANGE IN CONCENTRATION OF (I) AND (M-2) IN INCUBATIONS WITH RAT LIVER MICROSOMES (DEPENDENCE ON AMOUNT OF MICROSOMAL SUSPENSION).....	102
FIGURE 4.4	RELATIVE CHANGE IN CONCENTRATION OF (I) AND (M-2) IN INCUBATIONS WITH RAT LIVER MICROSOMES (DEPENDENCE ON TOTAL AMOUNT OF NADPH ADDED).....	103
FIGURE 4.5	RELATIVE CHANGE IN CONCENTRATION OF (I) AND (M-2) IN INCUBATIONS WITH RAT LIVER MICROSOMES (DEPENDENCE ON PRESENCE OF DNA).....	104
FIGURE 4.6	RELATIVE CHANGE IN CONCENTRATION OF (I) AND (M-2) IN INCUBATIONS WITH XANTHINE OXIDASE...	106
FIGURE 4.7	GRADIENT ELUTION 0→40% MeOH/H <sub>2</sub> O (V/V) #10 PROGRAM (WATERS GRADIENT PROGRAMER MODEL 660) HPLC ABSORBANCE PROFILE FOR ISOLATION OF METABOLITES (M-1) AND (M-2).....	109

		<u>Page</u>
FIGURE 4.8	ULTRAVIOLET ABSORPTION SPECTRA OF FRACTIONS COLLECTED BY HPLC FROM PREPARATIVE METABOLISM OF (I) BY 9000xg RAT LIVER HOMOGENATE SUPERNATANT.....	110A
FIGURE 4.9	DELOCALIZATION OF AMINE FREE ELECTRON PAIR INTO THE CONJUGATED SYSTEM IN 2,4-DIACETYL-AMINO-6-(5-AMINO-2-FURYL)-1,3,5-TRIAZINE; SUSPECTED AS (M-2).....	112
FIGURE 4.10	ELECTRON IONIZATION MASS SPECTRUM OF METABOLITE (M-2) ELUTED BY PREPARATIVE HPLC FROM <u>IN VITRO</u> METABOLISM OF (I) IN 9000xg RAT LIVER HOMOGENATE SUPERNATANT.....	113
FIGURE 4.11	POSTULATED STRUCTURES OF IMPORTANT FRAGMENTATION IONS IN MASS SPECTRA OF METABOLITE (M-2)	114
FIGURE 4.12	FOURIER TRANSFORM PROTON NUCLEAR MAGNETIC RESONANCE SPECTRA OF METABOLITE (M-2) ELUTED OFF PREPARATIVE HPLC FROM <u>IN VITRO</u> METABOLISM OF (I) IN 9000xg RAT LIVER HOMOGENATE SUPERNATANT.....	115
FIGURE 4.13	ISOCRATIC 40% MeOH/H <sub>2</sub> O (V/V) HPLC ABSORBANCE/RADIOACTIVITY PROFILES AFTER INCUBATION OF (I-ACETYL-H-3) WITH 9000xg RAT LIVER HOMOGENATE SUPERNATANT.....	121
FIGURE 4.14	ISOCRATIC 40% MeOH/H <sub>2</sub> O (V/V) HPLC ABSORBANCE/RADIOACTIVITY PROFILES AFTER INCUBATION OF (I-ACETYL-1-C-14) WITH 9000xg RAT LIVER HOMOGENATE SUPERNATANT.....	122- 123

FIGURE 4.15	ISOCRATIC 40% MeOH/H <sub>2</sub> O (V/V) HPLC ABSORBANCE/ RADIOACTIVITY PROFILES OF INCUBATION OF (I- C-14) WITH 9000xg RAT LIVER HOMOGENATE SUPER- NATANT AND XANTHINE OXIDASE.....	Page 130
FIGURE 4.16	ISOCRATIC 7% MeOH/H <sub>2</sub> O (V/V) HPLC ABSORBANCE/ RADIOACTIVITY PROFILES AFTER INCUBATION OF (I-C-14) WITH 9000xg RAT LIVER HOMOGENATE SUPERNATANT AND XANTHINE OXIDASE.....	131
FIGURE 4.17	GRADIENT ELUTION 0→40% MeOH/H <sub>2</sub> O (V/V) #10 PROGRAM (WATERS GRADIENT PROGRAMER MODEL 660) HPLC ABSORBANCE/RADIOACTIVITY PROFILE AFTER INCUBATION OF (I-C-14) WITH 9000xg RAT LIVER HOMOGENATE SUPERNATANT.....	132
FIGURE 4.18	GRADIENT ELUTION 0→40% MeOH/H <sub>2</sub> O (V/V) #10 PROGRAM (WATERS GRADIENT PROGRAMER MODEL 660) HPLC ABSORBANCE/RADIOACTIVITY PROFILE AFTER INCUBATION OF (I-C-14) WITH XANTHINE OXIDASE.	133
FIGURE 4.19	ISOCRATIC 40% MeOH/H <sub>2</sub> O (V/V) HPLC ABSORBANCE/ RADIOACTIVITY PROFILES AFTER CONTROL INCUBA- TIONS OF (I-C-14) IN 50 mM POTASSIUM PHOS- PHATE BUFFER pH 5.8 CONTAINING 2.5 mg HYPO- XANTHINE AND IN 50 mM POTASSIUM PHOSPHATE BUFFER pH 5.8 CONTAINING 3.3 mg BSA AND 2.5 mg HYPOXANTHINE.....	134
FIGURE 4.20	ISOCRATIC 7% MeOH/H <sub>2</sub> O (V/V) ABSORBANCE/RADIO- ACTIVITY PROFILE AFTER CONTROL INCUBATION OF (I-C-14) IN 50 mM POTASSIUM PHOSPHATE BUFFER pH 5.8 CONTAINING 2.5 mg HYPOXANTHINE.....	135



FIGURE 4.21	CREATED HPLC ABSORBANCE/RADIOACTIVITY CHROMATOGRAMS FOR ISOCRATIC 40% AND 7% MeOH/H <sub>2</sub> O (V/V) AFTER INCUBATION WITH XANTHINE OXIDASE OR 9000xg RAT LIVER HOMOGENATE SUPERNATANT...	<u>Page</u> 139-140
-------------	---	------------------------

## CHAPTER FIVE

IN VITRO NITROREDUCTASE CATALYZED BINDING OF  
2,4-DIACETYLAMINO-6-(5-NITRO-2-FURYL)-1,3,5-TRIAZINE-  
(6-C-14) TO DNA

FIGURE 5.1	ABSORBANCE/RADIOACTIVITY HYDROXYAPATITE COLUMN CHROMATOGRAMS OF TRIALS OF INCUBATION OF (I-C-14) WITH 9000xg RAT LIVER HOMOGENATE SUPERNATANT AND ADDED DNA.....	148
FIGURE 5.2	ULTRAVIOLET SPECTRAL SCANS OF DNA ISOLATED FROM A CONTROL INCUBATION OF (I-C-14) WITH RAT LIVER MICROSOMES BY THE PROTEIN PHENOLIC EXTRACTION/PRECIPITATION SEPARATION TECHNIQUE (FOR COMPARISON PURPOSES THE ULTRAVIOLET SPECTRA OF A BIS-TRIS/EDTA BUFFER SOLUTION OF COMMERCIAL DNA IS ALSO PRESENTED).....	156
FIGURE 5.3	PEAK HEIGHT, (I) AND AMINO METABOLITE (M-2), AND NUMBER OF ADDUCTS PER ONE-MILLION NUCLEOTIDE RESIDUES AS A FUNCTION OF INCUBATION TIME FOR INCUBATION OF (I) OR (I-C-14) WITH XANTHINE OXIDASE.....	161
FIGURE 5.4	PEAK HEIGHT, (I) AND AMINO METABOLITE (M-2), AND NUMBER OF ADDUCTS PER ONE-MILLION NUCLEOTIDE RESIDUES AS A FUNCTION OF AMOUNT OF XANTHINE OXIDASE ADDED TO THE INCUBATION AFTER 2.0 min INCUBATION TIME.....	162

	SUMMARY AND CONCLUSIONS	<u>Page</u>
FIGURE S/C-1	MECHANISTIC SCHEME FOR NUCLEOPHILIC BIOMACRO- MOLECULE ATTACK ON ACTIVATED ELECTROPHILIC INTERMEDIATE FROM HYDROXYLAMINOFURAN.....	171

LIST OF ABBREVIATIONS

AAF	2-acetylaminofluorene
Ac	acetyl
Aq	aqueous
AR	analytical reagent
BSA	bovine serum albumin
C	centigrade
cm	centimeter
<u>d</u> or D	deuterium
d	density
dia	diameter
DNA	deoxyribonucleic acid
DMF	dimethyl formamide
DMSO	dimethyl sulfoxide
DPM	disintegrations per minute
EDTA	ethylene diamine tetra-acetic acid
Et	ethyl
Et <sub>2</sub> O	ethyl ether
EtOAc	ethyl acetate
EtOH	ethyl alcohol
eV	electron volt
g	gravity
gm	gram
His	histidine
HPLC	high pressure liquid chromatography
hr	hour

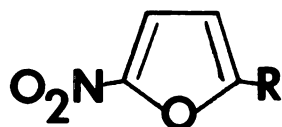
Hz	cycles per second
J	coupling constant
kg	kilogram
lb	pound
<u>M</u>	moles per liter
mCi	millicurie
m/e	mass to charge ratio
MeOH	methyl alcohol
mcgm	microgram
mg	milligram
min	minute
ml	milliliter
mm	millimeter
<u>mM</u>	millimoles per liter
<u>N</u>	gram equivalents per liter
NADH	reduced nicotinamide adenine dinucleotide
NADPH	reduced nicotinamide adenine dinucleotide phosphate
nm	nanometer
NMR	nuclear magnetic resonance
OD	optical density
RPM	revolutions per minute
TMS	trimethyl silane
t-RNA	transfer ribonucleic acid
u	micron
U	units xanthine oxidase; One unit will convert 1.0 umole of xanthine to uric per minute at pH 7.5 at 25 <sup>o</sup> C
uCi	microcurie

ul	microliter
UV	ultraviolet
V	volume
W	weight
xg	times gravity
$\lambda_{\max}$	maximum absorption frequency

## CHAPTER ONE

INTRODUCTION AND STATEMENT OF THE PROBLEMI. 5-Nitrofurans, History and Uses

The 5-nitrofurans, which do not occur naturally, consist of a furan ring nucleus substituted in the 5-position with a nitro group and in the 2-position with a variety of functional groups. Scheele first discovered



the furans in 1780 when furoic acid was obtained in the dry distillation of mucic acid. The next furan compound was discovered in 1832 by Dober-einer when furfural was accidentally formed from an attempted preparation of formic acid from sugar and manganese dioxide. Nearly one-hundred years elapsed before the first 5-nitrofuran was successfully prepared in 1930 by Gilman and Wright (1) when they synthesized 5-nitro-2-furaldehyde by nitration of 2-furaldehyde diacetate. In 1939 an organized effort was initiated by Eaton Laboratories to develop new 5-nitrofurans for use as medicinal agents (2). This program led to the discovery in 1944, by Dodd and Stillman (3), of nitrofurazone when they made the important observa-tion that a nitro group in the 5-position of 2-substituted furans confer-red antibacterial activity on these compounds (4). Concurrently, inves-tigators in Germany (5) were also studying the bacteriostatic effects of 5-nitrofurans and nitrothiophenes, but did not report their observations

until 1947. These early efforts stimulated attempts in many countries to find additional 5-nitrofurans with medicinal properties and ultimately resulted in the synthesis of several thousand 5-nitrofuran analogues, some of which have been used commercially.

Today, 5-nitrofurans are used clinically as antibiotics (6). The most widely used topical 5-nitrofuran for human use is nitrofurazone. It is used as an antibacterial/antifungal agent for the treatment for prevention of a variety of infections involving the skin, eyes, ears, and nose (7). The only 5-nitrofuran still used for systemic treatment of infections in humans in the United States is nitrofurantoin (4). It is used almost exclusively for urinary tract infections. Other 5-nitrofurans were used systemically, until quite recently, for similar purposes until reports of their oncogenicity were presented (2). Recently, 5-nitrofurans have been investigated for use as radiosensitizers to enhance the efficacy of radiotherapy in solid tumors (8,9). However, at the doses required side effects limit their usefulness.

Veterinary uses of 5-nitrofurans include topical application to surface infections and wounds as well as systemic medicinal uses for the treatment of various genitourinary tract and other specific bacterial infections (6). In addition to antibacterial properties, certain 5-nitrofurans have been shown to exhibit antifungal, antischistosomal, and anti-protozoan properties. Because of this broad spectrum of activity, 5-nitrofurans can keep animals disease-free and are used extensively in animal feeds as growth promoters (10).

The use of 5-nitrofurans as food preservatives began in Japan in 1950 with the approval of nitrofurazone for use in various meats and fish at concentrations of 5 mg/kg and up to 20 mg/kg in some fish and shellfish (11).

Other 5-nitrofurans, that were more effective as food preservatives, replaced nitrofurazone and were used at levels up to 250 mg/kg (12) until 1974. In 1974 the use of 5-nitrofurans was withdrawn in Japan when furylfuramide was demonstrated to be mutagenic and carcinogenic (13).

Other 5-nitrofurans are used as pesticides (13). In Czechoslovakia one is used as a wine stabilizer (14). With these many varied uses of 5-nitrofurans it is probable that they represent the largest group of nitro-compounds in use (7). Because of this exposure and the recent demonstration of the strong mutagenic and carcinogenic activity of many 5-nitrofurans, concern has developed over their use and their risk/benefit ratio is being reevaluated (15).

## II. Pharmacology and Toxicology

Although the broad spectrum of antibacterial, antifungal, and anti-protozoal activity of 5-nitrofurans has been studied for almost 40 years the mechanism of action has been poorly understood. Recently, Herrlich and Schweiger suggested a mechanism of action for nitrofurantoin. They reported that the bacteriostatic effect of nitrofurantoin was mediated through the inhibition of the inducible enzyme synthesis essential for the use of carbon sources (16) and the bacteriocidal activity results from its ability to damage bacterial DNA (16,17). The use of 5-nitrofurans as radiosensitizers has led to much speculation as to their mode of action. While 5-nitrofurans are known to be more cytotoxic under the hypoxic conditions found in tumor cells (18), their mode of action as radiosensitizers is not simply the sum effect of the damage due to ionizing radiation and hypoxic cell toxicity of the 5-nitrofuran. It is thought that radiosensitizers act by combining with short-lived radical species produced by ionizing



radiation in the target tumor molecules. This synergistic combination "fixes" the radiation damage and prevents its repair (19).

In the United States, nitrofurantoin is the only 5-nitrofurans currently administered systemically to patients. Its more serious toxic effects include pulmonary toxicity, peripheral polyneuropathies and hepatotoxicity. The lung toxicity, ranges from acute reactions to chronic lung disease. It is usually reversible but fatal reactions have been reported (20). The pulmonary toxicity was originally thought to represent various forms of a hypersensitivity reaction. More recently studies suggest that nitrofurans, like paraquat, may act by enhancing lipid peroxidation in the lung (21). A mechanism of action of this toxicity has been suggested by Mason and Holtzman (22) and Sesame and Boyd (23). They have demonstrated that under the aerobic conditions in the lung, the cyclic reduction/oxidation of nitrofurans could generate large amounts of superoxide responsible for the lung damage.

The peripheral polyneuropathy seen with nitrofurantoin therapy is very rare. It usually occurs within the first 45 days of administration and usually is reversible. Because patients who develop this toxicity frequently show renal function impairment, it has been suggested that accumulated metabolites are responsible. However, it has been reported in patients with normal renal function at recommended dosage levels (24). Polyneuropathies, following systemic administration of other 5-nitrofurans, are much more prevalent. Nitrofurazone, produces severe peripheral polyneuropathy at doses required for effective therapy (25). The clinical use of 5-nitrofurans as radiosensitizers has been limited by the frequencies of polyneuropathies encountered following the necessary dose (26). The hepatotoxicities observed following systemic nitrofurantoin

therapy include chronic active hepatitis and severe hepatic necrosis, and occur following long term therapy (27,28). The mechanism of action is still unknown, but, metabolism of the nitrofurantoin to reactive intermediates has been suggested to be a cause of the damage.

First reports of 5-nitrofurans possessing effects now recognized as associated with genotoxicity came from Szybalski and Nelson in 1954 when they reported evidence that nitrofurazone could interact with DNA (29). This was followed in 1958 when Szybalski reported bacterial reversion from streptomycin dependence to streptomycin independence following exposure to several 5-nitrofurans (30). Then, in 1966 the first report of animal oncogenicity was reported by Stein et al. (31). These early studies were followed by an increasing number of reports showing a large number of 5-nitrofurans to be mutagenic in bacterial, eukaryotic and mammalian systems (13, 32, 33) as well as carcinogenic in animals (32, 34).

Attempts to elucidate the mechanism of these oncogenetic effects have focused on their interaction with DNA. 5-Nitrofurans have been shown to bind to bacterial and mammalian DNA (9, 35), inhibit DNA synthesis (36), prevent bacterial transformation (36), induce chromosomal aberrations in rats (37), and cause single-strand breaks in DNA (38). Mutations produced in bacterial tester strains are of the single-base substitution type as well as the frameshift type (39).

Studies of the interaction of 5-nitrofurans with DNA have strongly suggested that the reactive intermediates from reductive metabolism are responsible for their toxic and oncogenic effects. McCalla et al. (40) have shown that carcinogenic 5-nitrofurans when incubated with E. coli B/r produce single-strand breaks in DNA. However, when incubated with E. coli nfr-207, a mutant lacking nitroreductase, no DNA breaks were

detected. Olive and McCalla (38) showed that nitrofurazone was metabolized in mouse liver homogenates at the maximum rate under hypoxic conditions. They also showed that under hypoxic conditions single-strand breaks were produced in DNA in mammalian cells in vivo. The toxicity and rate of metabolism of nitrofurazone to cultured mouse L cells and Chinese hamster ovary cells has been shown to increase as the oxygen content of the incubation mixture is lowered (41).

Specific studies defining the quantitative aspects of DNA binding are limited. Using C-14-nitrofurazone and C-14-furfylfuramide, Tatsume et al. have detected radiolabel covalently bound to liver and kidney DNA of rats fed these 5-nitrofurans (42). With C-14 radiolabeled 2-(2-furyl)-3-(5-nitro-2-furyl)-acrylamide (AF-2), enzymatically activated metabolites were bound to DNA (43). The nature of the bound adducts of 5-nitrofurans have not been reported, probably because of the difficulty inherent in performing these studies.

Structure activity relationships of 5-nitrofurans have shown that the 5-nitro group is an absolute, but not sufficient, requirement for mutagenicity and carcinogenicity (33, 44). In addition it has been suggested that the wide-ranging physical/chemical properties, resulting from substitution at the 2-position, are responsible for the variety of target tissues of carcinogenicity (26).

The evidence presented above indicates that activated reduced metabolites of 5-nitrofurans are responsible for their pharmacological and toxicological activity. More specifically, their antibacterial, mutagenic, and carcinogenic effects have been shown to be correlated with the ability of their reduced metabolites to covalently bind to DNA.

### III. Metabolism

The metabolism of 5-nitrofurans has been studied in both bacterial and mammalian systems. Because of the importance of biotransformation of the nitro-group, metabolism is divided into those pathways involving the nitro-group and those pathways not involving the nitro-group. As discussed above the reductive metabolism of the nitro-group has been implicated in the pharmacological and toxicological activity, and therefore, has been the subject of much study. In this pathway the nitro-group has been shown to be reduced to the corresponding 5-aminofuran (45, 46) which may undergo furan ring cleavage to form an open-chain nitrile (47, 48) or be acetylated (48). During the process of this reduction the radical nitro anion, nitroso, hydroxylamine radical, and hydroxylamine have been suggested to be transient intermediates (49). The inherent reactivity of one or all of these intermediates is thought to be responsible for their pharmacological effects. The hydroxylamine is especially suspect because of the demonstrated carcinogenic activity of N-hydroxylamine metabolites of aromatic amines (50). The formation of the nitro anion free radical in aerobic conditions is thought to lead to the production of superoxide, which in the presence of superoxide dismutase could form hydrogen peroxide. These toxic agents have been proposed to be responsible for the lung toxicities observed with 5-nitrofurans (51).

Upon metabolic reduction of some 5-nitrofurans, evidence of formation of the 5-aminofuran was not observed and the open-chain nitrile was obtained immediately. Initially, Beckett and Robinson (52) attributed this to the extreme lability of the 5-aminofuran. However, when Gavin et al. (53) observed that E. coli metabolized 1-((5-nitrofurfurylidene)-

amino)-2-imidazolidinone similarly to the open-chain nitrile but the synthetically prepared 5-aminofuran analogue was not metabolized to the open-chain nitrile, he proposed an alternate metabolic scheme in which the amine was not an intermediate precursor in the formation of the open-chain nitrile. His proposal was that reduction occurs to the hydroxylamine which undergoes tautomerization to yield the cis- and trans- oximes. The cis-oxime could be reduced to the amine but the trans- could open directly to the nitrile without going through the amine.

Other biotransformations involving the nitro-group include metabolism of the 5-nitrofuran to the 5-methylthiofuran (54) and production of a pyrrole derivative (45). The pyrrole derivative has been postulated to form from furan ring cleavage following nitroreduction and then re-cyclization. All the known pathways of nitro-group metabolism are depicted in Figure 1.1.

Biotransformations not involving the nitro-group include hydroxylation of the furan ring at the 4-position (55), 2-substituent oxidation (56) and modification (47) (hydrolysis, conjugation), and acid hydrolysis of the azomethine bond in those 5-nitrofurans which contain this structure (48). Hydroxylation at the 4-position results in tautomeric mixtures of the hydroxyl and corresponding aci-nitro forms. Hydrolysis of the azomethine bond results in 5-nitro-2-furaldehyde which undergoes further oxidation to 5-nitro-2-furoic acid. These pathways are all depicted in Figure 1.2.

Nitroreductase enzymes in bacterial systems have been shown to be made up of at least two separate types (57). One type is oxygen independent, utilizes NADH or NADPH, and is absent in 5-nitrofuran resistant

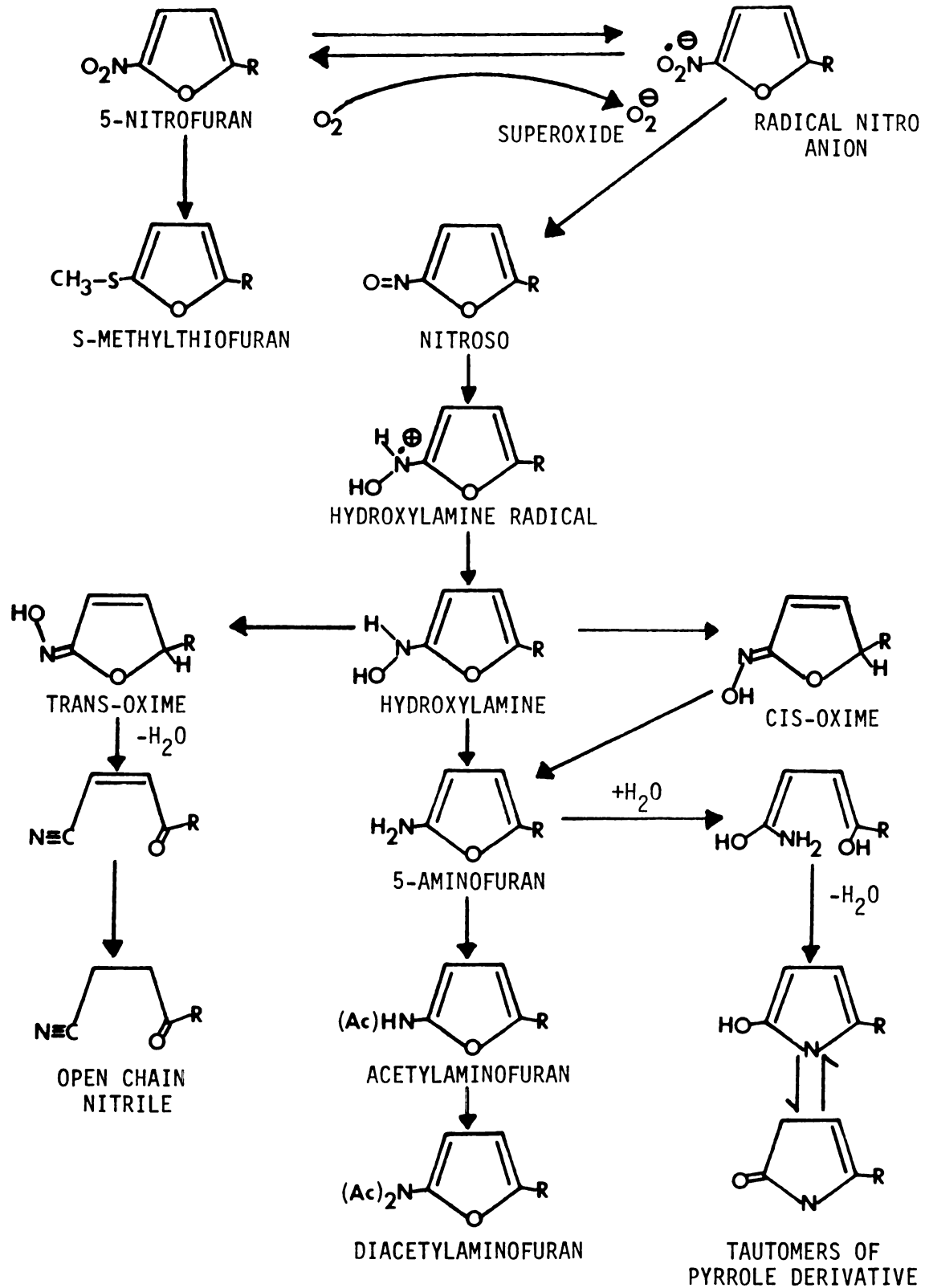


FIGURE 1.1

POSTULATED METABOLIC PATHWAYS OF THE 5-NITRO GROUP ON 5-NITROFURANS

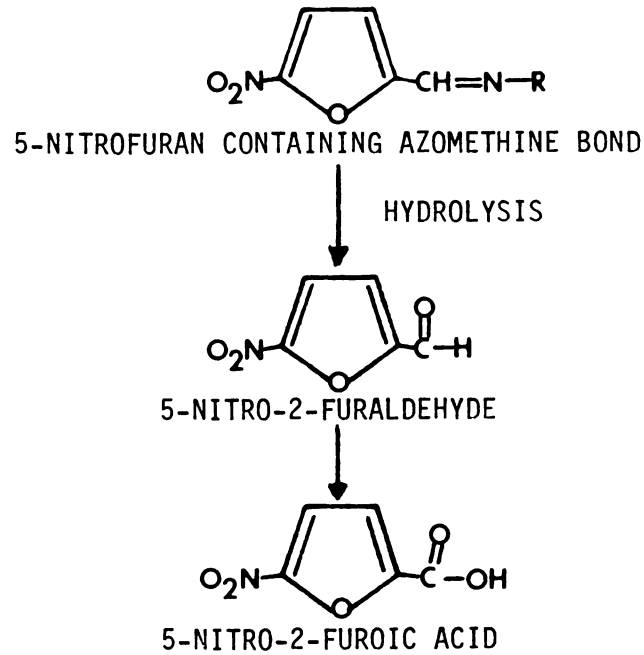
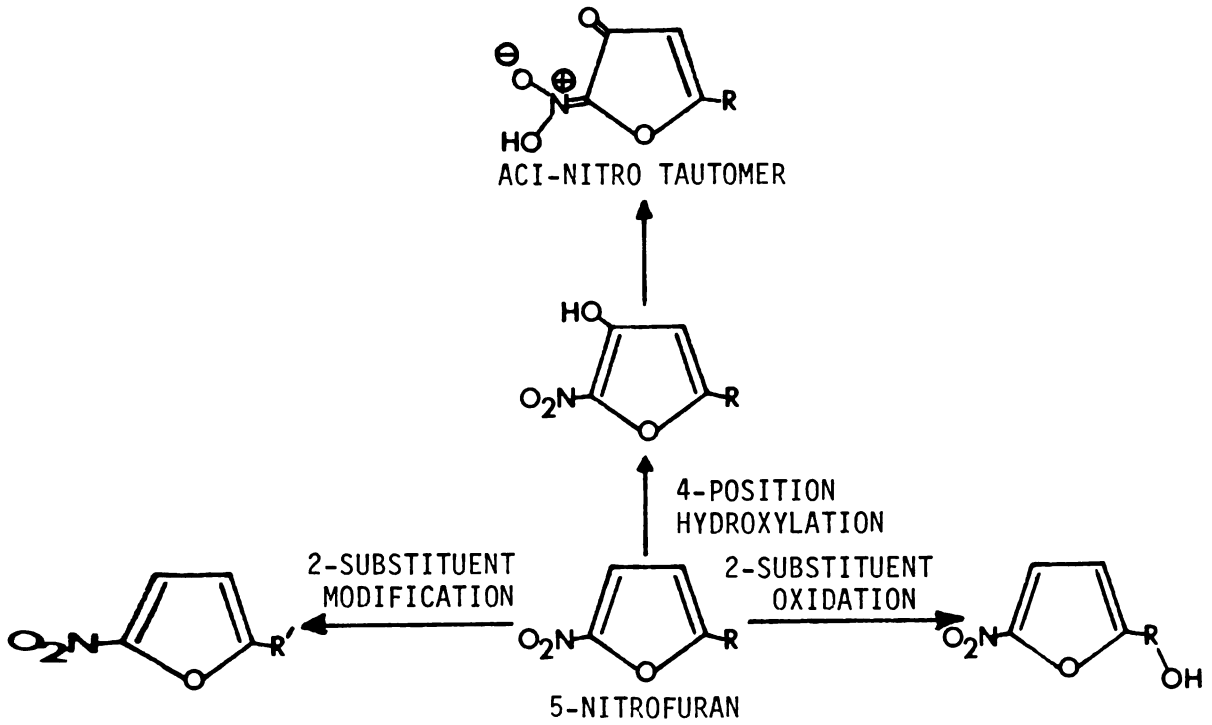


FIGURE 1.2

**METABOLIC PATHWAYS NOT INVOLVING THE 5-NITRO GROUP ON 5-NITROFURANS**

mutants (58). The end product of nitroreduction for this reductase is thought to be the open-chain nitrile derivative. The second type is inhibited by oxygen and has been shown to produce metabolites that break DNA in vitro and that are cytotoxic and mutagenic (33, 40).

Nitroreductase enzymes in mammalian tissues are found in the cytosol and microsomal fractions (59). The cytosol reductase has been shown to be dependent of NADH or hypoxanthine, and inhibited by oxygen and allopurinol (60). Therefore, this reductase activity is attributed, at least partially, to xanthine oxidase. Microsomal reductase activity has been shown to be NADPH dependent, inhibited by oxygen, and insensitive to inhibition by allopurinol (61). This activity is attributed to NADPH-cytochrome C reductase. A minor contribution to nitroreductase activity which is carbon monoxide sensitive in the microsomal fraction has also been attributed to cytochrome P-450 (62).

Other enzymes that have been shown to possess nitroreductase activity in mammalian tissues are aldehyde oxidase, cytosol DT diaphorase, and lipoyl dehydrogenase (61, 63). However, the majority of nitroreduction activity is primarily NADPH-cytochrome C reductase mediated. An assessment of the relative roles the major and minor reductase enzymes contribute in the production of biologically active metabolites and resulting toxicities has not been made.

#### IV. Mutagenicity and Carcinogenicity of 2,4-Diacetylamino-6-(5-Nitro-2-Furyl)-1,3,5-Triazine

The mutagenicity of 2,4-diacetylamino-6-(5-nitro-2-furyl)-1,3,5-triazine (I) has been tested in Salmonella typhimurium tester strains TA 100 and TA 98 (32). These tester strains were developed by Ames



et al. (64) from the standard tester strains TA 1535 and TA 1538 by the incorporation of an R-factor plasmid, pKM101, and are reported to be sensitive indicators of 5-nitrofurantoin mutagenic activity. The dose-response curve (His<sup>+</sup> revertant colonies/plate as a function of mcgms (I) applied to the plate) is presented in Figure 1.3 (32). Low doses are seen to result in a linear dose-response curve, followed by almost complete killing with no reversions. Relative mutagenic potency can be assessed by comparison of number of revertant colonies per plate at low doses for (I), nitrofurantoin, and nitrofurazone, also included in the study. From this (I) is 1.4 and 2.1 times more potent than nitrofurantoin and nitrofurazone respectively.

The carcinogenic activity of (I) was tested in a chronic feeding study in rats at 0.2% (W/W) of the diet for 46 weeks (34). The results showed (I) to be strongly carcinogenic. After 10 weeks on the diet 26 of 33 rats had tumors. Breast tumor incidence was the highest and pathologically consisted of mostly adenocarcinomas and a few fibroadenomas. Other tumors that were observed included intestinal adenocarcinoma and uterine sarcoma.

#### V. Statement of the Problem

Many questions concerning the pharmacological and toxicological effects of 5-nitrofurans and their relationship to nitroreductase metabolism are unanswered. These include the identity of transient intermediates that current evidence suggests play an important part in these effects. Also, an understanding of the mechanisms of metabolic activation and interaction with critically important biomacromolecules is necessary. Finally, no reasons have been discovered to account for the

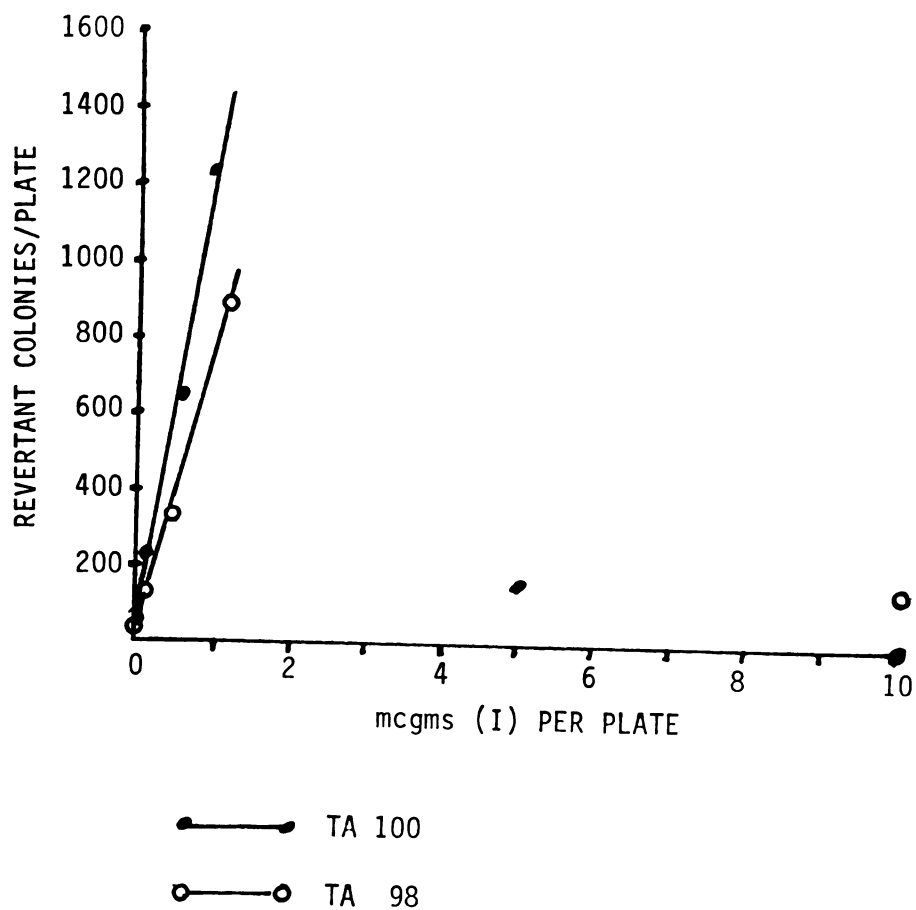


FIGURE 1.3

DOSE RESPONSE CURVE OF THE MUTAGENICITY OF  
2,4-DIACETYLAMINO-6-(5-NITRO-2-FURYL)-1,3,5-TRIAZINE (I).  
His<sup>+</sup> REVERTANTS OF *S. TYPHIMURIUM* TA 100 & TA 98 AS A  
FUNCTION OF mcgms/plate (FROM REF. 32)

differing abilities, both qualitative and quantitative, of the many 5-nitrofurans to elicit their pharmacological and toxicological effects.

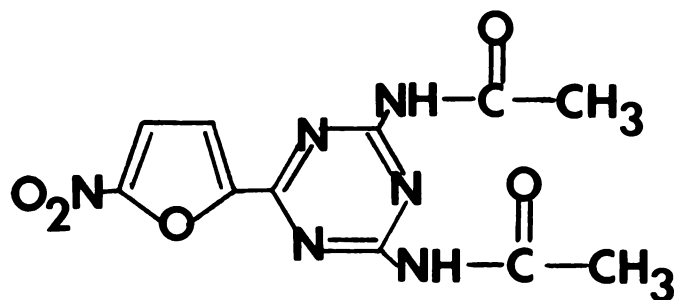
In order to begin answering some of these questions, studies with the highly carcinogenic/mutagenic 5-nitrofurans, 2,4-diacetylamino-6-(5-nitro-2-furyl)-1,3,5-triazine (I) were undertaken. Specifically, the anaerobic in vitro reductive metabolism of (I) was studied with the goals of identifying the metabolites and determining the amounts of each metabolite produced. The nitroreductase catalyzed binding of (I) to DNA was also studied. Studies were conducted using the 9000xg rat liver homogenate supernatant, rat liver microsomes, and xanthine oxidase as the source of nitroreductase. To determine conditions under which DNA binding studies could be conducted, it was necessary to study the relative metabolic rate dependence on the amount of enzyme and cofactors. Finally, because radiolabeled (I) was required in order to conduct the DNA binding studies and determine amounts of metabolites produced, it was necessary to develop a radiochemical synthesis of (I).

## CHAPTER TWO

PHYSICAL PROPERTIES, STABILITY, AND SYNTHESIS OF  
2,4-DIACETYLAMINO-6-(5-NITRO-2-FURYL)-1,3,5-TRIAZINE

I. Physical Properties

2,4-Diacetylamino-6-(5-nitro-2-furyl)-1,3,5-triazine (I) is an anti-bacterial agent first synthesized by Abbott Laboratories, North Chicago, Illinois. It was designated as A-14150 but never marketed as a therapeutic agent. Later it was found to be mutagenic and carcinogenic. It may also be found in the literature as 2,4-diacetamido-6-(5-nitro-2-furyl)-s-triazine, N,N'-(6-amino-1,3,5-triazine-2,4-diyl) bisacetamide, or (N,N')-(6-(5-nitro-2-furyl)-s-triazine-2,4-diyl) bisacetamide. Its chemical abstracts registry number is (3351-49-3).



(I)

The molecular formula for (I) is  $C_{11}H_{10}O_5N_6$  and its molecular weight is 306.24. The dry solid material is odorless and appears as very small tan-colored crystals.

#### A. Melting Range

Pure (I) has a melting point of 269-270°C after which decomposition is observed (65).

#### B. Ultraviolet Absorption Spectrum

The ultraviolet absorption spectrum of a 3.5 mcgms/ml solution of (I) in 40% MeOH/H<sub>2</sub>O (V/V) is given in Figure 2.1. The spectrum was recorded on a Cary model 118 (Varian Instruments Division, Cary Products, Palo Alto, California) double-beam spectrophotometer using 40% MeOH/H<sub>2</sub>O (V/V) as the reference. Two absorption maxima ( $\lambda_{\max}$ ) were observed at 231 nm and 324 nm.

#### C. Proton Nuclear Magnetic Resonance Spectrum

Because of the low solubility of (I), it was necessary to obtain the proton nuclear magnetic resonance spectrum with a Varian XL-100 Fourier transform NMR spectrometer equipped with a Nicolet Instrument Corporation model TT-100 accessory. The spectrum was obtained in d<sub>6</sub>-DMSO (99.5 atom % D, gold label, Aldrich Chemical Company, Milwaukee, Wisconsin). One-hundred pulses (pulse width 5 mcsec, acquisition time 3.4 sec, acquisition delay 400 mcsec) were used for the Fourier transform. The spectrum along with the proton assignments and coupling constants are presented in Figure 2.2.

#### D. Electron Ionization Mass Spectrum

Approximately 50-100 mcgms (I) was used to obtain the electron ionization mass spectrum by direct probe insertion. The spectra was taken on an Associated Electrical Industries model MS 12 mass spectro-

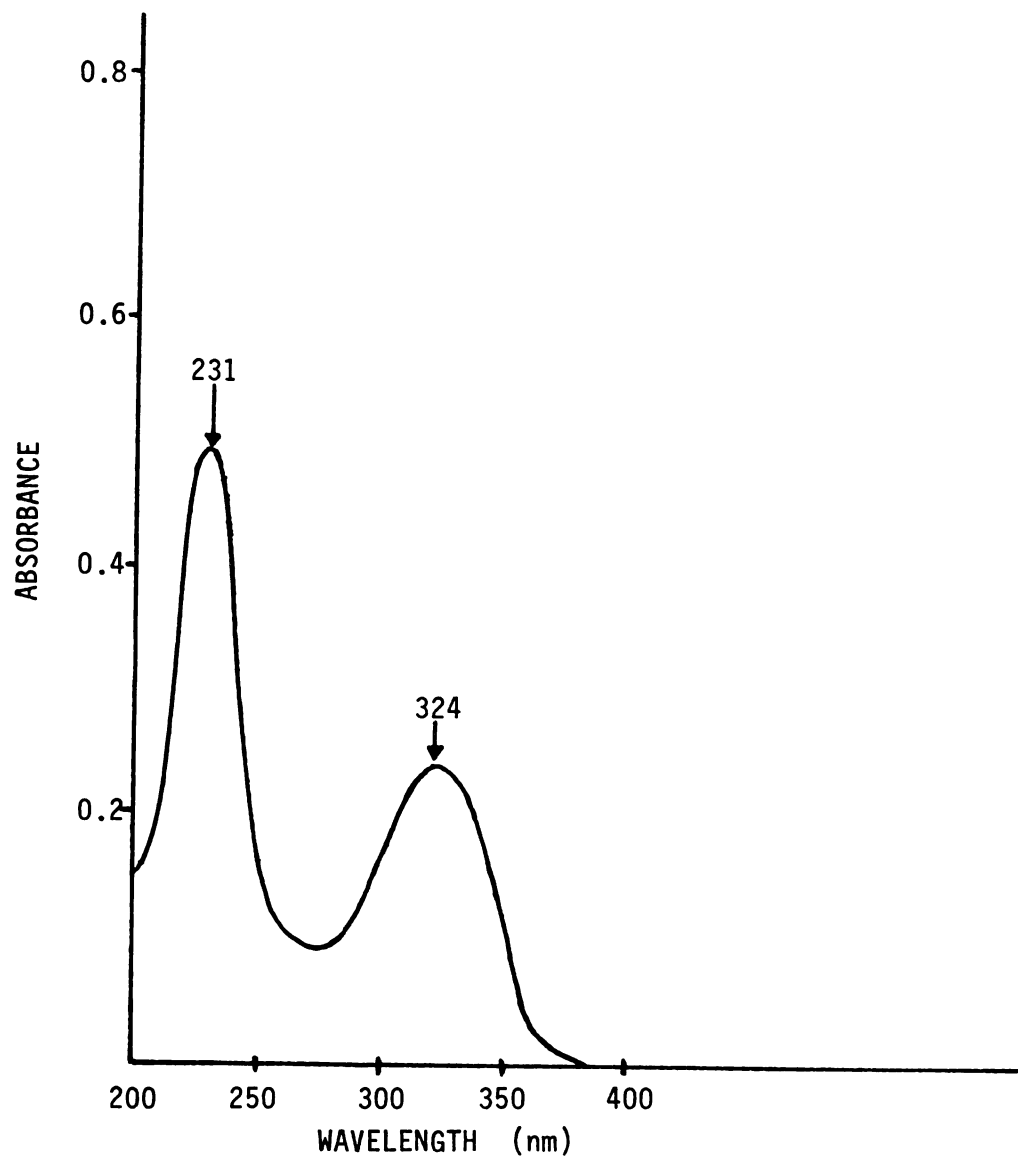


FIGURE 2.1

ULTRAVIOLET ABSORPTION SPECTRUM OF  
2,4-DIACETYLAMINO-6-(5-NITRO-2-FURYL)-1,3,5-TRIAZINE (I) IN  
40% MeOH/H<sub>2</sub>O (V/V) AND THE REFERENCE OF 40% MeOH/H<sub>2</sub>O (V/V)

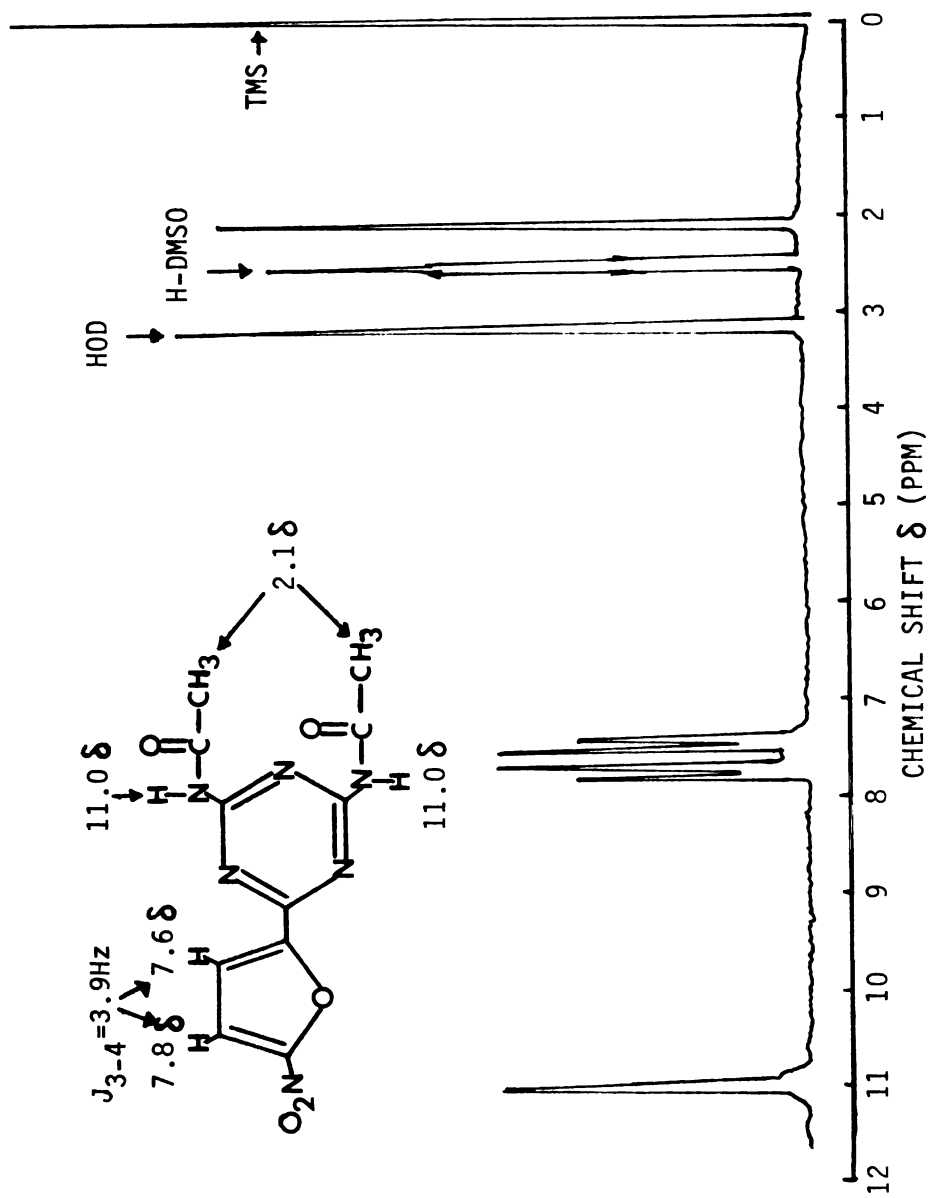


FIGURE 2.2

PROTON NUCLEAR MAGNETIC RESONANCE SPECTRUM OF  
 2,4-DIACETYLAMINO-6-(5-NITRO-2-FURYL)-1,3,5-TRIAZINE (I)  
 IN  $d_6$ -DMSO

meter. Sample probe temperatures ranged from 20 to 300°C and the voltage of the ionizing electron beam maintained at 70 eV.

The electron ionization mass spectrum of (I) is shown in Figure 2.3. The molecular ion at  $m/e$  306, the nominal molecular weight of this structure, is clearly observed. The fragmentation pattern giving ions of high relative abundance at  $(M-46)^+$ ,  $m/e$  260, and  $(M-84)^+$ ,  $m/e$  222, is the result of the expected loss of the neutral  $\text{NO}_2$  radical and the two acetyl groups from the parent compound respectively. Apparently the acetyl groups are so labile that upon heating the sample for volatilization into the ionizing electron beam, considerable deacetylation occurs before electron impact ionization takes place resulting in the ion at  $m/e$  222. Finally the base peak (relative abundance 100) at  $m/e$  43 is taken as the result of extensive homolytic cleavage of the bond between nitrogen and the carboxyl group of the amide functionality producing the  $(\text{CH}_3\text{-C}\equiv\text{O})^+$  ion. The postulated structures of these ions are all presented in Figure 2.4.

#### E. Solubility

The solubility of (I) in aliphatic and aromatic hydrocarbons (ie. hexane and benzene) was found to be very low. The best of those solvents tested appeared to be DMSO. Solubility values are not found in the literature. It was found that solutions of (I) could be made by first dissolving the compound in a small amount of DMSO and then slowly diluting with the solvent of choice. In this manner solutions of (I) in water, methanol, or ethanol were prepared at concentrations up to 60 mcgms/ml with as little as 5% (V/V) DMSO in the final solution.



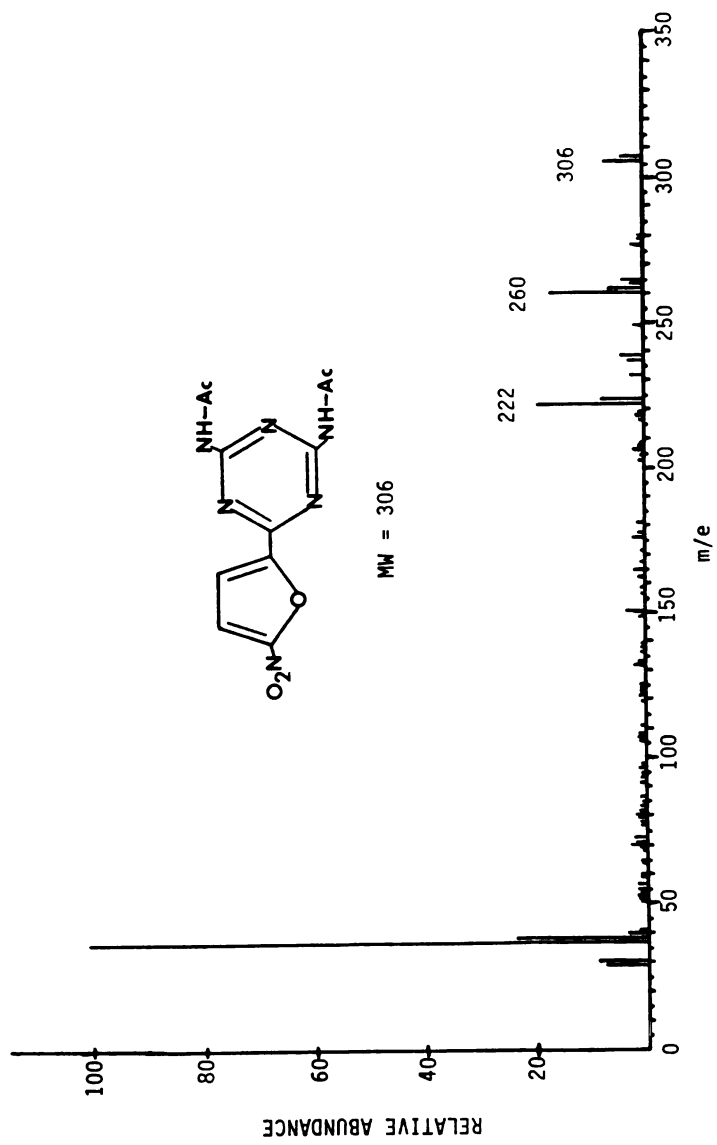


FIGURE 2.3  
ELECTRON IONIZATION MASS SPECTRUM OF  
2,4-DIACETYLAMINO-6-(5-NITRO-2-FURYL)-1,3,5-TRIAZINE (I)

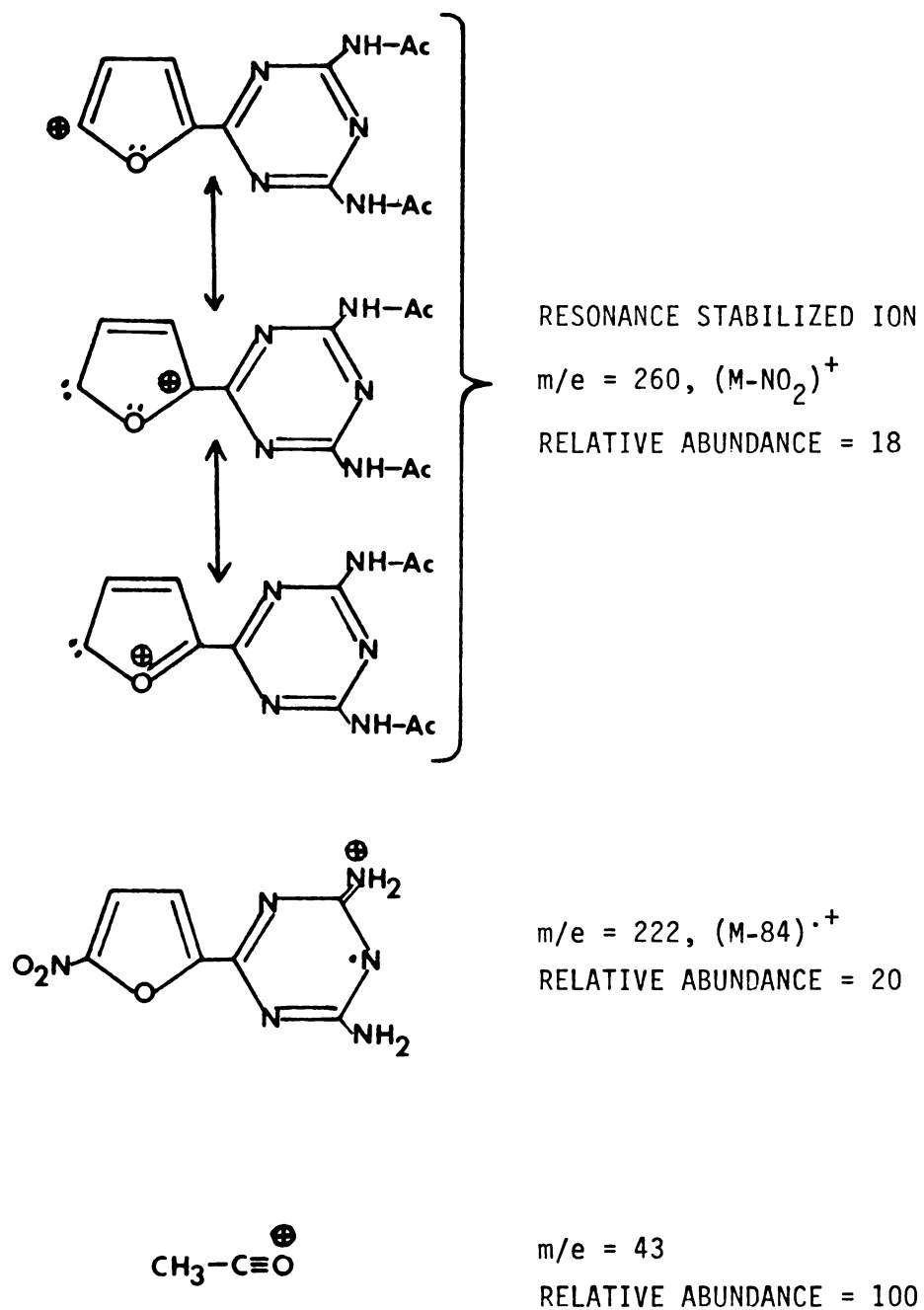


FIGURE 2.4

POSTULATED STRUCTURES OF IMPORTANT IONS IN THE ELECTRON IONIZATION MASS SPECTRUM OF 2,4-DIACETYLAMINO-6-(5-NITRO-2-FURYL)-1,3,5-TRIAZINE (I)

## II. Stability Study

Because 5-nitrofurans in general are considered photochemically unstable and the acetyl groups of (I) are of questionable chemical stability, a study was conducted to examine these two degradation pathways.

### A. Materials and Methods

The photochemical and acetyl lability of (I) was investigated in 50% MeOH/H<sub>2</sub>O (V/V) and 100 mM potassium phosphate buffer pH 7.35. Five mg (I) was dissolved in a total volume of 25.0 ml DMSO and 200 ul of this solution diluted to 2.00 ml in a small glass vial with either 50% MeOH/H<sub>2</sub>O (V/V) or 100 mM potassium phosphate buffer pH 7.35. Three solutions in each solvent system were prepared. One solution was left out under the normal laboratory lighting conditions at ambient temperature (labeled-light/ambient temperature). A second was wrapped in aluminum foil to block light exposure and left out at ambient temperature (labeled-dark/ambient temperature). The last sample of each solution was wrapped in aluminum foil and stored at 0-2<sup>0</sup>C in a refrigerator (labeled-dark/0-2<sup>0</sup>C).

Photochemical and acetyl lability were evaluated by determination of the relative amounts of (I) and the monodesacetyl derivative of (I) after the initial preparation of the solutions and at 1, 2, and 7 days. The HPLC analysis used a 10u C<sub>18</sub>-uBondapak 3.9 mm X 30 cm column (Waters Associates, Milford, Massachusetts) with 40% MeOH/H<sub>2</sub>O (V/V mobile phase at 2.0 ml/min and 365 nm detection. The monodesacetyl derivative of (I) and (I) eluted at retention times of 8.2 and 13.8 min respectively.

## B. Results

Photochemical stability of (I) in the two solvent systems was assessed by plotting the per cent of peak height of (I) at time zero as a function of time (Figure 2.5). The difference between samples labeled dark/ambient temperature and light/ambient temperature represents the photochemical instability of (I). The difference between the plots of the samples labeled dark/ambient temperature and dark/0-2°C represents the difference in chemical instability at the two different temperatures.

Acetyl lability was assessed by plotting the peak height of the desacetyl degradation product of (I) as a function of time (Figure 2.6). The difference between samples labeled dark/ambient temperature and dark/0-2°C represents the difference in acetyl lability at the two different temperatures. Only a small amount of the desacetyl (I) was formed in the light/ambient temperature sample because most of (I) was photochemically degraded.

After 7 days of sample aging an additional peak was observed on the chromatograms at a retention time of 4.8 min. This peak was suspected to be the product of complete deacetylation of (I). It was found to co-chromatograph with the di-desacetyl synthetic intermediate of (I) 2,4-diamino-6-(5-nitro-2-furyl)-1,3,5-triazine (II).

## C. Discussion

Due to the demonstrated photochemical instability of (I), all incubation and analytical procedures were carried out under subdued light. Also, because of the observed solvolysis of the acetyl groups, solutions of (I) in alcohol or buffers could not be stored for future use. Therefore, fresh solutions were prepared on the day of use.

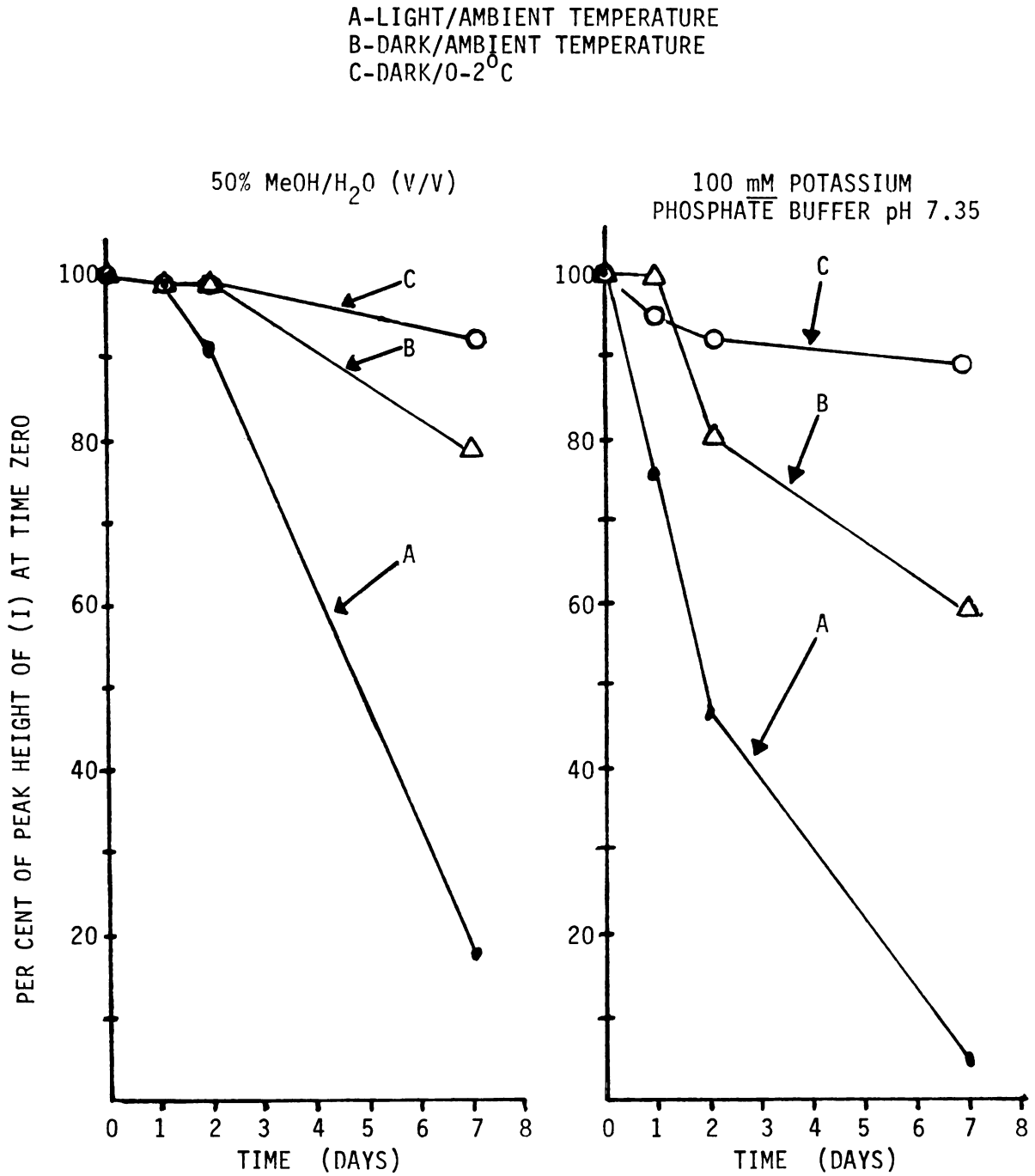
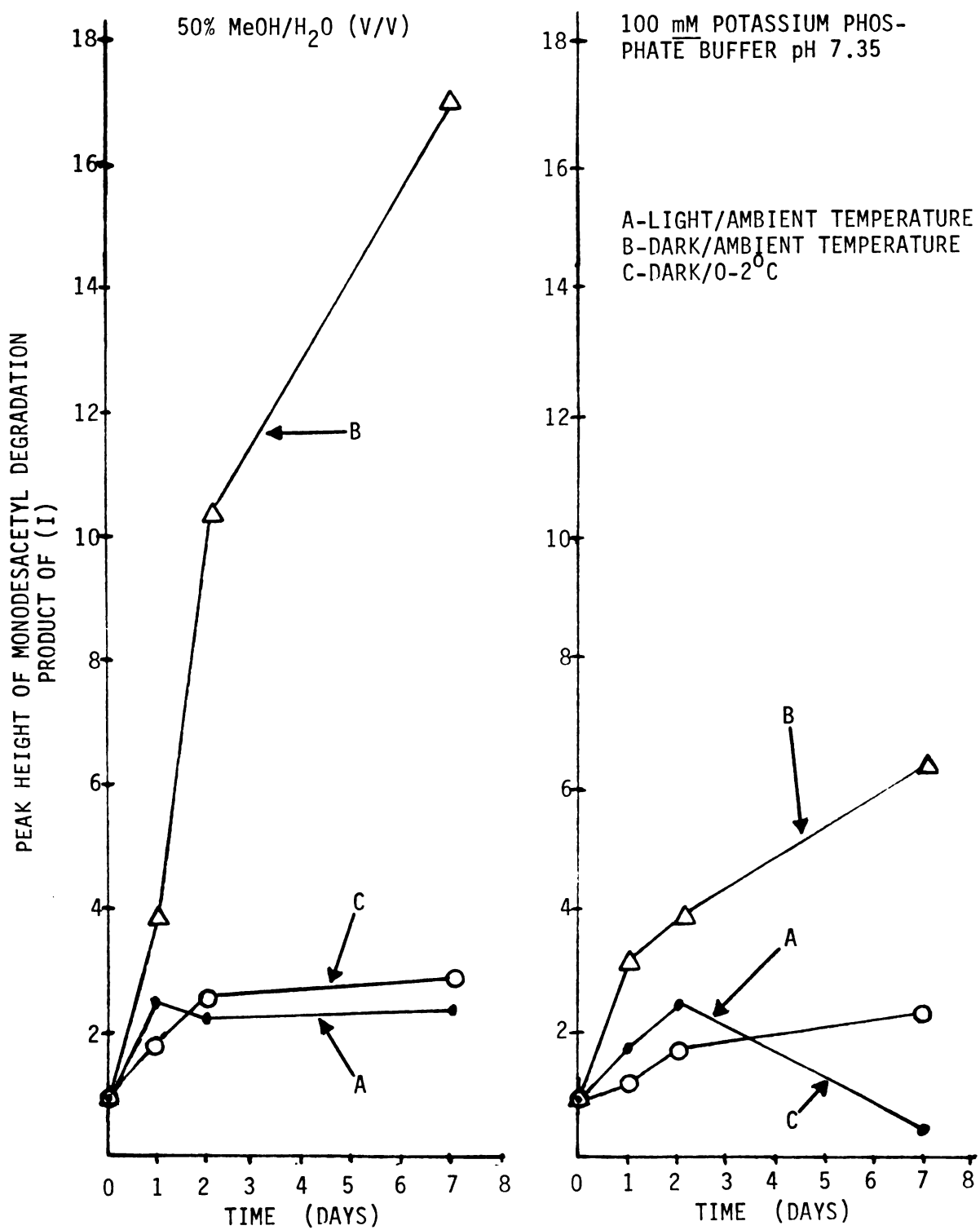


FIGURE 2.5

PHOTOCHEMICAL STABILITY OF (I), PER CENT OF PEAK HEIGHT  
OF (I) AT TIME ZERO AS A FUNCTION OF TIME



**FIGURE 2.6**

ACETATE STABILITY OF (I), PEAK HEIGHT OF MONODESACETYL DEGRADATION PRODUCT OF (I) AS A FUNCTION OF TIME

### III. Synthesis

Initial metabolism studies were carried out with samples of (I) supplied from Abbott Laboratories, North Chicago, Illinois. However, this supply was soon exhausted and it became necessary to synthesize more (I). The synthesis is based upon the patented Abbott process (66) in which an ester of a heterocyclic acid condenses with biguanide to form a diaminotriazine derivative. The diaminotriazine derivative is then acetylated in refluxing acetic anhydride. Synthetic work was begun using biguanide obtained from Aldrich Chemical Company, Milwaukee, Wisconsin. However, the purity of this material was questionable (depressed melting point) and Aldrich subsequently discontinued it. Therefore, it was necessary to synthesize it.

#### A. Synthesis of Biguanide

##### 1. Materials and Methods

Biguanide was first prepared by ammoniation of dicyanodiamide (cyanoguanidine) through reaction of an ammonium salt in the molten state. The cooled melt, containing impure biguanide, was then converted into the sulfate salt and purified by recrystallization (67). The free base was obtained from the biguanide sulfate by treating a solution of the sulfate with sodium hydroxide (68).

Dicyanodiamide (25.22 gms, 300 mmoles) (Aldrich Chemical Company, Milwaukee, Wisconsin) and ammonium chloride (40.1 gms, 750 mmoles) (Aldrich Chemical Company, Milwaukee, Wisconsin) were separately ground to a fine powder state and then intimately mixed in a 250 ml beaker. While constantly stirring the mixture with a spatula, gentle heat from

a Bunsen burner was applied until a liquid melt was obtained. The melt was held at 160 to 165°C for 10 min with constant stirring.

After the melt had cooled, the solid was crushed into small lumps and dissolved in 150 ml water at 90 to 100°C. The resulting suspension was filtered and the precipitate washed with two 25 ml portions of hot water. The filtrate was then treated with a slight excess of ammoniacal copper (II) sulfate solution. The excess was noted by the appearance of a slight purple color. After the rose-red copper biguanide sulfate precipitated, it was washed with 20 ml cold water and dissolved in 35 ml hot 10% sulfuric acid at a temperature no higher than 90°C. The resulting solution was then cooled in an ice bath for 1 hr and the crude crystals which formed were separated by filtration. The crystals were recrystallized two more times by dissolving in 25 ml boiling water and cooling in an ice bath for 1 hour. Finally, the resulting colorless crystals of biguanide sulfate 2-hydrate were washed first with 10 ml cold water and then 10 ml absolute ethanol, and dried at 110°C for 24 hours.

To obtain the free base pure anhydrous biguanide sulfate (9.95 gms, 0.10 mole) was added to a solution of 8 gms (0.4 mole) sodium hydroxide in 175 ml anhydrous methanol. The mixture was stirred for 2 hrs at room temperature and then refluxed for 45 min. The resulting sodium sulfate precipitate was filtered and the cake washed with 40 ml hot anhydrous methanol. The combined filtrate and wash were concentrated by roto-evaporation under reduced pressure at 40-45°C until crystals of biguanide started to separate. Then, further precipitation was promoted by the addition of 150 ml anhydrous ethyl ether. Finally, the crystals were filtered, washed with 10 ml anhydrous ethyl ether, and dried in a vacuum desiccator, with  $\text{CaSO}_4$  as the desiccant, for 24 hours. Because



biguanide decomposes on exposure to atmospheric moisture, the product was stored in the vacuum desiccator.

## 2. Results

Pure biguanide sulfate was synthesized with a yield of 7.47 gms (0.0375 mole), 12.5% of the theoretical yield, 81.2% of the reported literature yield, and a melting point of 243-244<sup>0</sup>C. The literature reports a melting point of 231-233<sup>0</sup>C. The prepared biguanide sulfate was apparently of significantly higher purity than the sample in the literature.

The free base biguanide was synthesized with a yield of 3.82 gms (0.0378 mole), 76.4% of the theoretical yield, 85.8% of the reported literature yield, and a melting point of 132-133<sup>0</sup>C. The literature reports a melting point of 133-134<sup>0</sup>C.

### B. Synthesis of 2,4-Diacetylamino-6-(5-Nitro-2-Furyl)-1,3,5-Triazine

Synthesis of (I) was accomplished by condensation of ethyl 5-nitro-2-furoate with biguanide to form a diaminotriazine derivative. The two free amino groups were then acetylated with acetic anhydride. Because ethyl 5-nitro-2-furoate was not available commercially it was necessary to synthesize it.

#### 1. Materials and Methods

Ethyl 5-nitro-2-furoate was synthesized by the method of Prousek *et al.* (84) in which ethyl 2-furoate is nitrated in acetic anhydride. A mixture consisting of fuming nitric acid (52 gms, d=1.5) and concentrated sulfuric acid (3.5 gms, d=1.83) was added dropwise to acetic

anhydride (84 gms) in a 500 ml three neck flask at  $-10^{\circ}\text{C}$  (dry ice/acetone bath). Under continuous magnetic stirring the temperature of this nitrating mixture was lowered to  $-20$  to  $-30^{\circ}\text{C}$  and a solution of ethyl 2-furoate (21.6 gms, 0.150 mole) (Aldrich Chemical Company, Milwaukee, Wisconsin) in 31 gms acetic anhydride was added. The temperature was maintained at  $-20$  to  $-30^{\circ}\text{C}$  for an additional 1 hr after which the mixture was poured onto approximately 300 gms crushed ice. Pyridine (40 ml) was added to neutralize the mixture which was heated to  $50^{\circ}\text{C}$  for 15 minutes. On cooling in an ice bath crystals of ethyl 5-nitro-2-furoate separated. The crystals were suction filtered in a Büchner funnel, washed three times with 25 mls of water and recrystallized in ethanol.

The condensation of biguanide with ethyl 5-nitro-2-furoate was performed by adding a stirred suspension of 9.26 gms (0.050 mole) ethyl 5-nitro-2-furoate in 60 ml absolute methanol to a solution of 5.06 gms (0.050 mole) biguanide in 15 ml absolute methanol. The suspension which formed was stirred overnight at room temperature in the absence of light. A green-tan colored solid was collected by suction filtration in a Büchner funnel and washed with 100 ml methanol. The reference reports that the product, 2,4-diamino-6-(5-nitro-2-furyl)-1,3,5-triazine (II), is purified by recrystallization from DMF. However, (II) would not crystallize from the DMF without the addition of one-half the volume of water. In this manner a tan colored crystalline product was obtained. Drying of the final product was done at  $153^{\circ}\text{C}$  in vacuo to give the pure diaminotriazine derivative.

The acetylated diaminotriazine product (I) was obtained by refluxing (II) in acetic anhydride according to the method of Sherman (65).

Acetic anhydride (50 ml) was placed in a 100 ml round bottom flask and 2.22 gms (0.010 mole) (II) were added. The suspension was refluxed for 1.5 hours. On cooling the diacetyl compound separated. No further purification was necessary.

## 2. Results

Ethyl 5-nitro-2-furoate was obtained in a yield of 15.0 gms (0.0810 mole), 54.0% of the theoretical yield, 64% of the reported literature yield. The melting point was 100-101<sup>0</sup>C, in agreement with the literature value.

A yield of 3.95 gms (0.0178 mole), 35.6% of the theoretical yield, 48% of the reported literature yield, (II), was obtained following DMF/H<sub>2</sub>O recrystallization. The melting point with decomposition was 362-363<sup>0</sup>C, in agreement with the literature value.

The final diacetyl product, (I), was obtained in a yield of 2.10 gms (0.0069 mole), 69% of the theoretical yield, 95% of the reported literature yield. A melting point of 274-275<sup>0</sup>C with decomposition was found, in agreement with the literature value.

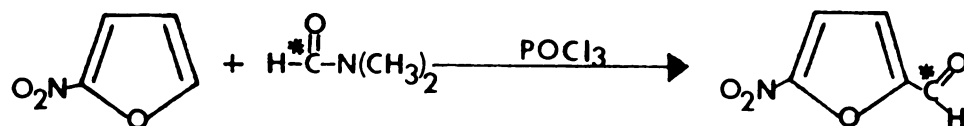
## CHAPTER THREE

RADIOCHEMICAL SYNTHESIS OF 2,4-DIACETYLAMINO-  
6-(5-NITRO-2-FURYL)-1,3,5-TRIAZINE

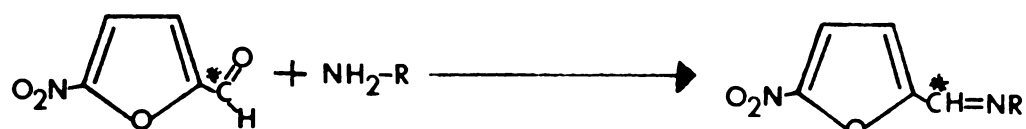
I. Background

There are two commercial procedures for radiolabeling 5-nitrofurans. The first is the condensation of a radiolabeled 5-nitrofuran electrophilic precursor with an appropriate nucleophile. The radiolabeled 5-nitrofuran electrophilic precursor is obtained by the Vilsmeier formylation of 5-nitrofuran using C-14 DMF (Figure 3.1 (A) (69)). The second pathway is the condensation of a non-radiolabeled 5-nitrofuran electrophilic precursor with an appropriately radiolabeled nucleophile (Figure 3.1 (B)) (70).

In deciding where and how to radiolabel 2,4-diacetylamino-6-(5-nitro-2-furyl)-1,3,5-triazine (I) (Figure 3.2) the following concerns were most important. A reasonably high specific activity was required in order to facilitate the detection of nucleotide adducts formed by reductive metabolic activation. The radiolabel could not be lost during metabolic activation and subsequent covalent binding to macromolecules or during any workup procedures. The final constraint was cost. The commercial procedures for making radiolabeled 5-nitrofurans that are applicable to (I) all involve starting materials available only with low specific activity and/or at high cost. In addition, tritium substitution at the three and four positions of the furan ring

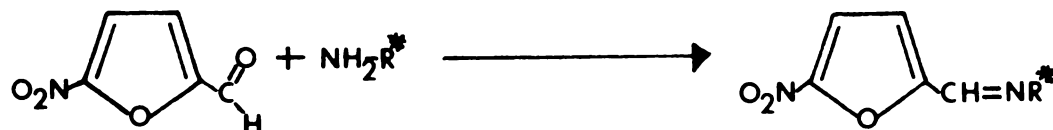


(VILSMEYER FORMYLATION OF 5-NITROFURAN)



RADIOLABELED 5-NITRO-2-FURFURAL-CARBONYL-<sup>14</sup>C  
CONDENSATION WITH NUCLEOPHILIC AMINE

A



RADIOLABELED NUCLEOPHILIC AMINE CONDENSATION  
WITH 5-NITRO-2-FURFURAL

B

FIGURE 3.1

COMMERCIAL PROCEDURES FOR RADIOLABELING 5-NITROFURANS

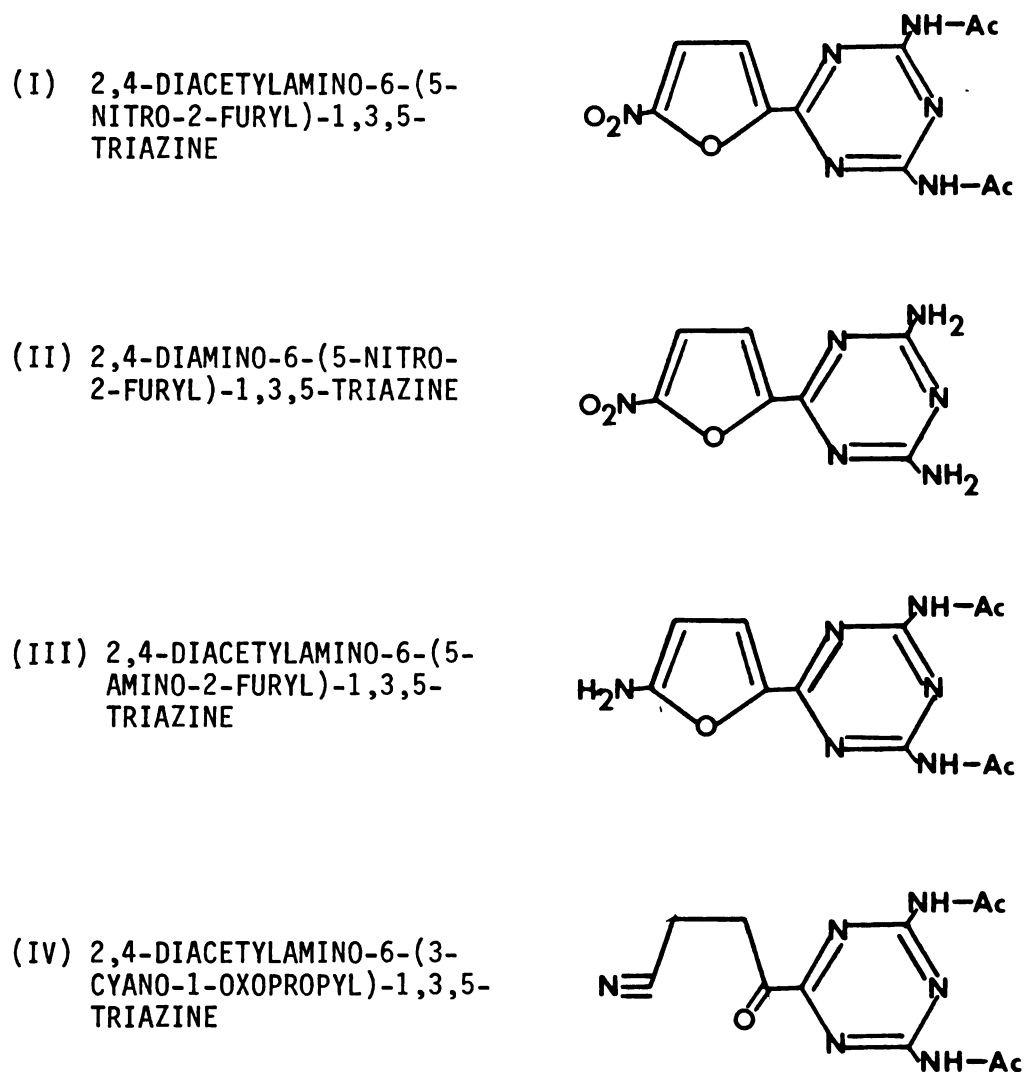


FIGURE 3.2

IMPORTANT CHEMICAL STRUCTURES AND POTENTIAL METABOLITES

was not considered because of the possibility of loss during covalent binding of the activated reduced metabolites to macromolecules (see Figure S/C-1 on p 171).

With these constraints taken into consideration the following synthetic program was initiated. First, because of the relative ease with which the two acetyl groups could be radiolabeled using either C-14 or H-3 radiolabeled acetic anhydride, acetylation of 2,4-diamino-6-(5-nitro-2-furyl)-1,3,5-triazine (II) (Figure 3.2) was attempted. However, as discussed below, the lability of this position, either by acetate hydrolysis or tritium loss by enolization, made this choice unacceptable. Subsequently various procedures to introduce a C-14 label at the two position of the furan ring using the relatively inexpensive C-14 sources of barium carbonate-(C-14) or cyanide-(C-14) were attempted.

## II. Synthesis of 2,4-Diacetylamino-6-(5-Nitro-2-Furyl)-1,3,5-Triazine-(Acetyl-H-3)

### A. Materials and Methods

A 22.5 umole aliquot of (II) was placed in a microscale refluxing apparatus (Figure 3.3). Acetic anhydride-(H-3) (100 mCi, 500 mCi/mole, ICN, Chemical and Radioisotope Division, Irvine, California) in a break-seal tube was centrifuged at 2000 RPM (IEC NH-SII centrifuge to bring all the liquid to the bottom. The radiolabeled acetic anhydride was removed as completely as possible by syringe, diluted with cold acetic anhydride to a calculated specific activity of 89 mCi/mole and transferred to the refluxing apparatus containing (II). The resulting suspension was refluxed for four hours in a 140°C oil bath. After four

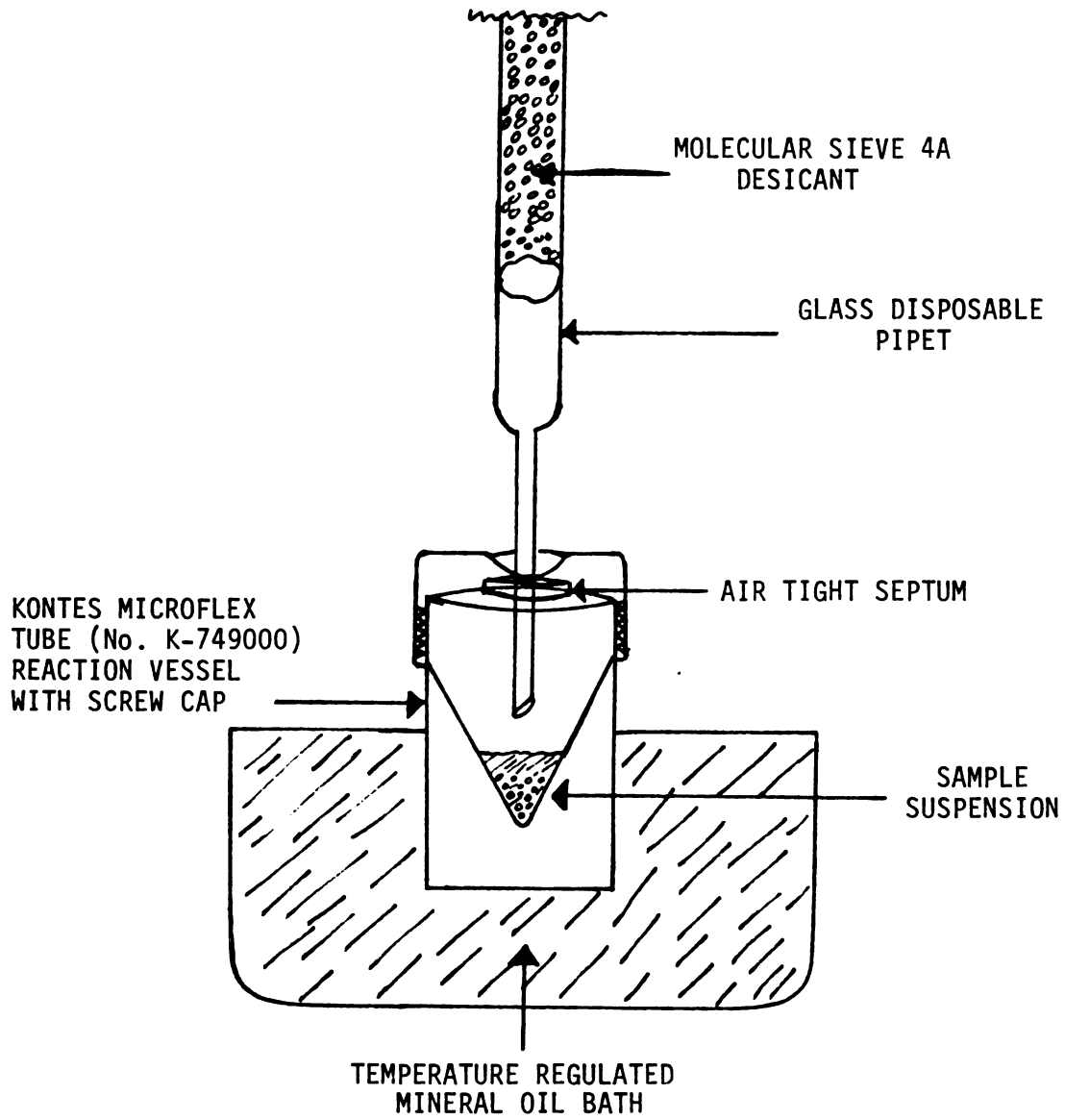


FIGURE 3.3

MICROSCALE REFLUXING APPARATUS



hours of refluxing the suspension was dissolved in 5.0 ml of DMF and purified by preparative HPLC using a 10 $\mu$  C<sub>18</sub>-u-Bondapak 7.8 mm X 30 cm column (Waters Associates, Milford Massachusetts) and 4.0 ml/min 40% MeOH/H<sub>2</sub>O mobile phase with 365 nm UV detection. Fractions of tritiated (I), retention time 13.2 min, were collected following many 200  $\mu$ l injections. The combined fractions were lyophilized and reconstituted with DMF.

The yield, radiochemical purity, and specific activity of the tritiated (I) were determined by HPLC analysis using the same system as described for purification. Fraction collection over the entire chromatogram and measurement of the peak height of the sample were used to determine radiochemical purity and specific activity respectively. HPLC fractions were counted on a Packard Tri-Carb liquid scintillation spectrometer on the tritium channel with quench correction by channels ratio method.

## B. Results

The HPLC absorbance/radioactivity profile of the purified 2,4-diacetylamino-6-(5-nitro-2-furyl)-1,3,5-triazine-(acetyl-H-3) is shown in Figure 3.4. A radiochemical purity of 82% was calculated by dividing the radioactivity collected in the chromatogram. The yield and specific activity were calculated from the amount of tritiated (I) injected. The concentration of (I) was determined by comparison with a standard curve constructed using samples of 8, 20, 40, and 100 mcgms/ml (I). A specific activity of 32 mCi/mole and a overall yield of 13.5  $\mu$ moles, 0.432 mCi (60% chemical yield, 0.43% radiochemical yield) were obtained.

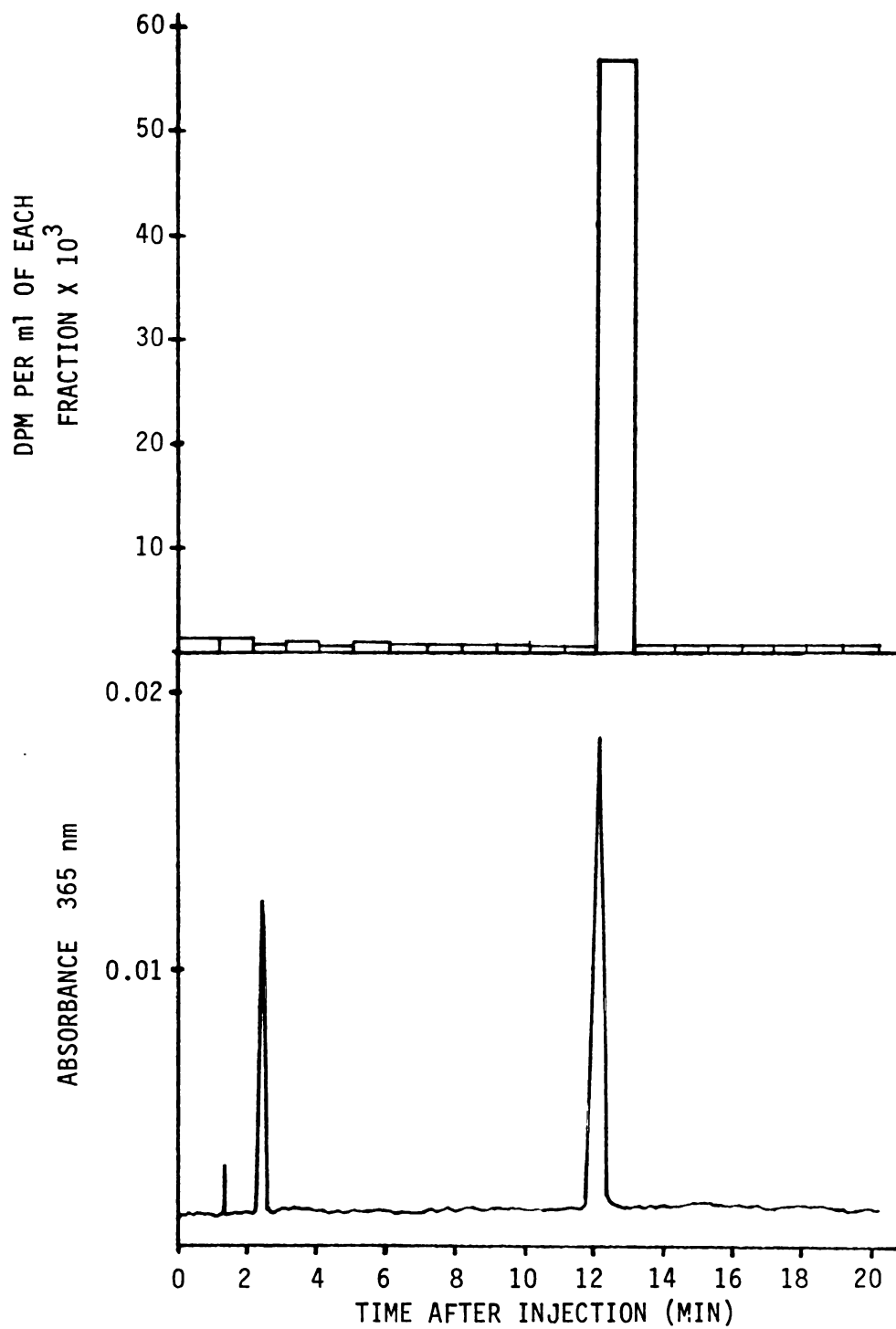


FIGURE 3.4

HPLC ABSORBANCE/RADIOACTIVITY PROFILE OF PURIFIED  
2,4-DIACETYLAMINO-6-(5-NITRO-2-FURYL)-1,3,5-TRIAZINE-(ACETYL-H-3)

### C. Discussion

The relatively low radiochemical purity obtained in the final product compromised the acceptability of this position for radiolabeling. It appeared that considerable radiolabel was lost during the purification process. As described in the metabolism section of this study (p 118) tritiated acetyl (I) was found to be unacceptable because of the high lability of the radiolabel in this position either because of acetate hydrolysis and/or enolization. Therefore, assuming that the loss was due to enolization, acetate labeling using acetic anhydride-(1-C-14) was tried.

### III. Synthesis of 2,4-Diacetylamino-6-(5-Nitro-2-Furyl)-1,3,5-Triazine-(Acetyl-1-C-14)

#### A. Materials and Methods

2,4-Diamino-6-(5-nitro-2-furyl)-1,3,5-triazine (II) (9 umole) and 70 ul freshly distilled acetic anhydride were added to a microscale refluxing tube. The refluxing tube (Figure 3.5) was attached to a high vacuum manifold (Figure 3.6) and the contents frozen with liquid nitrogen. Valve A to the high vacuum system was opened and the system was allowed to pump down for twenty minutes. This valve was then closed and the contents allowed to thaw. Acetic anhydride-(1-C-14) (1.0 mCi, 10 mCi/mmole, in 80% V/V benzene, New England Nuclear, Boston, Massachusetts) in a breakseal tube with an outer 14/35 ground glass fitting and containing a heavy magnet as described in Figure 3.7 was also attached to the high vacuum manifold at valve B. Once again the reflux tube was frozen with liquid nitrogen, valve A and B opened, and the system pumped

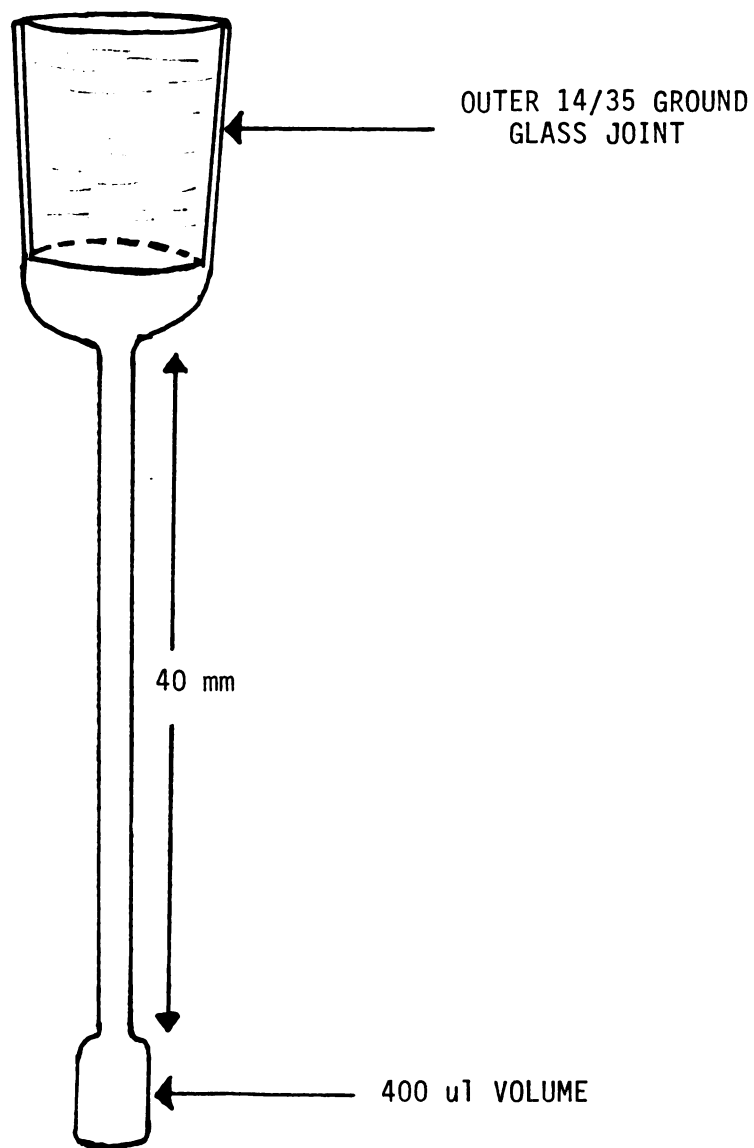


FIGURE 3.5

MICROSCALE REFLUXING TUBE  
(PYREX GLASS)

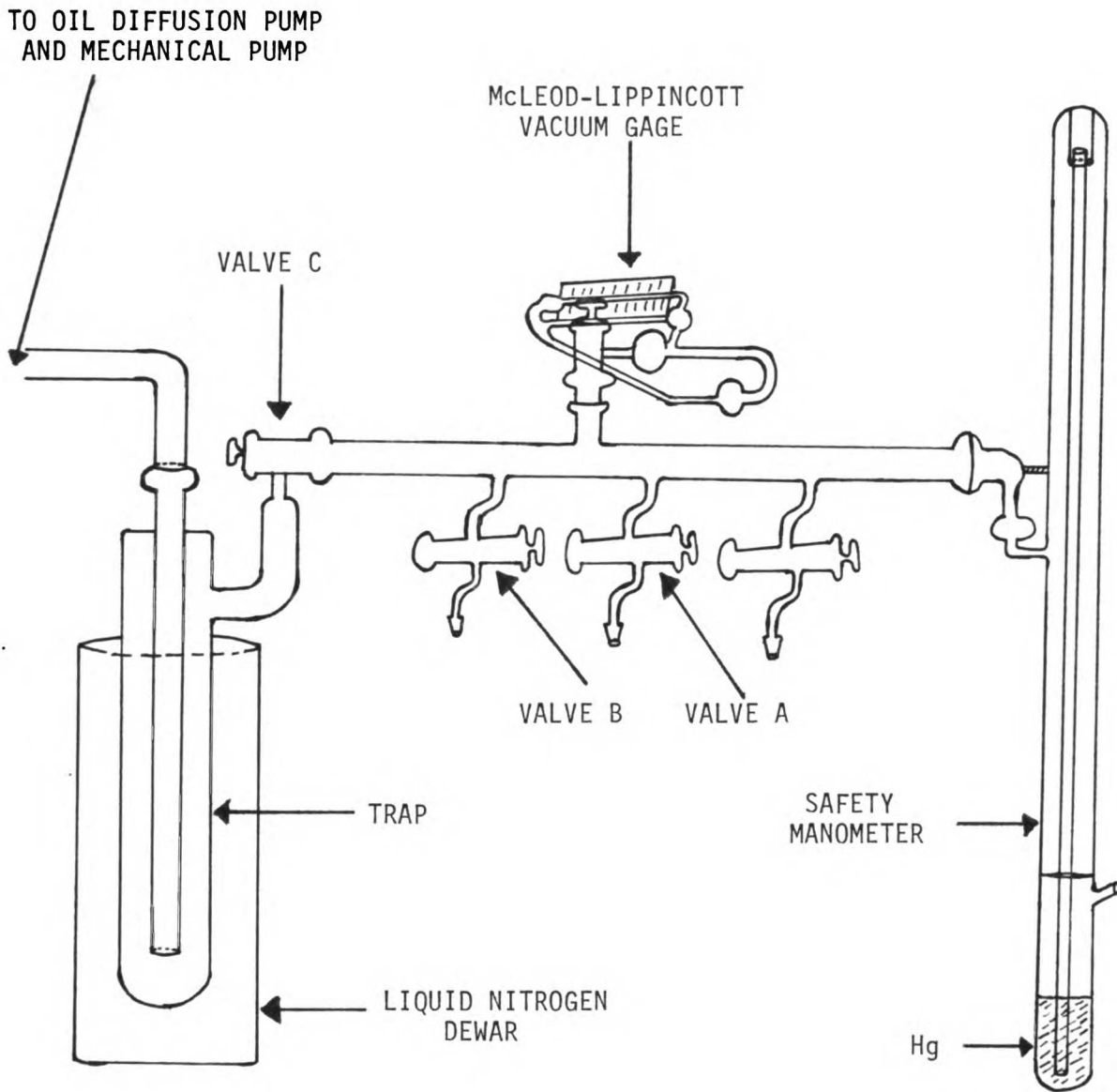


FIGURE 3.6

HIGH VACUUM MANIFOLD  
(KONTES, K-925100)

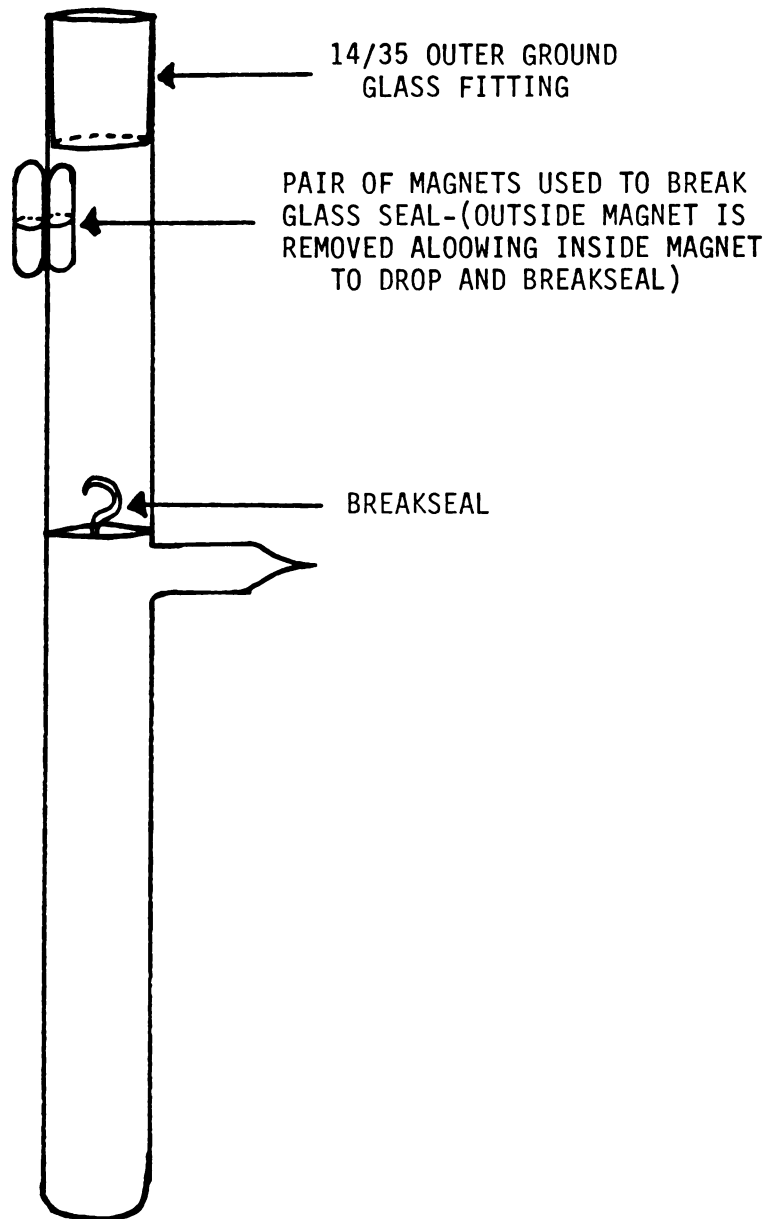


FIGURE 3.7

BREAKSEAL TUBE CONTAINING  
ACETIC ANHYDRIDE-1-<sup>14</sup>C

down for twenty minutes. The manifold was then isolated from the pumping system by closing off valve C; the heavy magnet was dropped on the breakseal and the radiolabeled acetic anhydride allowed to transfer into the frozen micro reflux tube. Valve A was closed after the transfer was complete and the contents allowed to thaw.

This suspension was then treated as described in the synthesis of 2,4-diacetylamino-6-(5-nitro-2-furyl)-1,3,5-triazine-(acetyl-H-3). Yield, radiochemical purity, and specific activity were also determined using the same analytical techniques as previously described.

#### B. Results

The HPLC radioactivity profile of the purified 2,4-diacetylamino-6-(5-nitro-2-furyl)-1,3,5-triazine-(acetyl-1-C-14) is shown in Figure 3.8. A 97.2% radiochemical purity, 0.18 mCi/mmol specific activity, and 5.4  $\mu$ moles, 0.972  $\mu$ Ci (60% chemical yield, 0.10% radiochemical yield).

#### C. Discussion

The very high radiochemical purity obtained in the final product suggests this radiolabel may be suitable for use in metabolism studies. It appears that the radioactive impurities seen in the tritiated acetyl (I) after HPLC purification were due to tritium loss through enolization. However, as described in the metabolism section of this study (p 118) the C-14 acetyl (I) was found to be unacceptable because the acetate group was easily hydrolyzed in subsequent studies.

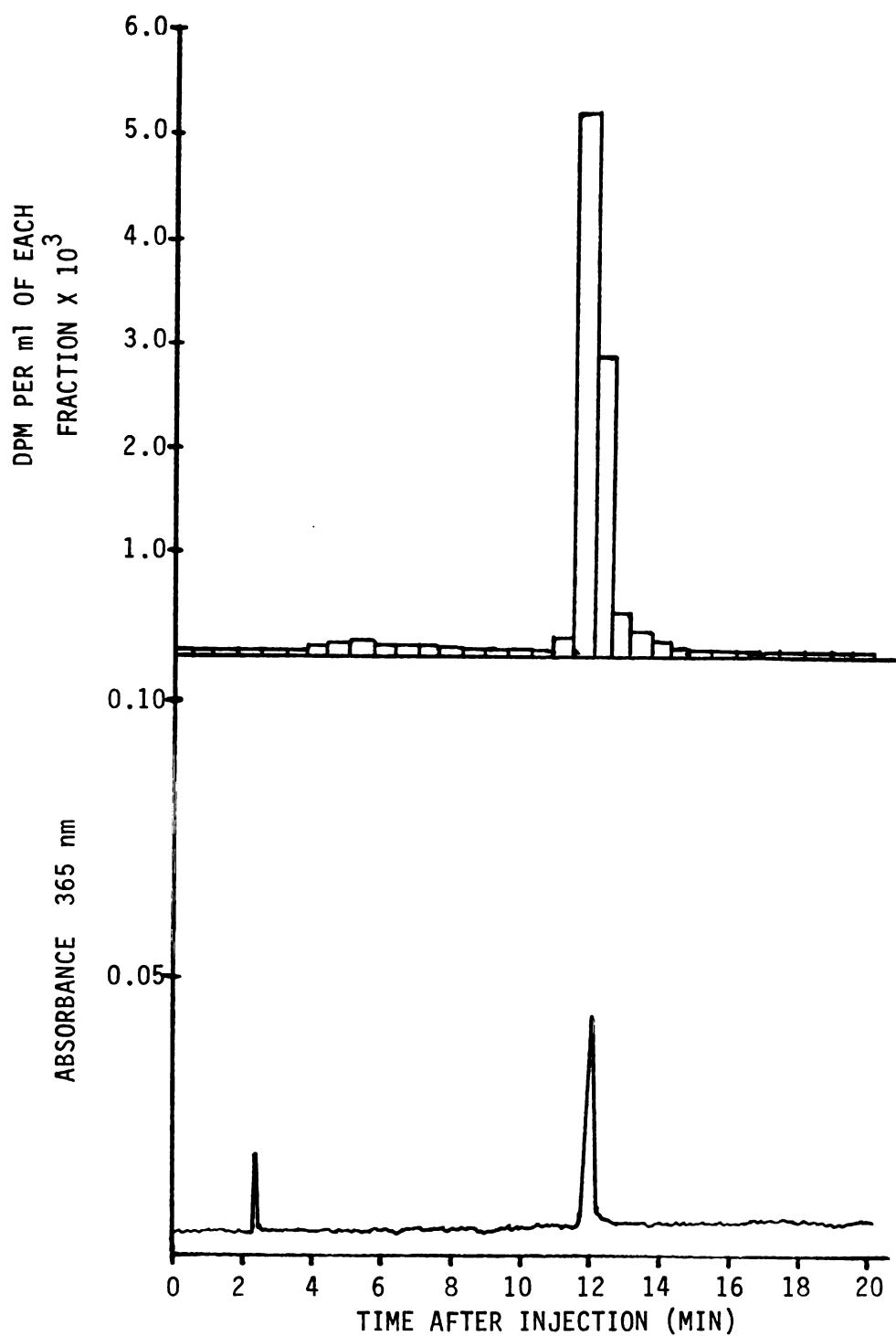


FIGURE 3.8

HPLC ABSORBANCE/RADIOACTIVITY PROFILE OF PURIFIED  
2,4-DIACETYLAMINO-6-(5-NITRO-2-FURYL)-1,3,5-TRIAZINE-(ACETYL-1-<sup>14</sup>C)



#### IV. Attempted Development of Microsynthesis of 2,4-Diacetylamino-6-(5-Nitro-2-Furyl)-1,3,5-Triazine From 5-Nitro-2-Bromofuran

##### A. Background

Since both the H-3 and C-14 acetate labeling of (I) were unacceptable for subsequent metabolic study, the following series of studies were undertaken to introduce a C-14 label at the two position of the furan ring. Figure 3.9 shows all of the pathways considered along with the scheme for the total synthesis of (I).

Because technical problems would be greatly reduced by introducing the radiolabel after the nitro group was attached, attempts were made at lithium halogen exchange, Grignard reagent preparation, and nucleophilic aromatic cyanide substitution of 5-nitro-2-bromofuran. First, however it was necessary to synthesize 5-nitro-2-bromofuran and to dry it completely.

##### B. Synthesis of 5-Nitro-2-Bromofuran

###### 1. Materials and Methods

The synthesis used is a modification of the procedure of Nazarova and Novikov (71) in which 5-bromo-2-furoic acid undergoes decarboxylative nitration. To 50 mls acetic anhydride in a 200 ml three-neck flask at  $-10^{\circ}\text{C}$  (ice/salt bath) were added 50 gms  $\text{HNO}_3$  ( $d=1.5$ ) (Mallinckrodt Inc., Paris, Kentucky) dropwise over a 20 min period. In a separate 100 ml two-neck flask 12 gms (62.8 mmole) 5-bromo-2-furoic acid (Pfaltz and Bauer, Inc., Stamford, Connecticut) were dissolved in 50 ml acetic anhydride with gentle heating. After complete solution this mixture

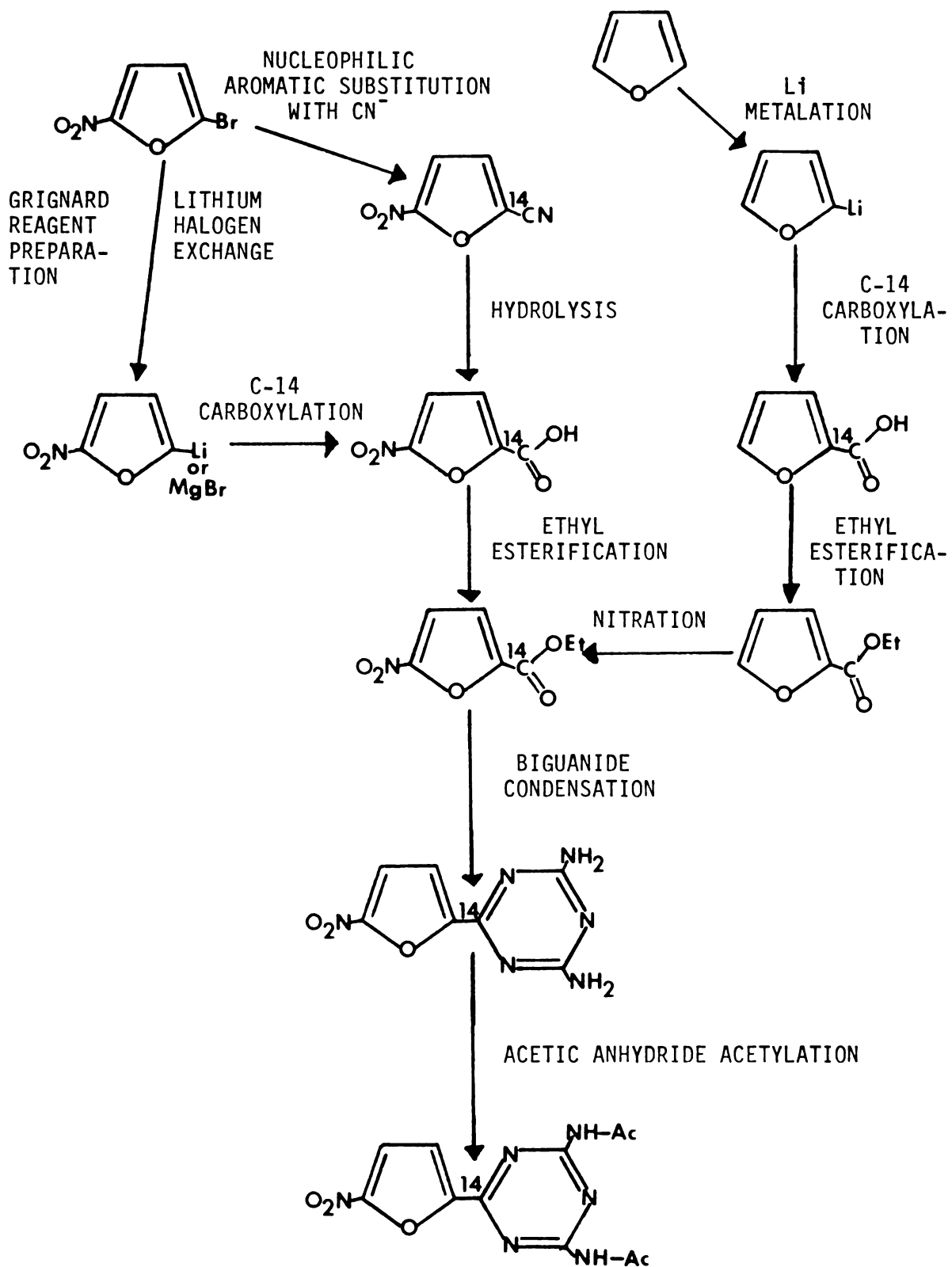


FIGURE 3.9

PATHWAYS FOR C-14 RADIOLABELING OF THE FURAN RING AND THE SUBSEQUENT SCHEME FOR THE TOTAL SYNTHESIS

was cooled to about 20°C and slowly added to the nitrating mixture over a 1 hr period. The temperature of the mixture was kept at -10°C. The mixture was further stirred for an additional hour at -10°C and during the next 2 hrs stirred while the temperature was gradually increased to 0°C. After an additional 1 hr of stirring, the solution was poured on about 200 ml ice with stirring and 1.0 gm NaCl added. This mixture was extracted with 100 ml ethyl ether, an additional 2.0 gms of NaCl were added to facilitate phase separation, and the ethyl ether layer removed. This ether extraction was repeated with 100 ml, 50 ml, 50 ml, and 30 ml portions without additional NaCl. Then 180 ml of saturated Na<sub>2</sub>SO<sub>4</sub> aqueous solution were added to the combined ethyl ether extracts and the mixture stirred vigorously. This two phase mixture was steam distilled. The 5-nitro-2-bromofuran crystalized in the condensor. After recovery, the 5-nitro-2-bromofuran was first dried in a vacuum desiccator with CaSO<sub>4</sub> as desiccant. Then, it was further dried in an Abderhalden drying apparatus (Kontes Scientific Glassware, San Leandro, California) under high vacuum using P<sub>2</sub>O<sub>5</sub> as a desiccant with the temperature maintained by acetone reflux. During this final drying step the 5-nitro-2-bromofuran sublimed and condensed in the side tube assuring the totally anhydrous state necessary for preparation of organo-metallic compounds.

## 2. Results

The 6.38 gms (33.2 mmoles) of product obtained had a melting point of 48.2°C. The yield obtained was 52.9% of the theoretical and 112% of the reported literature value (71). The reported melting point is 48°C.

### 3. Discussion

The synthesis of 5-nitro-2-bromofuran was successful. In addition this compound was dried to a highly anhydrous state in preparation for attempts at introducing a C-14 label for the bromide atom by metalation, with either lithium or magnesium, followed by carboxylation, or nucleophilic substitution with cyanide.

#### C. Attempt at Lithium Halogen Exchange With 5-Nitro-2-Bromofuran

##### 1. Background

Heterocyclic organolithium compounds prepared by lithium halogen exchange reactions are prepared by reaction of the heterocyclic bromides or iodides with n-butyllithium or phenyllithium (72). Preparation of organolithium compounds containing the nitro functionality are complex and not generally useful in synthesis because of competitive side reactions (73). However, a general feature of the metal halogen exchange reaction is its speed even at low temperatures. It is reported that it is usually possible to devise conditions leading to metal-halogen exchange almost exclusive of side reactions at low temperatures (73). For example, o-nitrophenyl lithium was prepared from o-nitrobromobenzene at very low temperatures (73). Therefore, with some optimism, the following work was begun in an attempt to prepare 5-nitro-2-furyllithium as a precursor for C-14 carboxylation in radiochemical synthesis of (I).

##### 2. Materials and Methods

Dry 5-nitro-2-bromofuran, 1.92 gms (10 mmoles), and a magnetic stir bar were placed in a flame dried two neck 50 ml round bottom flask with

one neck fitted with a septum and the other neck connected to a nitrogen bubble trap. Anhydrous ethyl ether (30 mls) was added by dry syringe and the mixture stirred until solution was complete. The solution was then cooled to  $-80^{\circ}\text{C}$  (dry ice/acetone bath) and 10 mmole n-butyllithium in hexane (Aldrich Chemical Company, Milwaukee, Wisconsin) or 10 mmoles phenyllithium in 70/30 benzene/ether (V/V) (Aldrich Chemical Company, Milwaukee Wisconsin) was slowly added through the septum by syringe.

After 1.0 hr of stirring at  $-80^{\circ}\text{C}$  a small amount of crush dry ice was added and the mixture stirred for 10 min at  $-80^{\circ}\text{C}$ . After 10 min the mixture was warmed to room temperature and poured into a separatory funnel containing an equal volume of water. The separatory funnel was shaken to extract any 5-nitro-2-furoate, and the aqueous phase separated and acidified with dilute HCl and re-extracted with ethyl ether. The ethyl ether was then evaporated on a steam bath and the yield of 5-nitro-2-furoic acid used to evaluate the success of lithium halogen exchange on the 5-nitro-2-bromofuran.

### 3. Results

Upon addition of the n-butyllithium or phenyllithium the reaction solution turned from clear colorless to reddish then brown and finally to tar black with precipitation indicating decomposition and polymerization. In using n-butyllithium or phenyllithium no yield of 5-nitro-2-furoic acid was obtained in the final ethyl ether extract indicating that lithium halogen exchange of 5-nitro-2-bromofuran cannot be used to make 5-nitro-2-furyllithium as a precursor to C-14 carboxylation.

#### 4. Discussion

A lithium halogen exchange reaction on a substrate containing a nitro group would be expected to be complicated by many side reactions. The presence of lithium, a reactive reducing reagent, and a nitro group, a readily reducible group, suggest redox side reactions as possible reasons for the unsuccessful attempt at lithium halogen exchange. The less reactive magnesium organo-metallic compound, if formed, would be less likely to undergo these side reactions.

#### D. Attempt at Grignard Reagent Formation With 5-Nitro-2-Bromofuran

##### 1. Background

Halides that contain a second functional group other than tertiary amines, ethers, alkenes, aromatic rings, and a few inert halides are usually reported not to be able to be converted to stable Grignard reagents (74). However, because the more reactive organolithium compound of o-nitrophenyllithium had been successfully prepared an attempt was made at preparation of 5-nitro-2-furyl magnesium bromide from 5-nitro-2-bromofuran.

##### 2. Materials and Methods

In a 50 ml three-neck round bottom flask containing a magnetic stir bar and fitted with a coil-type condenser and a 10 ml dropping funnel with a pressure equalizing side tube was added 0.4 gm magnesium turnings suitable for Grignard reagent preparations (Aldrich Chemical Company, Milwaukee, Wisconsin). Dry nitrogen was introduced at the top of the condenser and allowed to sweep through the apparatus and escape

at the mouth of the dropping funnel. Under continuous nitrogen flow the flask was heated gently with a free flame to ensure elimination of moisture adhering to the surface of the glass or metal. After cooling, the dropping funnel was stoppered and a slight positive pressure of nitrogen was maintained by allowing the nitrogen to divert through a bubbler by the use of a T-connector from the nitrogen source to the bubbler and the reaction apparatus. Ten milliliters of anhydrous ethyl ether were added to the flask containing the magnesium and 2.96 gms (15.4 mmoles) 5-nitro-2-bromofuran dissolved in 7.5 ml anhydrous ethyl ether added to the dropping funnel. After stirring was begun the contents of the dropping funnel were introduced. When about 20% of the dropping funnel contents had been added and no reaction initiation had been noted, by the appearance of bubbling, attempts were made to initiate the reaction by inserting a flattened glass stirring rod through the third neck of the flask and crushing a piece of the metal with a twisting motion. Promotion of reaction initiation was also attempted by adding a small crystal of iodine as suggested in the literature (75). At this point even though no reaction initiation had been observed the remaining contents of the dropping funnel were added and stirred with gently heat from an oil bath ( $\sim 35^{\circ}\text{C}$ ) for three hours.

Subsequently an entrainment procedure (76) used for converting an unreactive halide to its Grignard reagent was attempted using ethylene dibromide as the entraining reagent (77). In this procedure the ethylene dibromide is mixed with an ethereal solution of the halide in the dropping funnel. Upon addition, the entrainment reagent reacts readily with the magnesium keeping it clean and active and probably functioning as an exchange reaction for possible reaction with the refractory halide.

The procedure used in the attempted Grignard reagent preparation using the entrainment technique was the same as that used without the entrainment reagent except three times the mass of magnesium turnings were used and 2.89 gms (15.4 mmoles) ethylene dibromide (Aldrich Chemical Company, Milwaukee, Wisconsin) were added to the dropping funnel.

For both procedures Gilman's test (78) was used to determine if the Grignard reagent was present. About 0.5 ml of the ethereal solution was removed with a disposable pipet and treated with an equal volume of a 1% solution of Michler's ketone in dry benzene and then 1.0 ml of water was added slowly. Addition of several drops of 0.2% solution of iodine in acetic acid produces a greenish-blue color if the Grignard reagent is present.

### 3. Results

In the first attempts at Grignard reagent preparation, any Grignard reagent formation would have been evidenced by the loss of magnesium, the bubbling of the solution, or an increased turbidity of the reaction solution. None of these positive observations were made. The failure of any Grignard reagent to form was confirmed by a negative Gilman's test.

Using the entrainment procedure, Grignard reagent formation could only be evaluated by the Gilman's test since the entrainment procedure gives the appearance of Grignard reagent formation by its very nature. With this entrainment procedure the Gilman's test was negative.

### 4. Discussion

There are reports in the literature that halogenated furans are



unreactive toward Grignard reagent preparation (79). This appears to also be true for 5-nitro-2-bromofuran. All attempts at Grignard reagent preparation were unsuccessful. Therefore, nucleophilic aromatic substitution of the 5-nitro-2-bromofuran with cyanide was tried.

## E. Attempt At Cyanide Substitution of Bromide on 5-Nitro-2-Bromofuran

### 1. Background

Nazarova suggested (71) that attack by a nucleophilic reagent on the 5 position of 5-nitro-2-bromofuran should occur with great facility. He confirmed this experimentally by showing that the bromide easily enters into exchange reactions with metal iodides, thiocyanates, and nitric acid. Therefore, the possibility of cyanide exchange was investigated as a means of radiolabeling 5-nitro-2-bromofuran (Figure 3.9).

The method of Cook et al. (80) for activating cyanide to a strong nucleophile was attempted. This method uses the 18-crown-6 crown ether complex to solubilize the cyanide ion in anhydrous acetonitrile.

### 2. Materials and Methods

Into a three-neck 50 ml round bottom flask fitted with a coil type condenser and drying tube containing a magnetic stir bar were added 25 mls anhydrous acetonitrile (dried by refluxing over  $\text{CaH}_2$ ). Then, 112 mg (0.42 mmole) 18-crown-6 crown ether (Aldrich) and 960 mg (5.0 mmole) 5-nitro-2-bromofuran were added. Potassium cyanide, 641 mg (10 mmole) (dried 24 hrs at  $100^\circ\text{C}$  under vacuum), was added and the mixture stirred at room temperature for 24 hrs. At this time a small aliquot was taken and analyzed for 5-nitro-2-cyanofuran as described below. The

reaction mixture was then heated to reflux for 8.0 hrs and again analyzed for 5-nitro-2-cyanofuran.

The extent of cyanide substitution was evaluated by HPLC using a 10u C<sub>18</sub>-uBondapak column (Waters Associates, Milford, Massachusetts), 3.9 mm X 30 cm, 40% MeOH/H<sub>2</sub>O mobile phase, and UV detection at 365 nm and 280 nm. The chromatograms from 20 ul injections of the reaction solution and an acetonitrile solution of 5-nitro-2-bromofuran were compared for retention time and peak height ratio at the two wavelengths.

### 3. Results

Both the samples, 24 hrs stirring at room temperature or 8 hrs of additional refluxing, gave only one peak on the chromatogram which was identical in retention time (5.9 min) and peak height ratio (1.29 = 365 nm/280 nm) to the peak from the acetonitrile solution of 5-nitro-2-bromofuran.

### 4. Discussion

Cyanide substitution of bromide on 5-nitro-2-bromofuran was found to be unsuccessful in acetonitrile using the 18-crown-6 ether complex. In the studies conducted by Nazarova and Novikov substitutions were only demonstrated using the relatively stronger nucleophiles of iodide and thiocyanate in solvents in which the nucleophiles were readily soluble. It is evident that the cyanide in the 18-crown-6 ether complex is not sufficiently strong nucleophile to allow for substitution.

### F. Summary

Labeling of the acetate group on (I) either by H-3 or C-14 was

shown to be unacceptable for use in anaerobic in vitro metabolic studies. In addition, attempts at introducing a C-14 radiolabel after the nitro group is attached to the furan ring using either lithium halogen exchange or Grignard reagent preparation followed by C-14 carboxylation or by direct cyanide substitution were unsuccessful.

Introduction of a C-14 radiolabel prior to nitration was the only remaining alternative. Hence, the very challenging technical problems associated with carrying a radiolabeled compound through many subsequent synthetic steps while still obtaining an acceptable yield of the final product were tackled.

## V. Development of Microsynthesis of 2,4-Diacetylamino-6-(5-Nitro-2-Furyl)-1,3,5-Triazine From 2-Furyllithium

### A. Background

As outlined in Figure 3.9, C-14 radiolabeling of (I) by introduction of the label prior to nitration consists of C-14 carboxylation of 2-furyllithium which must be followed by esterification, nitration, biguanide condensation, and acetylation in order to complete the synthesis. All of these separate synthetic steps must be maximized for yield and each intermediate obtained in sufficient purity to prevent interference in the subsequent step.

The development of the synthesis was undertaken by dividing it into four steps. The first was to maximize yield and purity of ethyl 2-furoate from a limited amount of barium carbonate. The second was to obtain ethyl 5-nitro-2-furoate from ethyl 2-furoate. Subsequently, (I) was synthesized from ethyl 5-nitro-2-furoate. Finally, all the steps

were taken in sequence to synthesize (I) from a limited amount of barium carbonate in order to confirm the synthetic methods. All steps in the synthetic scheme were developed on the assumption of starting with 0.50 mmole barium carbonate. The yield at the end of each step was taken as the starting amount for the succeeding step.

B. Development of Maximum Yield in Sufficient Purity of Ethyl-2-Furoate from Barium Carbonate

Ethyl 2-furoate was chosen as the intermediate to evaluate the yield from carboxylation of 2-furyllithium from 0.50 mmole barium carbonate because it can be readily quantitated by reverse phase HPLC. Diazoethane was chosen as the ethyl esterification reagent because it is well known to go to completion and leaves no reagent by-products that might interfere in succeeding steps.

1. Establishment of Complete Ethylation by Diazoethane

It was first necessary to establish that diazoethane completely esterified 2-furoic acid to the ethyl ester in quantitative yield. This was done by reacting excess diazoethane with 2-furoic acid and analyzing for ethyl 2-furoate by reverse phase HPLC using external standards.

a. Materials and Methods

i. Diazoethane Generation

The filtration procedure for diazoethane generation of McKay et al. (81) was used. All glassware was cooled to  $-10^{\circ}\text{C}$  prior to use. A 25 ml

round bottom flask containing a magnetic stir bar and 2.2 ml aqueous 10 N KOH was submerged in a  $-4^{\circ}\text{C}$  (salt/ice) bath. The aqueous solution was then covered with 16 ml ethyl ether and the flask stoppered and stirred magnetically for 5 minutes. Then 900 mg (5.6 mmole) N-ethyl-N'-nitro-N-nitrosoguanidine (Aldrich Chemical Company, Milwaukee, Wisconsin) was added in aliquots over a period of five to seven minutes. During the addition of the nitroso compound the reaction solution was stirred vigorously. About two minutes after the addition was complete, the liquid in the reaction solution was transferred by disposable pipet and filtered through a glass wool plugged funnel into a separatory funnel. The lower aqueous phase was drawn off and the remaining undried, yellow, ethereal solution of diazoethane was used immediately for ethyl esterification.

ii. Ethyl Esterification of 2-Furoic Acid

Then, 58.5 mgs (0.522 mmole) 2-furoic acid (Aldrich Chemical Company, Milwaukee, Wisconsin) were dissolved in 10 ml ethyl ether in a 25 ml Erlenmeyer flask. The ethereal diazoethane was added with stirring until the diazo reagent remained and no further bubbling was observed. Sufficient ethanol to make 25 ml was added and 1.0 ml diluted to 25 ml again with ethanol. This final solution was then analyzed by reverse phase HPLC.

iii. HPLC Analysis of Ethyl 2-Furoate

A 10u  $\text{C}_{18}$ -uBondapak 3.9 mm X 30 cm column (Waters Associates, Milford, Massachusetts) with 40% MeOH/ $\text{H}_2\text{O}$  mobile phase at 2.0 ml/min and 20 ul injection volume was used. Absorbance was monitored at 280 nm.

External standards of 40, 120, 200, and 320 mcgms/ml of ethyl 2-furoate were used to construct a standard curve, fitted by least squares linear regression analysis.

b. Results

The HPLC assay of ethyl 2-furoate gave 114 mcgms/ml for the diazoethane esterified 2-furoic acid. This concentration was calculated to be a quantitative yield (103%) after multiplication with the appropriate dilution factors.

2. Carboxylation of 2-Furyllithium

a. Background

To quantitatively carboxylate furan with carbon dioxide from barium carbonate it was necessary to prepare 2-furyllithium from n-butyllithium in ethyl ether using excess furan so that the only organolithium reagent available for carboxylation was 2-furyllithium. Thus, four trials were conducted using different ratios of furan to n-butyllithium followed by high vacuum carboxylation using a limited amount of barium carbonate.

b. Materials and Methods

i. Preparation of n-Butyllithium in Ether

A scaled down method of the procedure of Gilman *et al.* (82) was used for the preparation of n-butyllithium in ether. A dry, oxygen-free nitrogen source was attached to a 50 ml three-neck flask equipped with a magnetic stir bar, low temperature thermometer (-30 to -50°C), and 50 ml

dropping funnel with pressure equalizing tube to purge the entire system. With nitrogen flowing, the system was flame dried and cooled to room temperature. After cooling a slight positive pressure of nitrogen was maintained by sealing the nitrogen exit and allowing nitrogen to divert through a bubbler by use of a T- connector. Then, 26 ml anhydrous ethyl ether and 1.2 gms (172 mmoles) lithium wire were added (3.2 mm dia., Alfa Products, Danvers, Massachusetts). The wire had been wound in a loose coil rinsed with pentane once and ether twice, flattened with pliers, and cut into pieces about 7 mm in length. Into the dropping funnel was added 13 ml anhydrous ethyl ether and 6.9 ml (64 mmoles) n-butyl bromide (Aldrich Chemical Company, Milwaukee, Wisconsin). Once the stirrer was started, 15 drops of the solution in the dropping funnel were added and the reaction mixture cooled to  $-10^{\circ}\text{C}$  with a dry ice/acetone bath kept at approximately  $-30$  to  $-40^{\circ}\text{C}$ . The remainder of the ethereal n-butyl bromide was then added at an even rate over a thirty-minute period while maintaining the internal temperature at  $-10^{\circ}\text{C}$ . After this addition was complete, the reaction mixture was allowed to warm to  $0$  to  $10^{\circ}\text{C}$  while stirring for two hours. The reaction mixture was then filtered through a nitrogen filled 20 ml syringe, plugged with glass wool, into a dry nitrogen-filled flask. The yield of n-butyl-lithium was not determined but assumed to be 80% (50 mmoles) as reported by Gilman et al.. Since n-butyllithium is not stable in ether it was used immediately to prepare 2-furyllithium.

ii. Preparation of 2-Furyllithium in Ether

A scaled down procedure of Ramanathan and Levine (83) was used to prepare 2-furyllithium from n-butyllithium. Forty milliliters (44 mmoles/

assumed) of the filtered n-butyllithium in ether was placed in a dry nitrogen filled 50 ml two neck round bottom flask fitted with a Dewar condenser and the means to keep a slight positive nitrogen pressure as described above. A few boiling chips and a dry magnetic stir bar were added and the contents of the flask cooled in an ice bath. The Dewar condenser was carefully filled with dry ice/2-propanol and the amount of furan (previously dried and fractionated from  $\text{CaH}_2$ ) (Aldrich Chemical Company, Milwaukee, Wisconsin) added by syringe to the round bottom flask over a one minute period with magnetic stirring. The magnetic stirring was stopped and the ice bath removed and replaced with an oil bath. The reaction solution was then refluxed for 4.0 hrs using oil bath heat as necessary. The Dewar condenser was kept cold by dry ice replenishment. The yield of 2-furyllithium was not determined but assumed to be 77% (34 mmoles) as reported by Ramanathan and Levine. Because of the instability of 2-furyllithium in ether it was carboxylated immediately.

### iii. High Vacuum Micro-Carboxylation of 2-Furyllithium

A 5 ml aliquot of ethereal 2-furyllithium was diluted to 50 ml in a dry nitrogen filled flask and a 10 ml (0.77 mmole/assumed) aliquot transferred to a dry, nitrogen-filled 25 ml pear-shaped flask. The pear flask was immediately connected to the high vacuum manifold and frozen with a Dewar filled liquid nitrogen flask. The reader is referred to Figure 3.10 for a graphic representation of the following sample treatments. With the sample still frozen valve A was opened and the system allowed to pump down for 10 minutes. Valve A was then closed and the liquid nitrogen Dewar flask removed and the sample allowed to thaw to room temperature. This freeze-thaw degassing procedure was



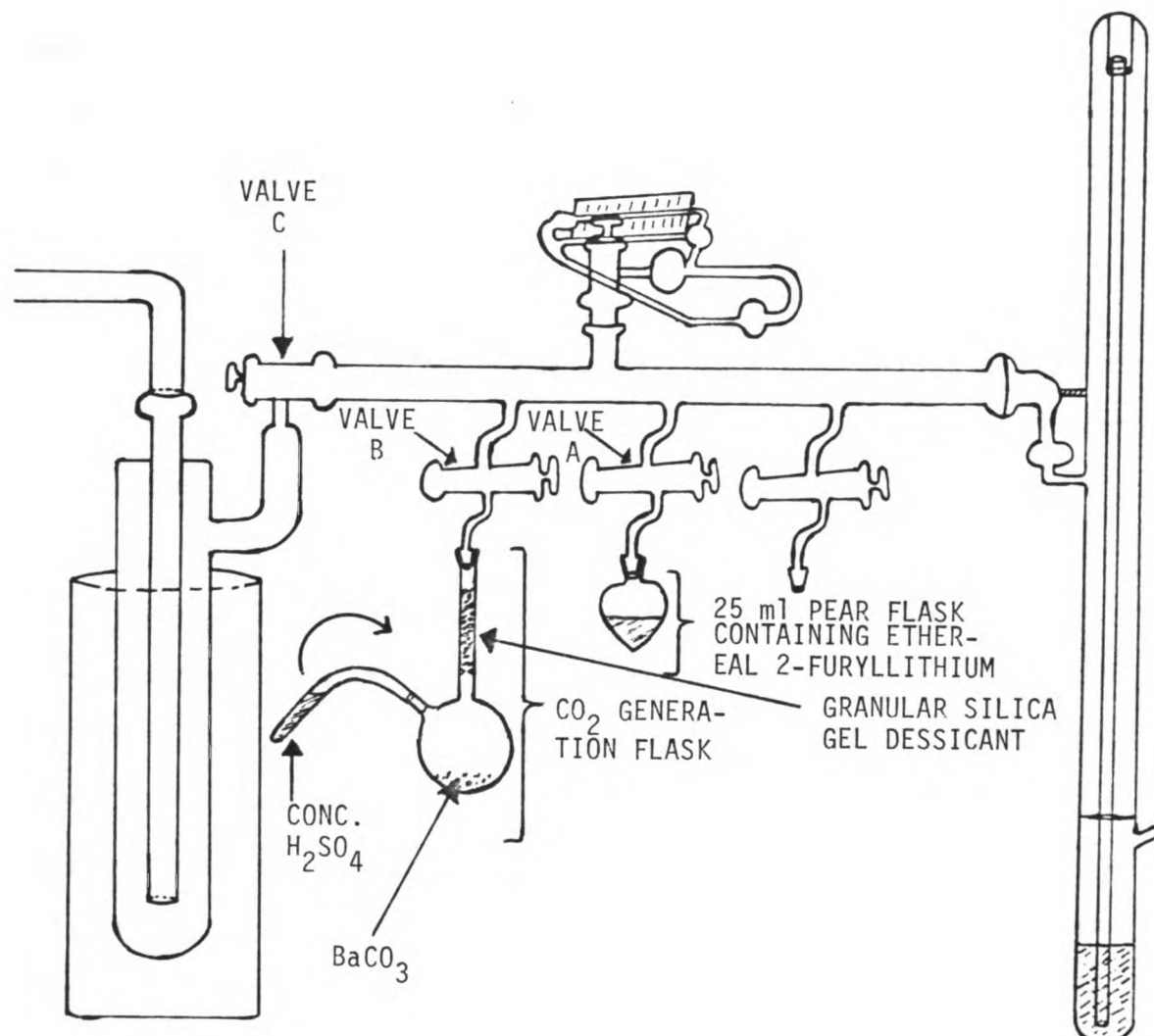


**FIGURE 3.10**

**HIGH VACUUM MANIFOLD  
(KONTES, K-925100)  
CARBOXYLATION OF 2-FURYL LITHIUM**

repeated and the sample again frozen with liquid nitrogen. The carbon dioxide generating flask, containing the barium carbonate, was attached to the manifold at valve B, both valves A and B opened and the system pumped down to a vacuum of less than 0.0005 mmHg. Valve C was then closed and the  $\text{H}_2\text{SO}_4$  tube on the carbon dioxide generating flask slowly rotated allowing the acid to drain onto the barium carbonate releasing carbon dioxide through the silica gel desiccant. This carbon dioxide condensed in the frozen 2-furyllithium. Valve A was closed after all the carbon dioxide had condensed and the liquid nitrogen Dewar replaced with a dry ice/acetone containing Dewar. The carboxylation was allowed to go over night at the temperature of the dry ice/acetone bath.

iv. Lithium 2-Furoate Extraction, Ethylation, and HPLC Analysis

After over night carboxylation, 10 ml water was added to dissolve the solids and the combined two-phase mixture transferred quantitatively to a 125 ml separatory funnel with an additional 10 ml water and 25 ml ethyl ether. The contents were shaken, the phases allowed to separate and the aqueous phase drawn off into another 125 ml separatory funnel. The remaining ether phase was then extracted twice with water and the aqueous extracts drawn into the same separatory funnel to insure complete removal of lithium 2-furoate. The combined aqueous extracts were acidified with 1.0 ml concentrated HCl and the 2-furoic acid extracted 3 times with 20 ml ethyl ether. The combined ethereal extracts were then ethylated with excess diazoethane and assayed for ethyl 2-furoate, as described previously.

c. Results

Table 3.1 shows the yield of ethyl 2-furoate from four separate trials. The results indicate that increasing amounts of furan increased ethyl 2-furoate yield probably because more complete reaction of the furan with n-butyllithium at the higher ratios resulted in exclusive carboxylation of 2-furyllithium.

3. Purification of Ethyl 2-Furoate for Nitration

a. Background

The purity of the ethyl 2-furoate in trial #4 (Table 3.1) was investigated by evaporating the ether and attempting to nitrate the residue as described on p 68. The results indicated that the ethyl 2-furoate residue contained impurities that significantly interfered with the nitration reaction. Therefore, it was necessary to develop a purification procedure that separated the ethyl 2-furoate from interfering substances without significantly lowering the yield.

Development of the purification procedure was undertaken in three steps. First, silicic acid column chromatography of the ethyl 2-furoate was investigated. Second, the stability of ethyl 2-furoate in different solvents was tested. Finally, a procedure was developed that incorporated the results of the first two steps.

b. Materials and Methods

i. Silicic Acid Column Chromatography of Ethyl 2-Furoate

Silicic acid column chromatograms of ethyl 2-furoate (Aldrich

TABLE 3.1  
 ETHYL 2-FUROATE YIELDS  
 FROM CARBOXYLATION OF 2-FURYLITHIUM

TRIAL #	BaCO <sub>3</sub> USED IN CARBOXYLATION		FURAN USED FOR 2-FURYLITHIUM		ETHYL 2-FUROATE YIELD	
	mg	mmoles	ml	mmoles	mmoles <sup>a</sup>	% YIELD <sup>b</sup>
1	98.3	0.498	3.0	41.2	0.269	54%
2	101.1	0.512	6.0	82.4	0.404	79%
3	95.4	0.483	9.0	124	0.454	94%
4	100.1	0.507	10.0	137	0.512	101%

a As determined by HPLC assay

b As % of BaCO<sub>3</sub>

Chemical Company, Milwaukee, Wisconsin) using Bio-Sil A/100-200 mesh (Bio-Rad, Richmond, California) are shown in Figure 3.11. Different relative amounts of hexanes and ethyl acetate were used as eluents to obtain a retention time of approximately ten minutes. Sample application was done in both ethyl ether and the eluent being used to determine the effect of ethyl ether as a sample loading solvent. Fractions of 8.6 ml were collected and assayed for ethyl 2-furoate. The HPLC assay used a 10u C<sub>18</sub>-uBondapak column (Waters Associates, Milford, Massachusetts), 50% MeOH/H<sub>2</sub>O mobile phase at 2.0 ml/min and UV detection at 280 nm.

The silicic acid column chromatographs indicated that sample application in ethyl ether caused spreading and tailing of the peak. In addition the retention time of ethyl 2-furoate was quite sensitive to the relative amount of ethyl acetate in the eluent. Reasonable retention times and peak shapes were achieved using a 1.5 cm X 17 cm column and a 98/2 hexanes/ethyl acetate (V/V) mobile phase with sample application in the eluting solvent. The next step in the purification of ethyl 2-furoate consisted of determining how to best remove the solvents, ethyl ether and hexanes/ethyl acetate, 98/2 (V/V), from solutions of ethyl 2-furoate in order to minimize solute degradation.

ii. Solvent Removal Techniques on Solutions of Ethyl 2-Furoate in Ethyl Ether and Hexanes/Ethyl Acetate, 98/2 (V/V)

Two different solvent removal techniques were investigated. One technique consisted of blowing a light stream of dry nitrogen gas on the solution of ethyl 2-furoate with oil bath heat applied at a temperature

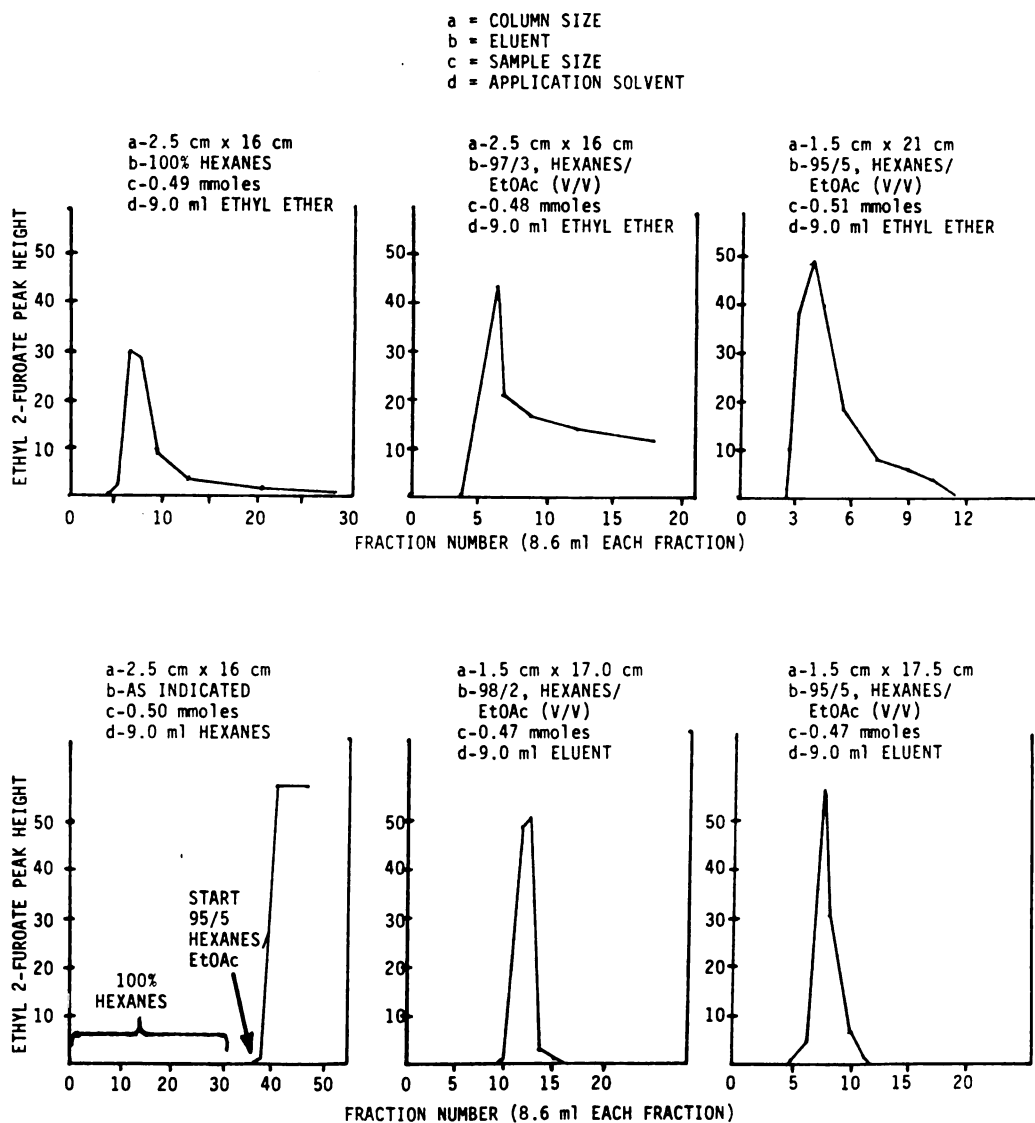


FIGURE 3.11

SILICIC ACID COLUMN CHROMATOGRAMS OF ETHYL 2-FUROATE

that allowed solvent removal to dryness to occur in 20 to 40 minutes. The other technique was roto-evaporative removal of the solvent at the reduced pressure supplied by a water vacuum aspirator at a significantly lower temperature.

Results of the amount of ethyl 2-furoate remaining after these solvent removal techniques are shown in Table 3.2. In addition Table 3.2 gives the results when the residue was reconstituted with a small amount of ethereal diazoethane in an attempt to re-esterify any 2-furoic acid that may have formed as a result of solvolysis. Ethyl 2-furoate was analyzed by HPLC as previously described.

The results in Table 3.2 indicate that solvent removal with minimal loss of ethyl 2-furoate occurs best at the lowest practical temperature. Also, reconstitution with ethereal diazoethane does not increase recovery suggesting ethyl 2-furoate loss is not simply loss of the ester. From the data in Table 3.2 it was decided that the best solvent removal technique was roto-evaporation at low temperatures.

### c. Results

From the results of the silicic acid column chromatography and solvent removal studies it was decided that the best method for purifying the ethyl 2-furoate was to use silicic acid column chromatography with 98/2 (V/V) hexanes/ethyl acetate as the mobile phase. Following diazoethane esterification, the ethyl ether would be removed by roto-evaporation at 2<sup>0</sup>C. Eluent solvent removal following chromatography would be done by roto-evaporative removal at 10<sup>0</sup>C.

In order to test the efficiency with which this purification technique removed interfering impurities in the nitration reaction

TABLE 3.2

## SOLVENT REMOVAL FROM SOLUTIONS OF ETHYL 2-FUROATE

AMOUNT ETHYL 2-FUROATE mg      mmoles		SOLVENT/VOLUME	SOLVENT REMOVAL TECHNIQUE	% ETHYL 2- FUROATE RECOVERED
69.8	0.498	Et <sub>2</sub> O/20 ml	N <sub>2</sub> BLOW DOWN WITH OIL BATH AT 60°C	94%
71.0	0.507	Et <sub>2</sub> O/20 ml	N <sub>2</sub> BLOW DOWN WITH OIL BATH AT 60°C FOLLOWED BY EXCESS DIAZOETHANE AND AGAIN N <sub>2</sub> BLOW DOWN AT 60°C	79%
69.4	0.495	Et <sub>2</sub> O/20 ml	ROTO-EVAPORATION WITH WATER ASPIRATOR VACUUM AND BATH AT 2°C	98%
70.6	0.504	$\frac{\text{HEXANES}}{\text{EtOAc}} / 40 \text{ ml}$ $\frac{98}{2}$	N <sub>2</sub> BLOW DOWN WITH OIL BATH AT 95°C	67%
70.4	0.502	$\frac{\text{HEXANES}}{\text{EtOAc}} / 40 \text{ ml}$ $\frac{98}{2}$	N <sub>2</sub> BLOW DOWN WITH OIL BATH AT 95°C FOLLOWED BY EXCESS DIAZOETHANE AND AGAIN N <sub>2</sub> BLOW DOWN AT 95°C	62%
76.1	0.543	$\frac{\text{HEXANES}}{\text{EtOAc}} / 40 \text{ ml}$ $\frac{98}{2}$	ROTO-EVAPORATION WITH WATER ASPIRATOR VACUUM AND BATH AT 10°C	87%



ethyl 2-furoate was prepared from 2-furyllithium and barium carbonate as previously described and then purified. Following purification the ethyl 2-furoate was nitrated as described below. Total yield of ethyl 5-nitro-2-furoate was then determined by HPLC as described on p 70.

The silicic acid column length was decreased to determine if a shorter column could be used in the purification procedure. Table 3.3 gives total yield of ethyl 5-nitro-2-furoate following the purification procedure as a function of the length of the silicic acid column. At a column length of 3.0 cm yellow impurity color in the ethyl 2-furoate solution was just separated. Shorter columns were not tested because the collected ethyl 2-furoate eluent contained significant color from impurities. In all subsequent procedures a 3.0 cm column was used.

C. Development of Maximum Yield in Sufficient Purity of Ethyl 5-Nitro-2-Furoate from Ethyl 2-Furoate

1. Background

Ethyl 2-furoate was nitrated by the method of Prousek et al. (84). The procedure was modified for microscale quantities and three purification techniques investigated to obtain the best yield of acceptable purity for condensation with biguanide.

2. Materials and Methods

a. Nitration of Ethyl 2-Furoate

Ethyl 2-furoate (Aldrich Chemical Company, Milwaukee, Wisconsin) (approximately 0.50 mmole) was placed in a 5 ml pear-shaped flask

TABLE 3.3

YIELD OF ETHYL 5-NITRO-2-FUROATE FROM 2-FURYLLITHIUM AND  
 $\text{BaCO}_3$  WITH SILICIC ACID COLUMN CHROMATOGRAPHIC PURIFICATION  
 USING DIFFERENT LENGTHS OF SILICIC ACID COLUMN

BaCO <sub>3</sub> USED AS CO <sub>2</sub> SOURCE IN CARBOXYLATION		SILICIC ACID COLUMN LENGTH, 1.5 cm DIA.	ETHYL 5-NITRO-2- FUROATE YIELD		
mg	mmole		mg	mmole	% YIELD <sup>a</sup>
99.2	0.503	17.0 cm	37.6	0.203	40.3%
98.0	0.496	11.0 cm	37.8	0.204	41.2%
98.5	0.499	7.0 cm	38.9	0.210	42.1%
96.5	0.489	4.0 cm	38.3	0.207	42.3%
96.8	0.490	3.0 cm	38.3	0.207	42.2%

a Based on BaCO<sub>3</sub>

containing a small magnetic triangular stir bar. Acetic anhydride (135  $\mu$ l) was added and the contents magnetically stirred until they were completely solubilized. The contents of the flask were then cooled to  $-20^{\circ}\text{C}$  in a dry ice/carbon tetrachloride bath while the nitrating reagent was prepared. The nitration reagent was prepared by adding 575  $\mu$ l  $\text{HNO}_3$  ( $d=1.5$ ) (Mallinckrodt, Paris, Kentucky) dropwise to 1.29 ml acetic anhydride at  $-20^{\circ}\text{C}$  with magnetic stirring. A 530  $\mu$ l aliquot of the nitrating mixture was then added dropwise to the cold acetic anhydride/ethyl 2-furoate solution and the nitration allowed to proceed for 1.0 hr at  $-20^{\circ}\text{C}$ . After 1.0 hr, 1.41 ml water and 310  $\mu$ l pyridine (Mallinckrodt AR, Paris, Kentucky) were added and the flask gradually heated to  $50^{\circ}\text{C}$  with an oil bath. After 15 min of heating at  $50^{\circ}\text{C}$  the solution was either directly analyzed for ethyl 5-nitro-2-furoate by HPLC or treated as described on pp 71-73.

b. HPLC Analysis of Ethyl 5-Nitro-2-Furoate

Diluted ethanolic solutions of ethyl 5-nitro-2-furoate were quantitated by HPLC using a 10 $\mu$   $\text{C}_{18}$ - $\mu$ Bondapak 3.9 mm X 30 cm column (Waters Associates, Milford, Massachusetts) with 50% MeOH/ $\text{H}_2\text{O}$  mobile phase at 2.0 ml/min, 20  $\mu$ l injection volumes, and UV detection at 280 nm. External standards of 29, 87, 145, and 232 mcgms/ml were used for the standard curve. The ethyl 5-nitro-2-furoate eluted at 4.0 minutes. The data was fitted using least squares linear regression analysis to construct a standard curve.

c. Purification of Ethyl 5-Nitro-2-Furoate from the Nitration Reaction Mixture for Condensation with Biguanide

i. Background

The three different techniques of silicic acid column chromatography, liquid/liquid ether extraction, and fractional crystallization were investigated as purification methods. Each method was evaluated for efficiency in removing impurities by submitting the purified ethyl 5-nitro-2-furoate to biguanide condensation, as described on p 77, and assaying for the resulting 2,4-diamino-6-(5-nitro-2-furyl)-1,3,5-triazine product by HPLC. The purification technique that gave the best yield was then selected as the one of choice for use in the microsynthesis.

ii. Silicic Acid Column Chromatography

The pyridine neutralized nitration reaction mixture was applied to the top of a 17 cm X 2.5 cm silicic acid column (Bio-Sil A, 100-200 mesh, Bio-Rad, Richmond, California) equilibrated with the carbon tetrachloride mobile phase. Ethyl 5-nitro-2-furoate was eluted (fractions 13 through 20) in 8.1 ml fractions. The previously described HPLC assay was used to determine relative amount of ethyl 5-nitro-2-furoate in each fraction (Figure 3.12). The fractions containing the product were combined and roto-evaporated to dryness and the residue submitted to biguanide condensation as described on p 77. The column size and carbon tetrachloride eluent were chosen to give complete separation of the desired product from the yellow/brown colored impurities.

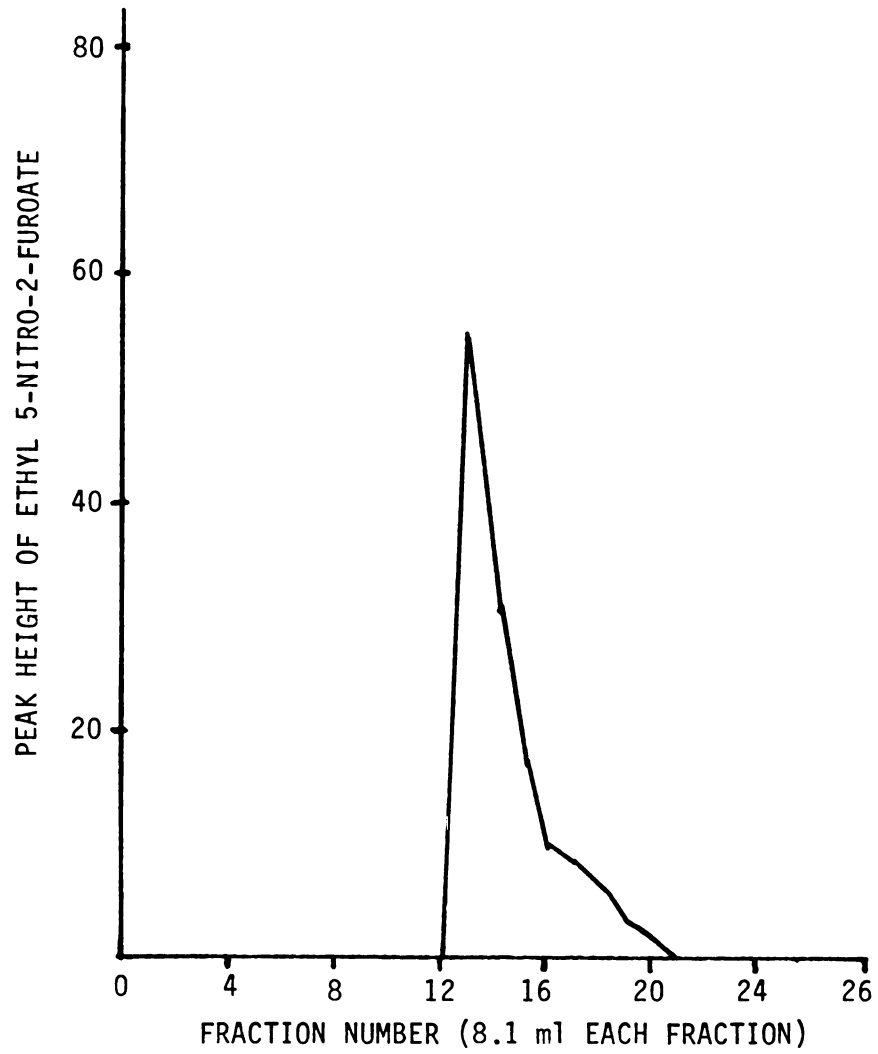


FIGURE 3.12

SILICIC ACID COLUMN CHROMATOGRAM OF THE SEPARATION  
OF ETHYL 5-NITRO-2-FUROATE FROM THE NEUTRALIZED  
NITRATION REACTION MIXTURE

### iii. Liquid/Liquid Ether Extraction

The pyridine neutralized nitration reaction mixture was transferred to a liquid/liquid ether extractor (Kontes, K-291700, San Leandro, California) and extracted for four hours with 25 ml of ethyl ether. The ether was then removed from the extract by roto-evaporation and the residue condensed with biguanide as described on p 77.

### iv. Fractional Crystallization

The pyridine neutralized nitration reaction mixture was transferred to a 25 ml microfiltration flask (Figure 3.13) containing a small triangular magnetic stir bar with one 10 ml portion of water rinsings for quantitative transfer. The mixture was stirred vigorously for two minutes and placed in an ice bath to crystallize out the ethyl 5-nitro-2-furoate. After 30 min in the ice bath the crystals were filtered by attaching a vacuum source to the microfiltration flask as pictured in Figure 3.13. The crystals were washed with an additional 6.0 ml ice cold water and filtered. A drying tube containing color indicating granular silica gel as desiccant was attached to the ground-glass fitting on the apparatus and the crystals dried by applying a vacuum and forcing dry air through the crystals. After 2.0 hrs of drying the crystals were condensed with biguanide as described on p 77.

## 3. Results

The yields of ethyl 5-nitro-2-furoate resulting from nitration of ethyl 2-furoate and each separate purification technique investigated are given in Table 3.4. Also in Table 3.4 are the yields of 2,4-diamino-6-(5-nitro-2-furyl)-1,3,5-triazine (II) obtained following biguanide

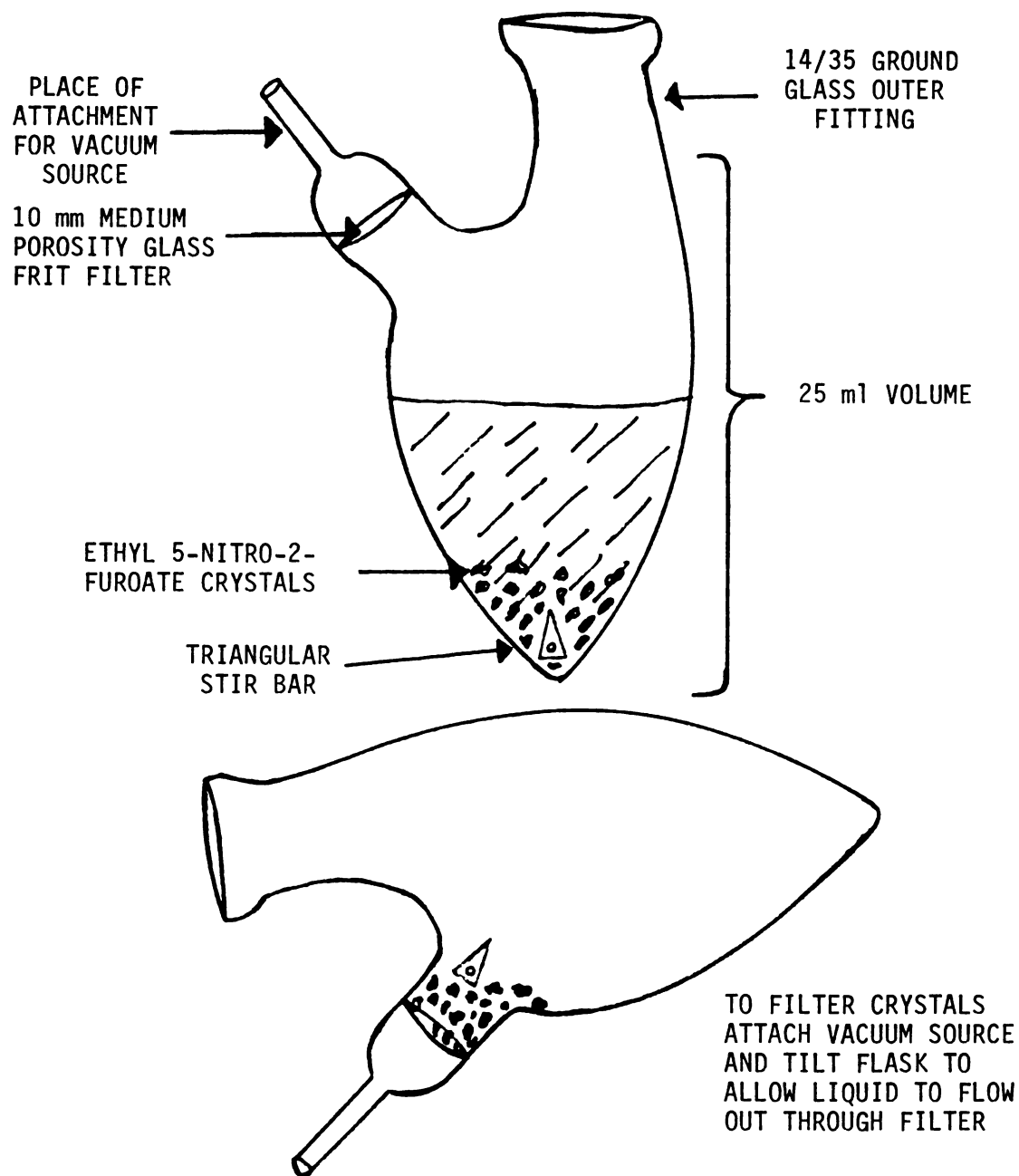


FIGURE 3.13

25 ml MICROFILTRATION FLASK

TABLE 3.4

YIELDS OF ETHYL 5-NITRO-2-FUROATE AND 2,4-DIAMINO-6-(5-NITRO-2-FURYL)-1,3,5-TRIAZINE (II) FROM NITRATION OF ETHYL 2-FUROATE FOLLOWED BY BIGUANIDE CONDENSATION

AMOUNT ETHYL 2-FUROATE		PURIFICATION TECHNIQUE	YIELD OF ETHYL 5-NITRO-2-FUROATE		YIELD (II)	
mg	mmole		mmole	% YIELD <sup>a</sup>	mmole	% YIELD <sup>a</sup>
69.2	0.494	SILICIC ACID COLUMN CHROM- ATOGRAPHY	0.224	45.3%	0.0188	3.8%
69.8	0.498	LIQUID/LIQUID ETHER EXTRAC- TION	0.234	47.0%	0.0085	1.7%
69.9	0.499	FRACTIONAL CRYSTALLIZATION	0.181	36.2%	0.108	21.7%

a Based on ethyl 2-furoate



condensation as described on p 77.

The results indicate unacceptable interfering impurities in the subsequent biguanide condensation reaction in the samples purified by silicic acid column chromatography and liquid/liquid ether extraction. The samples purified by fractional crystallization resulted in an isolated yield of 36.2% ethyl 5-nitro-2-furoate and a total yield of 21.7% 2,4-diamino-6-(5-nitro-2-furyl)-1,3,5-triazine (II) from ethyl 2-furoate. Therefore fractional crystallization was selected as the method of choice.

D. Development of Maximum Yield in Sufficient Purity of 2,4-Diacetyl-amino-6-(5-Nitro-2-Furyl)-1,3,5-Triazine from Ethyl 5-Nitro-2-Furoate

1. Background

The isolated yield of ethyl 5-nitro-2-furoate, 0.18 mmole, was used as the starting amount in the development of the final synthesis of 2,4-diamino-6-(5-nitro-2-furyl)-1,3,5-triazine (II) from the biguanide condensation with ethyl 5-nitro-2-furoate was first investigated for dependence on the source of biguanide, reaction solvent, and solvent volume. After these parameters were maximized for yield, (I) was prepared by acetylation of (II) with acetic anhydride and the yield determined without regard to purity. The stability of impure (I) in acetic anhydride was then investigated to determine suitability for storage in this solvent.

Because the final acetic anhydride suspension of (I) was black in color and obviously very impure, it was necessary to develop a purification technique that gave (I) in acceptable chemical and radiochemical purity for use in metabolism studies. Methods of purification were

evaluated by the color of the final purified material in acetic anhydride solution. Three different purification techniques were considered. First, silicic acid column chromatography and activated charcoal absorption of (I) were investigated. When these two purification techniques were determined to be unacceptable, fractional crystallization of (II) was attempted.

## 2. Biguanide Condensation, Acetylation, and Stability Studies

### a. Materials and Methods

#### i. Biguanide Condensation with Ethyl 5-Nitro-2-Furoate

Biguanide was condensed with ethyl 5-nitro-2-furoate according to a scaled down procedure patented by Abbott Laboratories (66). Ethyl 5-nitro-2-furoate (0.18 mmole) was placed into a 10 ml pear-shaped flask containing a small triangular magnetic stir bar. Then, 350 or 1000  $\mu$ l of methanol or ethanol was added and the suspension stirred. Biguanide (0.34 mmole) was dissolved in either 350 or 1000  $\mu$ l of methanol or ethanol for solvent and solvent volume trials. The biguanide was either obtained from Aldrich Chemical Company or synthesized as described on p 26.

The biguanide solution was then added to the ethyl 5-nitro-2-furoate suspension and the mixture was stirred overnight at room temperature in the absence of light. Dimethyl sulfoxide was added to the resulting tan colored suspension to dissolve the solids and the solution made to 25 ml in a volumetric flask with additional dimethyl sulfoxide. Three ml of this solution was diluted to 50 ml with ethanol. The yield of

(II) was then determined by HPLC assay of the ethanol diluted solution as described below.

ii. HPLC Analysis of 2,4-Diamino-6-(5-Nitro-2-Furyl)-1,3,5-Triazine and 2,4-Diacetylamino-6-(5-Nitro-2-Furyl)-1,3,5-Triazine

HPLC analysis of (I) and (II) were done using a 10 $\mu$  Bondapak C<sub>18</sub> 3.9 mm X 30 cm column (Waters Associates, Milford, Massachusetts) with 50% MeOH/H<sub>2</sub>O mobile phase at 2.0 ml/min and detection at 280 nm. Injection volumes were 15  $\mu$ l. External standards of (I) and (II) at 11.0, 33.0, 55.0, and 88.0 mcgms/ml were used for quantitation. Retention times of (I) and (II) were 4.3 and 2.3 minutes respectively. Standard curves were constructed by least squares linear regression analysis of peak height versus concentration.

iii. Acetylation of 2,4-Diamino-6-(5-Nitro-2-Furyl)-1,3,5-Triazine

Acetylation of (II) was done according to the method of Sherman (65). First the alcohol was removed from the biguanide condensation suspension by roto-evaporation. The dry residue was suspended in 4.0 ml acetic anhydride, a reflux condenser attached to the flask, and the mixture heated to reflux for 2.0 hours. After cooling the resulting suspension of (I) was solubilized and diluted with DMSO and ethanol as described above for (II). The reaction mixture was analyzed by HPLC.

iv. Stability of 2,4-Diacetylamino-6-(5-Nitro-2-Furyl)-1,3,5-Triazine

The stability of impure (I) following acetylation in acetic anhydride was investigated to determine suitability for storage in this

solvent. Stability at room temperature in the absence of light was determined over a two week period. At each point of determination the acetic anhydride suspension of (I) was heated to dissolve any crystallized (I) and then cooled to room temperature. Before any recrystallization of (I) had occurred a small aliquot was taken and analyzed for (I) by HPLC as described previously.

#### b. Results

Table 3.5 shows yields of (II) as a function of biguanide source, solvent, and solvent volume. The results indicate that the synthetic biguanide is superior to that obtained from Aldrich. There is no dependence of yield on solvent volume or methanol. Because sample manipulation is easier with the larger volume and ethyl 5-nitro-2-furoate stability greater in ethanol, these conditions were chosen for the condensation reaction.

Table 3.6 summarizes the stability of impure (I) in acetic anhydride. The results are expressed in terms of per cent of the concentration immediately following acetylation. The results indicate a suspension of (I) in acetic anhydride was suitable for storage.

### 3. Final Purification Studies

#### a. Materials and Methods

##### i. Silicic Acid Column Chromatography

A impure solution of (I) in acetic anhydride was prepared from ethyl 5-nitro-2-furoate condensation with biguanide and acetylation as

TABLE 3.5

DEPENDENCE OF YIELD OF 2,4-DIAMINO-6-(5-NITRO-2-FURYL)-  
1,3,5-TRIAZINE (II) ON BIGUANIDE SOURCE,  
SOLVENT, AND SOLVENT VOLUME

ETHYL 5-NITRO- 2-FUROATE USED		BIGUANIDE SOURCE	SOLVENT USED	TOTAL SOLVENT VOLUME	YIELD (II)	
mg	mmole				mmole	% YIELD <sup>a</sup>
34.7	0.187	ALDRICH	EtOH	700 u1	0.0748	40%
32.3	0.175	ALDRICH	EtOH	2000 u1	0.0700	40%
32.8	0.177	ALDRICH	MeOH	2000 u1	0.0726	41%
33.6	0.181	SYNTHETIC	EtOH	2000 u1	0.105	58%
32.1	0.173	SYNTHETIC	MeOH	2000 u1	0.106	61%

a Based on ethyl 5-nitro-2-furoate

TABLE 3.6

STABILITY OF 2,4-DIACETYLAMINO-6-(5-NITRO-2-FURYL)-  
1,3,5-TRIAZINE (I) AS A SUSPENSION  
IN ACETIC ANHYDRIDE

TIME AFTER ACETYLATION (DAYS)	PER CENT OF THE CONCENTRATION AT TIME IMMEDIATELY FOLLOWING ACETYLATION
0	100%
3	101%
6	102%
10	98%
14	97%

previously described (pp 77 & 78). A 500 ul aliquot containing 4.1 mg (I) was applied to the top of a 10 cm X 0.9 cm silicic acid column (Bio-Sil A/100-200 mesh, Bio-Rad, Richmond, California) and eluted with acetic anhydride. Fractions (3.0 ml) were collected and the relative amount of (I) determined in each fraction by HPLC as previously described. Fractions containing (I) were combined and the purity evaluated by color of the acetic anhydride solution of purified (I).

ii. Activated Charcoal Adsorption

Three impure solutions of (I) in acetic anhydride were prepared from ethyl 5-nitro-2-furoate condensation with biguanide and acetylation as previously described. Each solution was used in a separate trial to investigate impurity adsorption following addition of activated charcoal. After addition of 99, 204, or 311 mg of activated charcoal (Aldrich Chemical Company, Milwaukee, Wisconsin), the suspensions were heated to boiling for 10 min, a small amount of filter-aid (Aldrich Chemical Company, Milwaukee, Wisconsin) added to facilitate filtration of the fine particles, and the suspensions filtered through a medium porosity glass frit while still hot. The charcoal/filter-aid cake was then washed with 10 ml hot acetic anhydride and the resulting solution evaluated for purity by solution color. Because of the possibility that (I) may have irreversibly adsorbed to the activated charcoal the yield of (I) was determined by HPLC.

iii. Fractional Crystallization

A suspension of (II) in alcohol was prepared by condensation of ethyl 5-nitro-2-furoate with biguanide in a 25 ml microfiltration flask

(Figure 3.13). Dimethyl sulfoxide (3.0 ml) was added and the suspension magnetically stirred until all solids were in solution. Water (20 ml) was added, the solution stirred vigorously for 10 min, and (II) allowed to crystallize after placing the flask in a freezer at  $-10^{\circ}\text{C}$  for 1.0 hour. Following crystallization a small amount of filter-aid was added and the soluble impurities filtered by vacuum as pictured in Figure 3.13. The fine crystals of (II) intermixed with the filter-aid were further washed twice with 12 ml water and once each with 12 ml portions of methanol and ethyl ether.

The purified crystals of (I) intermixed in filter-aid were acetylated by refluxing for 2.0 hrs in 9.0 ml acetic anhydride. While still hot, the solution of purified (I) in acetic anhydride was filtered off by vacuum and the purity evaluated by solution color. Yields of (I) were determined by HPLC.

#### b. Results

Figure 3.14 shows the silicic acid column chromatogram of impure (I). As (I) was eluted most of the dark colored polar impurities were retained on the column. However, (I) did not elute as a single peak, but as a very broad split peak that contained significant amounts of colored impurities. Solvent systems of lesser eluting strength were not tested because of impractically low solubility of (I) in any less polar solvents.

Table 3.7 summarizes results of the purity of (I) obtained in each of three methods investigated. Listed in the table are the yields of (I), where applicable, and the evaluation of purity by color of the solution. The technique of activated charcoal adsorption appears to irreversibly adsorb impurities and (I) to the same extent resulting in a prohibitively

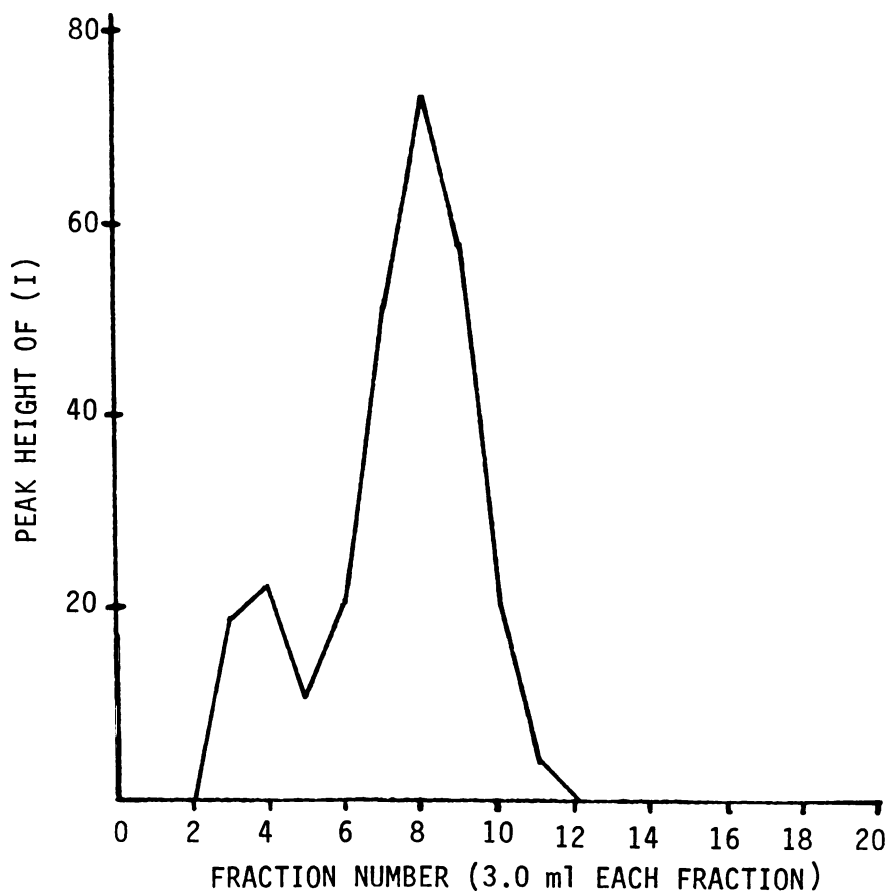


FIGURE 3.14

SILICIC ACID COLUMN CHROMATOGRAPHY OF IMPURE  
2,4-DIACETYLAMINO-6-(5-NITRO-2-FURYL)-1,3,5-TRIAZINE (I)  
WITH ACETIC ANHYDRIDE ELUTION



TABLE 3.7  
 PURITY AND YIELD OF (I) FOLLOWING DIFFERENT  
 PURIFICATION TECHNIQUES

PURIFICATION TECHNIQUE	PURITY OF (I) AS DETERMINED BY COLOR OF ACETIC ANHYDRIDE SOLUTION	PER CENT YIELD <sup>a</sup> (I)
SILICIC ACID COLUMN CHROMATOGRAPHY	IMPURE (YELLOW SOLUTION)	—————
ACTIVATED 99 mg	IMPURE (BROWN/YELLOW SOLUTION)	42.6%
CHARCOAL 204 mg	IMPURE (YELLOW SOLUTION/BETTER THAN 99 mg SAMPLE)	25.5%
ADSORPTION 311 mg	FAIRLY PURE (LIGHT YELLOW SOLUTION)	14.7%
FRACTIONAL CRYSTALLIZATION	VERY PURE (VERY LIGHT YELLOW SOLUTION)	58.2%

a Based on amount of ethyl 5-nitro-2-furoate

high loss of (I). From these results fractional crystallization was chosen as the method of choice for purification.

E. Microsynthesis of 2,4-Diacetylamino-6-(5-Nitro-2-Furyl)-1,3,5-Triazine from 0.50 mmole Barium Carbonate

1. Background

All the individual steps for the synthesis of (I) from 0.50 mmole barium carbonate had been developed. All these steps were now combined to refine the synthetic technique and confirm yield. However, as described below, sample handling procedures were slightly altered to reduce sample handling, a desirable factor in radiochemical synthesis. The final yield of (I) was determined by HPLC analysis.

2. Materials and Methods

a. Carboxylation of 2-Furyllithium

Ethereal 2-furyllithium (0.77 mmole) prepared from n-butyllithium and 10.0 ml furan was carboxylated by high vacuum transfer of carbon dioxide from 96.8 mg (0.490 mmole) barium carbonate as described on p 59.

b. Acidification and Extraction of 2-Furoic Acid into Ethyl Ether

Water (7.0 ml) and a small triangular magnetic stir bar were added to the ethereal lithium 2-furoate suspension. This suspension was stirred vigorously until all solids were dissolved. The two phase mixture was transferred to a 125 ml separatory funnel by disposable pipet with one 50 ml portion of ethyl ether rinsings. The separatory funnel was

shaken for 2.0 min, the phases allowed to separate, and the lower aqueous phase drained off into a 10 ml beaker. Then, the aqueous phase was transferred to a liquid/liquid ether extractor (Figure 3.15) by disposable pipet. The aqueous extraction transfer process was repeated two times with 3.0 ml water. The aqueous solution in the liquid/liquid ether extractor was then extracted for 0.5 hr with 30 ml ethyl ether. The ethyl ether extract was then discarded and the aqueous solution acidified with 1.0 ml concentrated hydrochloric acid. This acidified aqueous solution was then extracted with fresh ethyl ether (30 ml) for 2.0 hours.

c. Ethyl Esterification and Purification of Ethyl 2-Furoate by Silicic Acid Column Chromatography

After 2.0 hrs of ether extraction the internal coil cold finger condenser was removed, thus, allowing the ether extract to concentrate down to a volume of approximately 5 ml. When the ether extract of 2-furoic acid had cooled to room temperature, excess diazoethane was added, as described on p 56. Following esterification, the solution was roto-evaporated to dryness in an ice bath at 2-4<sup>0</sup>C. The residue was reconstituted with 3.0 ml hexanes/ethyl acetate, 98/2 (V/V), solution and swirled until complete solution was achieved. The impure sample of ethyl 2-furoate was then transferred to the top of a 1.5 cm X 3.0 cm silicic acid column (Bio-Sil A, 100-200 mesh, Bio-Rad, Richmon, California) equilibrated with hexanes/ethyl acetate, 98/2 (V/V), as the mobile phase, and eluted. Fractions (8.6 ml) were collected and the presence of ethyl 2-furoate in each fraction determined by HPLC. Those fractions containing ethyl 2-furoate were combined in a 50 ml pear-shaped flask and the solvent removed by roto-evaporation with the sample in a

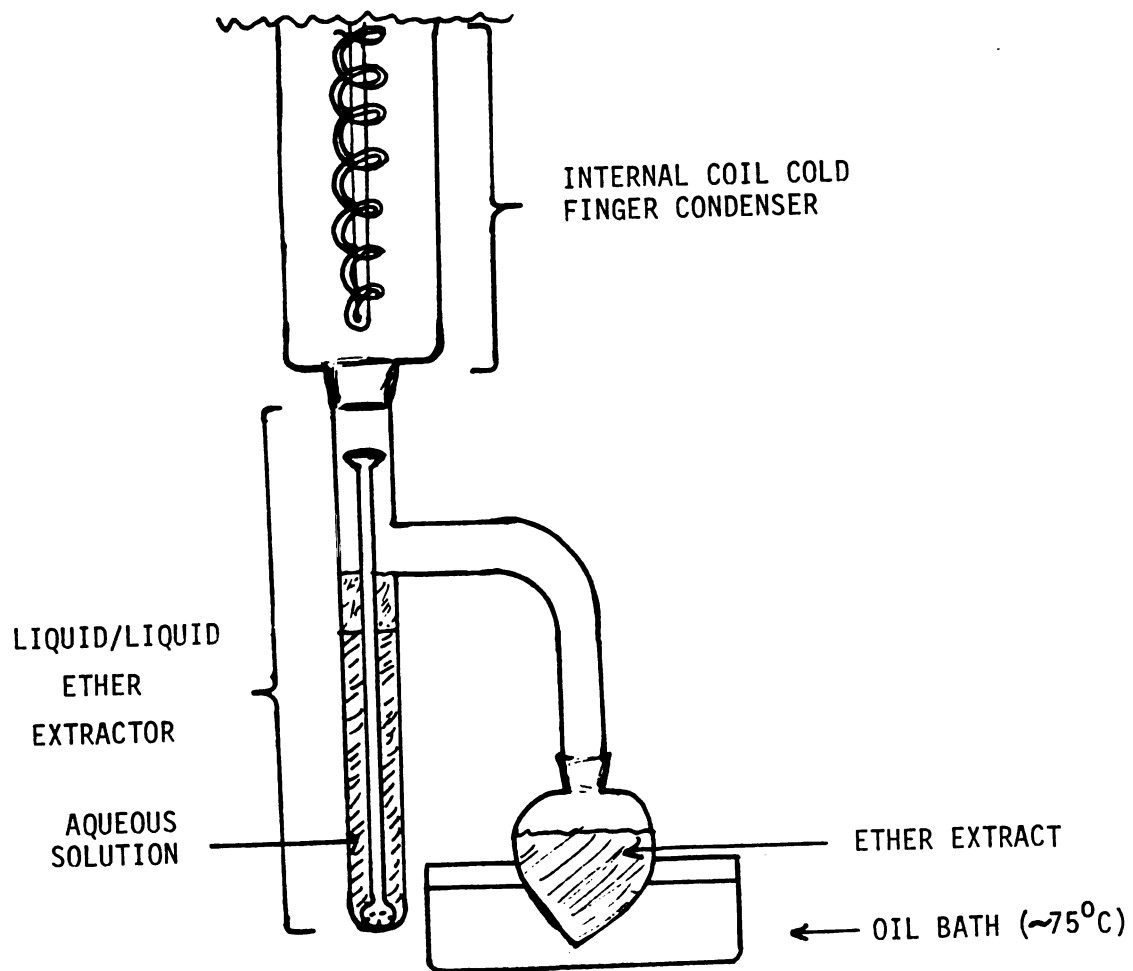


FIGURE 3.15

ETHER LIQUID/LIQUID EXTRACTOR

8-10<sup>0</sup>C bath in preparation for sample nitration.

d. Nitration of Ethyl 2-Furoate and Purification of Ethyl 5-Nitro-2-Furoate

The residue of purified ethyl 2-furoate was next nitrated and purified by fractional crystallization as described on pp 68 & 73.

e. Biguanide Condensation of Ethyl 5-Nitro-2-Furoate

Ethanol (1.0 ml) was added to the purified crystals of ethyl 5-nitro-2-furoate in the microfiltration flask by syringe through the glass frit filter. The filter opening was sealed with a septum and a cold finger condenser with drying tube on top attached to the flask. Heat from a oil bath (110<sup>0</sup>C) was applied to the bottom of the flask causing the ethanol to reflux up the sides bringing all the ethyl 5-nitro-2-furoate into solution at the bottom. After the ethanol solution had cooled to room temperature the sample was condensed with 34.4 mg (0.34 mmole) synthetic biguanide in 1.0 ml methanol as described on p 77.

f. Purification and Acetylation of 2,4-Diamino-6-(5-Nitro-2-Furyl)-1,3,5-Triazine

The suspension of (II) in alcohol was purified by fractional crystallization as described on p 73. Following purification (II) was acetylated as described on p 78.

3. Results

Analysis of (I) by HPLC gave a yield of 27.4 mg (0.0897 mmole). Based on the amount of barium carbonate used this resulted in a 18.3%

yield. This value was in agreement with the expected yield based on the preliminary work.

#### F. Summary

A microsynthesis of (I) starting with 0.50 mmole barium carbonate as the limiting precursor and giving 18% stoichiometric yield relative to barium carbonate has been developed. The overall synthetic scheme is outlined in Figure 3.16.

The microsynthesis was developed using non-radiolabeled barium carbonate and purity evaluation of the final product done by crude color comparison. To determine if the final product would be suitable for use in metabolism studies it was necessary to use C-14 barium carbonate and determine the radiochemical purity of the final product. If the final product proved to be of unacceptable radiochemical purity additional purification would be necessary.

### VI. Synthesis of 2,4-Diacetylamino-6-(5-Nitro-2-Furyl)-1,3,5-Triazine-(6-C-14)

#### A. Materials and Methods

Barium carbonate-(C-14) (0.55 mmole, 25.0 mCi, 45 mCi/mmole, New England Nuclear, Boston, Massachusetts) was used as the C-14 radiolabel to synthesize 2,4-diacetylamino-6-(5-nitro-2-furyl)-1,3,5-triazine-(6-C-14) according to the previously described methods (85). Yield, radiochemical purity, and specific activity were determined by HPLC using a 10 $\mu$  C<sub>18</sub>Bondapak 3.9 mm X 30 cm column (Waters Associates, Milford, Massachusetts) and 40% MeOH/H<sub>2</sub>O mobile phase and the other methods

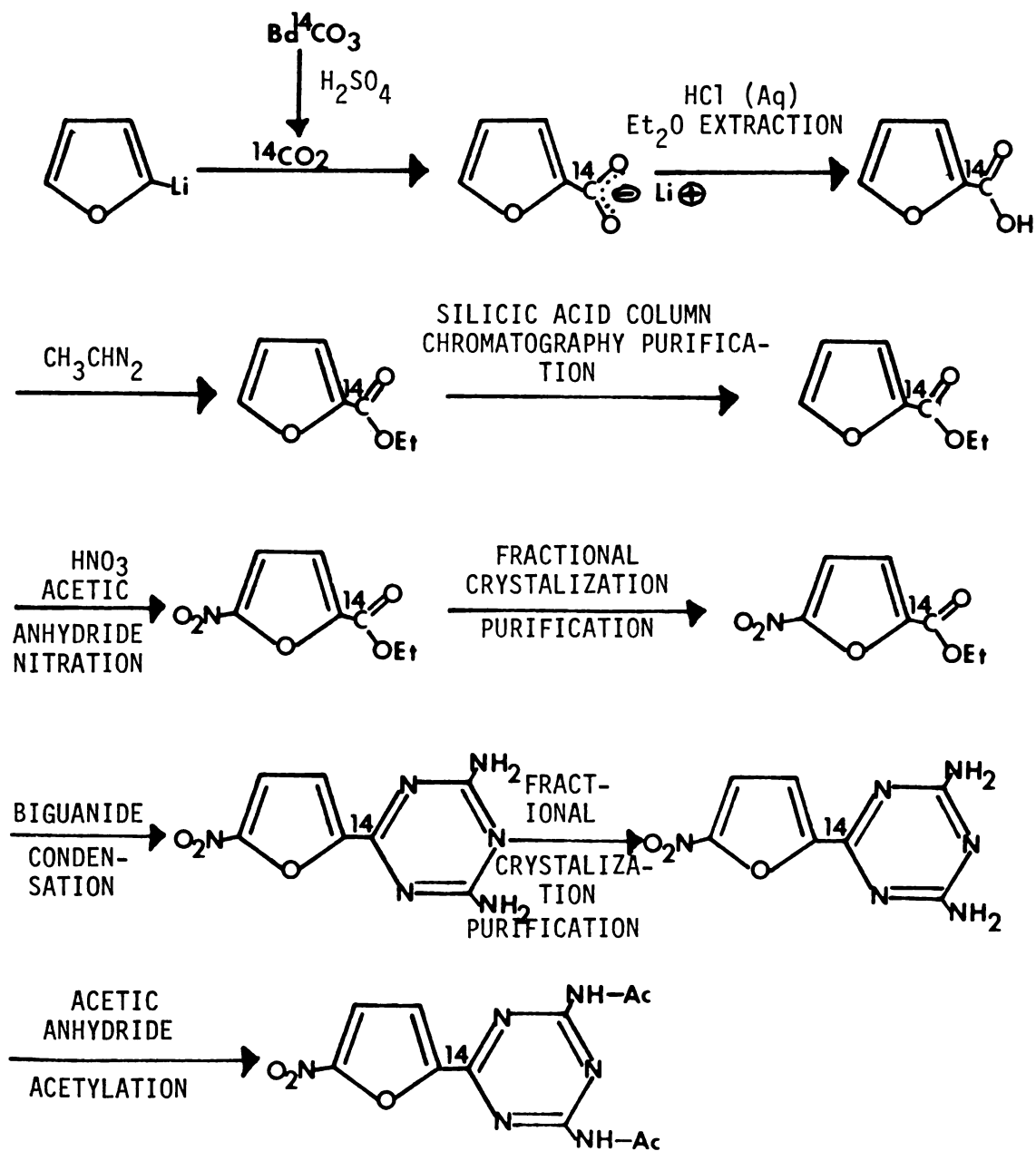


FIGURE 3.16

SYNTHETIC SCHEME FOR MICROSYNTHESIS OF  
 2,4-DIACETYLAMINO-6-(5-NITRO-2-FURYL)-1,3,5-TRIAZINE (I)

previously described for 2,4-diacetylamino-6-(5-nitro-2-furyl)-1,3,5-triazine-(acetyl-H-3) (p 36). Following the synthesis the solution of radiolabeled (I) was sealed and stored at  $-10^{\circ}\text{C}$  in the absence of light.

#### B. Results

The HPLC and radioactivity profile of the synthesized 2,4-diacetylamino-6-(5-nitro-2-furyl)-1,3,5-triazine-(6-C-14) is shown in Figure 3.17. A chemical yield of 0.123 mmole (22.3%) and a radiochemical yield of 5.31 mCi (21.2%) were determined by HPLC analysis. Similarly the radiochemical purity was determined to be 94.7%.

#### C. Discussion

The resulting yield of 22.3% was slightly higher than the yield obtained from the developed method (18.3%). The reason for the higher yield was probably because 0.55 mmole barium carbonate was used resulting in higher yields from the various purification techniques.

The radiochemical purity that results from the developed synthetic method was judged acceptable for use in metabolism studies.



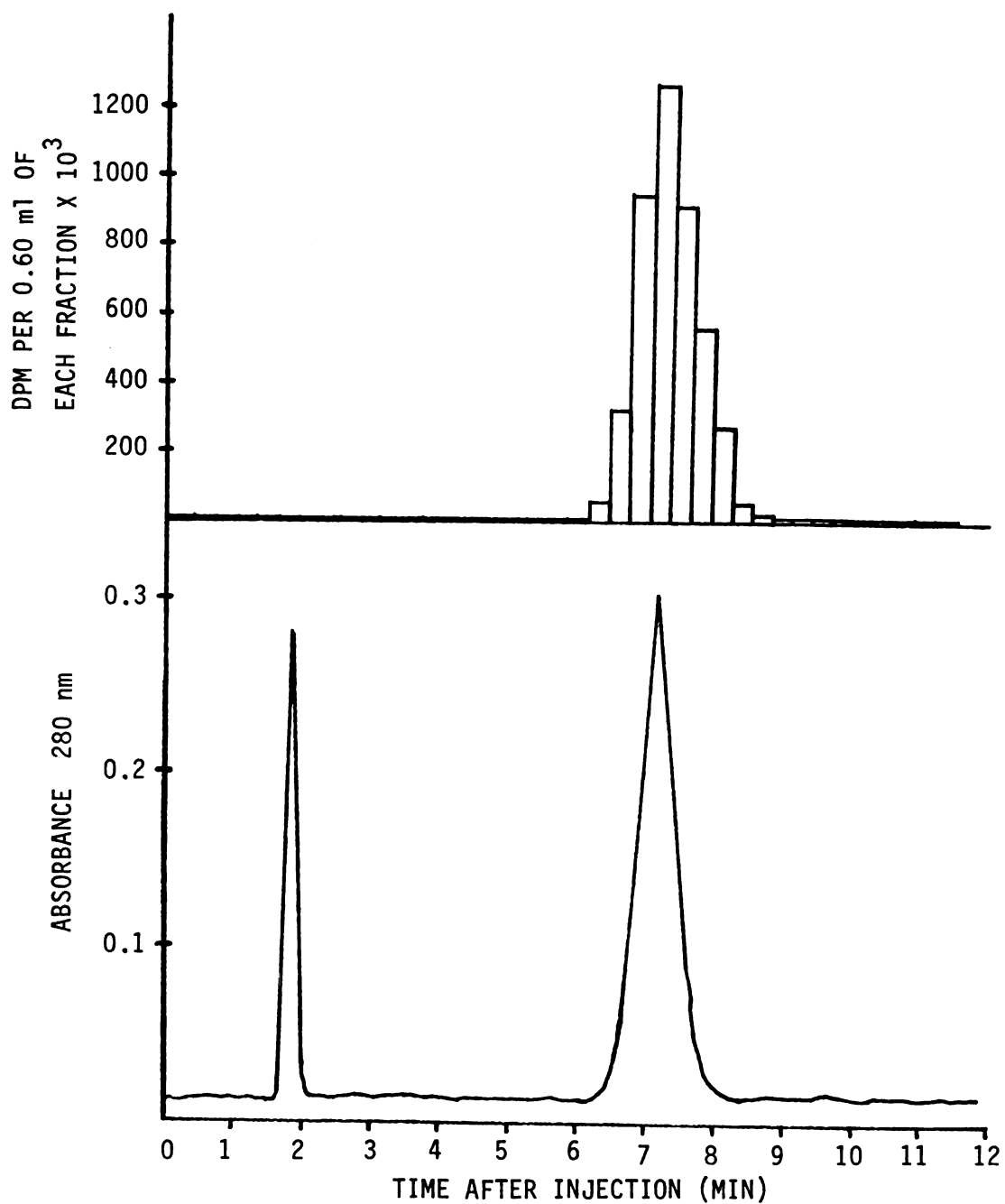


FIGURE 3.17

HPLC ABSORBANCE/RADIOACTIVITY PROFILE OF SYNTHESIZED  
2,4-DIACETYLAMINO-6-(5-NITRO-2-FURYL)-1,3,5-TRIAZINE-(6-<sup>14</sup>C)

## CHAPTER FOUR

ANAEROBIC IN VITRO REDUCTIVE METABOLISM OF  
2,4-DIACETYLAMINO-6-(5-NITRO-2-FURYL)-1,3,5-TRIAZINE

I. Background

The metabolism of (I) in vitro under anaerobic conditions was investigated using the three enzymatic systems, 9000xg rat liver homogenate supernatant, rat liver microsomes, and xanthine oxidase. The structures of the metabolites generated in these systems were elucidated by UV spectrometry, electron ionization mass spectrometry, and Fourier transform proton magnetic resonance spectrometry. The amino metabolite, 2,4-diacetylamino-6-(5-amino-2-furyl)-1,3,5-triazine (III), was prepared synthetically to confirm the structure. The relative rates of disappearance of (I) and appearance of the amino metabolite (III) were determined to define the conditions to be used in DNA binding studies. Using (I) radiolabeled with tritium and carbon-14 on the acetyl groups metabolism studies were done to determine the suitability of this position for DNA binding studies. These in vitro anaerobic metabolism studies were concluded with studies with 2,4-diacetylamino-6-(5-nitro-2-furyl)-1,3,5-triazine-(6-C-14) (I-C-14) to determine the total mass balance of (I) and its metabolites and to detect other metabolites in the 9000xg rat liver homogenate supernatant and xanthine oxidase incubation systems.

## II. Enzymatic Systems

### A. Preparation of 9000xg Rat Liver Homogenate Supernatant

Three male rats (Sprague-Dawley, 300 gms; Charles River Breeding Labs) were sacrificed by decapitation and the livers from each perfused with ice cold 1.15% KCl-10 mM potassium phosphate buffer pH 7.7 (buffer A) to remove blood. Each liver was then carefully removed from the animal, rinsed in two separate beakers of ice cold buffer A, blotted dry, and weighed. The livers were combined, minced into small pieces with scissors and homogenized in two parts (W/V) buffer A in a Potter-Elvehjem homogenizer with a Teflon pestle. The homogenate was then centrifuged for 20 min at 9000xg at 2°C in a Sorval RC-2 refrigerated centrifuge (Ivan Sorvall Inc., Norwalk, Connecticut) to remove nuclei and mitochondria. Finally the homogenate supernatant was filtered through cheese cloth to remove the fat layer and 4.0 ml aliquots placed in stoppered test tubes and stored at -10°C for up to three months before use in metabolism studies.

### B. Preparation of Rat Liver Microsomes

Because stability of nitroreductase activity in the microsomal preparation was unknown, only one rat was used to prepare a small amount of rat liver microsomal suspension which was used immediately in metabolism studies. The general method of liver microsome preparation of LaDu et al. (86) was used.

One male rat (Sprague-Dawley, 300 gms; Charles River Breeding Labs) was sacrificed by decapitation and the liver perfused with ice cold buffer A to remove blood. After carefully removing it, the liver was

rinsed twice in two separate beakers of ice cold buffer A, blotted dry, and weighed. The liver was then minced into small pieces with scissors and homogenized in five parts (W/V) of buffer A in a Potter-Elvehjem homogenizer with a Teflon pestle. The homogenate was then centrifuged for 20 min at 9000xg at 2<sup>0</sup>C in a Sorval RC-2 refrigerated centrifuge (Ivan Sorvall Inc., Norwalk, Connecticut) to remove nuclei and mitochondria. The 9000xg supernatant was then removed by pipet avoiding the lipid layer and four 9.0 ml aliquots transferred to 10 ml polycarbonate screw cap centrifuge tubes. These tubes were centrifuged for 60 min at 100,000xg in a Beckman L2-65B ultracentrifuge (Beckman Instruments Inc., Palo Alto, California) at 2<sup>0</sup>C to pull down the microsomal pellet. Following centrifugation, the clear supernatant containing soluble enzymes was discarded and the microsomal pellet resuspended by using a glass rod to break-up and transfer the pellet into a small Potter-Elvehjem homogenizer and re-homogenizing with three downward strokes of the Teflon pestle. The microsomal suspension was stored at 0<sup>0</sup>C until used in metabolism studies on the same day.

### C. Xanthine Oxidase

Xanthine oxidase, grade I from buttermilk, suspension in 2.3 M ammonium sulfate containing 0.02% sodium salicylate and substantially free from uricase was purchased from Sigma Chemical Company, St. Louis, Missouri. Twenty-five to fifty unit vials were received at concentrations of 28.1 to 16.7 U/ml and stored at 0-5<sup>0</sup>C before use in metabolism studies.

### III. Relative Rates of Metabolism

#### A. Materials and Methods

##### 1. In 9000xg Rat Liver Homogenate Supernatant

Incubation of (I) with 9000xg rat liver homogenate supernatant was carried out at 37<sup>0</sup>C in a Dubnoff metabolic incubator. Incubation mixtures contained 10 ml 100 mM potassium phosphate buffer pH 7.35 and 2.0 ml of an NADPH generating system consisting of NADP (2.0 umoles), glucose-6-phosphate (60 umoles) and MgCl<sub>2</sub> (30 umoles). To determine the sensitivity of metabolism to DNA one trial was run with 13.2 mgs DNA dissolved in the buffer. Incubation mixtures were kept anaerobic by saturation with nitrogen which was passed through a deoxygenizer consisting of a 0.4% sodium hydroxide solution containing 0.5% sodium dithionite and 0.05% of the sodium salt of 2-anthraquinone-sulfonic acid. One ml of the 9000xg rat liver homogenate supernatant (corresponding to 500 mg of tissue) was added to the anaerobic incubation mixture and the metabolism initiated by addition of 200 ul of 7.00 mM dimethyl sulfoxide solution of (I) (1.40 umole). Due to the photosensitivity of (I) all procedures were performed in subdued light and in amber glass vials. To insure complete anaerobic conditions throughout the incubation period, the vials were capped with a rubber septum perforated with needles to allow maintenance of a constant flow of nitrogen and for withdrawal of samples.

To characterize metabolism 1.0 ml aliquots of metabolism mixture were removed at 0.6, 6.0, 12.0 and 20.0 min, mixed with 1.0 ml ice-cold methanol and centrifuged at 9000xg at 2<sup>0</sup>C for 30 min to precipitate pro-

teins. Aliquots (50  $\mu$ l) of the supernatant were then analyzed by HPLC. Metabolite separation was obtained using a 10 $\mu$  C<sub>18</sub>Bondapak 3.9 mm X 30 cm column (Waters Associates, Milford, Massachusetts) and mobile phase gradient elution of 0-40% MeOH/H<sub>2</sub>O (V/V) on program 10 (Waters gradient elution programmer, model 660) over twenty minutes with a flow rate of 2.0 ml/min. Ultra-violet detection at 254 nm and 365 nm was used to monitor the appearance of metabolites.

After the metabolite elution profile had been characterized, the relative rates of disappearance of (I) and appearance of the major metabolite (M-2) were determined by HPLC using isocratic elution in order to avoid the long column equilibration times necessary in gradient elution. Aliquots (50  $\mu$ l) of the supernatant following protein precipitation were analyzed using a 40% MeOH/H<sub>2</sub>O mobile phase.

## 2. In Rat Liver Microsomes

Incubation of (I) with rat liver microsomes was carried out at 37<sup>0</sup>C in a Dubnoff metabolic incubator. Incubation mixtures contained 12.0 ml 50 mM potassium phosphate buffer pH 7.35 containing 60  $\mu$ moles MgCl<sub>2</sub>. Incubation mixtures were kept anaerobic with nitrogen and the procedures performed in subdued light as previously described. To determine metabolism sensitivity to DNA one trial was run with 15.75 mg DNA dissolved in the buffer. To determine metabolism dependence on amount of enzyme, 0.25, 0.50, 0.75, 1.00, 1.50, or 2.00 ml (corresponding to 50, 100, 150, 200, 300, and 400 mg tissue), of the rat liver microsomal suspension was added to the anaerobic incubation mixture along with the necessary amount of buffer to make a total volume of 13.5 ml. Next, 250  $\mu$ l of 11.2 mM dimethyl sulfoxide solution of (I)

(2.80 umoles) was added and the metabolism initiated by addition of one-half of the total amount of NADPH ( $\beta$ -form, tetrasodium salt, No. N-7505, Sigma Chemical Company, St. Louis, Missouri) in 1.0 ml buffer. The second portion of NADPH was added about half way through the total metabolism time. The total amount of NADPH added was 3, 5, 7, or 10 umoles to determine sensitivity to the amount of reducing cofactor. One ml aliquots were taken during the incubation time and prepared for HPLC analysis as previously described. Relative rates of disappearance of (I) and appearance of the major metabolite (M-2) were determined as previously described by isocratic HPLC analysis.

### 3. In Xanthine Oxidase

Incubation of (I) with xanthine oxidase was carried out at 37°C in a Dubnoff metabolic incubator. Incubation mixtures contained 4.5 ml 50 mM potassium phosphate buffer pH 5.8 containing 2.5 mg hypoxanthine. Incubation mixtures were kept anaerobic with nitrogen and the procedures performed in subdued light as previously described. To determine metabolism sensitivity to DNA one trial was run with 5.0 mg DNA dissolved in the buffer. To determine metabolism dependence on amount of enzyme, 0.25, 0.50, or 2.50 units xanthine oxidase were added to the anaerobic incubation mixture along with the necessary amount of buffer to make a total volume of 5.0 ml. Metabolism was initiated by the addition of 50  $\mu$ l of 2.0 mM dimethyl sulfoxide solution of (I) (0.10 umole) and sample aliquots (1.0 ml) taken at 1.0, 30, 60, 90, 150, and 160 minutes. Sample handling and determination of relative rates of disappearance of (I) and appearance of the major metabolite (M-2) were done as previously described.

## B. Results

The gradient elution HPLC profile of metabolites of (I) after 12.0 min of incubation in 9000xg rat liver homogenate supernatant without DNA is shown in Figure 4.1. Two metabolites, (M-1) and (M-2) with retention times of 20.1 and 22.9 min respectively were found. Similar profiles of metabolites were observed for the other sample times with peak height for the metabolites increasing with sample time and peak height for (I) decreasing with sample time.

Relative rates of disappearance of (I) and appearance of (M-2) in incubations with and without DNA were determined by isocratic HPLC as previously described to define conditions to be used in DNA binding studies. Metabolite (M-1) was not separated from interfering materials in the isocratic HPLC analysis and therefore, it was not followed. The relative change in the concentration of (I) and (M-2) are represented in Figure 4.2 (A) and (B) by plotting peak height of (I) and (M-2) as a function of time. The results indicate significant differences in the relative disappearance of (I) and appearance of (M-2) when DNA is added.

A gradient elution profile of metabolites of (I) after incubation with rat liver microsomes was not done because of assumed similarity to the 9000xg rat liver homogenate supernatant system. The relative dependence of the disappearance of (I) and the appearance of (M-2) on the amount of microsomal suspension used, total amount of NADPH added, and presence of DNA is represented in Figures 4.3, 4.4, and 4.5 respectively. In this system there was no difference in the disappearance of (I) when DNA was present. However, there was a significant difference



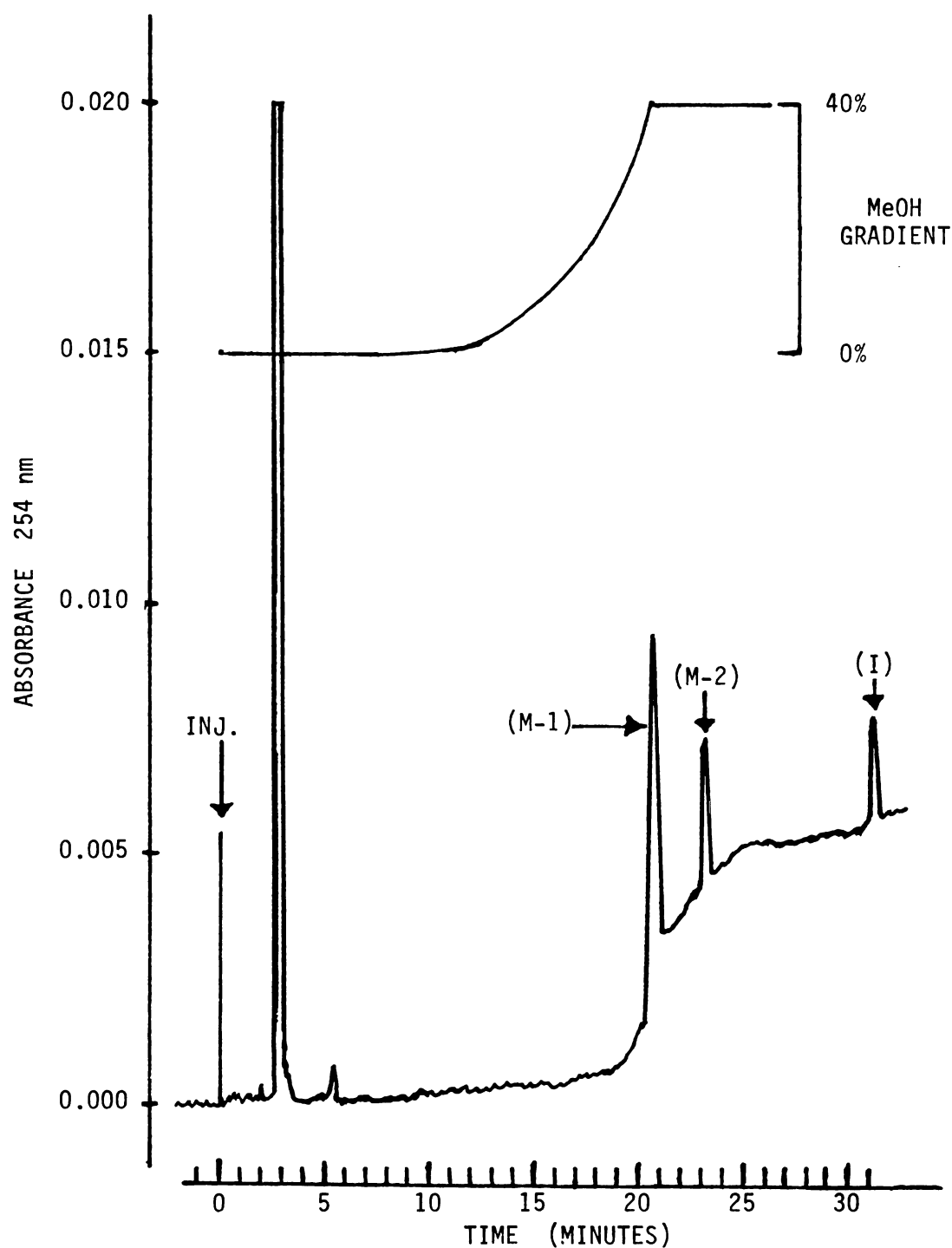


FIGURE 4.1

GRADIENT ELUTION 0→40% MeOH/H<sub>2</sub>O (V/V) #10 PROGRAM  
(WATERS GRADIENT PROGRAMER MODEL 660) HPLC ABSORBANCE PROFILE  
OF METABOLITES OF (I) AFTER 14 MIN INCUBATION WITH 9000xg  
RAT LIVER HOMOGENATE SUPERNATANT WITHOUT DNA

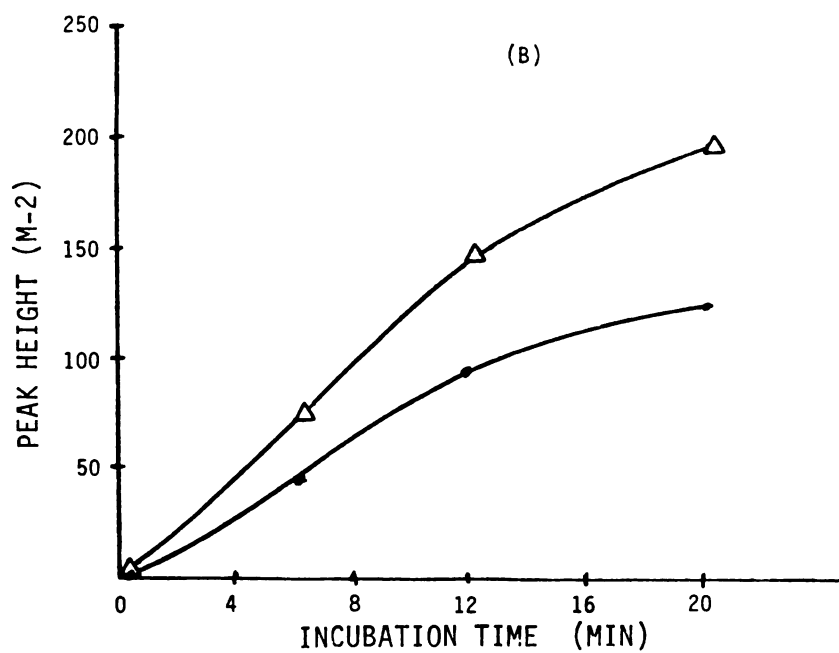
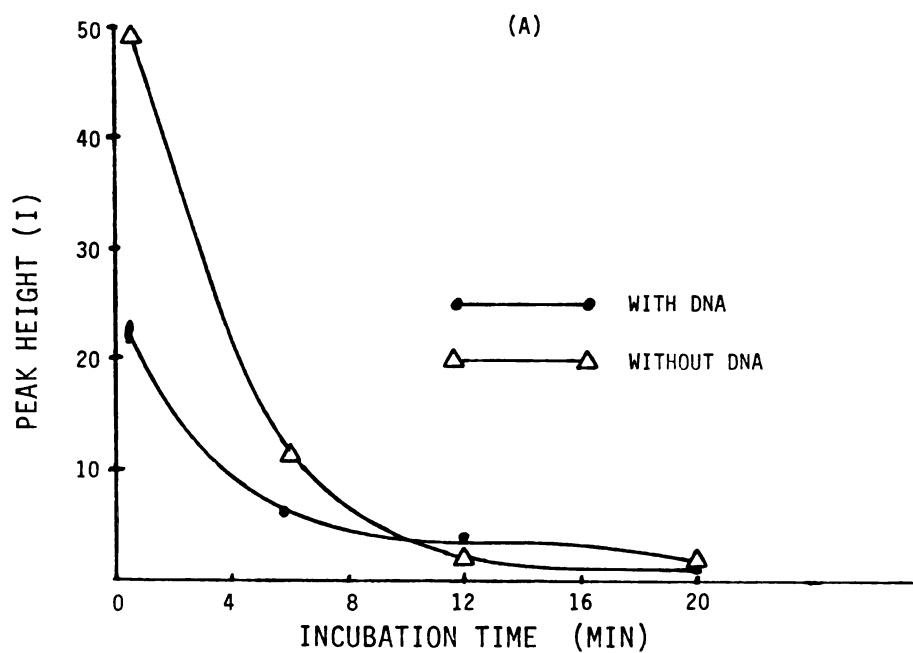
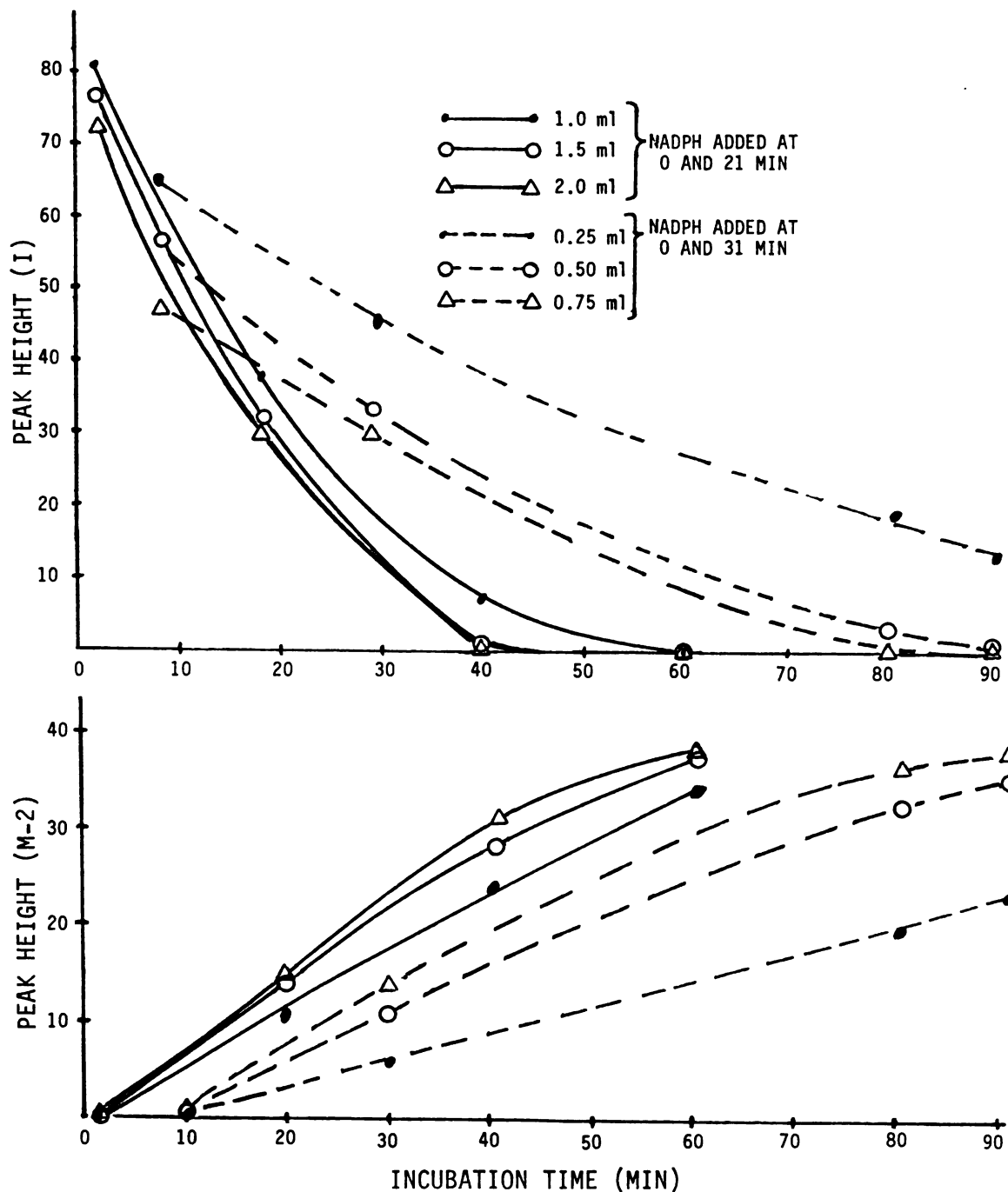


FIGURE 4.2

RELATIVE CHANGE IN CONCENTRATION OF (I) AND (M-2)  
IN INCUBATIONS WITH 9000xg RAT LIVER HOMOGENATE SUPERNATANT



**FIGURE 4.3**

(TOTAL NADPH ADDED-10  $\mu$ MOLES)

RELATIVE CHANGE IN CONCENTRATION OF (I) AND (M-2)  
IN INCUBATIONS WITH RAT LIVER MICROSOMES  
(DEPENDENCE ON AMOUNT OF MICROSOMAL SUSPENSION)

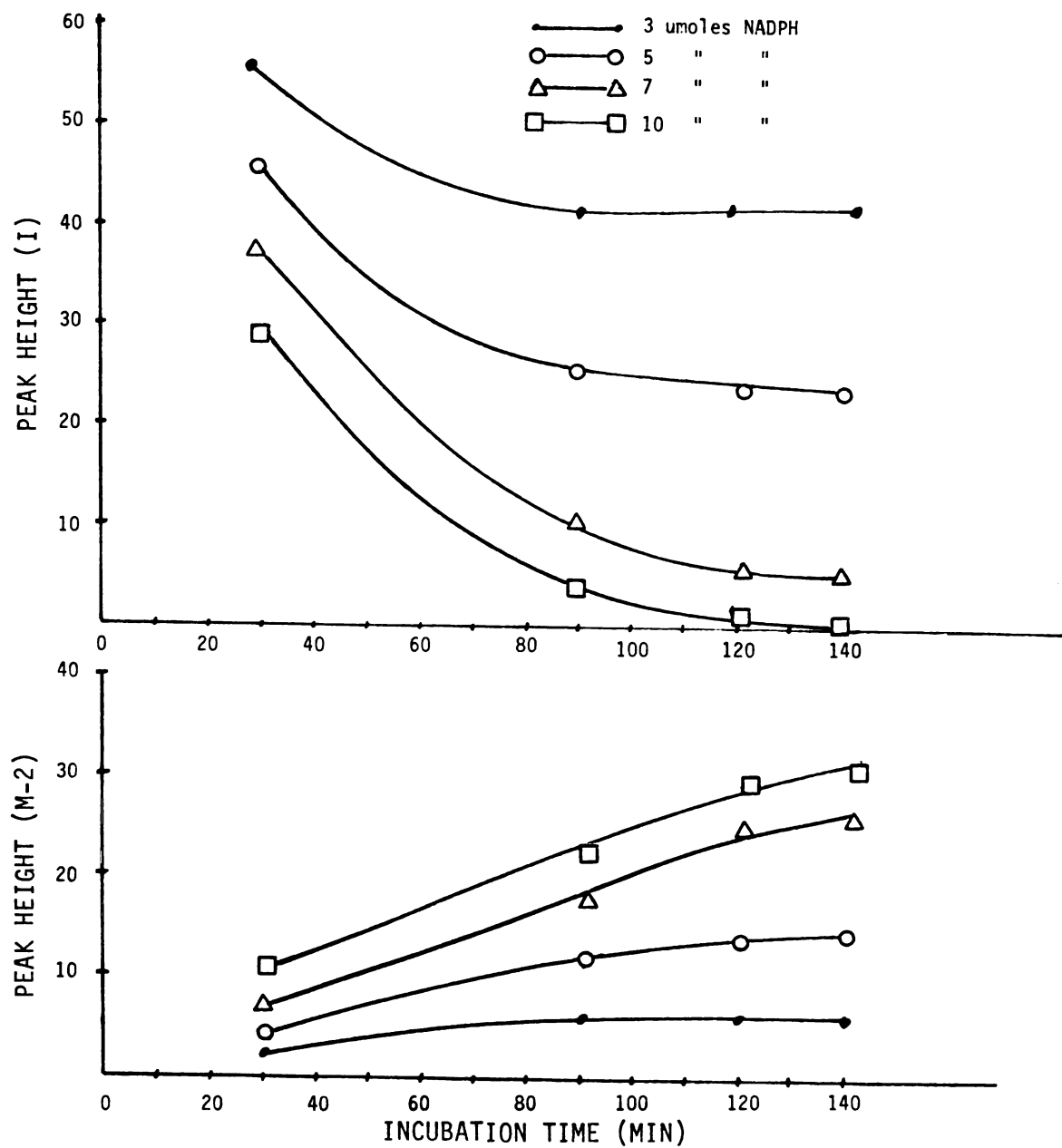


**FIGURE 4.4**

(MICROSOMAL SUSPENSION ADDED-0.5 ml)  
 RELATIVE CHANGE IN CONCENTRATION OF (I) AND (M-2)  
 IN INCUBATIONS WITH RAT LIVER MICROSOMES  
 (DEPENDENCE ON TOTAL AMOUNT OF NADPH ADDED)

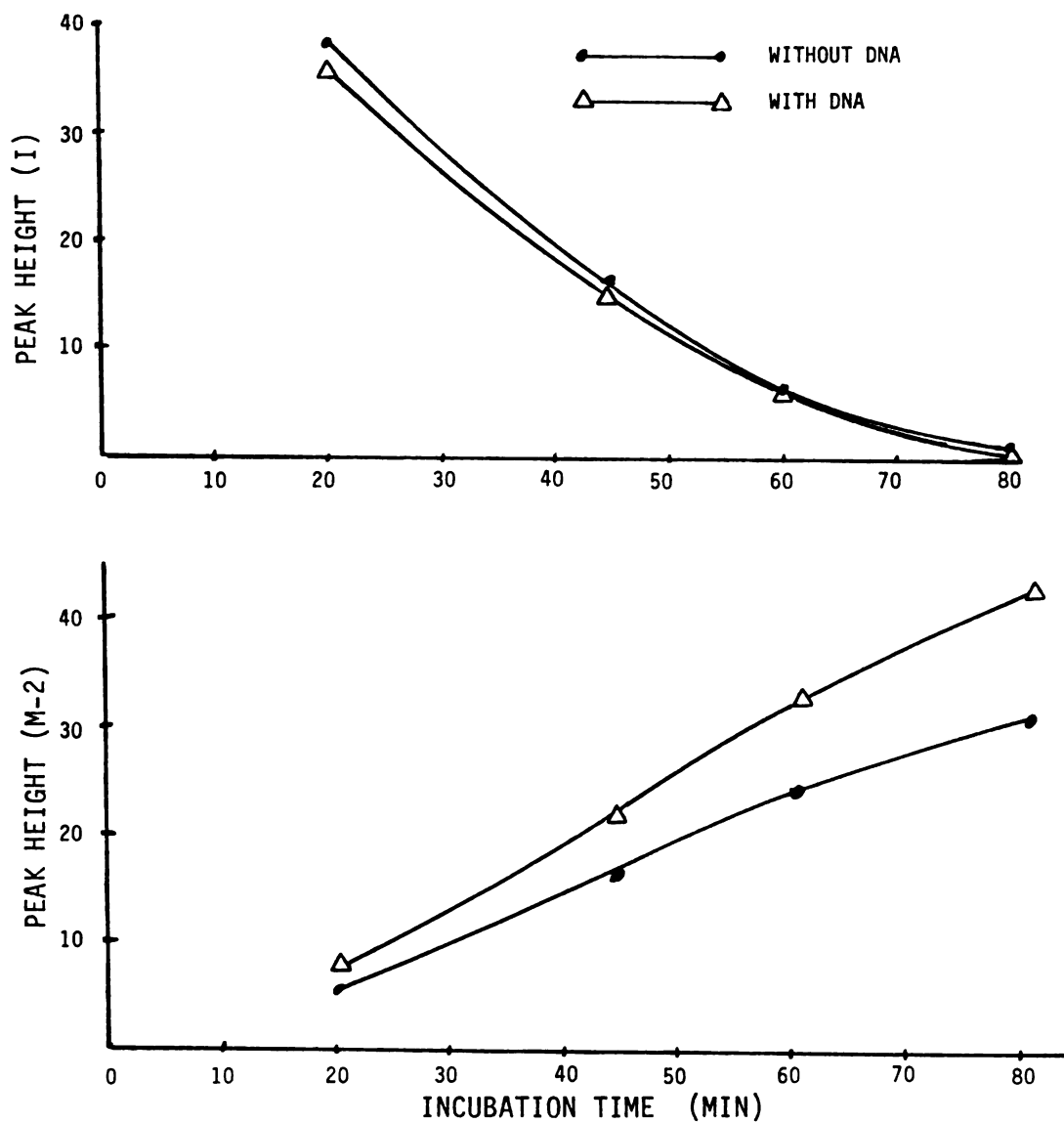


FIGURE 4.5

(NADPH ADDED-10  $\mu$ MOLES, MICROSOMAL SUSPENSION ADDED-0.5 ml)

RELATIVE CHANGE IN CONCENTRATION OF (I) AND (M-2)  
IN INCUBATIONS WITH RAT LIVER MICROSOMES  
(DEPENDENCE ON PRESENCE OF DNA)

in the appearance of (M-2) when DNA was added.

The gradient elution profile of metabolites of (I) after incubation with xanthine oxidase was identical with the 9000xg rat liver homogenate supernatant system and therefore is not shown. The relative disappearance of (I) and appearance of (M-2) as a function of the amount of enzyme and the addition of DNA are represented in Figure 4.6. In this system there was no significant difference in the disappearance of (I) and appearance of (M-2) when DNA was present.

### C. Discussion

The difference in the relative disappearance of (I) and appearance of (M-2) with and without added DNA using the 9000xg rat liver homogenate supernatant and rat liver microsomes may not be significant. If the observed dependences were caused totally by the addition of DNA, a similar effect would be expected in the 9000xg rat liver homogenate supernatant and rat liver microsomes if it were assumed that the enzyme responsible for nitroreduction was in the microsomes and not the cytosol. However, a comparable dependence was not observed suggesting possible cytosolic contribution to metabolism. Moreover, the difference might be explained by the different amounts of precipitated material in the incubations with DNA. It is possible that entrapment of (I) and/or its metabolites occurs in the protein precipitation step prior to HPLC analysis. This entrapment effect would be most prevalent when both DNA and high amounts of protein are present. When low amounts of protein are present, as with the xanthine oxidase system, the combined entrapment effect resulting from DNA and protein precipitation is not significantly different from the entrapment effect observed when only protein

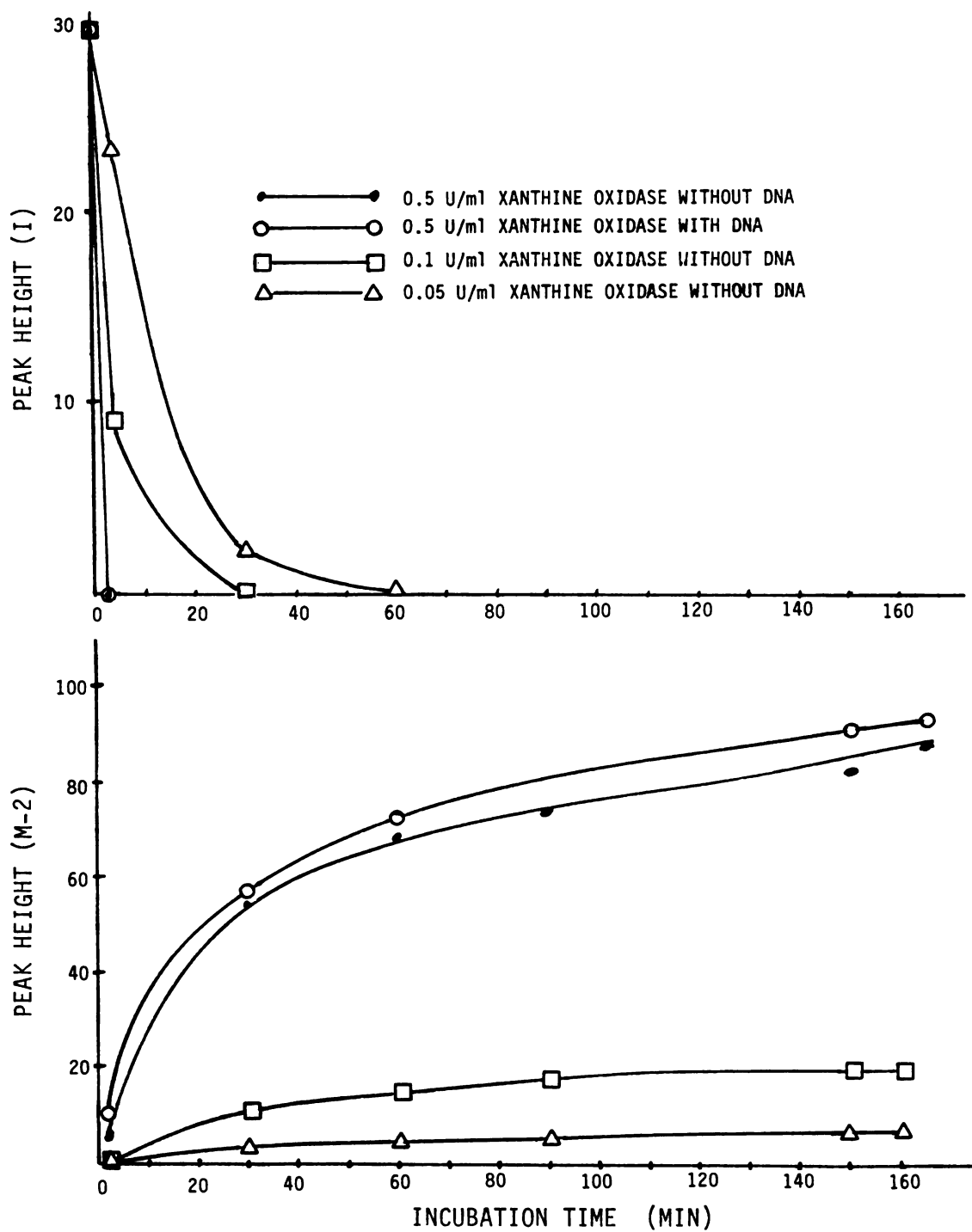


FIGURE 4.6

RELATIVE CHANGE IN CONCENTRATION OF (I) AND  
(M-2) IN INCUBATIONS WITH XANTHINE OXIDASE

is present.

In these enzymatic preparations a significant difference was observed between rat liver derived enzymes and xanthine oxidase. With xanthine oxidase the disappearance of (I) was much faster than the appearance of (M-2). Two rationalizations of this observed difference can be offered. In the first instance, it is probable that rat liver derived nitroreductase enzymes are heterogeneous and different enzymes could be responsible for each reductive step leading to the final end product. However, with xanthine oxidase only a single enzyme is involved. Secondly, if both enzymatic systems are considered to be homogeneous but different from each other then the observed differences could be due to the different individual rates of each reductive step. Whatever the cause of the difference, this observation may be of significance in determining which enzyme is responsible for the activation of (I) to its ultimate carcinogen/mutagen.

#### IV. Metabolite Structural Elucidation

##### A. Materials and Methods

###### 1. Preparative Scale Incubations

Large amounts of metabolites were prepared for structural elucidation by in vitro techniques similar to those used to characterize rates of metabolism for the rat liver homogenate supernatant. Six incubation mixtures containing 12 ml 100 mM potassium phosphate buffer pH 7.35, and 2.0 ml of NADPH generating system consisting of NADP (2.0 umoles), glucose-6-phosphate (60 umoles), and MgCl<sub>2</sub> (30 umoles), and 1.0 ml of



the 9000xg rat liver homogenate supernatant (corresponding to 500 mg of tissue) were prepared. All other conditions were identical to those described previously. Metabolism was initiated by the addition of 2.5 umoles (I), in 200 ul DMSO, to each incubation vial and the incubations allowed to proceed for 45 minutes. Metabolism was terminated by the addition of 15 ml ice cold methanol and the mixture centrifuged at 9000xg for 30 min to precipitate proteins. The supernatants from each incubation were pooled together and lyophilized to dryness overnight.

## 2. Metabolite Isolation

Following lyophilization the residue was reconstituted with 20 ml distilled water, filtered through a 0.45 um filter and 800 ul aliquots of the filtrate submitted to metabolite separation by preparative scale HPLC. The preparative scale HPLC system consisted of a 10u C<sub>18</sub>uBondapak column 7.8 mm X 30 cm (Waters Associates, Milford, Massachusetts) and the same gradient elution program as described for metabolite profile characterization with a flow rate of 4.0 ml/min. The HPLC fractions eluting between 19.4 and 20.4 min and 25.3 and 26.9 min (Figure 4.7) corresponding to metabolites (M-1) and (M-2) respectively, were collected from ten successive injections. The collections from each fraction were combined and treated as follows for structural elucidation.

## 3. Physical Characterization of Metabolites

### a. Ultraviolet Spectra

The UV absorption spectra of the (M-1) and (M-2) fractions as they eluted off the HPLC were recorded on a Cary model 118 double-beam

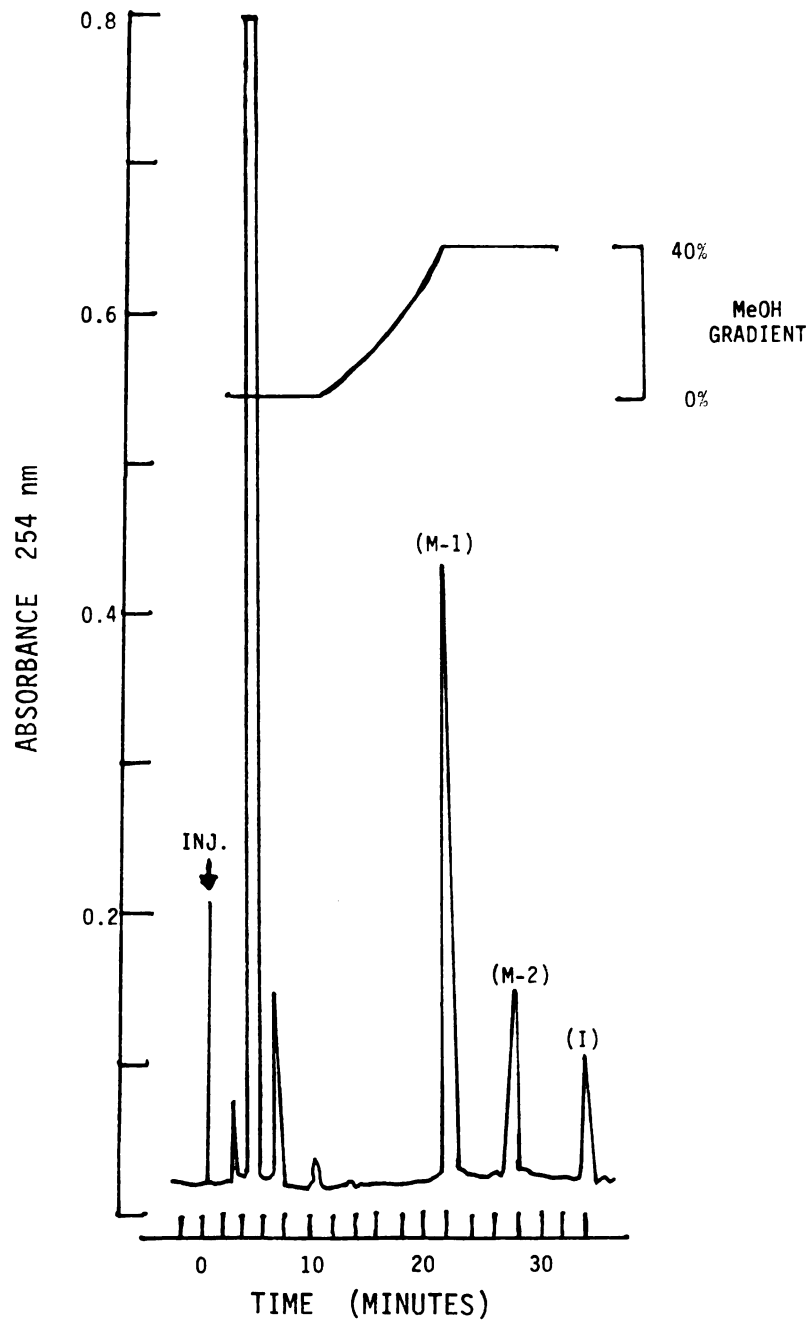


FIGURE 4.7

GRADIENT ELUTION 0→40% MeOH/H<sub>2</sub>O (V/V) #10 PROGRAM  
(WATERS GRADIENT PROGRAMER MODEL 660) HPLC ABSORBANCE  
PROFILE FOR ISOLATION OF METABOLITES (M-1) AND (M-2)

recording spectrophotometer with 40% MeOH/H<sub>2</sub>O as the reference.

b. Electron Ionization Mass Spectra

The combined fractions eluted off the HPLC representing (M-1) and (M-2) from ten successive HPLC injections were lyophilized. Approximately 0.05 mg of the dried samples were submitted for mass spectra analysis by direct probe insertion. Electron impact mass spectra were taken on an Associated Electrical Industries model MS 12 mass spectrometer. Sample probe temperature ranged from 20 to 300°C with the voltage of the ionizing electron beam maintained at 70 ev.

c. Fourier Transform Proton Nuclear Magnetic Resonance Spectra

The remaining residues of (M-1) and (M-2) were dissolved in approximately 0.6 ml of d<sub>6</sub>-DMSO (99.5 atom %D, gold label, Aldrich Chemical Company, Milwaukee, Wisconsin). Proton nuclear magnetic resonance spectra were recorded on a Varian XL-100 Fourier transform spectrometer equipped with a Nicolet Instrument Corporation model TT-100 accessory. Five-hundred pulses (pulse width 5 usec, acquisition time 3.4 sec, acquisition delay 400 usec) were used to generate the spectra.

B. Results

The UV absorption spectra for (M-1) and (M-2) are shown in Figure 4.8. Absorption maxima,  $\lambda_{\max}$ , for the metabolites showed the following: (M-1) (223 nm and 317 nm) and (M-2) (227 nm and 386 nm). The UV absorption spectrum of metabolite (M-2) has a pronounced bathochromic effect in  $\lambda_{\max}$  relative to (I) ( $\lambda_{\max}$  231 nm and 324 nm). This suggests formation of 2,4-diacetylamino-6-(5-amino-2-furyl)-1,3,5-triazine (III)

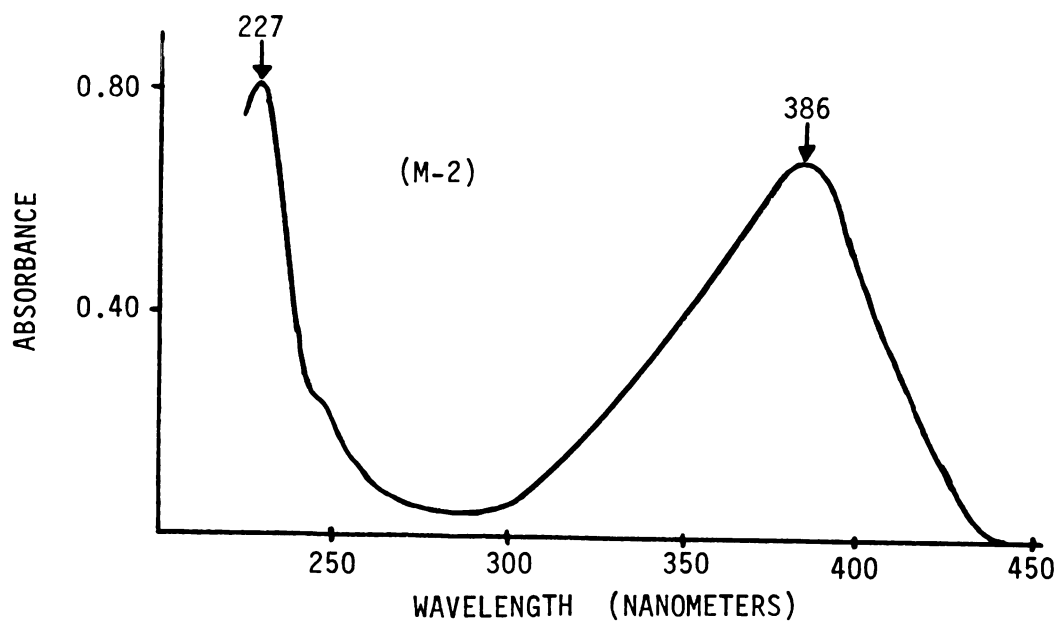
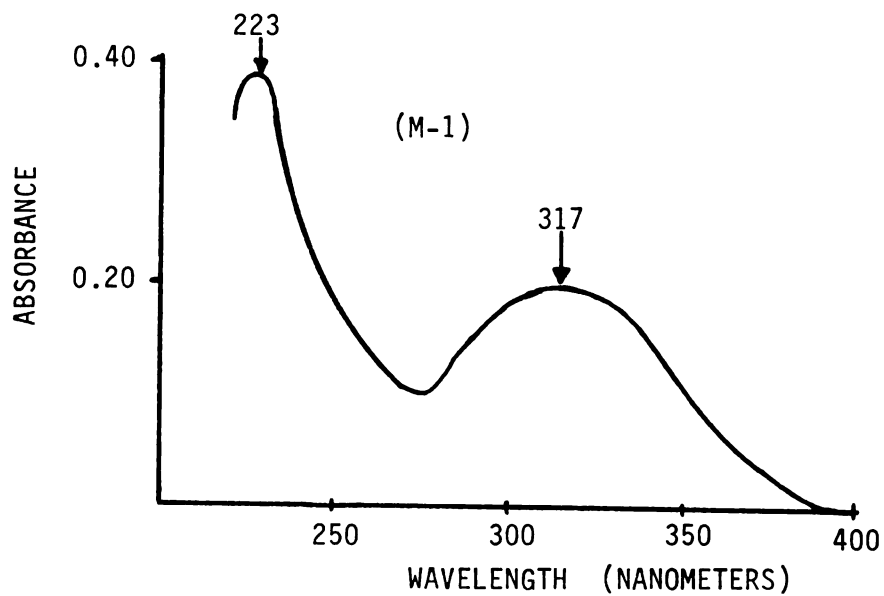


FIGURE 4.8

ULTRAVIOLET ABSORPTION SPECTRA OF FRACTIONS COLLECTED BY HPLC  
FROM PREPARATIVE METABOLISM OF (I) BY 9000xg RAT LIVER HOMOGENATE SUPERNATANT

through the expected bathochromic effect produced by delocalization of the amine free electron pair into the conjugated system (Figure 4.9). The UV absorption spectrum of metabolite (M-1) has a slight hypsochromic effect in  $\lambda_{\text{max}}$  relative to (I). This suggests the formation of the open chain nitrile structure 2,4-diacetylamino-6-(3-cyano-1-oxopropyl)-1,3,5-triazine (IV). However, the absorption maxima for (M-1) is relatively high compared to open chain nitrile metabolites isolated from nitro-furantoin by Aufrere et al. (46) and two other 5-nitrofurans by Tatsumi et al. (45) and Chapfield (47). They all report hypsochromic shifts of around 80-100 nm for the open chain nitrile metabolite relative to the 5-nitrofurans and absorption maxima between 270 and 290 nm.

The electron ionization mass spectrum of metabolite (M-2) is shown in Figure 4.10. This mass spectrum together with the UV spectroscopic data strongly suggests the structure of the amino metabolite (III) for (M-2). A strong molecular ion  $M^+$  (relative abundance 40) was observed at  $m/e$  276, the nominal molecular weight for this structure. The fragmentation pattern of  $(M-15^+)$ ,  $(M-42^+)$ , and  $(M-57^+)$  is in agreement with homolytic fission of bonds on the acetamino group of the triazine ring giving ions of the structure shown in Figure 4.11.

The apparent low volatility or high instability of (M-1), prevented the acquisition of its electron ionization mass spectra. Only peaks of  $m/e$  170 or less were obtained. Hence, no useful information was gathered for structural elucidation.

Because of the very low concentration of the metabolites in  $d_6$ -DMSO, Fourier transform NMR was necessary to obtain spectra. Figure 4.12 shows the NMR spectra of (M-2) along with chemical shift assignments of the suspected amino metabolite (III) protons. The NMR spectrum of the

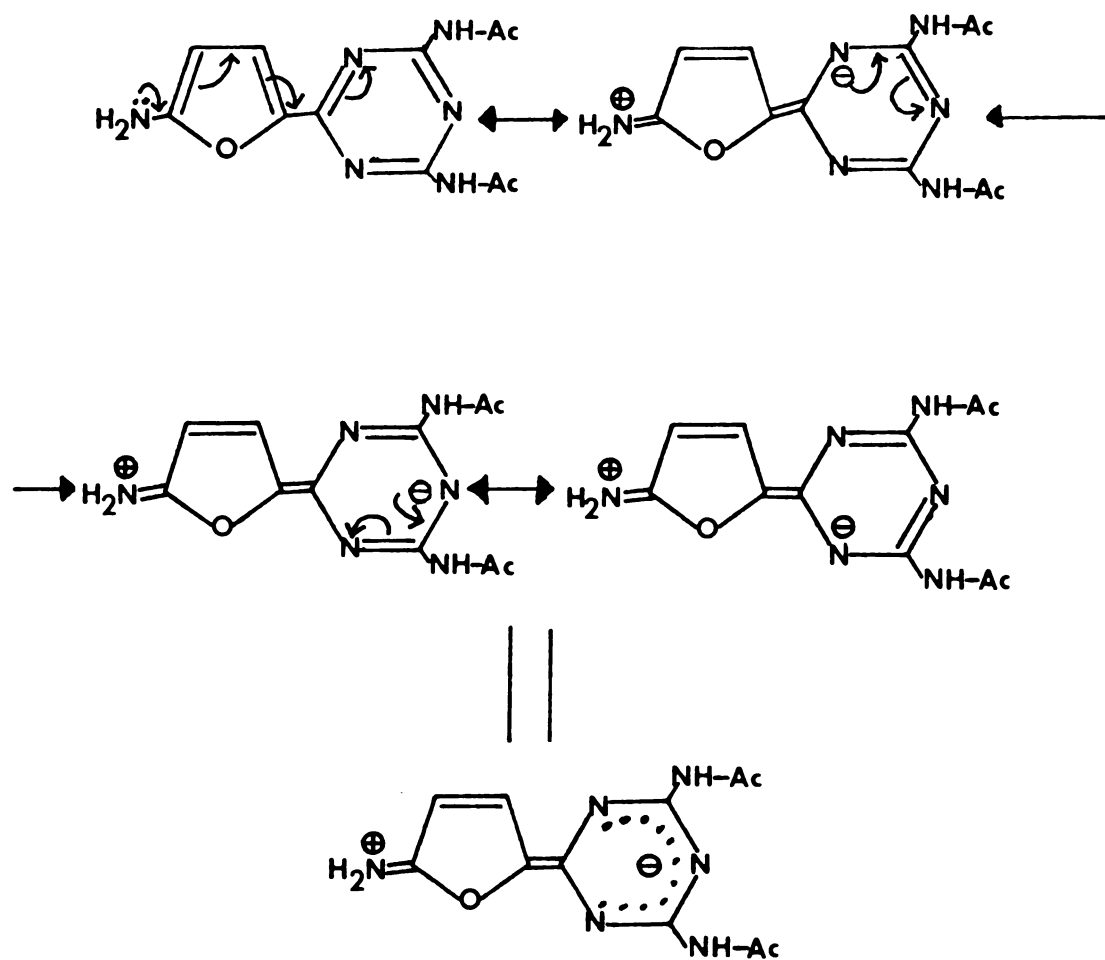


FIGURE 4.9

DELOCALIZATION OF AMINE FREE ELECTRON PAIR INTO THE CONJUGATED SYSTEM IN 2,4-DIACETYLAMINO-6-(5-AMINO-2-FURYL)-1,3,5-TRIAZINE; SUSPECTED AS (M-2)

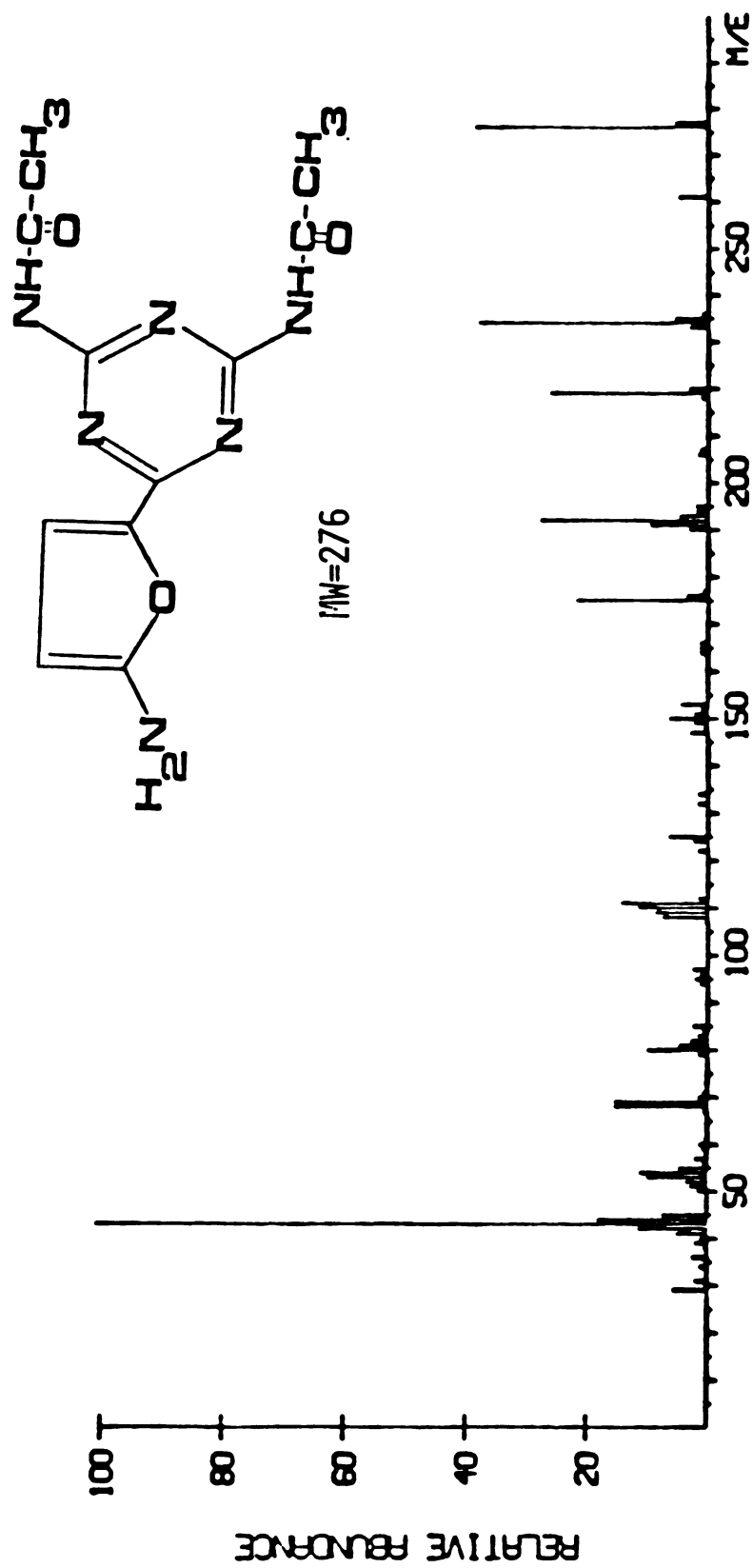
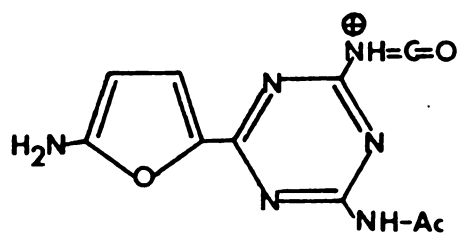
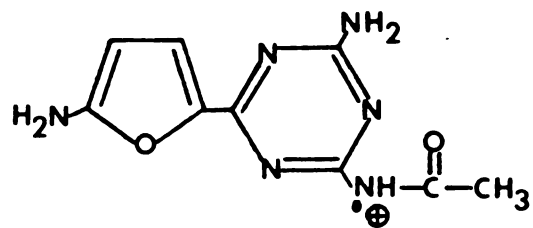


FIGURE 4.10

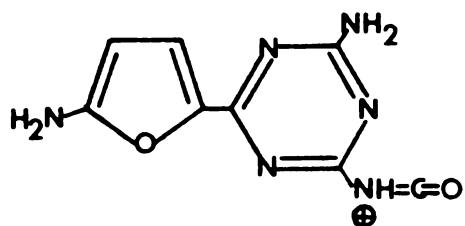
ELECTRON IONIZATION MASS SPECTRUM OF METABOLITE (M-2) ELUTED BY  
PREPARATIVE HPLC FROM IN VITRO METABOLISM OF (I) IN 9000xg  
RAT LIVER HOMOGENATE SUPERNATANT



(M-15)<sup>+</sup>, m/e = 261



(M-42)<sup>+</sup>, m/e = 234



(M-57)<sup>+</sup>, m/e = 219

FIGURE 4.11

POSTULATED STRUCTURES OF IMPORTANT FRAGMENTATION IONS IN  
MASS SPECTRA OF METABOLITE (M-2)



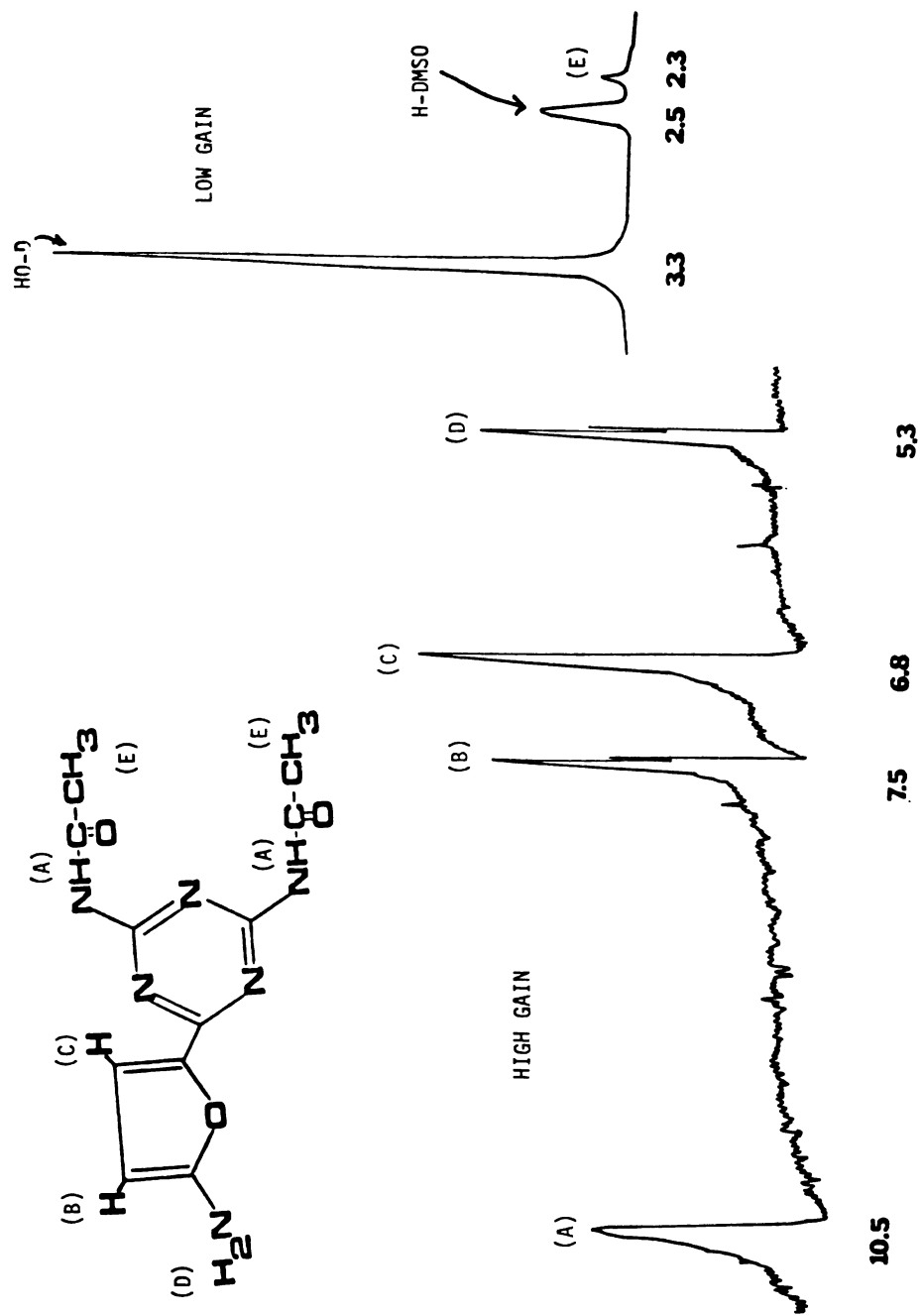


FIGURE 4.12

FOURIER TRANSFORM PROTON NUCLEAR MAGNETIC RESONANCE SPECTRA OF METABOLITE (M-2) ELUTED OFF PREPARATIVE HPLC FROM IN VITRO METABOLISM OF (I) IN 9000xg RAT LIVER HOMOGENATE SUPERNATANT

parent compound (I) in  $d_6$ -DMSO is shown in Figure 2.2 for reference purposes. From this spectra it is seen that the amide protons have shifted from  $\delta$  11.0 to  $\delta$  10.5 in (M-2). Similarly, the aromatic furan ring protons shifted from  $\delta$  7.8 and 7.6 to  $\delta$  7.5 and 6.8 respectively, and the methyl protons on the acetate groups shifted from  $\delta$  2.1 to 2.3. The additional NMR signal from the amine protons at  $\delta$  5.3 is consistent for aromatic amino protons and is not observed in the parent spectra. The furan ring protons would be expected to be observed as two sets of doublets with coupling constants in the range of 3 to 5 Hz (87). However, the spectra was taken under marginal conditions of low concentration and the resolution was not sufficient to observed the coupling.

When preparing the NMR sample for metabolite (M-1) it was apparant that there was significantly less material from the lyophilization residue than for the metabolite (M-2). This was confirmed in the NMR spectra by the observance of only large water and non-deuterated DMSO peaks. Further attempts at preparing greater quantities of (M-1) by the same procedures of metabolite generation and isolation gave similar results. These NMR results together with the electron ionization mass spectra results suggest (M-1) may be undergoing decomposition as a result of the isolation procedure.

### C. Discussion

Results from the combined UV, electron ionization, and NMR spectra strongly suggest that metabolite (M-2) is 2,4-diacetylamino-6-(5-amino-2-furyl)-1,3,5-triazine (III). To confirm this (III) was synthetically prepared by catalytic hydrogenation of (I) and characterized spectrally

and by HPLC for comparison to (M-2).

The combined spectral results for (M-1) were not definitive for structural elucidation. However, the UV spectra suggests an open chain nitrile structure and is supported by reports of instability of structures of this type (46).

## V. Preparation of 2,4-Diacetylamino-6-(5-Amino-2-Furyl)-1,3,5-Triazine

### A. Materials and Methods

Reduction of the 5-nitrofurans (I) to the 5-aminofurans (III) was achieved using the methods of Ebetino *et al.* (88) for the reduction of nitrofurans. The catalyst, 175 mg of 10% palladium on carbon (ICN, K and K Laboratories Inc., Irvine, California) was suspended in 50 ml methanol and placed in a Parr hydrogenation bottle. Then 440 mg (1.61 mmoles) of (I) was added. Catalytic hydrogenation was performed in a Parr pressure-reaction apparatus (Parr Instrument Company Inc., Moline, Illinois) at three atmospheres for one hour in subdued light. Crude (III) was separated from the catalyst by addition of 30 ml DMSO to promote complete dissolution and filtering off the catalyst. Final purification of (III) was achieved by preparative HPLC using the same procedures as described for preparative scale isolation of (M-2). Structural confirmation of the purified (III) was checked by NMR spectroscopy. In addition, comparison of synthetically prepared (III) to (M-2) in UV spectra and HPLC retention time was made to confirm that (III) was the structure of the biologically produced (M-2).

## B. Results

The NMR spectrum of the synthetically prepared (III) was identical to the biologically produced (M-2). With the use of the same HPLC elution program described for the isolation of metabolites, synthetically prepared (III) co-chromatographed with (M-2). The UV absorption spectra was also found to be identical to (M-2) with absorption maxima at 386 nm and 227 nm. From these data, it was concluded that metabolite (M-2) isolated from anaerobic in vitro incubation with the 9000xg rat liver homogenate supernatant was (III).

## VI. Anaerobic In Vitro Metabolism of 2,4-Diacetylamino-6-(5-Nitro-2-Furyl)-1,3,5-Triazine-(Acetyl-H-3) and 2,4-Diacetylamino-6-(5-Nitro-2-Furyl)-1,3,5-Triazine-(Acetyl-1-C-14) in the 9000xg Rat Liver Homogenate Supernatant

### A. Background

Following radiochemical synthesis and purification of H-3 and C-14 acetyl labeled (I), it was necessary to determine the suitability of these labeled positions for use in metabolism studies. Because the position of the label was on acetyl groups that are suspected to be chemically hydrolyzable and/or enolizable, the lability of the radiolabel had to be investigated. Radiolabel lability was evaluated by incubation with the 9000xg rat liver homogenate supernatant and the cofactors necessary for nitroreduction. Aliquots of the incubation mixture were then analyzed by HPLC with fraction collection and radioassay of the eluent fractions. Ideally, a suitably radiolabeled compound would show a radioactivity distribution in close correlation to the observed metabolite absorbance profile.

## B. Materials and Methods

### 1. For 2,4-Diacetylamino-6-(5-Nitro-2-Furyl)-1,3,5-Triazine-(Acetyl-H-3)

Incubation of 2,4-diacetylamino-6-(5-nitro-2-furyl)-1,3,5-triazine-(acetyl-H-3) (I-acetyl-H-3) with 9000xg rat liver homogenate supernatant was carried out at 37<sup>0</sup>C in a Dubnoff metabolic incubator with the same precautions for maintenance of anaerobic conditions and subdued light as previously described. The incubation mixture contained 11.0 ml 100 mM potassium phosphate buffer pH 7.35 and 2.0 ml of an NADPH generating system consisting of NADP (2.0 umoles), glucose-6-phosphate (60 umoles), and MgCl<sub>2</sub> (30 umoles). Following addition of 1.0 ml 9000xg rat liver homogenate supernatant (corresponding to 500 mg of tissue) metabolism was initiated by the addition of 3.0 ml 50% DMSO/H<sub>2</sub>O (V/V) solution containing 0.56 umole (18.0 uCi) HPLC-purified tritiated (I).

Immediately following addition of (I-acetyl-H-3) and at 2.0 and 5.0 min 1.0 ml aliquots of the incubation mixture were mixed with 1.0 ml ice cold methanol and centrifuged at 9000xg at 2<sup>0</sup>C for 30 min to precipitate proteins. Aliquots (100 ul) of the supernatant were then analyzed by HPLC using a 10u C<sub>18</sub>uBondapak (Waters Associates, Milford, Massachusetts) 7.9 mm X 30 cm column, 40% MeOH/H<sub>2</sub>O (V/V) mobile phase at 4.0 ml/min, and UV detection at 365 nm. Fractions of the HPLC eluent were collected and counted on a Packard Tri-Carb liquid scintillation spectrometer using PCS (Amersham, Arlington Heights, Illinois) cocktail and quench correction by sample channels ratio method.

2. For 2,4-Diacetylamino-6-(5-Nitro-2-Furyl)-1,3,5-Triazine-(Acetyl-1-C-14)

Incubation of 2,4-diacetylamino-6-(5-nitro-2-furyl)-1,3,5-triazine-(acetyl-1-C-14) (I-acetyl-1-C-14) in the 9000xg rat liver homogenate supernatant was performed as described for (I-acetyl-H-3). However, because the acetyl C-14 labeled (I) differed significantly in specific activity, the incubation mixture contained only 7.3 ml 100 mM potassium phosphate buffer pH 7.35 and 0.5 ml rat liver homogenate supernatant. Metabolism was initiated by the addition of a 200  $\mu$ l DMSO solution containing 1.0  $\mu$ mole (0.18  $\mu$ Ci) HPLC-purified (I-acetyl-1-C-14). The incubation contained the same NADPH generating system. HPLC analysis of samples immediately following addition of (I-acetyl-1-C-14) and at 15, 30, and 45 min and radioactivity counting of the collected fractions (1.0 min) were performed as described for (I-acetyl-H-3).

C. Results

The HPLC absorbance/radioactivity profiles from the incubation of (I-acetyl-H-3) and (I-acetyl-1-C-14) with the 9000xg rat liver homogenate supernatant are shown in Figure 4.13 and 4.14 respectively. In the incubation using (I-acetyl-H-3) constant time/volume increment fractions of the HPLC eluent were not collected. Instead, fractions of different volumes were collected to afford characterization of the amount of radioactivity associated with each absorbance peak on the HPLC profile. Examination of the HPLC absorbance/radioactivity profiles from the incubations using (I-acetyl-H-3) indicates that a significant amount of radioactivity is not associated with any peaks detected by UV absorption. Furthermore, no peak for (I-acetyl-H-3) is observed even in the

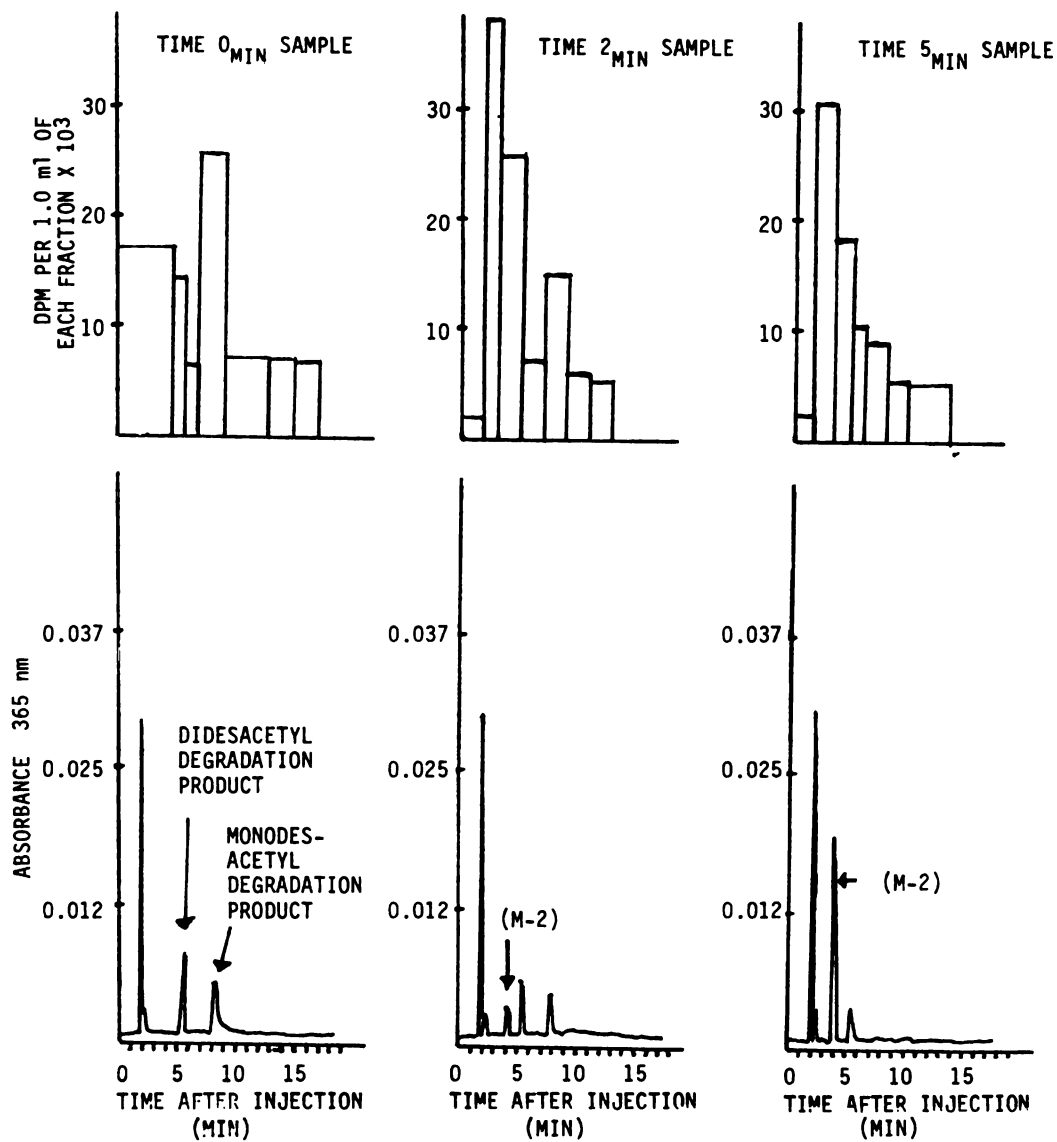


**FIGURE 4.13**

ISOCRATIC 40% MeOH/H<sub>2</sub>O (V/V) HPLC ABSORBANCE/RADIOACTIVITY PROFILES AFTER INCUBATION OF (I-ACETYL-H-3) WITH 9000xg RAT LIVER HOMOGENATE SUPERNATANT

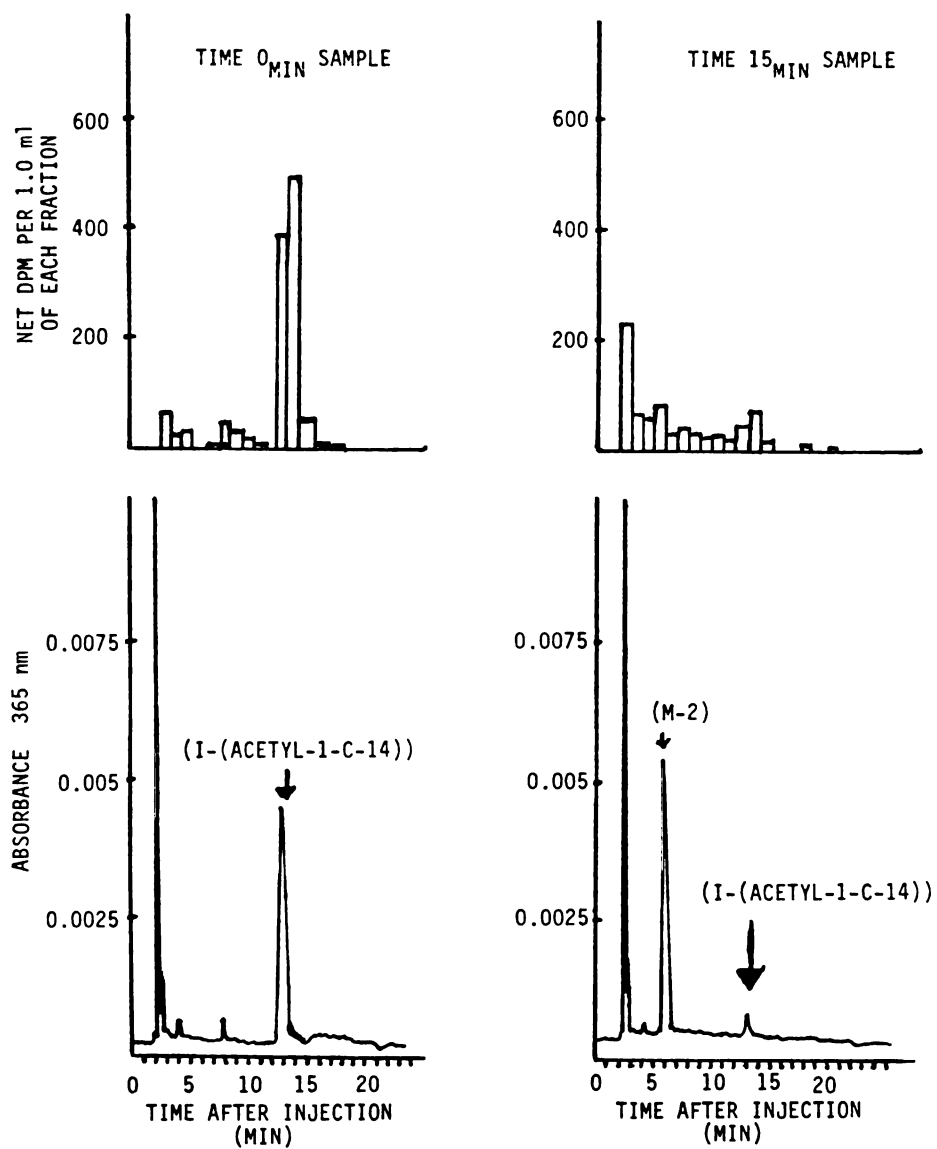


FIGURE 4.14

ISOCRATIC 40% MeOH/H<sub>2</sub>O (V/V) HPLC ABSORBANCE/RADIOACTIVITY PROFILES AFTER INCUBATION OF (I-ACETYL-1-C-14) WITH 9000xg RAT LIVER HOMOGENATE SUPERNATANT



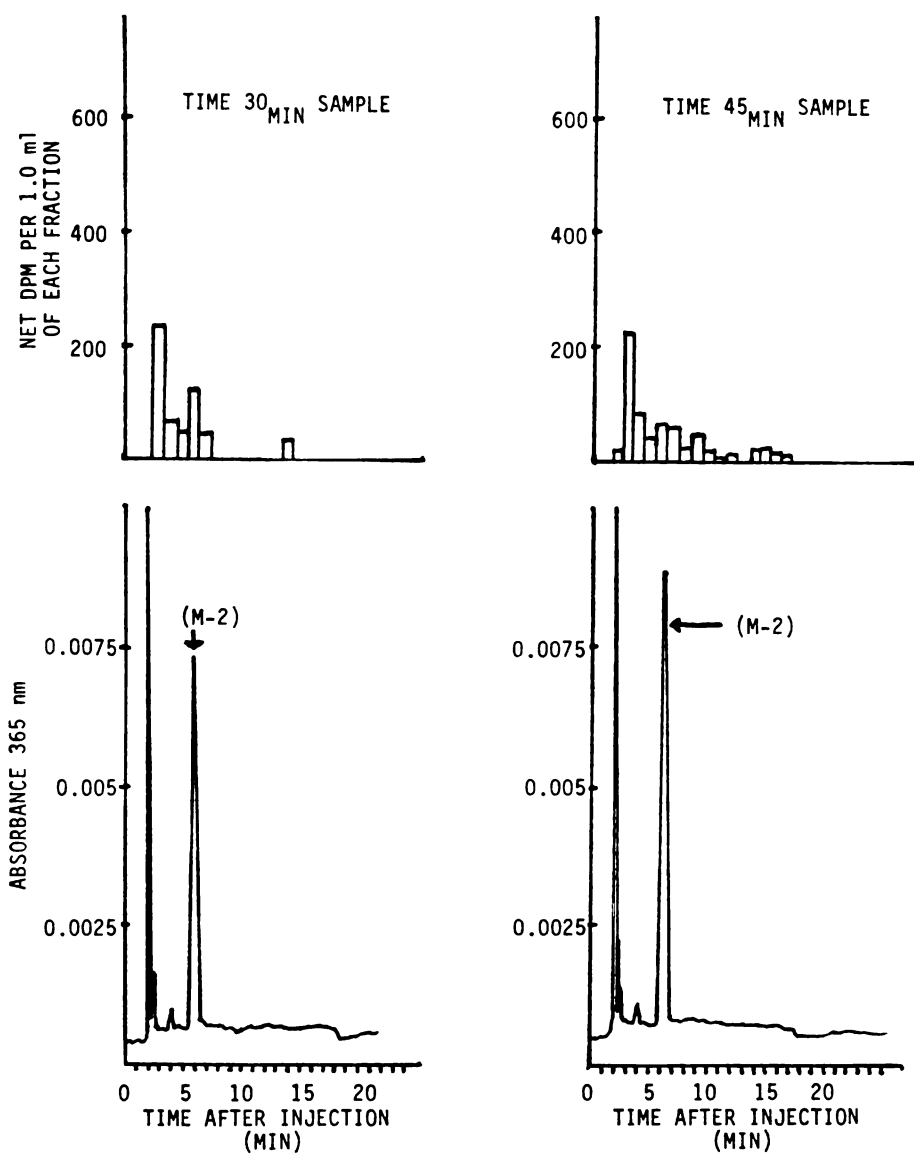


FIGURE 4.14

(CONTINUED)

ISOCRATIC 40% MeOH/H<sub>2</sub>O (V/V) HPLC ABSORBANCE/RADIOACTIVITY  
PROFILES AFTER INCUBATION OF (I-ACETYL-1-C-14) WITH 9000xg RAT  
LIVER HOMOGENATE SUPERNATANT

sample taken immediately after addition of the parent 5-nitrofuran. There are, however, two peaks at retention times 5.6 and 8.1 min that decrease with incubation time. Stability studies (p 22) identified these peaks as the di- and mono- desacetyl products resulting from hydrolysis of (I). The precise reason for the instability of (I-acetyl-H-3) observed here is unknown since neither deacetylated product was observed in metabolism studies using non-radiolabeled (I) or when using (I-acetyl-1-C-14). However, radiolabels are known to destabilize compounds. All of these observations led to the conclusion that tritium labeling on the acetyl groups was unexceptionable for metabolism studies.

In the incubation using (I-acetyl-1-C-14) constant time increment fractions of the HPLC eluent were collected to allow characterization of the radioactivity distribution over the total chromatogram. Because the amount of radioactivity being counted was so small relative to the background of radioactivity eluting from the column without any sample injection, net DPM values are reported in the HPLC radioactivity profiles. Net DPM values were calculated by subtraction of the amount of background radioactivity eluting immediately before sample injection from the radioactivity of the counted fraction. Examination of the HPLC net radioactivity/absorbance profiles (Figure 4.14), again, as with (I-acetyl-H-3) incubations, shows that a significant amount of radioactivity is not associated with any peaks detected by UV absorption. After 45 min of incubation the absorbance profile shows only a solvent front peak and (M-2) but the radioactivity profile shows a moderate solvent front followed by almost a continuous spread of radioactivity over the remaining HPLC profile. These observations led to the conclusion that acetyl-1-C-14 labeling was unacceptable for metabolism studies.

#### D. Discussion

Both H-3 and C-14 acetyl labeled (I) were evaluated for their suitability for use in metabolism studies by incubation with the 9000xg rat liver homogenate supernatant. For each compound the lability of the label made them unacceptable for use in metabolism studies. The HPLC absorbance/radioactivity profiles indicated substantial deacetylation for (I-acetyl-H-3) and after metabolism had occurred both compounds showed almost a continuous spread of radioactivity throughout the HPLC profile that was not associated with any peaks detected by UV absorbance. From these observations it was decided that metabolism studies could only be conducted with a radiolabel of C-14 in a non-labile position. A C-14 label such as that in 2,4-diacetylamino-6-(5-nitro-2-furyl)-1,3,5-triazine-(6-C-14) (I-C-14) seemed to be a logical choice.

#### VII. Determination of Total Mass Balance of Metabolites in the 9000xg Rat Liver Homogenate Supernatant and Xanthine Oxidase Incubation Systems with Radiolabeled 2,4-Diacetylamino-6-(5-Nitro-2-Furyl)-1,3,5-Triazine-(6-C-14) (I-C-14)

These studies were performed to determine the relative amounts of metabolites produced in the 9000xg rat liver homogenate supernatant and xanthine oxidase incubation systems. In addition, metabolites produced in too small amounts or without chromophores that allow for detection by UV absorption would be detected by radioactivity counting of HPLC fractions provided that these metabolites still contained the radiolabel.

## A. Materials and Methods

Because six weeks had elapsed since the preparation of 2,4-diacetyl-amino-6-(5-nitro-2-furyl)-1,3,5-triazine-(6-C-14) (I-C-14) radiochemical purity and specific activity were re-determined as previously described.

### 1. In the 9000xg Rat Liver Homogenate Supernatant

Incubation of (I-C-14) with 9000xg rat liver homogenate supernatant was carried out at 37<sup>0</sup>C in a Dubnoff metabolic incubator with the same precautions for maintenance of anaerobic conditions and subdued light as previously described. Incubation mixtures contained 3.43 ml 100 mM potassium phosphate buffer pH 7.35 and 1.0 ml of an NADPH generating system consisting of NADP (2.0 umoles), glucose-6-phosphate (60 umoles), and MgCl<sub>2</sub> (30 umoles). Following addition of 0.5 ml 9000xg rat liver homogenate supernatant (corresponding to 250 mg of tissue) to the incubation mixture, metabolism was initiated by the addition of 50 ul of the DMSO solution of (I-C-14). The DMSO solution containing 0.40 umoles (17.4 uCi) (I-C-14) per 50 ul was prepared by aliquoting out the appropriate amount of (I-C-14) in acetic anhydride, from the synthesis, removing the solvent by high vacuum distillation, and reconstituting with DMSO.

After 45 min of incubation a 500 ul aliquot was mixed with 1.0 ml ice cold methanol and centrifuged at 9000xg at 2<sup>0</sup>C for 30 min to precipitate proteins. Aliquots (100 ul) of the supernatant were then analyzed by HPLC using the following three separate elution schemes on a 10u C<sub>18</sub>-column (Alltech Associates, Deerfield, Illinois) 4.6 mm X 25 cm with UV detection at 280 nm and 365 nm. Elution scheme 1 of isocratic 40% MeOH/H<sub>2</sub>O (V/V) at 2.0 ml/min was used to quantitate (M-2) through

radioassay of eluted fractions every 0.3 min. Elution scheme 2 of isocratic 7% MeOH/H<sub>2</sub>O (V/V) at 2.0 ml/min was used to quantitate (M-1) through radioassay of eluted fractions every 0.3 min up to 12.0 min then 1.0 min fractions to 32 min. A final elution scheme of 0% to 40% MeOH/H<sub>2</sub>O (V/V) on gradient program 10 (Waters Associates gradient programmer model 660) in 20 min at 2.0 ml/min was used in an attempt to observe any previously non-detected metabolites and characterize radioactivity at the solvent front of the previous chromatograms by radioassay of 0.3 min fractions to 9.0 min and then 1.0 min fractions to 49 min.

HPLC fractions were radioassayed using a Beckman LS 7800 liquid scintillation counter (Beckman Instruments Inc., Irvine, California) with PCS (Amersham, Arlington Heights, Illinois) liquid scintillation cocktail and quench correction by sample channels ratio method. This counter contained a microprocessor that automatically determined quench correction by generating a third-order polynomial least-squares cubic fit regression of data from a set of quenched standards. All samples were counted to an accuracy of at least 2%.

To determine what percentage of the radioactivity in the HPLC injection was eluted in each of the collected fractions, 200  $\mu$ l of the supernatant following protein precipitation was diluted with 5.00 ml of the same buffer and 500  $\mu$ l samples counted. In order to determine radioactivity that was precipitated with protein, 200  $\mu$ l of incubation mixture was diluted with 10.00 ml 100 mM potassium phosphate buffer pH 7.35 and 500  $\mu$ l samples were counted.

## 2. In Xanthine Oxidase

Incubation of (I-C-14) with xanthine oxidase was carried out at 37°C in a Dubnoff metabolic incubator with the same precautions for maintenance of anaerobic conditions and subdued light as previously described. Incubation mixtures contained 4.86 ml 50 mM potassium phosphate buffer pH 5.8 containing 2.5 mg hypoxanthine. After anaerobic conditions were established 89 µl of commercial xanthine oxidase suspension containing 2.5 U xanthine oxidase were added and the metabolism initiated by the addition of 50 µl DMSO solution containing 0.44 µmole (19.2 µCi) (I-C-14) prepared as previously described. After 90 min of incubation HPLC/radioassay analysis was performed in the same manner as previously described for the 9000xg rat liver homogenate supernatant.

Because (I-C-14) was of relatively low radiochemical purity it was necessary to incubate (I-C-14) under the same conditions as described in the previous studies except without any enzymatic nitroreductase present. Two such control incubations were performed. The first incubation contained 4.95 ml 50 mM potassium phosphate buffer pH 5.8 containing 2.5 mg hypoxanthine and 50 µl DMSO solution containing 0.44 µmole (19.2 µCi). In order to determine if the radioactivity associated with the solvent front in the HPLC analysis was caused by non-enzymatic dependent binding to protein, the second control incubation contained the same constituents as the first with the addition of 3.3 mg of bovine serum albumin. Incubations were for 90 min and sample aliquots of supernatant, following protein precipitation, were analyzed by HPLC with radioactivity counting of eluent fractions as previously described for the 40% MeOH/H<sub>2</sub>O (V/V) and 7% MeOH/H<sub>2</sub>O (V/V) elution schemes.

Because results indicated significantly higher amounts of radio-

activity associated with protein in the 9000xg rat liver homogenate supernatant incubation, the relative protein concentration of the two systems was determined. Protein was determined by the method of Lowry et al. (89) using bovine serum albumin as a standard.

## B. Results

The results of the radiochemical purity and specific activity determination of (I-C-14) six weeks after preparation indicated that the compound had degraded to a radiochemical purity of 72.9% with the specific activity remaining fairly constant at 43.5 mCi/mmole. Because no procedure was developed to purify the compound it was used in this relatively low state of purity and all calculations take this into consideration.

The HPLC absorbance/radioactivity profiles from the metabolism and control studies of (I-C-14) are shown in Figures 4.15 through 4.20. Metabolites (M-1) and (M-2) were quantitated on the isocratic 7% MeOH/H<sub>2</sub>O (V/V) (Figure 4.16) and 40% MeOH/H<sub>2</sub>O (V/V) (Figure 4.15) elution HPLC's respectively. Quantitation was done by adding the total radioactivity associated with metabolite HPLC absorbance peaks and subtracting a background value calculated by estimating the radioactivity in each peak resulting from incomplete separation of metabolite from other radioactivity. Specifically, background estimation was by drawing a continuation line of the decreasing amount of radioactivity counted in each fraction following the solvent front through the metabolite peak to the value following metabolite elution.

Incubation times were selected from the relative rate metabolism studies (p 96) so that complete metabolism of the parent 5-nitrofurran

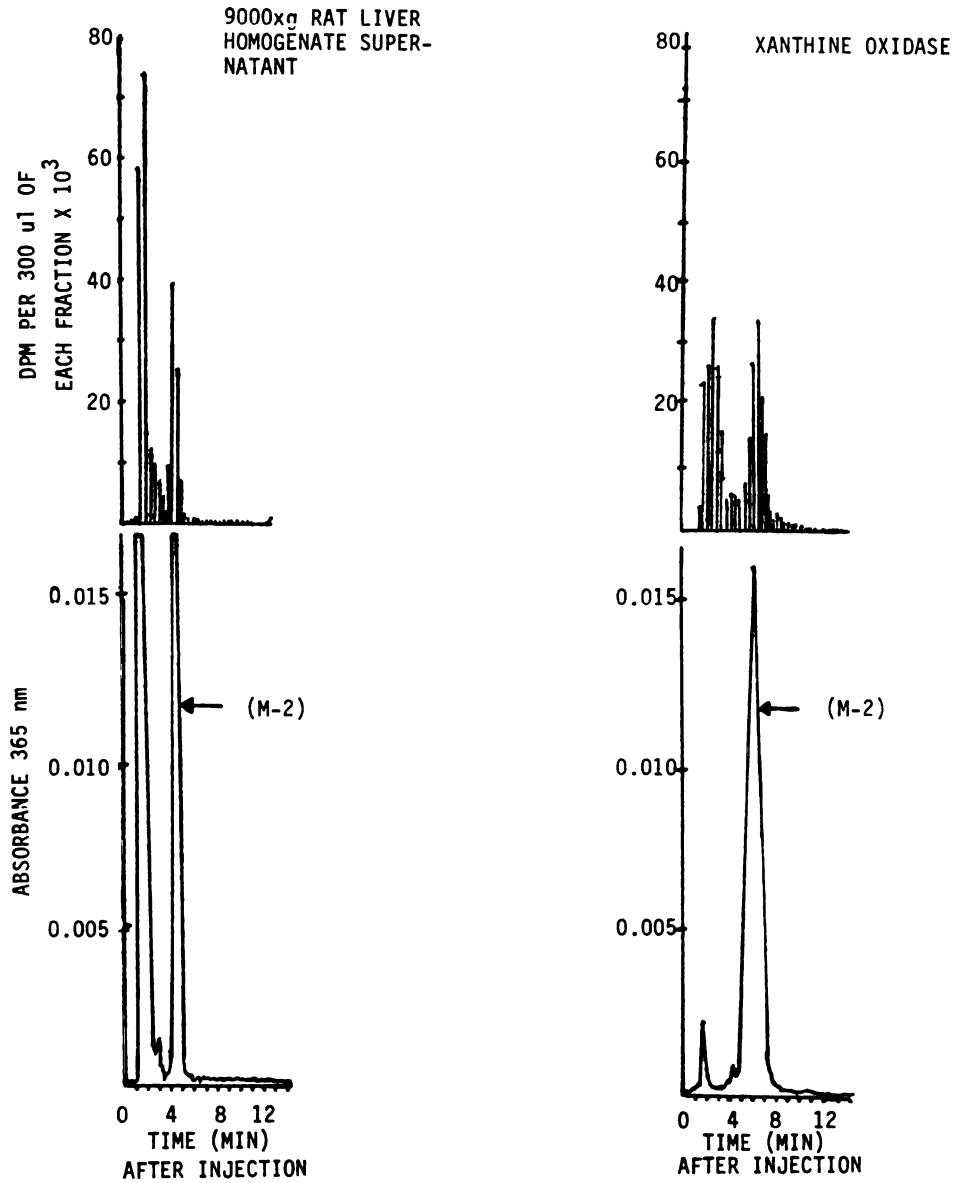


FIGURE 4.15

ISOCRATIC 40% MeOH/H<sub>2</sub>O (V/V) HPLC ABSORBANCE/RADIOACTIVITY  
PROFILES OF INCUBATION OF (I-C-14) WITH 9000xg RAT  
LIVER HOMOGENATE SUPERNATANT AND XANTHINE OXIDASE



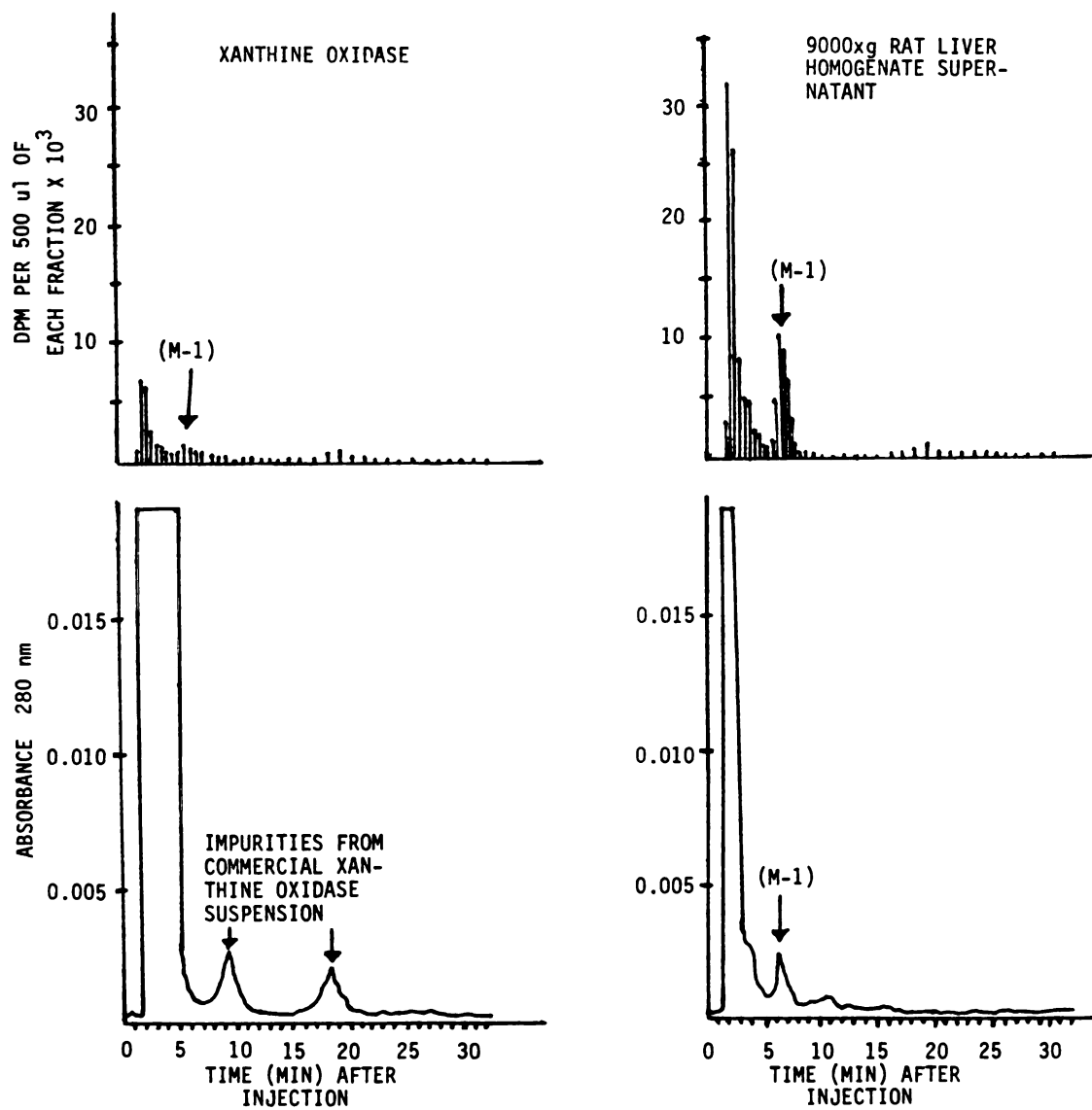


FIGURE 4.16

ISOCRATIC 7% MeOH/H<sub>2</sub>O (V/V) HPLC ABSORBANCE/RADIOACTIVITY PROFILES AFTER INCUBATION OF (I-C-14) WITH 9000xg RAT LIVER HOMOGENATE SUPERNATANT AND XANTHINE OXIDASE

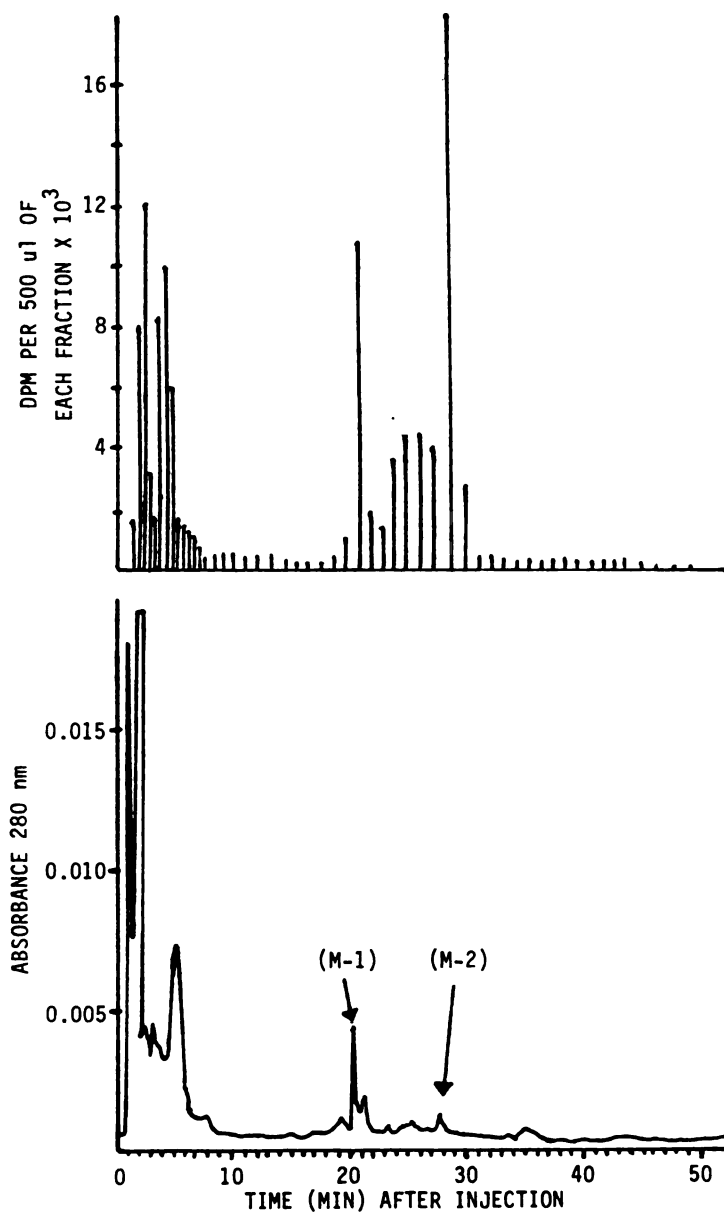
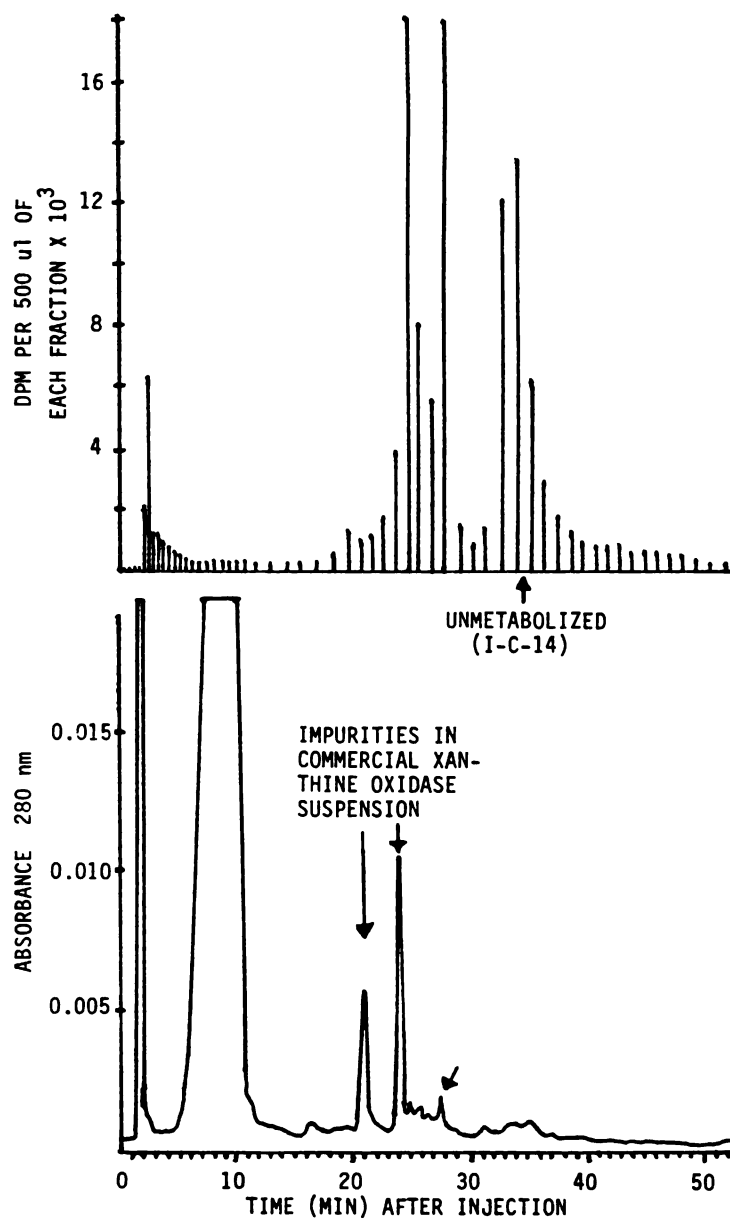


FIGURE 4.17

GRADIENT ELUTION 0 $\rightarrow$ 40% MeOH/H<sub>2</sub>O (V/V) #10 PROGRAM  
(WATERS GRADIENT PROGRAMER MODEL 660) HPLC  
ABSORBANCE/RADIOACTIVITY PROFILE AFTER INCUBATION OF (I-C-14)  
WITH 9000xg RAT LIVER HOMOGENATE SUPERNATANT



**FIGURE 4.18**

GRADIENT ELUTION 0 $\rightarrow$ 40% MeOH/H<sub>2</sub>O (V/V) #10 PROGRAM  
 (WATERS GRADIENT PROGRAMER MODEL 660) HPLC  
 ABSORBANCE/RADIOACTIVITY PROFILE AFTER INCUBATION OF  
 (I-C-14) WITH XANTHINE OXIDASE

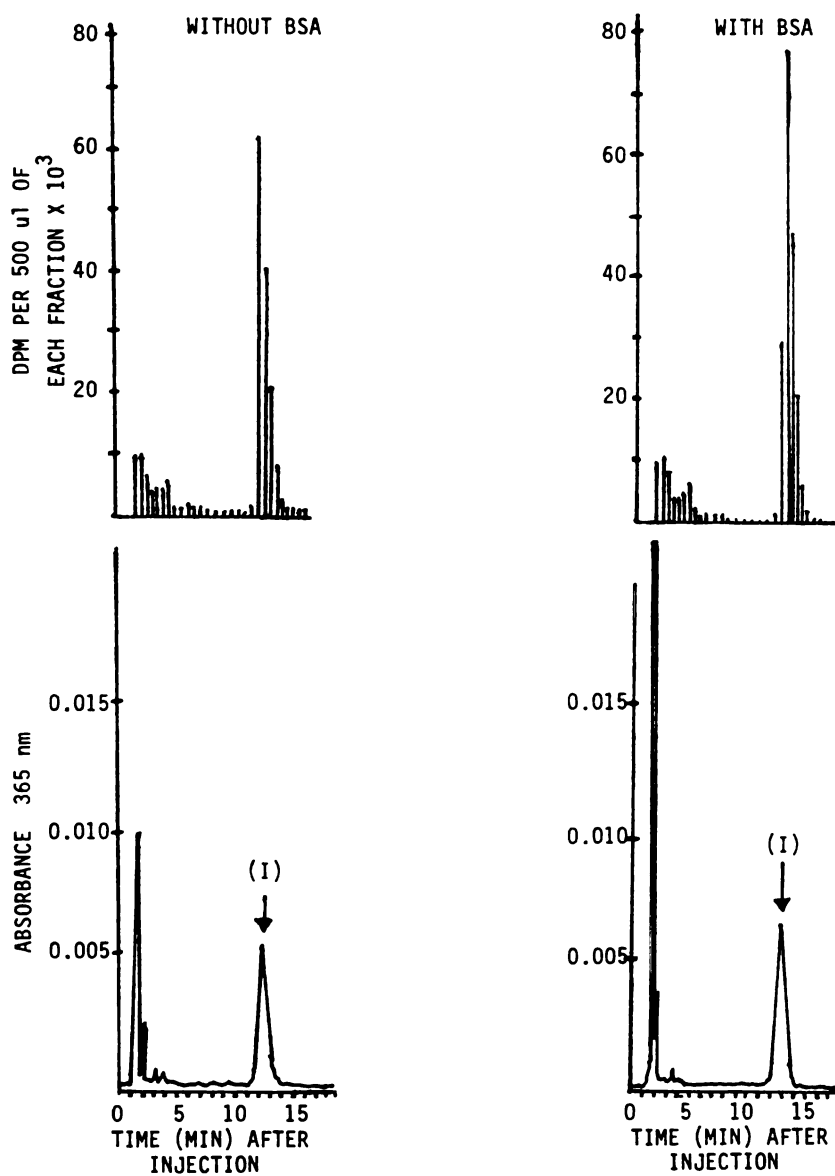


**FIGURE 4.19**

ISOCRATIC 40% MeOH/H<sub>2</sub>O (V/V) HPLC ABSORBANCE/RADIOACTIVITY PROFILES AFTER CONTROL INCUBATIONS OF (I-C-14) IN 50 mM POTASSIUM PHOSPHATE BUFFER pH 5.8 CONTAINING 2.5 mg HYPOXANTHINE AND IN 50 mM POTASSIUM PHOSPHATE BUFFER pH 5.8 CONTAINING 3.3 mg BSA AND 2.5 mg HYPOXANTHINE

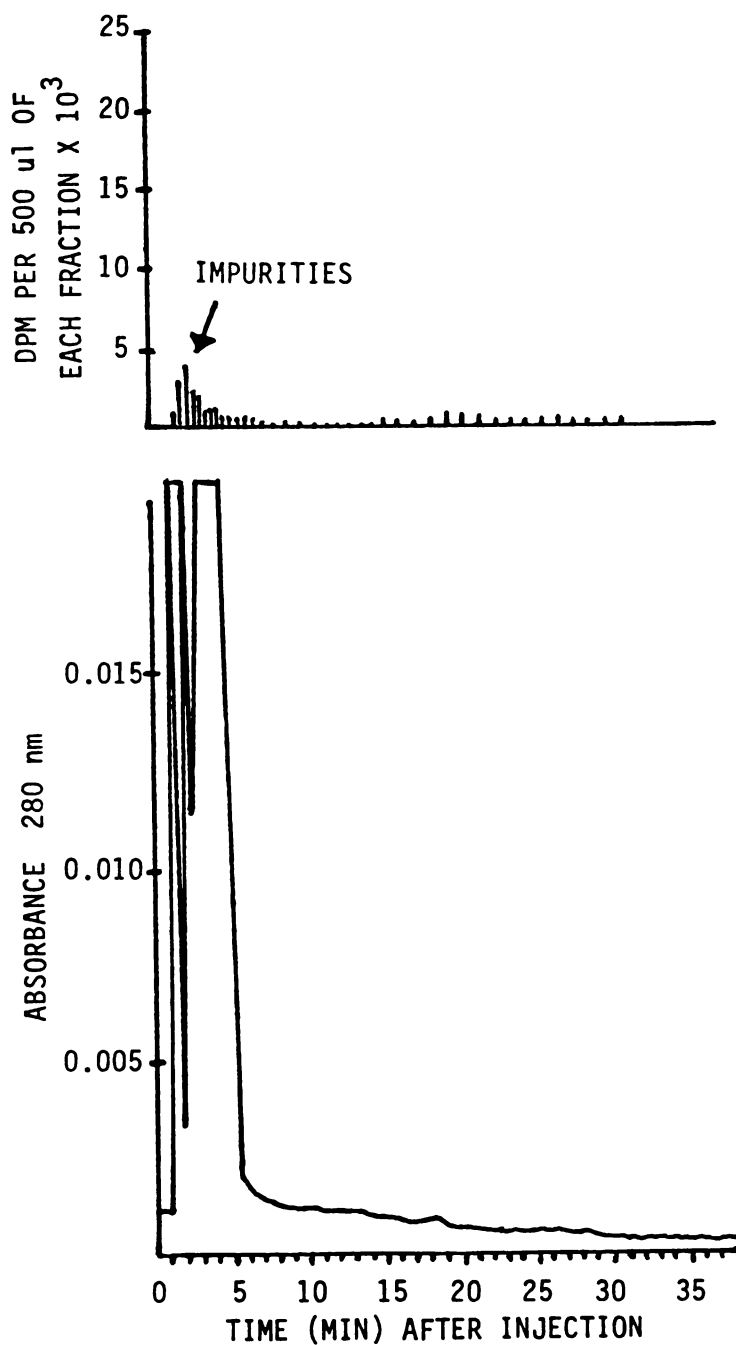


FIGURE 4.20

ISOCRATIC 7% MeOH/H<sub>2</sub>O (V/V) ABSORBANCE/RADIOACTIVITY  
PROFILE AFTER CONTROL INCUBATION OF (I-C-14) IN  
50 mM POTASSIUM PHOSPHATE BUFFER pH 5.8 CONTAINING  
2.5 mg HYPOXANTHINE

would be achieved. However, the gradient elution 0% to 40% MeOH/H<sub>2</sub>O (V/V) program 10 (Waters gradient programmer model 660) HPLC absorbance/radioactivity profile of incubation of (I-C-14) with xanthine oxidase (Figure 4.18) indicated the presence of unmetabolized (I-C-14). Apparently the commercial xanthine oxidase suspension used did not contain comparable nitroreductase activity to that used in the relative rate studies. Quantitation of remaining unmetabolized (I-C-14) was achieved with background subtraction for result calculation as previously described.

Results of the recovered radioactivity in each HPLC analysis and quantitation of (M-1) and (M-2) are reported in Table 4.1. Radioactivity (DPM) values are reported as the net values resulting from subtraction of estimated background from total DPM as previously described. The results indicate significantly different metabolite distribution from the two different systems. Xanthine oxidase produces almost exclusively the aminofuran metabolite (M-2) while the 9000xg rat liver homogenate supernatant distribution is approximately one-third (M-1) and two-thirds (M-2). However, the sum total of the metabolites accounted for represent remarkably similar amounts of 49.3% and 52.2% of metabolized parent 5-nitrofurans in both systems.

The percent recovery of HPLC injected radioactivity results indicates complete elution of all radioactivity for the isocratic 40% MeOH/H<sub>2</sub>O (V/V) and gradient 0% to 40% MeOH/H<sub>2</sub>O (V/V) elution. The recovery result for the isocratic 7% MeOH/H<sub>2</sub>O (V/V) elution was expected to be less than complete recovery since (M-2) and (I) were not eluted. However, there was a significant difference in the amount of radioactivity recovered on the 7% MeOH/H<sub>2</sub>O (V/V) system between the two

TABLE 4.1

RESULTS OF MASS BALANCE OF METABOLITES IN THE 9000xg RAT  
LIVER HOMOGENATE SUPERNATANT AND XANTHINE OXIDASE  
INCUBATION WITH (I-C-14) STUDIES

MEASURED/CALCULATED VALUE	9000xg RAT LIVER HOMOGENATE SUPERNATANT	XANTHINE OXIDASE
TOTAL (I-C-14) DPM IN 100 $\mu$ l INJECTED ON HPLC	257,520	284,160
NET DPM ASSOCIATED WITH UNMETABOLIZED (I-C-14) FROM GRADIENT 0-40% MeOH/H <sub>2</sub> O ELUTION	0	33,800
NET DPM ASSOCIATED WITH (M-1) FROM ISOCRATIC 7% MeOH/H <sub>2</sub> O ELUTION	39,151	3,738
NET DPM ASSOCIATED WITH (M-2) FROM ISOCRATIC 40% MeOH/H <sub>2</sub> O ELUTION	87,809	126,901
PER CENT OF TOTAL DPM INJECTED INTO HPLC THAT IS COUNTED IN COLLECTED FRACTIONS FOR-		
<u>ISOCRATIC 40% MeOH/H<sub>2</sub>O ELUTION</u>	108.5%	102.1%
<u>ISOCRATIC 7% MeOH/H<sub>2</sub>O ELUTION</u>	57.7%	16.5%
GRADIENT 0-40% MeOH/H <sub>2</sub> O ELUTION	105.3%	110.5%
PER CENT OF METABOLIZED (I-C-14) THAT RESULTS IN-		
<u>ISOLATED (M-1)</u>	15.2%	1.5%
ISOLATED (M-2)	34.1%	50.7%
PER CENT UNMETABOLIZED (I-C-14) REMAINING AT END OF INCUBATION	0%	11.9%

enzymatic systems which cannot be rationalized solely on the basis of the difference in amount of (M-1) eluted. Examination of the HPLC absorbance/radioactivity profiles (Figure 4.14 through 4.20) shows that the major amount of recovered radioactivity is associated with the solvent front where polar soluble molecules are expected to elute. These polar compounds may be from two different sources. First, in the 9000xg rat liver homogenate, where metabolite conjugate-forming enzymes and cofactors are present, polar conjugate metabolites may have formed. Second, because the protein concentration is much higher in the 9000xg rat liver homogenate, a larger amount of metabolite bound protein that remained soluble after protein precipitation could be eluting. This second explanation is further supported by comparison of the amount of radioactivity precipitated with protein (Table 4.2) with the amount of radioactivity associated with the solvent front as discussed below.

In order to represent the net result of metabolism on an HPLC profile, chromatograms were created by subtraction of the control radioactivity in the incubation of (I-C-14) with potassium phosphate buffer and hypoxanthine only from the enzyme incubations for isocratic 40% MeOH/H<sub>2</sub>O (V/V) and 7% MeOH/H<sub>2</sub>O (V/V) elutions (Figure 4.21). The 40% MeOH/H<sub>2</sub>O (V/V) chromatograms show a large solvent front peak of radioactivity that contains either label bound to non-precipitable protein and/or polar metabolites. Assuming this fraction to be radiolabeled proteins, the amount of radioactivity was quantitated and presented in Table 4.2 along with the results of the amount of radioactivity precipitated in the preparation of the samples used for HPLC analysis and the Lowry protein determination on the 9000xg rat liver homogenate supernatant. These results indicate that the 9000xg rat liver homogenate



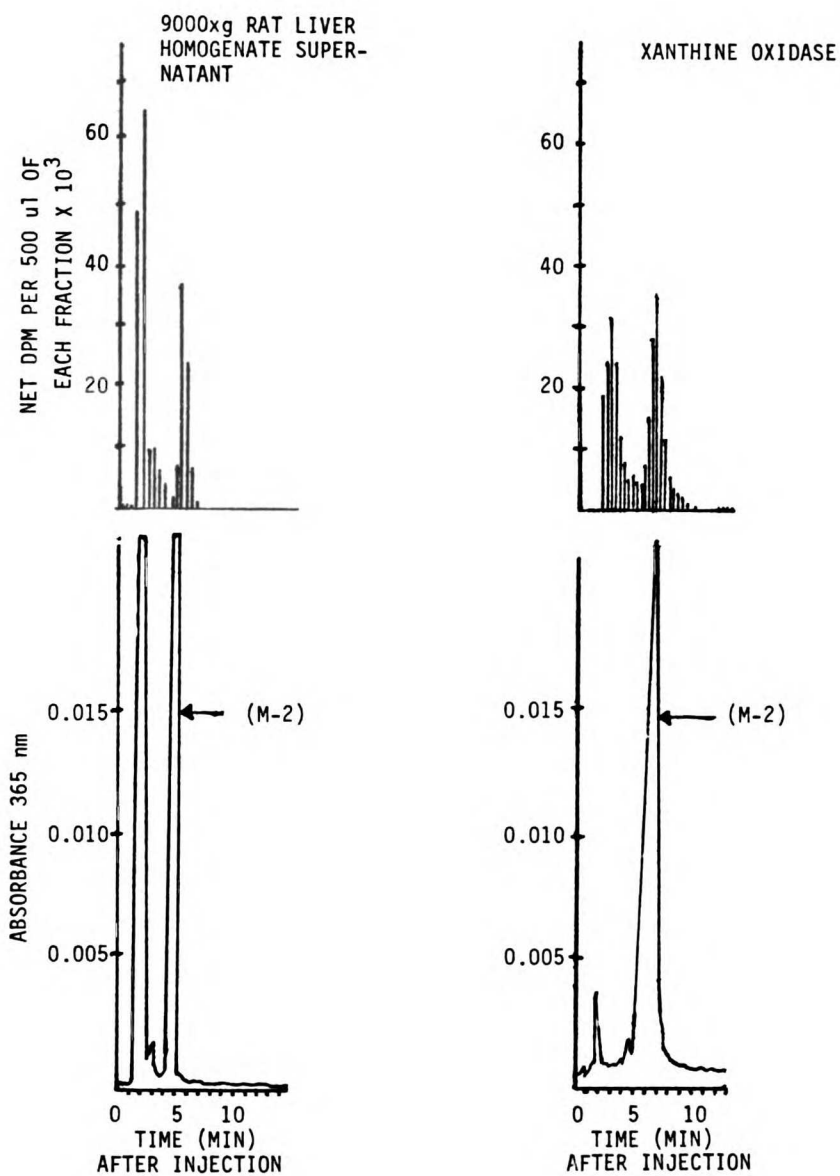


FIGURE 4.21

CREATED HPLC ABSORBANCE/RADIOACTIVITY CHROMATOGRAMS FOR  
 ISOCRATIC 40% MeOH/H<sub>2</sub>O (V/V) ELUTION  
 AFTER INCUBATION WITH XANTHINE OXIDASE OR  
 9000xg RAT LIVER HOMOGENATE SUPERNATANT

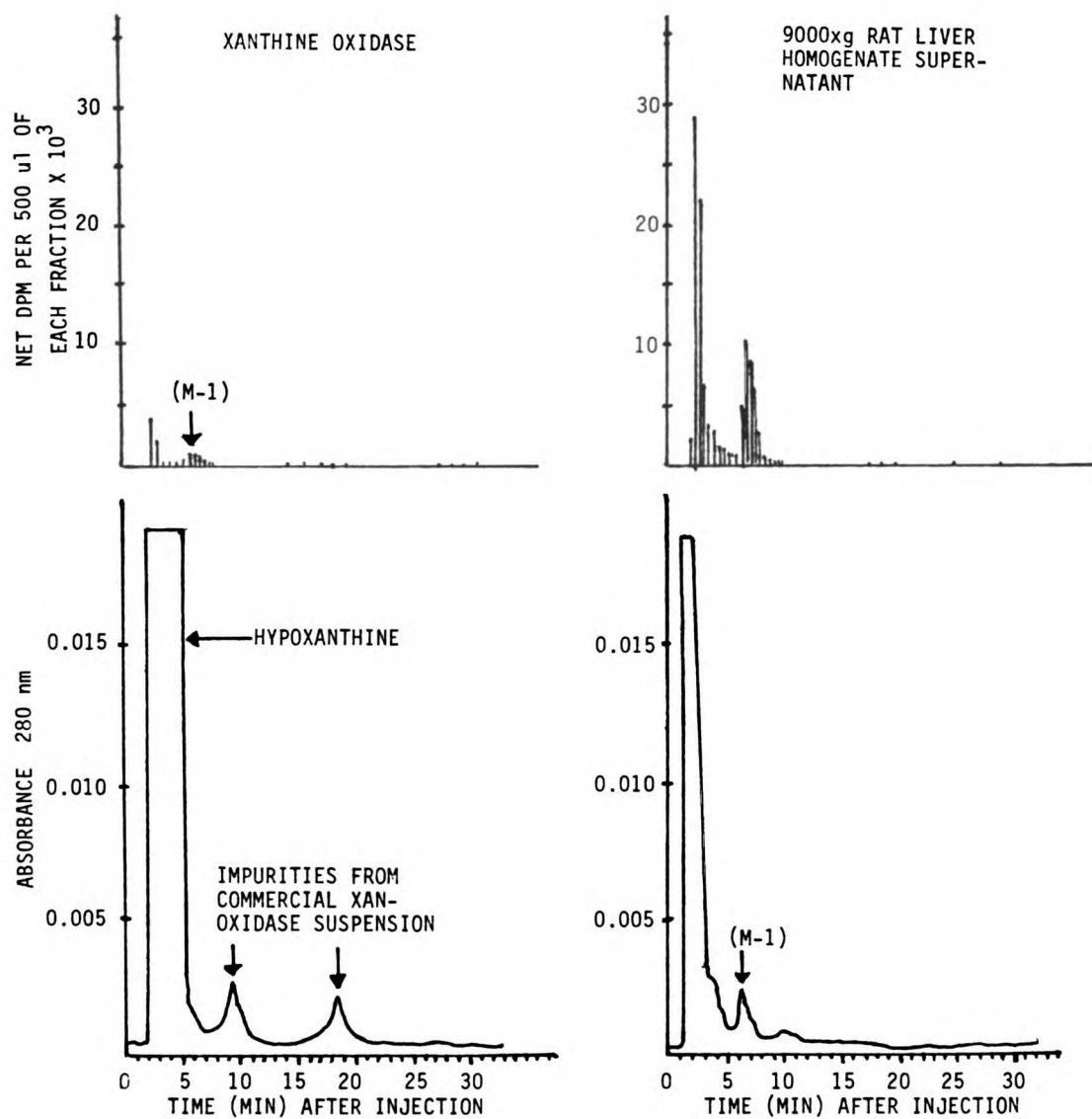


FIGURE 4.21

(CONTINUED)

CREATED HPLC ABSORBANCE/RADIOACTIVITY CHROMATOGRAMS FOR ISOCRATIC 7% MeOH/H<sub>2</sub>O (V/V) ELUTION AFTER INCUBATION WITH XANTHINE OXIDASE OR 9000xg RAT LIVER HOMOGENATE SUPERNATANT

TABLE 4.2

RESULTS OF QUANTITATION OF RADIOACTIVITY ASSOCIATED WITH  
 PROTEIN IN INCUBATION MIXTURES RESULTING FROM METABOLISM

CALCULATED/DETERMINED VALUE	9000xg RAT LIVER HOMOGENATE SUPERNATANT	XANTHINE OXIDASE
PER CENT OF DPM ADDED TO METABOLISM MIXTURE ASSOCIATED WITH SUSPECTED PROTEIN PEAK IN CREATED 40% MeOH/H <sub>2</sub> O CHROMATO- GRAM	43.9%	28.6%
PER CENT OF DPM PUT INTO INCUBATION THAT IS PRECIPITATED WITH PROTEIN IN THE PREPARATION OF THE HPLC ANALYSIS SAMPLE	15.4%	8.4%
PROTEIN CONCENTRATION IN THE INCUBATION MIXTURE (mg/ml)	4.1 <sup>a</sup>	0.97 <sup>b</sup>

a By Lowry protein determination

b As reported in the commercial brochure

supernatant incubation, which has a greater than four fold higher protein concentration than the xanthine oxidase incubation has more radioactivity precipitated with the protein and more radioactivity associated with the solvent front peak in the created 40% MeOH/H<sub>2</sub>O (V/V) chromatograms. This suggests that at least some of the radiolabel is associated with the non-precipitable protein.

#### VIII. Summary

Anaerobic in vitro metabolism studies on (I) using the 9000xg rat liver homogenate supernatant, rat liver microsomes, and xanthine oxidase, as the source of nitroreductase have been conducted. In all three enzymatic systems two metabolites were observed following reverse phase HPLC. The dependence on the presence of DNA on the rate of disappearance of (I) and appearance of (M-2) was determined for each nitroreductase system. There appeared to be a significant dependence for the 9000xg rat liver homogenate supernatant, only a slight dependence for the rat liver microsomes, and no dependence for xanthine oxidase. These results may be explained by a precipitation entrapment effect resulting when greater amounts of protein are precipitated.

Relative rates of metabolism studies were conducted to determine conditions to be used in DNA binding studies. From these studies a significant difference in the relative rates of loss of parent 5-nitro-furan and appearance of (M-2) between the rat liver derived enzymes and xanthine oxidase emerged. The rate of disappearance of (I) in relation to appearance of (M-2) was much faster in the xanthine oxidase catalyzed system.

Preparative scale incubations were performed in attempts to iso-

late and elucidate the structures of metabolites (M-1) and (M-2). Spectral measurements strongly suggested the 5-aminofuran structure (III) for (M-2) and confirmation that (M-2) was (III) was made by synthesis of (III) through catalytic hydrogenation of (I). The combined spectral measurements on (M-1) were unsatisfactory for structural elucidation. However, the UV spectra and the instability of (M-1) did suggest an open chain nitrile structure.

Studies to investigate the suitability of H-3 and C-14 acetyl labeled (I) for metabolism studies were conducted. The HPLC absorbance/radioactivity profiles of the incubation mixtures indicated extensive radiolabel lability that precludes their usefulness for such studies. From these results it was decided that metabolism studies could only be conducted with a radiolabel on one of the ring carbons.

Using (I-C-14), determination of total mass balance of metabolites in the 9000xg rat liver homogenate supernatant and xanthine oxidase incubation systems was achieved. Xanthine oxidase metabolized (I-C-14) to the aminofuran (M-2). The 9000xg rat liver homogenate supernatant produced an identified metabolite distribution of approximately one-third (M-1) and two-thirds (M-2). Both enzymatic systems produced about equivalent sum total amounts of identified metabolites suggesting that one metabolite was formed initially and other metabolite resulted from further metabolism or chemical instability.

Quantitation of the amount of radioactivity precipitated with protein in the preparation of the sample for HPLC analysis together with the observed radioactivity in the solvent front of the isocratic 40% MeOH/H<sub>2</sub>O (V/V) HPLC elution profiles suggests that large amounts of activated (I-C-14) were bound to protein material. It is also possible

that this solvent front peak could contain one or more polar metabolites. However, because the solvent front consisted of one large radioactive peak, resolution of possible additional polar metabolites could not be achieved. Moreover, because incubations that had higher protein concentrations also had higher amounts of radioactivity associated with the solvent front of the HPLC elution profile, it is suggested that activated (I-C-14) metabolites were bound to protein rather than subsequently metabolized to (M-1), (M-2), or other, as yet unidentified, metabolites.

## CHAPTER FIVE

IN VITRO NITROREDUCTASE CATALYZED BINDING OF  
2,4-DIACETYLAMINO-6-(5-NITRO-2-FURYL)-1,3,5-TRIAZINE-  
(6-C-14) TO DNA

I. Background

Incubation of 2,4-diacetylamino-6-(5-nitro-2-furyl)-1,3,5-triazine-(6-C-14) (I-C-14) in vitro under nitroreductase catalyzing conditions in the presence of added DNA was investigated using the three enzymatic systems, 9000xg rat liver homogenate supernatant, rat liver microsomes, and xanthine oxidase. Following incubation, the amount of DNA-bound radioactivity resulting from metabolic activation was quantitated. Isolation of DNA from incubation mixtures utilized two separation techniques. Hydroxylapatite column chromatography was used to isolate DNA from incubations containing the 9000xg rat liver homogenate supernatant. A protein phenolic extraction/DNA precipitation technique was used to isolate DNA from incubations containing rat liver microsomes and xanthine oxidase. The phenolic extraction technique could not be used with incubations containing the 9000xg rat liver homogenate supernatant because emulsions formed and phase separation was poor.

Preliminary studies used the 9000xg rat liver homogenate supernatant. After it was determined that little or no DNA-bound radioactivity resulted from metabolism, studies were conducted using the relatively purer rat liver microsomes as the source of nitroreductase. DNA bound radioactivity resulting from metabolism was determined and studies on the dependence on the amount of enzyme and time of incuba-

tion were performed. Final DNA binding studies were with xanthine oxidase as the source of nitroreductase. Again, DNA bound radioactivity dependence on the amount of enzyme and time of incubation were studied.

## II. Using the 9000xg Rat Liver Homogenate Supernatant

### A. Materials and Methods

Incubations of (I-C-14) with 9000xg rat liver homogenate supernatant were carried out at 37<sup>0</sup>C in a Dubnoff metabolic incubator. Precautions for maintenance of anaerobic conditions and subdued light were as previously described (p 96). Two incubation trials were performed with each containing 10.0 mg calf thymus DNA (Type I, No. D-1501, Sigma Chemical Company, St. Louis, Missouri) dissolved in 10.0 ml 100 mM potassium phosphate buffer pH 7.35. To each incubation was added 2.0 ml of an NADPH-generating system consisting of NADP (2.0 umoles), glucose-6-phosphate (60 umoles), and MgCl<sub>2</sub> (30 umoles). After anaerobic conditions were established, 1.0 ml of the 9000xg rat liver homogenate supernatant was added to one vial and 1.0 ml buffer added to the other control vial. Metabolism was then initiated by addition of 250 ul DMSO solution containing 2.78 umoles (120 uCi) (I-C-14) prepared as previously described (p 126).

After 30 min, the incubation mixtures were transferred to 50 ml screw cap polypropylene tubes and 26.5 ml ice cold ethanol were added with vortexing to precipitate proteins and DNA. Following centrifugation at 2000xg for 10 min at 2<sup>0</sup>C the supernatant was removed to separate soluble metabolites and the combined protein/DNA pellet was



resuspended in 10 ml 8 M urea 0.24 M sodium phosphate buffer pH 6.8. DNA was then separated according to the method of Shoyab (90) using hydroxylapatite column chromatography.

DNA separation consisted of applying the resuspended protein/DNA pellet in 8 M urea 0.24 M sodium phosphate buffer to the top of a 2.5 cm X 10 cm hydroxylapatite (16 gms hydroxylapatite, DNA-grade Bio-Gel HTP, Bio-Rad Laboratories, Richmond, California) column equilibrated with the same buffer. Proteins were eluted with 175 ml of the urea/phosphate buffer and then urea was removed with 175 ml 0.15 M sodium phosphate buffer pH 6.8. Finally double stranded DNA free of protein was eluted with 175 ml 0.4 M sodium phosphate buffer pH 6.8. Fractions (8.8 ml) of the entire elution process were collected. The absorbance, at 280 nm (Bausch & Lomb Spectronic 710 spectrophotometer, Bausch & Lomb Analytical Systems Division, Rochester, New York) of each fraction was determined together with radioactivity counting of 2.0 ml aliquots of selected fractions for construction of an absorbance/radioactivity chromatogram. Typical chromatography elutions took 17 hrs to complete. Liquid scintillation counting was done on a Beckman LS 7800 liquid scintillation spectrometer with quench correction by channels ration method as previously described (p 127).

## B. Results

The absorbance/radioactivity chromatograms of the two trials are shown in Figure 5.1. These chromatograms indicate comparable amounts of radioactivity eluting with the DNA for the trial with active enzyme and the control (without enzyme). The results were interpreted as evidence that no significant binding to DNA of activated reduced

I-8M UREA 0.24M SODIUM PHOSPHATE BUFFER pH 6.8  
 II-0.15M SODIUM PHOSPHATE BUFFER pH 6.8  
 III-0.40M SODIUM PHOSPHATE BUFFER pH 6.8

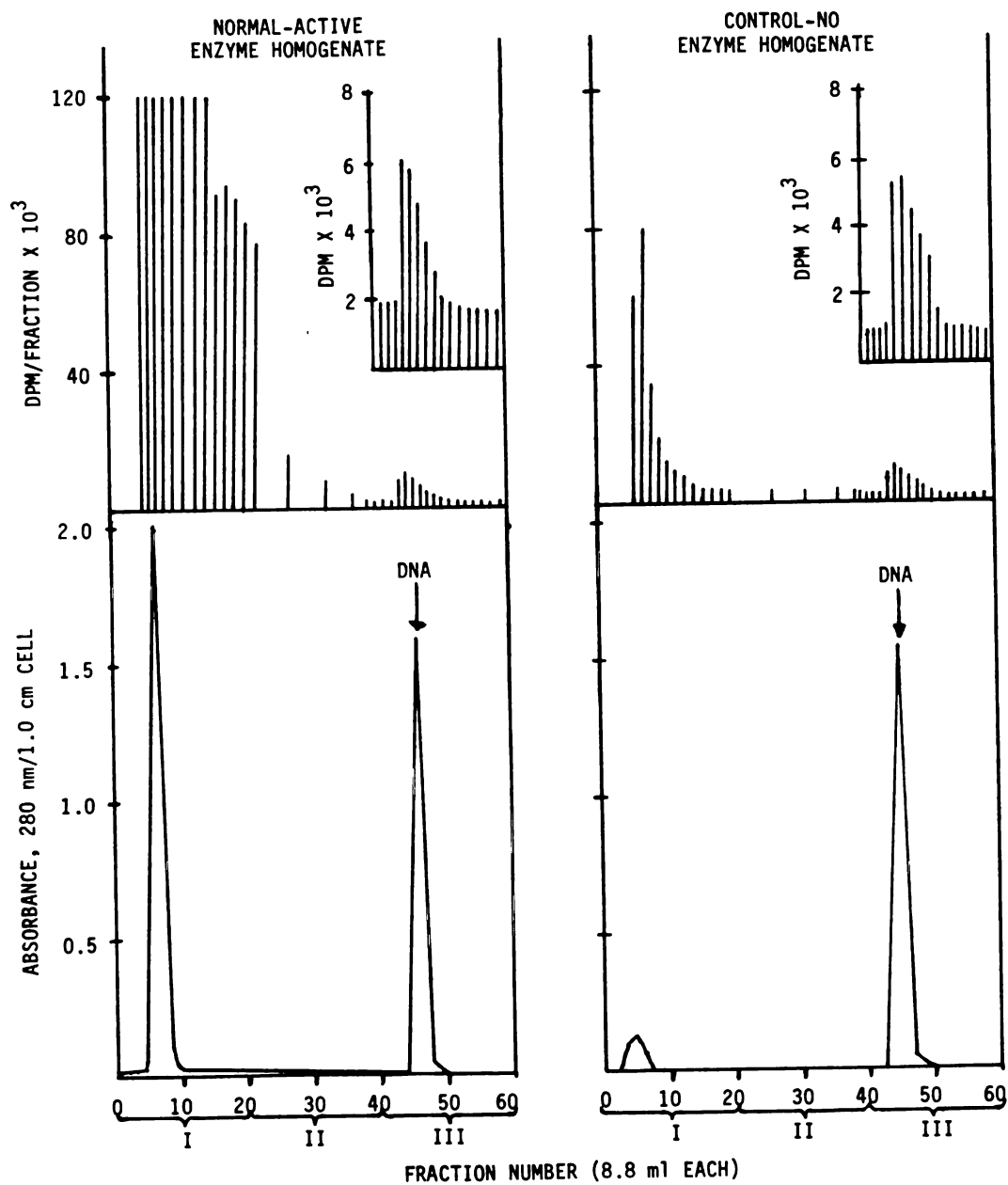


FIGURE 5.1

ABSORBANCE/RADIOACTIVITY HYDROXYLAPATITE COLUMN CHROMATOGRAMS  
 OF TRIALS OF INCUBATION OF (I-C-14) WITH 9000xg RAT LIVER  
 HOMOGENATE SUPERNATANT AND ADDED DNA

metabolites of (I-C-14) occurred.

### C. Discussion

The 9000xg rat liver homogenate supernatant is a very crude, impure source of nitroreductase. This fraction contains a relatively high concentration of protein material as well as glutathione. These components might be expected to reduce the amount of binding of activated metabolites to DNA by effectively competing for reactive intermediates. This appears to be the case in these studies as evidenced by the large amount of radioactivity eluting with protein on the chromatogram of the active enzyme trial. Apparently activated reduced metabolites of (I-C-14) became bound exclusively to protein and/or polypeptides as a result of their relatively high concentration in the incubation mixture.

If the previous conjectures are true, then a more highly purified source of microsomal nitroreductase would be expected to result in observable DNA-bound radioactivity. Such a source is the microsomal fraction of rat liver homogenate. This fraction is free of all soluble protein material and cofactors such as glutathione. Studies were therefore undertaken to observe DNA bound radioactivity resulting from incubation of (I-C-14) with rat liver microsomes.

## III. Using Rat Liver Microsomes

### A. Materials and Methods

Incubations of (I-C-14) with rat liver microsomes were carried out at 37°C in a Dubnoff metabolic incubator. Precautions for maintenance of anaerobic conditions and subdued light were as previously described

(p 96). Incubation mixtures had a total volume of 15.75 ml containing 15.75 mg dissolved calf thymus DNA, 60 umoles  $MgCl_2$ , 10 umoles NADPH tetrasodium salt ( $\beta$ -form, Sigma No. N-7505, Sigma Chemical Company, St. Louis, Missouri), and 2.78 umoles (120 uCi) (I-C-14) in 250 ul DMSO. In order to determine the amount of binding as a function of the amount of metabolism that had occurred, two separate studies were undertaken. In the first, the amount of microsomal suspension added to the incubation mixture was varied in three increments of 0.25, 0.50, and 0.75 ml. A metabolism time of 40 min was selected from the relative rate studies so that the relative amount of metabolism that had occurred was approximately 50%, 80%, and 85% respectively (see Figure 4.3). In the second study, metabolism time was varied from 1.0 hr to 2.5 hrs and 2.5 hrs to 4.0 hrs in one-half hour increments using 0.50 ml microsomal suspension from two separate rat liver preparations. For all incubations one-half of the NADPH was added at the start of incubation and the second half added approximately at one-half the total incubation time. The remaining volume in each incubation mixture consisted of 100 mM potassium phosphate buffer pH 7.3.

At the end of each incubation DNA was separated by the protein phenolic extraction/DNA precipitation technique of Howard and Beland (91). Incubation mixtures were transferred to a 25 mm X 200 mm glass screw cap tube containing 15.75 ml extraction mixture, phenol/isoamyl alcohol/chloroform, 25/1/24, (V/V), and immediately vortexed at high speed for 1.0 minutes. Following vortexing the emulsion was broken by centrifuging at 1200xg for 15 min and the lower organic phase, containing protein and metabolites, removed by disposable pipet. This extraction sequence was repeated two additional times and then the DNA was

precipitated from the aqueous phase by addition of 47 ml ice cold ethanol. The DNA was then pelleted by centrifugation at 1200xg for 5 min and the supernatant carefully removed by disposable pipet. The DNA was dissolved in 1.0 ml 5 mM (bis(2-hydroxyethyl)imino-tris(hydroxymethyl)methane)-HCl buffer pH 7.1 containing 0.1 mM EDTA (bis-tris/EDTA buffer) with vortexing to promote dissolution. The turbid solution of DNA was then transferred to a 1.5 ml plastic Eppendorf microcentrifuge tube and centrifuged at 12,000xg to bring down suspended particles. The clear supernatant was carefully transferred to a 13 mm X 100 mm glass tube and the DNA again precipitated by the addition of 3 ml ice cold ethanol. The tube was centrifuged to pellet the DNA. After removal of the supernatant the DNA was redissolved in 5.0 ml bis-tris/EDTA buffer and a 0.300 ml aliquot diluted to 10.0 ml with bis-tris/EDTA buffer for spectrophotometric determination of DNA content at 260 nm (Bausch and Lomb spectronic 710, Bausch and Lomb Analytical Division, Rochester, New York). The extent of radioactivity bound to DNA was determined with a Beckman LS 7800 liquid scintillation spectrometer (Beckman Instruments Inc., Irvine, California) with quench correction by channels ratio method as previously described (p 127). Two 2.00 ml aliquots of the final DNA solution were counted in PCS (Amersham, Arlington Heights, Illinois) cocktail.

Control studies using boiled enzymes were conducted to determine the extent of background radioactivity associated with the DNA following this separation procedure. Also, DNA isolated from these control studies was scanned in the UV range on a Cary model 118 spectrophotometer (Varian Instruments Division/Cary Products, Palo Alto, California) to confirm purity of the isolated DNA. In one other study  $MgCl_2$  was omitted from the incubation mixture to determine the influence it may have on the

amount of binding to DNA resulting from metabolic activation of (I).

In a final study attempts to determine if radioactivity bound DNA resulted from non-covalent binding of metabolites to DNA were made. This study was performed by first incubating active and boiled (control) enzymes without DNA. After 90 min, glutathione (reduced form, Sigma No. G-4254, Sigma Chemical Company, St. Louis, Missouri) (172 umoles) was added in 5.0 ml buffer. The glutathione should act as a nucleophilic trap for activated reduced metabolites of (I-C-14) effectively eliminating their ability to covalently bind to DNA. Following glutathione addition, incubation was continued for an additional hour after which DNA (15.75 mg) was added. When the DNA had gone into solution the samples were treated as already described for quantitation of DNA bound radioactivity.

## B. Results

Results of the quantitation of DNA-bound radioactivity are given in Table 5.1. From the specific activity of the isolated DNA and assuming each bound metabolite of (I-C-14) represents one nucleotide adduct the number of adducts per one-million nucleotides using 330 as the average nucleotide residue molecular weight was calculated. Control samples show background DNA radioactivity from the separation technique of approximately 20 adducts per million nucleotides. Almost all incubations done with active enzymes show more DNA-bound radioactivity than the controls. A correlation between the extent of metabolism, as determined by the amount of microsomal suspension or time of incubation, and DNA bound radioactivity is evident.

Results of the quantitation of DNA bound radioactivity for the

TABLE 5.1

RESULTS OF QUANTITATION OF DNA BOUND RADIOACTIVITY FOLLOWING  
 INCUBATION OF (I-C-14) WITH RAT LIVER MICROSOMES  
 (ENZYME AMOUNT AND INCUBATION TIME DEPENDENCE AND CONTROLS)

SAMPLE DESIGNATION <sup>a,b</sup>	AMOUNT OF MICROSOMAL SUSPENSION (ml)	INCUBATION TIME (MIN)	SPECIFIC ACTIVITY OF ISO-LATED DNA (DPM/mg)	CALCULATED NUMBER OF ADDUCTS PER 10 <sup>6</sup> NUCLEOTIDES
ACTIVE	0.25	40	6,974	24.0
ACTIVE	0.50	40	10,154	34.9
ACTIVE	0.75	40	14,893	51.2
ACTIVE	0.50	60	13,912	47.9
ACTIVE	0.50	90	12,138	41.8
ACTIVE	0.50	120	14,244	49.0
ACTIVE	0.50	150	23,567	81.1
ACTIVE	0.50	150	10,558	36.3
ACTIVE	0.50	180	12,478	42.9
ACTIVE	0.50	210	14,595	50.2
ACTIVE	0.50	240	16,405	56.4
CONTROL	0.25	40	6,501	22.4
CONTROL	0.50	40	4,752	16.4
CONTROL	0.75	40	5,974	20.6
CONTROL	0.50	90	6,129	21.1
CONTROL	0.50	90	7,155	24.6

a Control samples are boiled enzymes

b Grouped samples represent samples run from enzymes prepared from same rat

incubation without  $MgCl_2$  and the study using glutathione to block covalent binding are given in Table 5.2. The results indicate  $MgCl_2$  has no influence on the amount of DNA bound radioactivity. The results of the glutathione study are inconclusive. Very high DNA bound radioactivity was found with a fairly large variation between duplicate trials. However, because the control trial in this study had a relatively low amount of bound radioactivity this high binding may be important.

Ultraviolet spectral scans of DNA isolated from a control incubation and the commercial DNA put into the incubations are shown in Figure 5.2. The 260/280 nm optical density ratio was calculated and the values presented in the figure. A ratio of 1.85 is reported in the literature (92) to represent a pure DNA preparation free of protein.

### C. Discussion

The amount of binding to DNA resulting from metabolic activation was quite low. While other investigators (43, 93) have detected DNA-bound radioactivity from in vitro reductive metabolic activation of other radiolabeled 5-nitrofurans their studies did not quantitate the binding so a comparison can not be made. However, Swaminathan (94) reports that 2-amino-4-(5-nitro-2-furyl)-2-C-14-thiazole under reductive in vitro metabolic activation, utilizing rat liver microsomes, binds to t-RNA to a maximum of 10.2 nmoles per mg of t-RNA (3000 adducts per million nucleotides) at optimal conditions. The binding results reported here with (I-C-14) are about two orders of magnitude less. Comparison between binding studies using these two different nucleotides must be made cautiously since t-RNA has much less tertiary structure with more single stranded regions resulting in increased acces-



TABLE 5.2

RESULTS OF QUANTITATION OF DNA BOUND RADIOACTIVITY FOLLOWING  
INCUBATION OF (I-C-14) WITH RAT LIVER MICROSOMES

MgCl<sub>2</sub> DEPENDENCE STUDY

SAMPLE DESIGNATION <sup>a</sup>	AMOUNT OF MICROSOMAL SUSPENSION (ml)	INCUBATION TIME (MIN)	MgCl <sub>2</sub>	SPECIFIC ACTIVITY OF ISOLATED DNA (DPM/mg)	CALCULATED NUMBER OF ADDUCTS PER 10 <sup>6</sup> NUCLEOTIDES
ACTIVE	0.50	90	No	10,841	37.3
ACTIVE	0.50	90	No	11,061	38.1
ACTIVE	0.50	90	Yes	12,138	41.8
CONTROL	0.50	90	No	6,912	23.8

a Control samples are boiled enzymes

GLUTATHIONE STUDY

SAMPLE DESIGNATION <sup>a</sup>	AMOUNT OF MICROSOMAL SUSPENSION (ml)	INCUBATION TIME (MIN)	MgCl <sub>2</sub>	SPECIFIC ACTIVITY OF ISOLATED DNA (DPM/mg)	CALCULATED NUMBER OF ADDUCTS PER 10 <sup>6</sup> NUCLEOTIDES
ACTIVE	0.50	SEE MATERIALS AND METHODS	Yes	38,270	132
ACTIVE	0.50	SEE MATERIALS AND METHODS	Yes	50,998	175
CONTROL	0.50	SEE MATERIALS AND METHODS	Yes	9,448	32.5

a Control samples are boiled enzymes

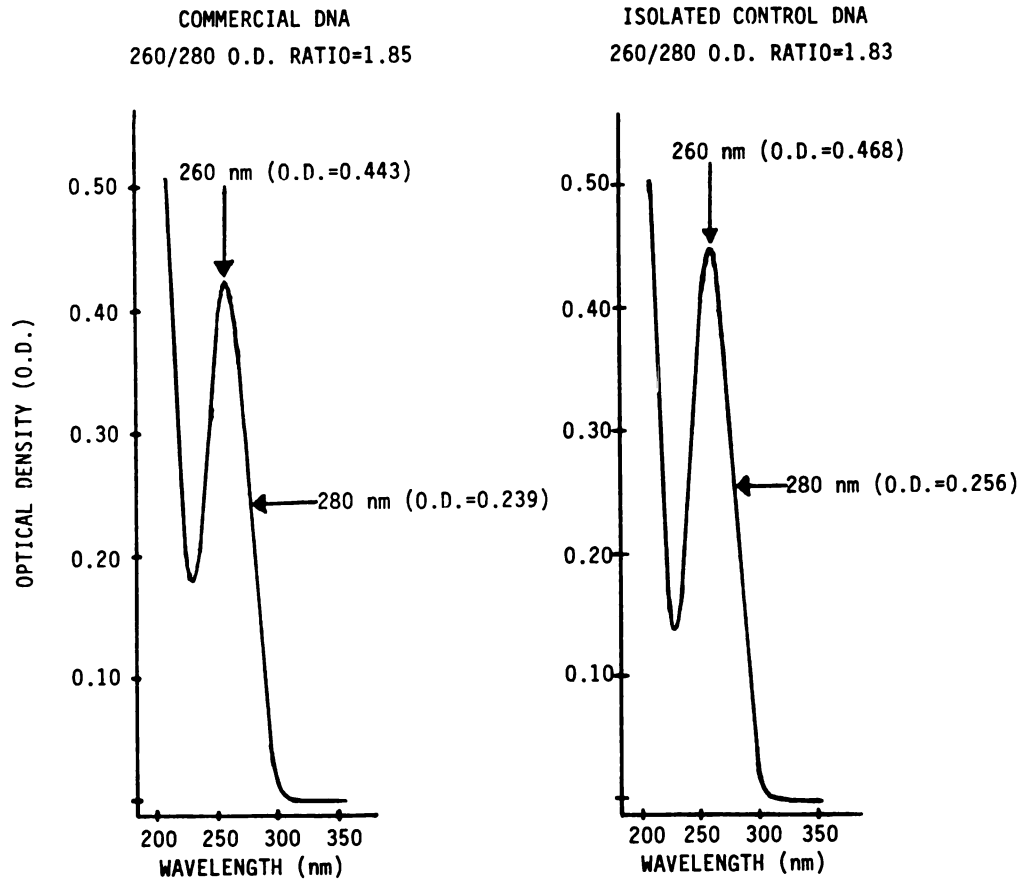


FIGURE 5.2

ULTRAVIOLET SPECTRAL SCANS OF DNA ISOLATED FROM A CONTROL INCUBATION OF (I-C-14) WITH RAT LIVER MICROSOMES BY THE PROTEIN PHENOLIC EXTRACTION/PRECIPITATION SEPARATION TECHNIQUE (FOR COMPARISON PURPOSES THE ULTRAVIOLET SPECTRA OF A BIS-TRIS/EDTA BUFFER SOLUTION OF COMMERCIAL DNA IS ALSO PRESENTED)

sibility of the bases to electrophiles.

The relatively high amounts of DNA bound radioactivity from control studies may be the result of binding without metabolic activation. Tatsumi *et al.* (93) has reported a similar non-enzymatic mediated binding of C-14 labeled AF-2 to biological macromolecules. Whatever the cause for this high binding in control samples, *in vitro* metabolic activation increases binding by a factor of two.

The binding resulting from incubations using different amounts of microsomal suspension and time of incubation show a correlation between the amount of metabolism and extent of binding. It could be argued that incubation times should have been much shorter to more closely coincide with the relative metabolism rate of the parent 5-nitrofurantoin (see Figure 4.2). If, however, the amount of binding closely correlated with the rate of disappearance of (I-C-14) from the incubation mixture, the results from the time dependence studies conducted should have all been constant at the maximum binding level. The results reported here suggest that initial loss of parent compound is not the rate determining step in binding. Perhaps, subsequent metabolism of the intermediates or activation by conjugation with sulfate or other small molecules which form better leaving groups is the rate determining step. For other aromatic carcinogens such as AAF this has been suggested (95).

There are reports in the literature (96) that magnesium ion influences the amount metabolically activated carcinogens bound to DNA. It is postulated that high magnesium ion concentration tightens the coil of the double helix preventing access of the activated metabolite to nucleophilic sites. In the incubation study of (I-C-14) without  $MgCl_2$  no quantitative difference in binding was found suggesting that binding

of metabolically activated (I-C-14) to DNA may not be dependent on the tertiary structure of DNA.

The results from the incubations with glutathione, in an attempt to block covalent binding, are at first analysis perplexing. The presence of reduced glutathione would be expected to reduce if not completely eliminate DNA binding by acting as a nucleophilic trap for the activated, electrophilic metabolites. However, there was increased DNA binding in incubations with glutathione. This may be interpreted as suggesting that activated reduced metabolites of (I-C-14) form a very reactive complex with glutathione that goes on to bind at a greater extent with DNA. Further studies are required to clearly define the mechanism of this observed increase in binding.

#### IV. Using Xanthine Oxidase

##### A. Materials and Methods

Incubation of (I-C-14) with xanthine oxidase was carried out at 37<sup>0</sup>C in a Dubnoff metabolic incubator. Precautions for maintenance of anaerobic conditions and subdued light were as previously described (p 96). Incubation mixtures had a total volume of 15.00 ml containing 15.0 mg dissolved calf thymus DNA, 7.5 mg hypoxanthine, and 0.30 umole (13.0 uCi) (I-C-14) in 50 ul DMSO. In order to determine the amount of binding as a function of the amount of metabolism that had occurred two separate studies were undertaken. In the first, using 7.5 U xanthine oxidase, incubation time was varied by stopping metabolism at 0.0, 2.0, 5.0, 9.0, 20.0, 50.0, 110.0, and 150.0 minutes. In the second, the amount of xanthine oxidase was varied using 0.00, 0.75, 1.5, 4.5, or 7.5

units xanthine oxidase. For this study an incubation time of 2.0 min was selected as a result of the time dependence study. The remaining volume of each incubation mixture consisted of 50 mM potassium phosphate buffer pH 5.8. At the end of each incubation DNA was separated by the protein phenolic extraction/DNA precipitation technique and the amount of DNA-bound radioactivity determined as described previously (p 150).

## B. Results

Results of the quantitation of DNA-bound radioactivity are given in Table 5.3. The samples at 0.0 min incubation time and 0.00 U xanthine oxidase should be considered as controls. Both indicate relatively low binding.

In order to clarify the relationship between the amount of binding and the amount of metabolism the two graphs shown in Figures 5.3 and 5.4 were constructed. In the first, peak height of (I) and amino metabolite (M-2) (replotted from Figure 4.6) as well as number of adducts per one-million nucleotide residues are plotted as a function of amount of xanthine oxidase added to the incubation. The time dependence graph shows a maximum number of DNA adducts after 2.0 min of incubation which decreases rapidly and then decrease very slowly. The enzyme dependence graph shows a linear relationship between amount of amino metabolite produced (replotted from Figure 4.6) and binding after a minimum of 1.5 U xanthine oxidase added.

## C. Discussion

Lower amounts of (I-C-14) were used in these studies so that comparison could be made of the amount of DNA binding with a study similarly

TABLE 5.3

RESULTS OF QUANTITATION OF DNA BOUND RADIOACTIVITY  
 FOLLOWING INCUBATION OF (I-C-14) WITH XANTHINE OXIDASE

INCUBATION TIME (MIN)	XANTHINE OXIDASE ADDED (UNITS)	SPECIFIC ACTIVITY OF ISOLATED DNA (DPM/mg)	CALCULATED NUMBER OF ADDUCTS PER $10^6$ NUCLEOTIDES
0.0	7.5	4,542	15.5
2.0	7.5	14,441	49.3
5.0	7.5	10,798	36.9
9.0	7.5	10,957	37.4
20.0	7.5	10,263	35.1
50.0	7.5	8,570	29.3
110.0	7.5	7,449	25.4
150.0	7.5	8,166	27.9
2.0	0.00	5,576	19.0
2.0	0.75	4,491	15.3
2.0	1.50	3,850	13.2
2.0	4.50	8,904	30.4
2.0	7.50	14,441	49.3

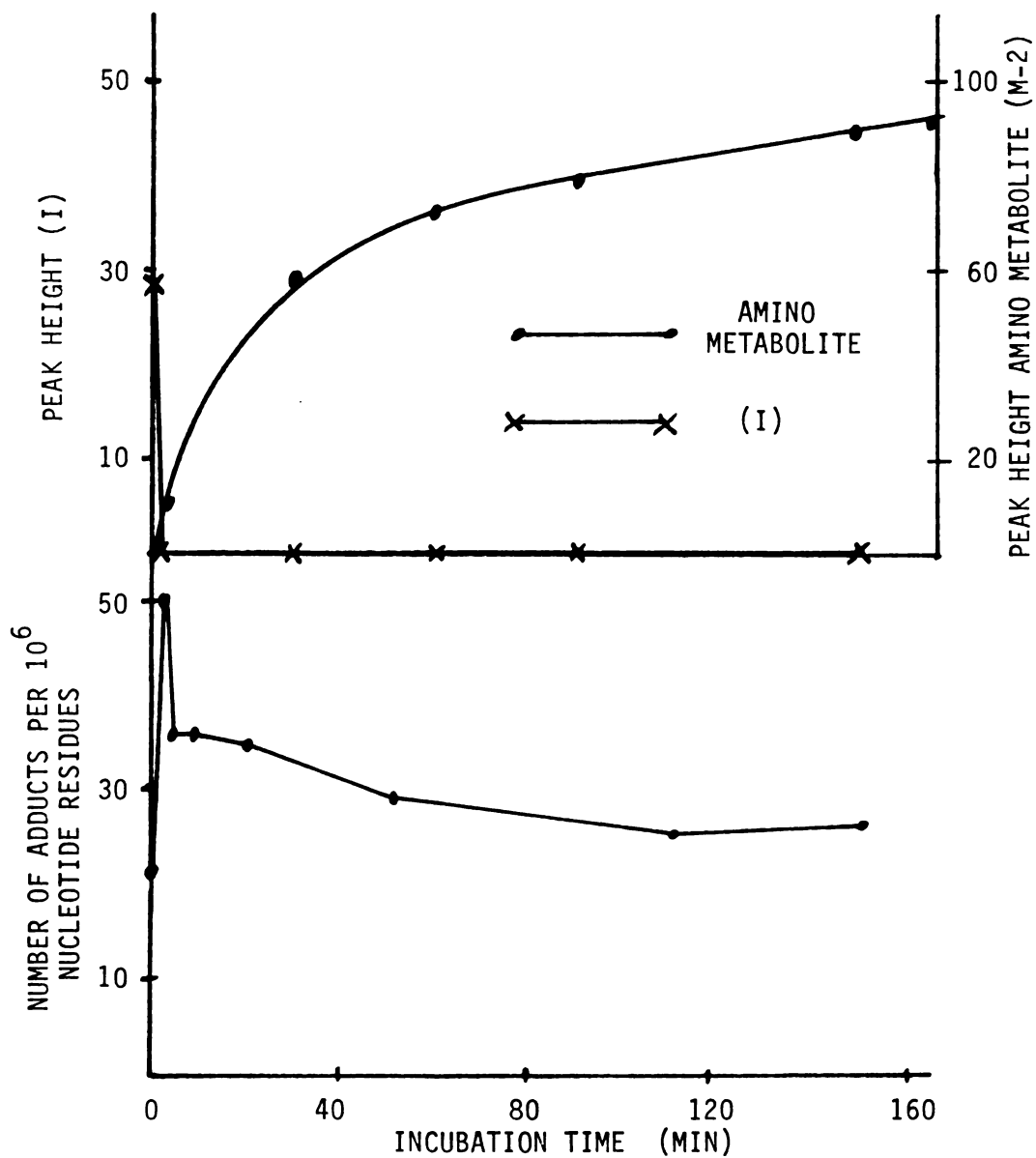


FIGURE 5.3

PEAK HEIGHT, (I) AND AMINO METABOLITE (M-2), AND NUMBER OF ADDUCTS PER ONE-MILLION NUCLEOTIDE RESIDUES AS A FUNCTION OF INCUBATION TIME FOR INCUBATION OF (I) OR (I-C-14) WITH XANTHINE OXIDASE

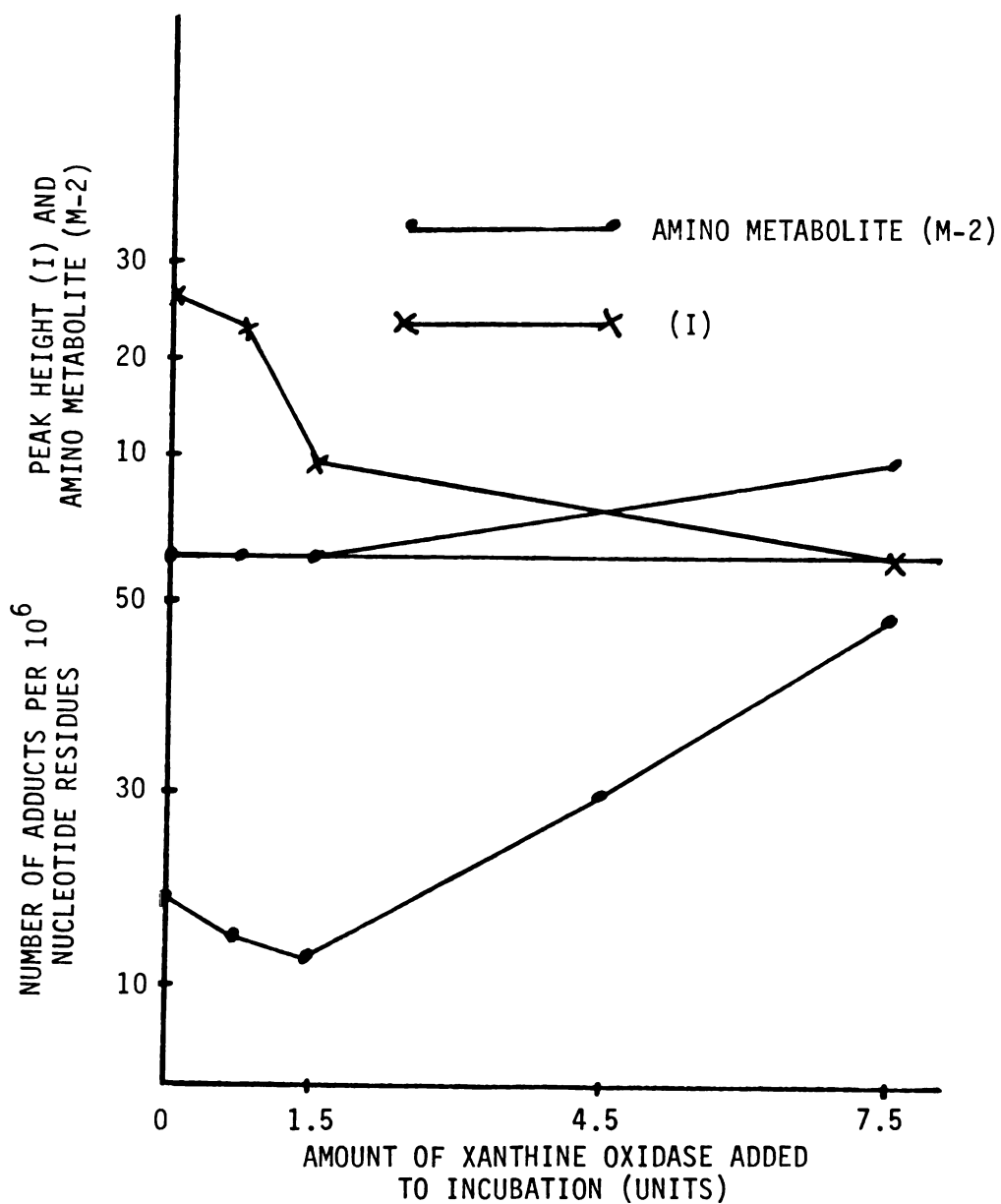


FIGURE 5.4

PEAK HEIGHT, (I) AND AMINO METABOLITE (M-2), AND NUMBER OF ADDUCTS PER ONE-MILLION NUCLEOTIDE RESIDUES AS A FUNCTION OF AMOUNT OF XANTHINE OXIDASE ADDED TO THE INCUBATION AFTER 2.0 min INCUBATION TIME



conducted with 1-nitropyrene (91). With 1-nitropyrene a maximum DNA binding of about 500 adducts per one-million nucleotide residues was obtained using 7.5 U xanthine oxidase after 1.0 hr incubation. Furthermore, exponential time dependent and enzyme dependent binding relationship were demonstrated.

In studies with (I-C-14) the binding dependence on time and enzyme amount are more complex. It appears that a relatively high amount of labile DNA binding occurs very quickly after metabolism is initiated followed by loss of bound, activated (I-C-14). Examination of the enzyme dependence graph confirms a correlation between amount of labile binding at 2.0 min incubation time and appearance of amino metabolite. A linear increase in binding and amount of amino metabolite is observed when amount of xanthine oxidase is increased above 1.5 U.

The complex time course of binding may be interpreted by speculating that at least two types of adducts are being formed. These adducts differ substantially in their lability under incubation conditions. This lability may be the result of different activated metabolites binding to DNA, or the same activated metabolite binding to different sites on DNA, or a combination of both these mechanisms. The second possibility has been demonstrated for certain O-adducts of other DNA-bound carcinogens (97). At this time the data are not definitive enough to ascertain which mechanism(s) is in operation.

#### V. Summary

Anaerobic in vitro DNA binding studies on (I-C-14) using the 9000xg rat liver homogenate supernatant, rat liver microsomes, and xanthine oxidase, as the source of nitroreductase, have been conducted. A protein

phenolic extraction/DNA precipitation separation procedure was used to characterize DNA binding following metabolic activation with studies using rat liver microsomes and xanthine oxidase. DNA isolated by this procedure was analyzed in the UV spectrum and determined to be of high purity. Because this DNA separation procedure was not amendable for use with the 9000xg rat liver homogenate studies, a hydroxylapatite column chromatographic procedure was used for those studies.

The DNA binding results using the 9000xg rat liver homogenate supernatant indicate that no binding of activated reduced metabolites of (I-C-14) to DNA occurred. The impurity of the nitroreductase source and the presence of known competitive inhibitors of DNA binding, including proteins and other nucleophiles, are offered as reasons for this observation.

When the purer rat liver microsomes were used, DNA binding was observed. A correlation between amount of metabolism and amount of DNA binding was demonstrated in incubations using different amounts of microsomal suspension and incubation time. Because no difference in the amount of DNA binding was observed in incubations without  $MgCl_2$ , a inhibitor of DNA binding when binding is dependent on the tertiary structure of DNA, it was suggested that binding of metabolically activated (I-C-14) is not limited by the tertiary structure of DNA. The enhanced DNA binding in incubations of the metabolism study containing large amounts of reduced glutathione suggests that a highly activated complex forms between reduced metabolites of (I-C-14) and glutathione. This complex may bind to a greater extent with DNA. However, further studies are needed to confirm this possibility.

With the purest form of nitroreductase studied, xanthine oxidase,

binding to DNA was observed. The relationship between amount of binding and the amount of metabolism was evaluated by constructing two graphs. The time dependence graph showed a peak in amount of binding after 2.0 min of incubation followed by rapid and then a slow decrease in binding. The enzyme dependence graph showed a correlation between amount of amino metabolite produced and amount of binding. Comparison was made between the amount of observed binding of (I-C-14) and literature results of 1-nitropyrene studied under the same conditions. Maximum 1-nitropyrene binding to DNA was about ten times higher than studies conducted with (I-C-14). The time and enzyme dependence results taken together are offered as evidence that the observed binding is the result of covalent binding and not merely the result of non-covalent binding of metabolites to DNA.

### SUMMARY AND CONCLUSIONS

Following in vitro anaerobic metabolism of 2,4-diacetylamino-6-(5-nitro-2-furyl)-1,3,5-triazine (I) in rat liver 9000xg homogenate supernatant, rat liver microsomes, and xanthine oxidase, two metabolites were separated by HPLC. Structural elucidation of these metabolites indicated the production of the 5-aminofuran, 2,4-diacetylamino-6-(5-amino-2-furyl)-1,3,5-triazine (III) (M-2). This structure was confirmed by synthetic preparation of (III). The structure of the other metabolite (M-1) could not be elucidated because of poor spectroscopic results. However, the open-chain nitrile structure, 2,4-diacetylamino-6-(3-cyano-1-oxopropyl)-1,3,5-triazine (IV), was suggested by UV spectroscopy and the apparent instability of the product.

A carbon-14 radiochemical synthesis of (I) was developed for use in the determination of the amounts of metabolites produced and DNA binding studies. Preliminary metabolic studies on synthesized C-14 and H-3 acetyl labeled (I) indicated that these positions were not acceptable for use because of lability of the radiolabel. A satisfactory radiolabeled compound was synthesized by radiocarbonylation of 2-furyllithium, followed by ethyl esterification of the acid, nitration of the ethyl 2-furoate, condensation of the ethyl 5-nitro-2-furoate with biguanide, and acetylation to yield 2,4-diacetylamino-6-(5-nitro-2-furyl)-1,3,5-triazine-(6-C-14) (I-C-14).

Using (I-C-14), the amount of metabolites (M-1) and (M-2) were determined in anaerobic in vitro reductive metabolism studies with the 9000xg rat liver homogenate supernatant and xanthine oxidase as the source

of nitroreductase. Xanthine oxidase was found to produce almost exclusively the 5-aminofuran (M-2). The 9000xg rat liver homogenate supernatant produced approximately one-third (M-1) and two-thirds (M-2). In addition, with xanthine oxidase (I) disappeared more quickly than (M-2) appeared. Both enzymatic systems produced about equivalent sum total amounts of identified metabolites, corresponding to about 50% of all metabolized (I). Additional polar metabolites that could not be resolved by UV absorbance also could not be resolved by radioactivity counting of fractions because of a large broad radioactive peak eluting on the HPLC chromatograms. Quantitation of the amount of radioactivity precipitated with protein following incubations and the observed large radioactivity peak at the solvent front on HPLC profiles, where polar protein material would elute, suggested large amounts of metabolized (I-C-14) were bound to protein material.

Nitroreductase catalyzed binding of (I-C-14) to DNA using the 9000xg rat liver homogenate supernatant was not observed. The impurity of the nitroreductase source and the presence of known inhibitors of carcinogen-DNA binding are offered as the reasons for this result. With a purer rat liver microsome preparation DNA binding was indeed observed. A correlation between amount of metabolism and amount of DNA binding was demonstrated in incubations using different amounts of microsomal suspension and in incubations of different time. The amount of DNA binding was found to be independent of the presence of  $MgCl_2$ . However, a nearly 4-fold increase in DNA binding was observed when metabolites were generated first followed by addition of glutathione and DNA.

With the purest nitroreductase studied, xanthine oxidase, binding to DNA was also observed. The maximum amount of binding occurred at 2.0 min

followed by first a rapid and then a slow decrease in binding. There was a correlation between amount of amino metabolite (M-2) produced and amount of binding.

The significance of the results of this work as assessed in the following discussion and conclusions. Anaerobic in vitro reductive metabolism of the highly carcinogenic/mutagenic (I) resulting in reduction of the nitro-group to form the 5-aminofuran metabolite (M-2) was the major metabolite isolated by HPLC. Other 5-nitrofurans, that exhibit a broad range of pharmacological and toxicological activities, also are reported to produce the 5-aminofuran derivative which may undergo further metabolism to an open-chain nitrile derivative. There is some evidence that metabolism of (I) leads to such a product, however, this could not be confirmed. As with other 5-nitrofurans, isolation of the intermediates of reductive metabolism was not possible. Because of the similarity in carcinogenicity between some arylamines and aryl nitro compounds, it has been suggested that these compounds are subject to convergent routes of metabolic activation. It has been shown that arylamines are oxidatively metabolized to N-hydroxylamines that have been identified as the proximate carcinogen. Hence, nitroreduction is suspected to produce the same N-hydroxylamine when they are reduced to the amine. However, as in other studies, the hydroxylamine was not isolated. Instability appears to be the cause, since synthetic approaches to the preparation of N-hydroxylamines of furan compounds have also been unsuccessful.

Results from anaerobic in vitro reductive metabolism studies with (I-C-14) accounted for only 50% of the metabolites. The remaining 50% may be bound to proteins or may be very polar metabolites. The quantita-

tive difference in the rate of reductive metabolism of (I) between xanthine oxidase and rat liver derived enzymes illustrates that the various nitroreductase enzymes found in mammalian systems differ significantly. This observation must be taken into consideration in future assessments of the factors influencing metabolic activation and interaction with critical biomacromolecules in different target tissues.

DNA binding studies with (I-C-14) indicated that only very low amounts of binding occurred. Comparable studies with other carcinogens, both from oxidative and reductive metabolic activation, generally results in 5 to 10 times greater amounts of DNA bound metabolites. However, only the quantitative aspects of DNA binding were investigated and it is generally accepted that a qualitative analysis of the formed adducts is of comparable, if not of equally or more importance. Characterization of such adducts is rendered extremely difficult because of the very minute amount of DNA.

The time dependence of DNA binding indicates that the rate of disappearance of (I) is not the rate determining step in the formation of DNA bound metabolites. Subsequent metabolic steps are required and may include conjugation or other as yet undetermined metabolic pathways. Another possibility is that more than one reductive metabolite becomes covalently bound to DNA. In addition several different adducts with differing labilities may be formed under the incubation conditions.

The  $MgCl_2$  independence of DNA binding suggests that binding of metabolically activated (I-C-14) is not dependent upon the tertiary structure of DNA. The results of the increased DNA binding with glutathione suggests that activated reduced metabolites form an even more activated complex with glutathione that binds to an even greater extent with DNA.

If the hydroxylamine is considered as the activated electrophilic intermediate responsible for covalent binding to critical biomacromolecules, a mechanistic scheme can be drawn in which furan ring positions 3 and 4 are the sites of attack by nucleophiles. Loss of the OH-group of the hydroxylamine would form the electrophilic cation "A" in Figure S/C-1. Nucleophilic attack by biomacromolecules at positions 3 or 4 could result in re-aromatization to the 5-aminofuran adduct. Nucleophilic attack at furan ring positions 2 or 5 would not be expected to be as favorable because re-aromatization could only occur by loss of the poorer leaving groups  $\text{NH}_2^+$  or  $\text{R}^+$ .



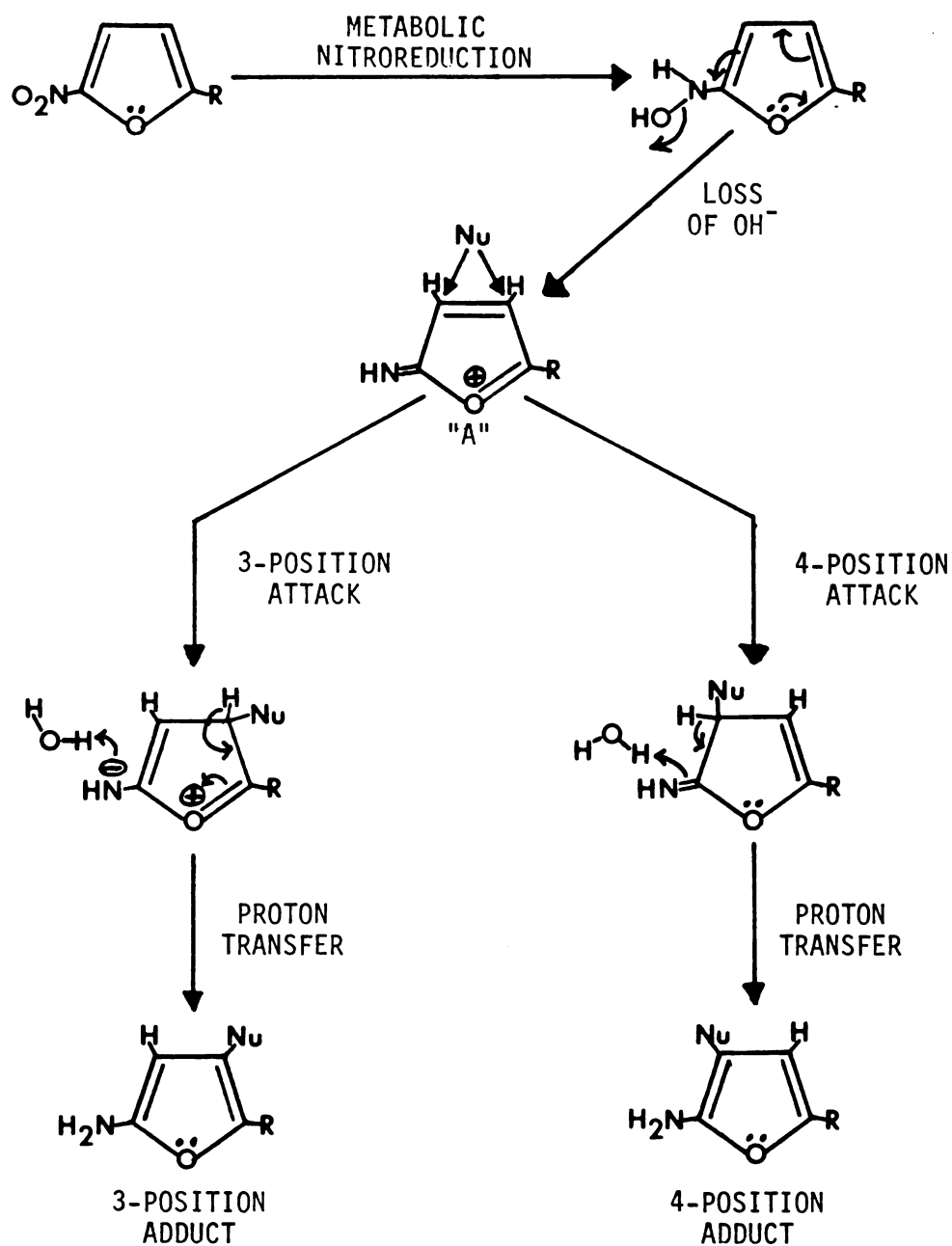


FIGURE S/C-1

MECHANISTIC SCHEME FOR NUCLEOPHILIC BIOMACROMOLECULE ATTACK ON ACTIVATED ELECTROPHILIC INTERMEDIATE FROM HYDROXYLAMINOFURAN

REFERENCES

1. Gilman, H., and G.F. Wright. (1930). Nitrofurfural and nitro-furylacrylic acid. J. Am. Chem. Soc. 52, 2550-2554.
2. Miura, K., and H.K. Reckendorf. (1967). The nitrofurans. In: Progress in Medicinal Chemistry (G.P. Ellis and G.B. West, eds.), Vol. 5, Plenum Press, New York, 320-381.
3. Dodd, M.C., and W.B. Stillman. (1944). The in vitro bacteriostatic action of some simple furan derivatives. J. Pharmacol. Exp. Ther. 82, 11-18.
4. Paul, H.E., and M.F. Paul. (1964). The nitrofurans-Chemotherapeutic properties. In: Experimental Chemotherapy (R.J. Schnitzer and F. Hawking, eds.), Vol. 2, Part 1, Academic Press, New York, 307-370.
5. Dann, O., and E.F. Möller. (1947). Bakteriostatisch wirkende Nitroverbindungen des Thiophens und Furans. Chem. Ber. 80, 23-36.
6. Bryan, G.T. (1978). Occurrence, Production and Uses of Nitrofurans. In: Nitrofurans (G.T. Bryan ed.), Raven Press, New York, 1.
7. IARC. (1974). IARC Monographs on the evaluation of carcinogenic risk of chemicals to man. Some antithyroid and related substances, nitrofurans and industrial chemicals. Vol. 7:27, 143-193.
8. Reuvers, A.P., J.D. Chapman, and J. Borsa. (1972). Potential use of nitrofurans in radiotherapy. Nature 237, 402-403.

9. Chapman, J.D., A.P. Reuvers, J. Borsa, A. Petkau, and D.R. McCalla. (1972). Nitrofurans as radiosensitizers of hypoxic mammalian cells. Cancer Res. 32, 2616-2624.
10. Federal Register. (1976). Nitrofurazone (NF-73): Opportunity for hearing on proposal to withdraw approval of certain new animal drug applications. Federal Register 41 (160), August 17, 1976, 31899-31908.
11. Matsuda, T. (1966). Review on recent nitrofurans used as food preservatives. J. Ferment. Technol. 44, 495-508.
12. Obatake, A., and T. Matsuda. (1965). Studies of new nitrofurans derivatives as food preservatives. I. On the preservative effect of AF-2 and AF-5. Bull. Jpn. Soc. Sci. Fisheries 31, 138-145.
13. Tazima, Y., T. Kada, and A. Murakami. (1975). Mutagenicity of nitrofurans derivatives, including furylfuramide, a food preservative. Mut. Res. 32, 55-80.
14. Sram, R.J., P. Rossner, V.S. Zhurkov, and I. Katytikova. (1979). Mut. Res. 68, 367.
15. Office of Toxic Substances, U.S. Environmental Protection Agency (1977). A study of industrial data on candidate chemicals for testing. Final Report. National Technical Information Service, Springfield, Virginia, 4-259-4-261.
16. Herrlich, P., and M. Schweiger. (1976). Nitrofurans, a group of synthetic antibiotics, with a new mode of action: Discrimination of specific messenger RNA classes. Proc. Natl. Acad. Sci. USA, 73, 3386-3390.

17. Hirsch-Kauffman, M.P. Herrlich, and M. Schweiger. (1978). Klin. Wschr. 56, 405.
18. Olive, P.L., and D.R. McCalla. (1977). Cytotoxicity and DNA damage to mammalian cells by nitrofurans. Chem. Biol. Interact. 16, 223-233.
19. Chapman, J.D., C.L. Greenstock, A.P. Reuvers, E. McDonald, and I. Dunlop. (1973). Radiation chemical studies with nitrofurazone as related to its mechanism of radiosensitization. Radiat. Res. 53, 190-203.
20. Geller, M., H.E. Dickie, D.A. Kass, G.R. Hafez, and J.J. Gillespie. (1976). The histopathology of acute nitrofurantoin-associated pneumonitis. Ann. Allergy 37, 275-279.
21. Boyd, M.R., G.L. Catignani, H.A. Sasame, J.R. Mitchell, and A.W. Stiko. (1979). Acute pulmonary injury in rats by nitrofurantoin and modification by vitamin E, dietary fat, and oxygen. Am. Rev. of Resp. Dis. 20, 93-98.
22. Mason, R.P., and J.L. Holtzman. (1975). Biochem. Biophys. Res. Comm. 67, 1267.
23. Sesame, H.A., and M.R. Boyd. (1979). Superoxide and hydrogen peroxide production and NADPH oxidation stimulated by nitrofurantoin in lung microsomes: Possible implications for toxicity. Life Sci. 24, 1091-1096.
24. Jackowitz, A.I., J.L. FeFroch, and R.A. Prince. (1977). Nitrofurantoin polyneuropathy: Report of two cases. Am. J. Hosp. Pharm. 34, 759-761.

25. Koch-Weser, J., V.W. Sidel, M. Dexter, C. Parish, D.C. Finer, and P. Kanarek. (1971). Adverse reactions to sulfisoxazole, sulfamethoxazole, and nitrofurantoin. Arch. Intern. Med. 128, 399-404.
26. Olive, P.L. (1978). Macromolecular, Antineoplastic, and Radiosensitization Effects of Nitrofurans. In: Nitrofurans (G.T. Bryan ed.), Raven Press, New York, 131.
27. Sharp, J.R., K.G. Ishak, and H.J. Zimmerman. (1980). Chronic active hepatitis and severe hepatic necrosis associated with nitrofurantoin. Ann. Int. Med. 92, 14-19.
28. Black, M., L. Rabin, and N. Schatz. (1980). Nitrofurantoin-induced chronic active hepatitis. Ann. Int. Med. 92, 62.
29. Szybalski, W., and T.C. Nelson. (1954). Genetics of bacterial resistance to nitrofurans and radiation. Bacteriol. Proc. 51, 52.
30. Szybalski, W. (1958). Special microbiological systems, II. Observations on chemical mutagenesis in micro-organisms. Ann. N.Y. Acad. Sci. 76, 474-489.
31. Stein, R.J., D. Yost, F. Petroluinas, and A. Von Esch. (1966). Carcinogenic activity of nitrofurans. A histologic evaluation. Fed. Proc. 25, 291.
32. Goodman, D.R., P.J. Hakkinen, J.H. Nemenzo, and M. Vore. (1977). Mutagenic evaluation of nitrofuran derivatives in Salmonella Typhimurium, by the micronucleus test, and by in vivo cytogenetics. Mut. Res. 48, 259-306.

33. McCalla, D.R., and D. Voutsinos. (1974). On the mutagenicity of nitrofurans. Mut. Res. 26, 3-16.
34. Cohen, S.M., E. Erturk, A.M. Von Esch, A.J. Crovetti, and G.T. Bryan. (1973). Carcinogenicity of 5-nitrofurans, 5-nitroimididazoles, 4-nitrobenzenes and related compounds. J. Natl. Cancer Inst. 51, 403-417.
35. McCalla, D.R., A. Reuvers, and C. Kaiser. (1970). Mode of action of nitrofurazone. J. Bacteriol. 104, 1126-1134.
36. Terawaki, A., and J. Greenberg. (1965). Effect of some radio-mimetic agents on deoxyribonuclei acid synthesis in Escherichia coli and transformation in Bacillus subtilis. Biochim. Biophys. Acta 95, 170-173.
37. Sugiyama, T., K. Goto, and H. Uenaka. (1975). Acute cytogenetic effect of 2-(2-furyl)-3-(5-nitro-2-furyl) acrylamide (AF-2), (a food preservative) on rat bone marrow cells in vivo. Mut. Res. 31, 241-246.
38. Olive, P.L., and D.R. McCalla. (1975). Damage to mammalian cell DNA by nitrofurans. Cancer Res. 35, 781-784.
39. Rosenkranz, H.S. (1977). Studies on the mutagenicity of nitrofurans in Salmonella typhimurium. Biochem. Pharmacol. 26, 896-898.
40. McCalla, D.R., A. Reuvers, and C. Kaiser. (1971). Breakage of bacterial DNA by nitrofuran derivatives. Cancer Res. 31, 2184-2188.
41. McCalla, D.R., D. Voutsinos, and P.L. Olive. (1975). Mutagen screening with bacteria: niridazole and nitrofurans. Mut. Res. 31, 31-37.

42. Tatsumi, K., S. Kitamura, and H. Yoshimura. (1977). Binding of nitrofurans derivatives to nucleic acids and proteins. Chem. Pharm. Bull. 25, 2948-2952.
43. Matsushima, T., M. Sawamura, K. Hara, and T. Sugimura. (1976). In Vitro Metabolic Activation in Mutagenesis Testing (F.J. de Serres, J.R. Fouts, J.B. Bend, R.M. Philpot, and Elsevier eds.), 81.
44. Cohen, S.M., E. Ertürk, A.M. Von Esch, A.J. Crovetti, and G.T. Bryan. (1975). J. Nat. Cancer Inst. 54, 841.
45. Tatsumi, K., S. Kitamura, and H. Yoshimura. (1976). Reduction of nitrofurans derivatives by xanthine oxidase and microsomes. Isolation and identification of reduction products. Arch. Biochem. Biophys. 175, 131-137.
46. Aufrère, M.B., B. Hoener, and M. Vore. (1978). Reductive metabolism of nitrofurantoin in the rat. Drug Met. Disp. 6, 403-411.
47. Chatfield, D.H. (1976). The disposition and metabolism of some nitrofuranylthiazoles possessing antiparasitic activity. Xenobiotica 6, 509-520.
48. Olivard, J., S. Valenti, and J.A. Buzard. (1962). The metabolism of 5-nitro-2-furaldehyde acetylhydrazone. J. Med. Pharm. Chem. 5, 524-531.
49. Kato, R., T. Oshima, and A. Takanaka. (1969). Studies on the mechanism of nitro reduction by rat liver. Mol. Pharmacol. 5, 487-498.

50. Miller, E.C., and J.A. Miller. (1976). The metabolism of chemical carcinogens to reactive electrophiles and their possible mechanisms of action in carcinogenesis. In: Chemical Carcinogens (C.E. Searle ed.), 737-762.
51. Biaglow, J.E., O.F. Nygaard, and C.L. Greenstock. (1976). Electron transfer in Ehrlich ascites tumor cells in the presence of nitrofurans. Biochem. Pharmacol. 25, 393-398.
52. Beckett, A.H., and A.E. Robinson. (1959). The reactions of nitrofurans with bacteria. II. Reduction of a series of antibacterial nitrofurans by Aerobacter aerogenes. J. Med. Chem. 1, 135-154.
53. Gavin, J.J., F.F. Ebetino, R. Freedman, and W.E. Waterbury. (1966). The aerobic degradation of 1-(5-nitrofurfurylideneamino)-2-imidazolidinone (NF-246) by Escherichia coli. Arch. Biochem. Biophys. 113, 399-404.
54. Ou, T., K. Tatsumi, and H. Yoshimura. (1977). Isolation and identification of urinary metabolites of AF-2 (3-(5-nitro-2-furyl)-2-(2-furyl) acrylamide) in rabbits. Biochem. Biophys. Res. Comm. 75, 401-405.
55. Olivard, J., G.M. Rose, G.M. Klein, and J.P. Heotis. (1976). Metabolic and photochemical hydroxylation of 5-nitro-2-furancarboxaldehyde derivatives. J. Med. Chem. 19, 729-731.
56. Pugh, D.L., J. Olivard, H.R. Snyder, and J.P. Heotis, (1972). Metabolism of 1-((5-nitrofurfurylidene)amino)-2-imidazolidinone. J. Med. Chem. 15, 270-273.



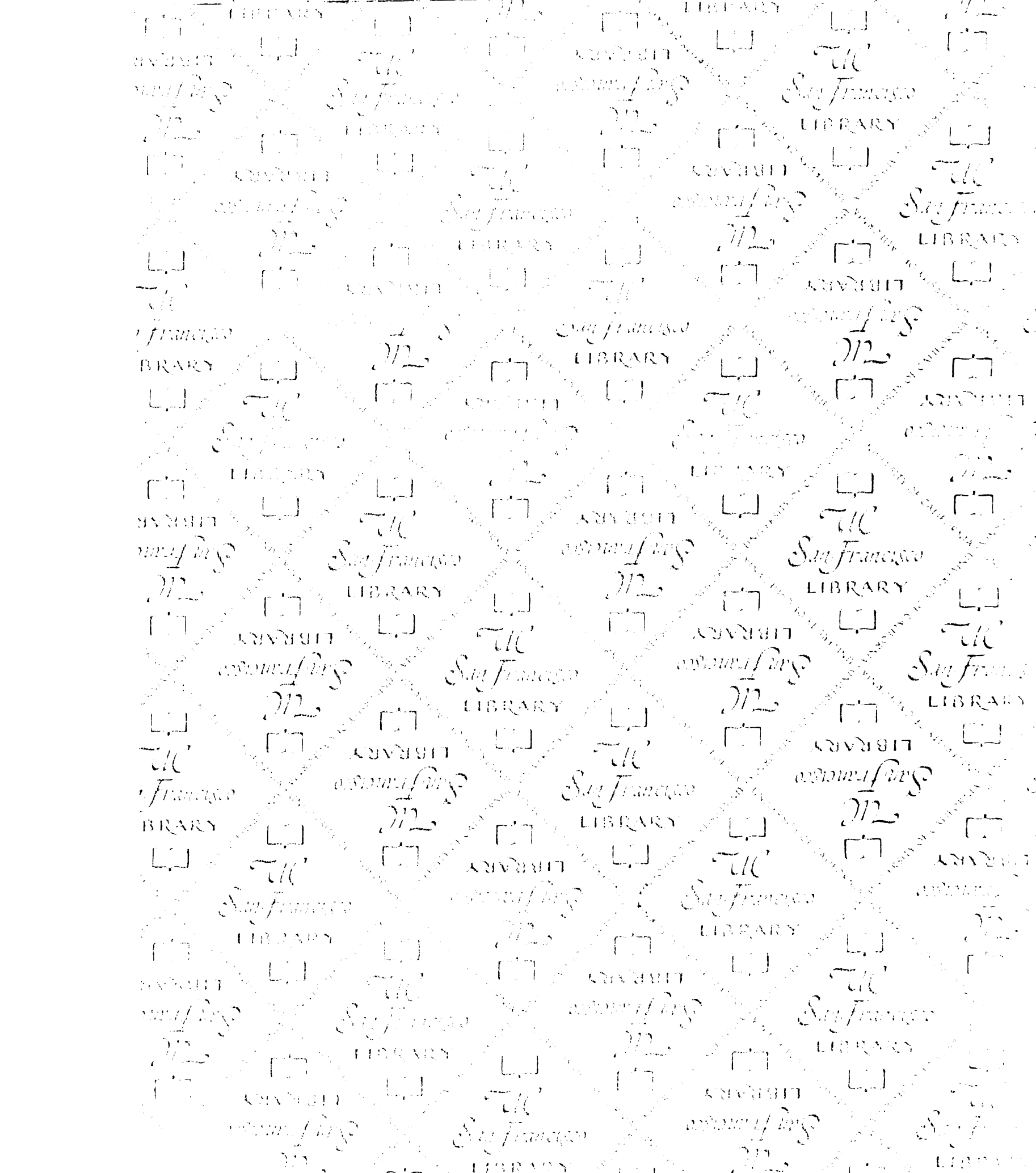
57. Asnis, R.E. (1957). The reduction of furacin by cell-free extracts of furacin-resistant and parent-susceptible strains of Escherichia coli. Arch. Biochem. Biophys. 66, 208-216.
58. McCalla, D.R., P. Olive, Y. Tu, and M.L. Fan. (1975). Nitrofurazone-reducing enzymes in E. coli and their role in drug activation in vivo. Can. J. Microbiol. 21, 1484-1491.
59. Wang, C.Y., B.C. Behrens, M. Ichikawa, and G.T. Bryan. (1974). Nitroreduction of 5-nitrofuran derivatives by rat liver xanthine oxidase and reduced nicotinamide adenine dinucleotide phosphate-cytochrome C reductase. Biochem. Pharmacol. 23, 3395-3404.
60. Lower, G.M., Jr., and G.T. Bryan. (1971). Metabolic activation of N-(4-(5-nitro-2-furyl)-2-thiazolyl)formamide (FANFT), a bladder carcinogen. Proc. Am. Assoc. Cancer Res. 12, 3.
61. Gillette, J.R. (1971). Reductive enzymes. In: Handbook of Experimental Pharmacology, Concepts in Biochemical Pharmacology (B.B. Brodie and J.R. Gillette eds.), Vol. 28, Part 2, Springer, New York, 349-361.
62. Gillette, J.R., J.J. Kamm, and H.A. Sasame. (1968). Mechanism of p-nitrobenzoate reduction in liver: The possible role of cytochrome P-450 in liver microsomes. Mol. Pharmacol. 4, 541-548.
63. Wolpert, M.K., J.R. Althaus, and D.G. Johns. (1973). Nitroreductase activity of mammalian liver aldehyde oxidase. J. Pharmacol. Exp. Ther. 185, 202-213.
64. Ames, B.N., F.D. Lee, and W.E. Durston. (1973). An improved bacterial test system for the detection and classification of mutagens and carcinogens. Proc. Natl. Acad. Sci. (USA) 70, 782-786.

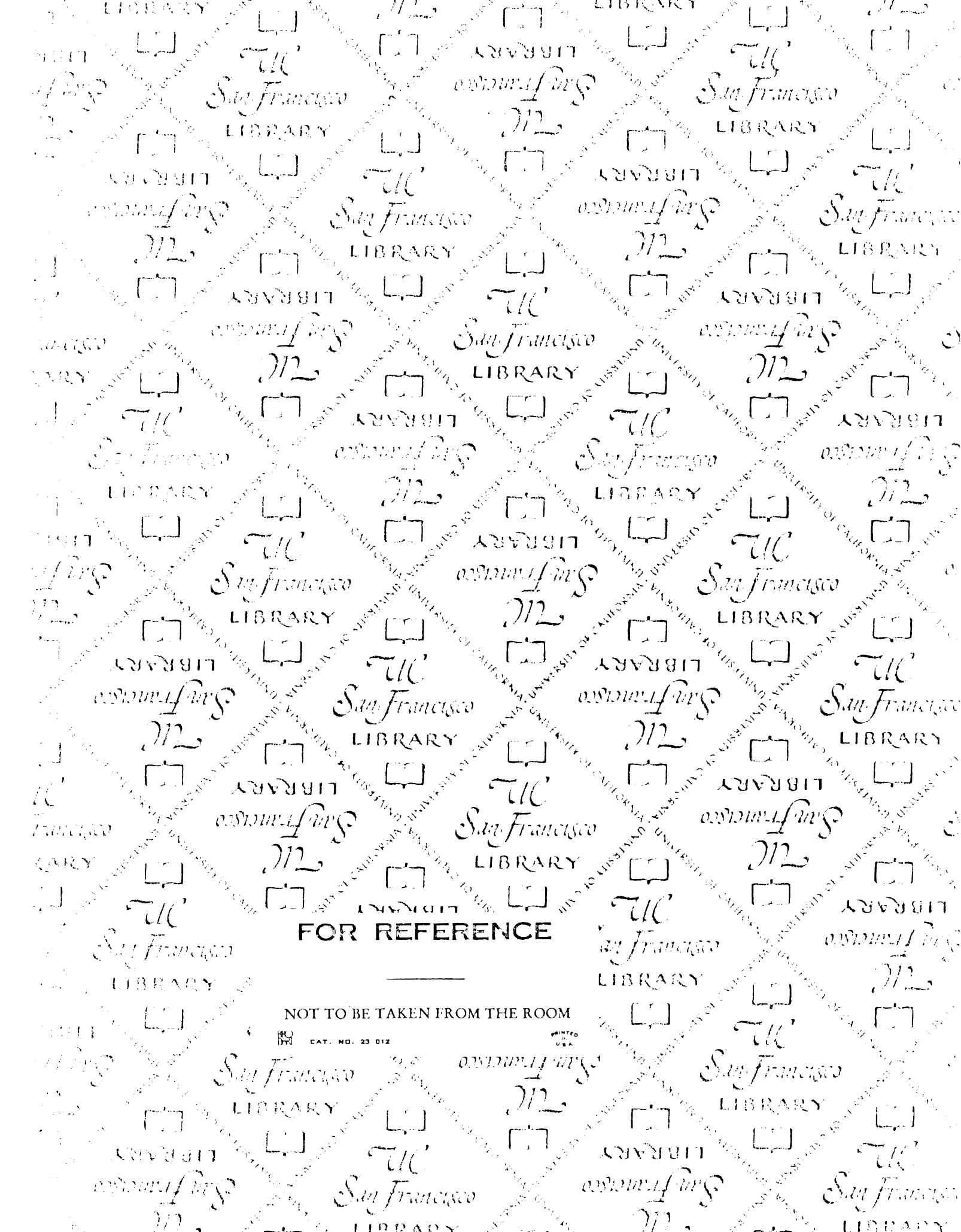
65. Sherman, W. (1961). 5-Nitro-2-furyl-substituted 1,3,4-oxidiazoles, 1,3,4-thiadiazoles, and 1,3,5-triazines. J. Org. Chem. 26, 88.
66. Schock, R.U., and A. Alter. (1959). Unpublished results from Abbott Laboratories; R.U. Schock, U.S. Patent 2,885,400 (May 5, 1959), Chemical Abstracts 53, 17159h.
67. Karipides, D., and W. Fernelius. (1963). 14. Biguanide sulfate. Inorg. Syn. 7, 56.
68. Holter, S., and W. Fernelius. (1963). 15. Biguanide. Inorg. Syn. 7, 58.
69. Norwich Pharmaceutical, personal communication.
70. Swaminathan, S., G.M. Lower, and G.T. Bryan. (1978). Binding of 2-amino-4-(5-nitro-2-furyl)-2-<sup>14</sup>C-thiazole (ANFT) to rat liver microsomes. Proc. Am. Assoc. Cancer Res. 19, 150.
71. Nazarova, Z.N., and V.N. Novikov. (1961). The chemistry of 5-halo-furans. J. General Chem., U.S.S.R. 31, 243.
72. Jones, R.G., and H. Gilman. (1951). Organic Reactions, John Wiley and Sons, New York, 339.
73. Wakefield, B.J. (1974). The Chemistry of Organolithium Compounds, Pergmon, Oxford.
74. Hendrick, J.B., D.J. Cram, and G.S. Hammond. (1970). Organic Chemistry, 3rd ed., McGraw-Hill, New York.
75. Fieser, L.F., and M. Fieser. (1967). Reagents for Organic Synthesis, John Wiley and Sons, New York, 1, 415.
76. Fieser, L.F., and M Fieser. (1967). Reagents for Organic Synthesis, John Wiley and Sons, New York, 1, 417-418.

77. Pearson, D.E., D. Cowan, and J.D. Beckler. (1959). A study of the entrainment method for making Grignard reagents. J. Org. Chem. 24, 504.
78. Gilman, H., and F. Schulze. (1925). A qualitative color test for the Grignard reagent. Am. Soc. 47, 2002.
79. Gilman, H., J.M. Peterson, and F. Schulze. (1928). An improved activated magnesium for the preparation of the Grignard reagent, and a comparative study of various catalysts. Rec. trav. chim. 47, 19.
80. Cook, F.L., C.W. Bowers, and C.L. Liotta. (1974). Chemistry of "naked" anions. III. Reactions of the 18-crown-6 complex of potassium cyanide with organic substrates in aprotic organic solvents. J. Org. Chem. 39, 3416.
81. McKay, A.F., W.L. Ott, G.W. Taylor, M.N. Buchanan, and J.F. Crooker. (1950). Diazohydrocarbons. Can. J. Res., Section B: Chemical Sciences 288, 683-688.
82. Gilman, H., J.A. Beel, C.G. Brannen, M.W. Bullock, G.E. Dunn, and L.S. Miller. (1949). The preparation of n-butyllithium. J.A.C.S. 71: 2, 1500.
83. Ramanathan, V., and R. Levine. (1962). Some reactions of 2-furyllithium. J. Org. Chem. 27, 1216.
84. Prousek, J., A. Jurasek, and J. Kovac. (1980). Reactions and spectral properties of ethyl 5-aminofuroate and its derivatives. Col. Czech. Chem. Comm. 45, 135-141.

85. Doose, D.R., and B. Hoener. (1983). Synthesis of the 5-nitrofuran 2,4-diacetylamino-6-(5-nitro-2-furyl)-1,3,5-triazine-(6-C-14). J. Rad. Comp. Radiopharm. XX, No 4, 495-500.
86. LaDu, B.N., H.G. Mandel, and E.L. Way. (1971). Fundamentals of Drug Metabolism and Disposition, Chapter 27, The Williams and Wilkins Company.
87. Williams, D.H., and I. Fleming. (1973). Spectroscopic Methods in Organic Chemistry, 2nd ed., McGraw Hill, New York, 139.
88. Ebetino, F.F., J.J. Carroll, and G. Gever. (1962). Reduction of nitrofurans. I. Aminofurans. J. Med. Pharm. Chem. 5, 513-523.
89. Lowry, O.H., N.J. Rosebrough, A.L. Farr, and R.J. Randall. (1951). Protein measurement with the folin phenol reagent. J. Biol. Chem. 193, 265-275.
90. Shoyal, M. (1979). Binding of polycyclic aromatic hydrocarbons to cells in culture: A rapid method for its analysis using hydroxyl-apatite column chromatography. Chem. Biol. Inter. 25, 77-85.
91. Howard, P.C., and F.A. Beland. (1982). Xanthine oxidase catalyzed binding of 1-nitropyrene to DNA. Biochem. Biophys. Res. Comm. 104, No. 2, 727-732.
92. Kuchler, R.J. (1977). Biochemical Methods in Cell Culture and Virology. Macromolecular Analysis, Ultraviolet Spectral Analysis, Dowden, Hutchinson and Ross, Inc. Stroudsburg, Pennsylvania, 223.
93. Tatsumi, K., K. Shigeyuki, and H. Yoshimura. (1977). Binding of nitrofuran derivatives to nucleic acids and protein. Chem. Pharm. Bull. 25, 2948-2952.

94. Swaminathan, S., C. Wong, G. Lower, and G. Bryan. (1977). Binding of 2-amino-4-(5-nitro-2-furyl)-2-C-14-thiazole to yeast transfer RNA, using rat liver microsomes. AACR Abstracts, 745.
95. Irving, C.C., and R.A. Veazey. (1969). Persistent binding of 2-acetylaminofluorene to rat liver DNA in vivo and consideration of the mechanism of binding of N-hydroxy-2-acetylaminofluorene to rat liver nucleic acids. Cancer Res. 29, 1799.
96. MacLeod, M., and J. Selkirk. (1982). Physical interactions of isomeric benzo(a)pyrene diol-epoxides with DNA. Carcinogenesis, 3, No. 3, 287-292.
97. Singer, B. (1977). Sites in nucleic acids reacting with alkylating agents of differing carcinogenicity of mutagenicity. J. Toxicol. and Envir. Health 2, 1279-1295.





FOR REFERENCE

NOT TO BE TAKEN FROM THE ROOM

NO. CAT. NO. 23 012

San Francisco LIBRARY

San Francisco LIBRARY

San Francisco LIBRARY

San Francisco LIBRARY

San Francisco LIBRARY

San Francisco LIBRARY

